Non-invasive Diagnostic Tests for Renal Osteodystrophy

Syazrah Salam

Submitted for the degree of Doctor of Philosophy

Academic Unit of Bone Metabolism

University of Sheffield

May 2019

Table of Contents

Acknowledgement 6
Statement of Attribution 8
Summary 10
Abbreviations 12
Publication and Abstracts 15
Chapter 1. Introduction 17
1.1 Chronic Kidney Disease 18
1.1.1 Prevalence 18
1.1.2 Classification 18
1.1.3 Complications 19
1.2 Pathogenesis of CKD-MBD 21
1.2.1 Overview 21
1.2.2 FGF23 and Phosphate 23
1.2.3 Vitamin D 26
1.2.4 Secondary Hyperparathyroidism 30
1.2.5 Treatment of Secondary Hyperparathyroidism 33
1.3 Bone in Chronic Kidney Disease 36
1.3.1 Fracture 36
1.3.2 Bone Physiology in Health and CKD 38
1.3.3 Renal Osteodystrophy and Osteoporosis in CKD 42
1.3.4 Bone-specific Treatment to Reduce Fracture Risk 45
1.4 Diagnostic Test for Renal Osteodystrophy 47
1.4.1 Bone Biopsy 47
1.4.2 Overview of Non-invasive Tests 50
1.4.3 Bone Turnover Markers (BTMs) 52
1.4.4 Bone Imaging 56
1.5 Vascular Calcification in CKD 58
1.5.1 Prevalence and Complications 58
1.5.2 Pathogenesis 59
1.5.3 Relationship with Biochemistry and Bone Abnormalities 62
1.5.4 Treatment 63
1.6 Summary 64

1.7 Study Aims and Hypothesis....65
Chapter 2. Methodology....67
2.1 Study Design and Participants....68
2.2 Bone Biopsy....69
2.2.1 Bone Biopsy Procedure....69
2.2.2 Pain Assessment....71
2.2.3 MicroCT....72
2.2.4 Sample Preparation and Histomorphometry....74
2.3 Imaging....77
2.3.1 Dual-energy X-ray Absorptiometry (DXA)....77
2.3.2 High Resolution Peripheral Quantitative Computed Tomography (HR-pQCT)....89
2.3.3 Vascular Calcification Imaging....94
2.4 Biochemistry....99
2.4.1 Principles of Immunoassays....99
2.4.2 Principles of Enzymatic Assay....103
2.4.3 CKD-MBD Biochemistry....103
2.4.4 Bone Turnover Markers....107
2.4.5 Vascular Calcification Markers....112
2.5 Statistical Analysis....114
2.5.1 Normality Testing....114
2.5.2 Summary Statistics....115
2.5.3 Testing Group Differences....115
2.5.4 Testing Relationship between Variables....116
2.5.5 Z-scores....116
2.5.6 Receiver Operating Characteristic (ROC) Analysis....117
Chapter 3. Bone Biopsy Patterns in Advanced CKD....123
3.1 Introduction....124
3.2 Methodology....125
3.2.1 Bone Biopsy Procedure, MicroCT and Histomorphometry....125
3.2.2 Statistical Analysis....125
3.3 Results....127
3.3.1 Patient Characteristics, Pain Score and Sample Adequacy....127
3.3.2 Bone Turnover....129

3.3.3 Bone Mineralization....132
3.3.4 Bone Volume....134
3.3.5 Diagnostic Accuracy of Static Parameters to Identify Low and High Bone Turnover....138
3.4 Discussion....141
Chapter 4. Bone Microstructure in Advanced CKD....151
4.1 Introduction....152
4.2 Methodology....154
4.2.1 Bone Imaging....154
4.2.2 Statistical Analysis....156
4.3 Results....157
4.3.1 Participants' Demographics....157
4.3.2 Bone Microstructure in CKD and Controls....157
4.3.3 Bone Microstructure in CKD patients with Low BMD on DXA....160
4.3.4 Relationship between Bone Microstructure on Bone Biopsy and Bone Imaging 164
4.4 Discussion....165
Chapter 5. Diagnostic Accuracy of Bone Turnover Markers and Bone Imaging to diagnose Renal Osteodystrophy....173
5.1 Introduction....174
5.2 Methodology....175
5.2.1 Study Design and Population....175
5.2.2 Bone Biomarkers....176
5.2.3 Bone Imaging....176
5.2.4 Bone Biopsy and Histomorphometry....177
5.2.5 Statistical Analysis....177
5.3 Results....178
5.3.1 Participants and the Bone Turnover on Histomorphometry....178
5.3.2 Biomarkers and Imaging in CKD and Controls....181
5.3.3 Relationship between Bone Turnover on Histomorphometry and Biomarkers and Imaging in CKD....182
5.3.4 Diagnostic Accuracy of Biomarkers and Imaging for Low Bone Turnover....185
5.3.5 Diagnostic Accuracy of Biomarkers and Imaging for High Bone Turnover....187
5.4 Discussion....188
Chapter 6. Vascular Calcification Relationship with Biomarkers and Bone in CKD....193

6.1 Introduction 194
6.2 Methodology 197
6.2.1 Vascular Calcification and Bone Imaging 197
6.2.2 Vascular Calcification Biomarkers 197
6.2.3 Statistical Analysis 197
6.3 Results 198
6.3.1 Vascular Calcification in CKD and Controls 198
6.3.2 Vascular Calcification Biomarkers 201
6.3.3 Vascular Calcification and Bone Microstructure 203
6.3.4 Vascular Calcification and Bone Biopsy 205
6.3.5 Independent Factors for Vascular Calcification 205
6.4 Discussion 207
Chapter 7. Conclusions and Future Research 218
References 224
Appendix 1. Lifestyle Questionnaire 249

Acknowledgement

I would like to express my sincere gratitude to Professor Richard Eastell and Dr Arif Khwaja who are my mentors. They have given me support and guidance throughout the study and in preparing this thesis. Their enthusiasm and involvement have made the experience on this project invaluable and I have learnt a great deal. Their patience and advice during my PhD have allowed me to get to this stage. I would also like to thank Dr Jennifer Walsh for giving her feedback in preparing this thesis.

I am grateful to Kidney Research UK for awarding me the Research Training Fellowship, and Immunodiagnostic Systems PLC and the Sheffield Hospitals Charity for funding the study. Thank you also to Professor Martin Wilkie for supporting the funding applications.

I would like to thank the following people:

- Dr Margaret Paggiossi who performed bone image acquisition, bone image analysis and teaching me on bone imaging techniques
- Ms Fatma Gossiel for carrying out bone turnover markers analyses
- Ms Orla Gallagher for bone biopsy histomorphometry and teaching me on the techniques
- Mrs Selina Bratherton who also performed bone image acquisition and responsible for setting up the study database
- The staff at the Northern General Hospital NIHR Clinical Research Facility especially Sister Angela Green, Sister Julie Walker, Mrs Carol McGurk and Mrs Jill Thompson for recruiting control participants and assisting with sample collection including bone biopsy.

- Professor Mark Wilkinson for trans-iliac bone biopsy training
- Dr David Hughes for histomorphometry support and advice
- Ms Louese Dunn for assisting and co-ordinating the research approvals
- Dr Richard Jacques for his statistical support
- CKD participants from Sheffield Kidney Institute and control participants who gave up their time and provided samples for the study
- All the staff and students at the Academic Unit of Bone Metabolism
- My husband, Anthony, for his unwavering support and my son, Thomas, for cheering me on.

Statement of Attribution

Study Protocols

Study protocol and study documents were initially written by Dr Arif Khwaja and Professor Richard Eastell. I attended the Research Ethics Committee (REC) meeting for approval. I revised the study protocol and the associated documents for substantial amendment for REC approval once during the study and was assisted by Ms Louese Dunn, Renal Research Co-ordinator.

Funding

I wrote the grant application and was awarded the Clinical Research Training Fellowship from Kidney Research UK. I also wrote the grant application for Sheffield Hospitals Charity funding. Professor Eastell wrote the application for grant funding from Immunodiagnostic Systems PLC.

Recruitment

I recruited and consented all the CKD participants in this study. Sister Angela Green from the Northern General NIHR Clinical Research Facility (NGH CRF) recruited and consented all the healthy control participants from an existing research volunteer database stored at the Academic Unit of Bone Metabolism, Northern General Hospital.

Bone Imaging

All scans were performed by Dr Margaret Paggiosi and Mrs Selina Bratherton. Image analyses were performed by Dr Paggiosi.

Bone Biochemistry

Blood samples were collected by myself or the staff at the NGH CRF. Samples preparation and storage were done by the NGH CRF staff. Ms Fatma Gossiel performed all the bone turnover marker analyses at the Bone Biochemistry Lab, Medical School, the University of Sheffield.

Bone Biopsy

I performed all the trans-iliac bone biopsy procedures in the study. Ms Orla Gallagher performed bone samples preparation, microCT and histomorphometry. Dr David Hughes provided support and advice.

Statistical Analysis

I performed all the statistical analyses.

Summary

Chronic Kidney Disease – Mineral Bone Disorder (CKD-MBD) is a common complication of advanced chronic kidney disease (CKD). Bone abnormalities of CKD-MBD are known as renal osteodystrophy (ROD) and are characterised by abnormal bone turnover and mineralization. ROD results in bone microstructural and mechanical changes which increases bone fragility. Thus, fracture risk is increased and subsequent mortality is high in these patients. Correct diagnosis of ROD is required before potential treatment to reduce fracture risk can be commenced. This can only be done with bone biopsy which is the gold standard test but this is an invasive and painful procedure. We conducted a cross sectional study with the primary aim of testing new non-invasive tests to diagnose and classify ROD as shown on bone biopsy.

Sixty-nine advanced CKD stages 4-5D and their age and gender-matched healthy controls were recruited. All participants had blood samples collected for bone turnover markers (BTMs) analysis and had bone scan using high resolution peripheral quantitative computed tomography (HR-pQCT). Forty-three CKD patients had trans-iliac bone biopsy samples evaluable for histomorphometry. We also used a new technique using HR-pQCT to simultaneously assess bone and vascular calcification (VC) relationship in CKD.

We found that advanced CKD patients have worse bone microstructure compared to controls. Importantly, BTMs such as bone alkaline phosphatase (bALP), intact procollagen type 1 N-terminal propeptide (intact PINP) and tartrate-resistant acid phosphatase 5b (TRAP5b), and bone imaging of radius using HR-pQCT were able to discriminate low bone turnover in advanced CKD patients. These non-invasive tests are robust diagnostic tools and have the potential to be translated into clinical practice. We also found that ankle arteries

VC was associated with worse bone microstructure of cortical bone at the tibia. These non-invasive tests could be instrumental in further research into treatment to reduce fracture risk in advanced CKD.

Abbreviations

25(OH)D	25-hydroxyvitamin D
AAC	Abdominal aortic calcification
ABD	Adynamic bone disease
Ac.f	Activation frequency
AUC	Area under the ROC curve
bALP	Bone alkaline phosphatase
BFR/BS	Bone formation rate/bone surface
BMC	Bone mineral content
BMD	Bone mineral density
BMI	Body mass index
BTMs	Bone turnover markers
BV/TV	Bone volume/tissue volume
CAC	Coronary artery calcification
CaSR	Calcium sensing receptor
CaxPO4	Calcium x phosphate
CKD	Chronic kidney disease
CKD-MBD	Chronic kidney disease – mineral bone disorder
CLIA	Chemiluminescence immunoassay
Cr	Creatinine
CRP	C-reactive protein
CTX	C-terminal telopeptides of type I collagen
Dkk-1	Dickkopf-1
dp-uc MGP	Dephosphorylated-uncarboxylated Matrix Gla protein
DXA	Dual energy X-ray absorptiometry
ECLIA	Electrochemiluminescence immunoassay

eGFR	Estimated Glomerular Filtration Rate
EIA	Enzyme immunoassay
ELISA	Enzyme-linked immunosorbent assay
ES/BS	Erosion surface/bone surface
FGF23	Fibroblast growth factor 23
FN	False negative
FP	False positive
HD	Haemodialysis
HR-pQCT	High resolution peripheral quantitative computed tomography
IGF-1	Insulin-like growth factor-1
iPTH	Intact parathyroid hormone
LS	Lumbar spine
LVH	Left ventricular hypertrophy
MAR	Mineral apposition rate
MGP	Matrix Gla protein
MLT	Mineralization lag time
MS/BS	Mineralising surface/bone surface
NPV	Negative predictive value
NTX	N-terminal telopeptides of type I collagen
O.Th	Osteoid thickness
OB	Osteoblast
ObS/BS	Osteoblast surface/bone surface
OC	Osteoclast
OcS/BS	Osteoclast surface/bone surface
OMT	Osteoid maturation time
OPG	Osteoprotegerin
OS/BS	Osteoid surface/bone surface

OV/BV	Osteoid volume/bone volume
PD	Peritoneal dialysis
PICP	Procollagen type 1 C-terminal propeptide
PINP	Procollagen type 1 N-terminal propeptide
PPV	Positive predictive value
PTH	Parathyroid hormone
QC	Quality control
RANKL	Receptor-activator of NF-κB ligand
ROC	Receiver operating characteristics
ROD	Renal osteodystrophy
ROI	Region of interest
RRT	Renal replacement therapy
SHPT	Secondary hyperparathyroidism
tALP	Total alkaline phosphatase
Tb.Th	Trabecular thickness
TBS	Trabecular bone score
TH	Total hip
TN	True negative
TP	True positive
TRAP5b	Tartrate-resistant acid phosphatase 5b
t-uc MGP	Total uncarboxylated Matrix Gla protein
VAS	Visual analogue scale
vBMD	Volumetric bone mineral density
VC	Vascular calcification
VDBP	Vitamin D binding protein
VDR	Vitamin D receptor
VSMCs	Vascular smooth muscle cells

Publication and Abstracts

Publication

Diagnostic Accuracy of Biomarkers and Imaging for Bone Turnover in Renal Osteodystrophy.

Salam, S, Gallagher, O, Gossiel, F, Paggiosi, M, Khwaja, A, Eastell, R. *J Am Soc Nephrol. 2018 May;29(5):1557-1565. doi: 10.1681/ASN.2017050584.*

Abstracts

Vascular calcification relationship to bone microstructure in advanced chronic kidney disease. Salam S, Paggiosi M, Gallagher O, Khwaja A, Eastell R.

- European Calcified Tissue Society Congress 2019. Calcif Tissue Int (2019) 104:S1–S151
- UK Kidney Week 2019 Conference
- European Renal Association – European Dialysis and Transplantation Association (ERA-EDTA) 2019 Congress. Nephrology Dialysis Transplantation, Volume 34, Issue Supplement_1, June 2019, gfz106.FP610

Diagnostic accuracy of a novel TRAP5b assay in diagnosing renal osteodystrophy. Salam S, Gallagher O, Gossiel F, Khwaja A, Eastell R.

- European Calcified Tissue Society Congress 2019. Calcif Tissue Int (2019) 104:S1–S151

Diagnostic accuracy of biomarkers and imaging in predicting bone turnover in advanced chronic kidney disease. Salam S, Gallagher O, Gossiel F, Jacques R, Paggiosi M, Khwaja A, Eastell R.

- UK Kidney Week Conference 2017
- European Calcified Tissue Society Congress 2017. Calcif Tissue Int (2017) 100:S1–S174.

Periostin as a novel bone biomarker for renal osteodystrophy in advanced chronic kidney disease. Salam S, Gallagher O, Gossiel F, Paggiosi M, Khwaja A, Eastell R.

- European Calcified Tissue Society Congress 2017. Calcif Tissue Int (2017) 100:S1–S174.

Bone mineral density and micro-architectural changes in advanced chronic kidney disease. Salam S, Paggiosi M, Khwaja A, Eastell R.

- UK Kidney Week Conference 2014
- European Calcified Tissue Society Congress 2014. Bone Abstracts (2014) 3

Peripheral vascular calcification and bone changes in advanced chronic kidney disease using high resolution peripheral quantitative computed tomography (HR-pQCT). Salam S, Paggiosi M, Khwaja A, Eastell R.

- Clinical Research Facility Conference 2014
- American Society of Nephrology Kidney Week Conference 2014. J Am Soc Nephrol 25, 2014: Page 232.
- European Renal Association-European Dialysis and Transplantation Association (ERA-EDTA) Congress 2015. Nephrology Dialysis Transplantation, Volume 30, Issue suppl_3, May 2015, Pages iii286–iii287

Chapter 1. Introduction

1.1 Chronic Kidney Disease

1.1.1 Prevalence

Chronic kidney disease (CKD) is increasingly common worldwide. In England alone, moderate to severe CKD affects 6% of the population which is equivalent to 2.6 million people {PHE 2014}. Meanwhile, National Health and Nutrition Examination Study (NHANES 1988-1994) showed that CKD affected 10% of the United States of America (USA) population and this prevalence had increased to 13% in the NHANES 1999-2004 {Coresh et al 2007}. This was equivalent to 26 million adults in the USA and 700,000 of those had severe CKD.

Increasing CKD prevalence is associated with risk factors such as ageing, diabetes, obesity and hypertension. Although moderate to severe CKD is rare (0.2%) in those below the age of 40 years, the NHANES data showed that a quarter of adults ages 70 or above had moderate to severe CKD {Coresh et al 2003}. The trend is similar in England where only 2% of those below the age of 65 years had moderate to severe CKD but a third of those over the age of 75 were affected {PHE 2014}. Given our ageing population, the prevalence of moderate to severe CKD in England alone is expected to increase to 3.2 million people in 2021 and 4.2 million in 2036.

1.1.2 Classification

CKD severity is classified based on estimated glomerular filtration rate (eGFR) which is a measure of excretory renal function and is derived from serum creatinine (Cr). Cr is produced at a fairly constant rate from the muscles and is excreted by the kidneys through glomerular filtration with a degree of proximal tubular secretion. Serum Cr alone is a poor reflection of kidney function as the level only becomes elevated when around 40% of GFR is lost. There

are also a number of non-renal determinants of Cr including individual's muscle mass and dietary protein intake. Meanwhile, eGFR calculation using CKD-EPI (Chronic Kidney Disease Epidemiology Collaboration) equation takes into account Cr, gender, body weight and race which gives a better estimation of glomerular filtration rate {Levey et al 2009}. ***Table 1.1*** shows the classification of CKD based on eGFR categories as set out by the National Institute of Clinical Excellence (NICE) and Kidney Disease: Improving Global Outcomes (KDIGO) guidelines {Kidney Disease: Improving Global Outcomes 2013; NICE 2014}.

Table 1.1

Chronic kidney disease (CKD) categories based on estimated glomerular filtration rate (eGFR). Taken from KDIGO CKD Guideline 2012.

CKD categories	eGFR range (ml/min/1.73m^2)	Description
Stage 1	≥ 90	Normal
Stage 2	60 – 89	Mildly decreased
Stage 3a	45 – 59	Mildly to moderately decreased
Stage 3b	30 – 44	Moderately to severely decreased
Stage 4	15 - 29	Severely decreased
Stage 5 (or 5D)	<15 (or on dialysis)	Kidney failure

1.1.3 Complications

Chronic kidney disease-mineral and bone disorder (CKD-MBD) is a common complication of CKD. The term CKD-MBD was first introduced by KDIGO in 2005 to describe a constellation of biochemical, bone, and vascular abnormalities associated with CKD (***Figure 1.1***) {S. Moe et al 2006}. It is defined as a systemic disorder of bone and mineral metabolism due to CKD manifested by either one or a combination of the following: (1) abnormalities of calcium,

phosphorus, parathyroid hormone (PTH), or vitamin D metabolism; (2) abnormalities in bone turnover, mineralization, volume, linear growth, or strength; and (3) vascular or other soft tissue calcification. A Clinical Practice Guideline for the Diagnosis, Evaluation, Prevention, and Treatment of CKD-MBD was published by KDIGO in 2009 and an update was published in 2017 {KDIGO 2009; KDIGO 2017}.

Figure 1.1

Manifestations of Chronic Kidney Disease - Mineral Bone Disorder (CKD-MBD) {KDIGO 2009}.

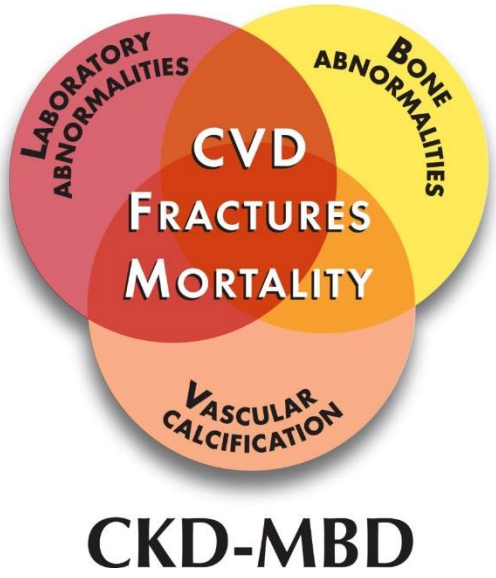

Other complications of CKD are anaemia, fluid and electrolyte abnormalities, metabolic acidosis, hypertension, cardiovascular disease and malnutrition. Importantly, CKD is associated with increased mortality. A systematic review by Tonelli et al showed that the risk of mortality in those with mild to moderate CKD is 2 - 4 times higher than those without CKD {Tonelli et al 2006}. A Swedish population based cohort study involving over 5500 patients

with CKD 4 and 5 pre-dialysis, haemodialysis and peritoneal dialysis (PD) patients also showed that the risk of mortality is increased 4 times in pre-dialysis CKD, 9 times in PD and 13 times in haemodialysis patients compared to age and gender-matched general population controls {Neovius et al 2014}.

Cause of death in advanced CKD is mainly cardiovascular disease which includes heart failure, thromboembolic events and arrhythmia. Reports have shown that 30% of deaths in renal replacement therapy (RRT) patients in the United Kingdom (UK) and 50% of deaths in RRT patients in the USA are due to cardiovascular disease {Methven et al 2017; USRDS 2015}. Other main causes of death in these patients included malignancy and infection.

The cost of RRT which includes dialysis or kidney transplantation is substantial. The National Health Service (NHS) in the UK spends 3% of its total budget on renal care. There were 63,162 patients with end stage renal disease receiving RRT in the UK in 2016 {MacNeill et al 2017}. The average cost of care for a dialysis patient is £31,000 annually and for a renal transplant patient, the cost is £22,000 in the first year and £3,000 annually thereafter {Li et al 2015}.

1.2 Pathogenesis of CKD-MBD

1.2.1 Overview

There are a number of CKD-MBD biochemical changes which occur as CKD progresses as summarised in ***Figure 1.2***. One of the earliest changes is an increase in the phosphaturic hormone fibroblast growth factor 23 (FGF23) which starts in the early stages of CKD with one study showing that a third of CKD stage 1 and nearly half of CKD stage 2 patients have raised FGF23 level whilst parathyroid hormone (PTH) level remained normal {Evenepoel et al 2010}.

A number of studies consistently showed that FGF23 rise is well established by the time eGFR is less than 60 ml/min/1.73m^2 and there is an exponential increase in its level in stage 5 CKD and dialysis {Evenepoel et al 2010; Wolf 2010}. The rise in FGF23 in early CKD is quickly followed by a reduction in 1,25-dihydroxyvitamin D (calcitriol) but both of these markers are not measured routinely in clinical practice {O. M. Gutierrez et al 2008; Isakova et al 2011}. This is partly because the methodology is challenging and partly because it is currently unclear if early intervention affects patient-related outcomes.

Secondary hyperparathyroidism (SHPT) is usually detected when eGFR is less than 45 mls/min/1.73m^2. PTH measurement is routinely available and normal reference range is well established. KDIGO CKD-MBD guidelines have also recommended a range of target PTH level as uncontrolled SHPT is associated with increased mortality {Floege et al 2011}. However, it is now accepted that SHPT is a relatively late change in CKD-MBD compared to FGF23 and calcitriol. The final detectable biochemical change is hyperphosphataemia which is usually observed in CKD stage 4 - 5D. Importantly, all these biochemical abnormalities ubiquitously worsen on dialysis and are associated with worse outcomes such as mortality {Block et al 2004; Tentori et al 2008}.

Figure 1.2

An overview of the onset of biochemical abnormalities with CKD progression {Wolf 2010}.

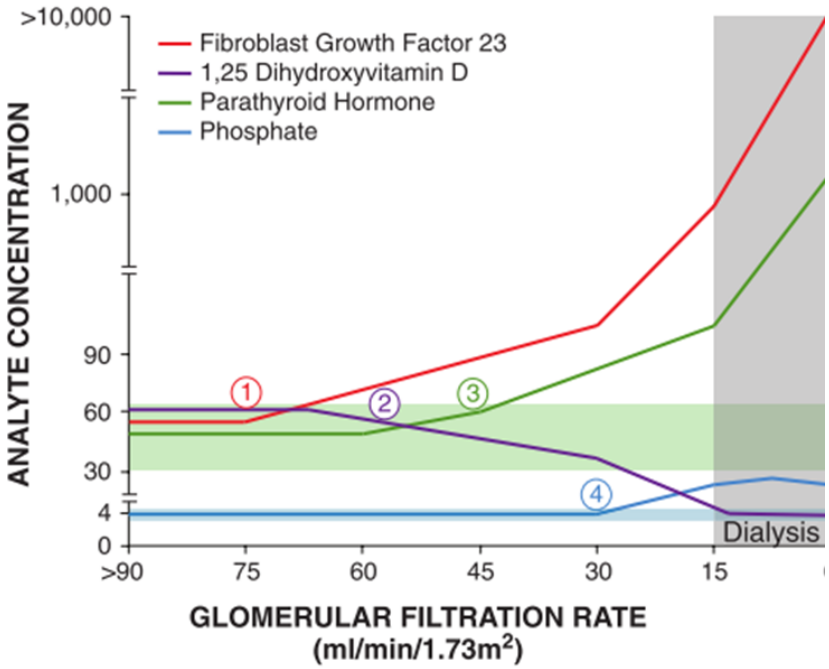

1.2.2 FGF23 and Phosphate

FGF23 is a hormone produced mainly by osteocytes but some are also produced by osteoblasts. It regulates phosphate handling via its high affinity to bind with its co-receptor, klotho, in the kidneys to promote phosphaturia by inhibiting the sodium-phosphate co-transporter in the proximal tubule {Saito et al 2003}. Another important FGF23 action is the inhibition of 1α-hydroxylase activity in the kidneys and increased 24-hydroxylase activity which in turn reduces the level of calcitriol {Antoniucci et al 2006; O. Gutierrez et al 2005; Hasegawa et al 2010}. This is shown in ***Figure 1.3***. Low calcitriol level impairs intestinal absorption of phosphate.

Figure 1.3

FGF23 roles in Vitamin D metabolism in CKD-MBD. Taken from SIMPLIFIED Study presentation slide by Hiemstra T (https://slideplayer.com/slide/10843676/)

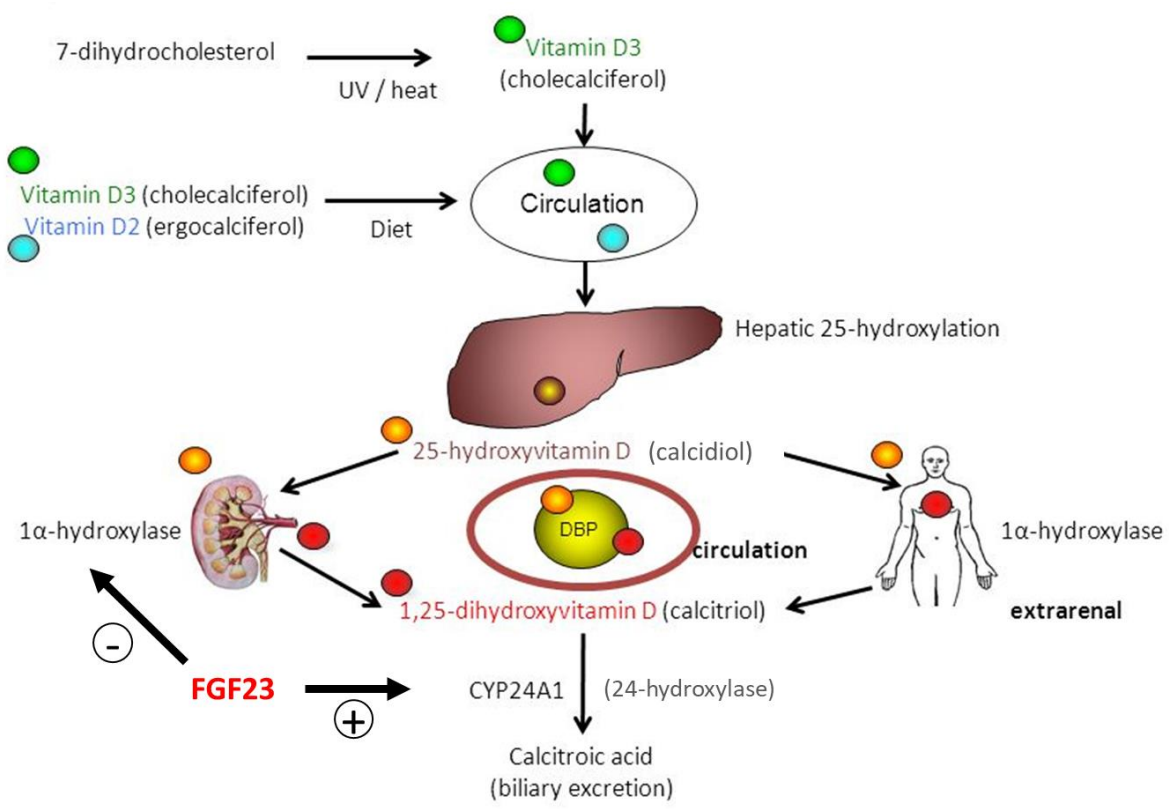

The importance of FGF23 in phosphate regulation is demonstrated in various genetic conditions. FGF23 excess in X-linked hypophosphataemia, autosomal dominant hypophosphotaemic rickets and tumor-induced osteomalacia results in severe hypophosphataemia due to renal phosphate wasting. In contrast, reduced production of intact FGF23 in tumoral calcinosis results in hyperphosphataemia. FGF23 production is also sensitive to dietary phosphate intake. A study in healthy men showed that dietary phosphate supplementation increases FGF23 and urinary fractional excretion of phosphate whereas dietary phosphate restriction has the opposite effects {Antoniucci et al 2006}.

Controversies exist on the aetiology of the sustained FGF23 rise in early CKD which eventually reaches extremely high level (in the 1000s) in dialysis patients. Hyperphosphataemia does not occur in early CKD but increased urinary excretion of phosphate is observed which suggests a compensatory mechanism in which FGF23 plays a crucial role {Craver et al 2007}. A number of studies have shown that although serum phosphate is still within the normal range, there is an inverse relationship between serum phosphate and kidney function {Evenepoel et al 2010; O. Gutierrez et al 2005; Isakova et al 2011}. At the same time, urinary phosphate excretion increases (measured as daily urinary phosphate and fractional excretion of phosphate) with worsening CKD and it is independently associated with FGF23 increase. This supports the hypothesis that the FGF23 rise in early CKD is driven by relatively small increases in serum phosphate. Another possibility is the reduction in FGF23 degradation in CKD {Bhattacharyya et al 2012; Shimada et al 2010}. A study showed that FGF23 expression by osteocytes in bone was increased in CKD stages 2 - 5D compared to normal controls but FGF23 expression was similar across all CKD stages including dialysis despite the exponential rise in circulating FGF23 found in advanced CKD {Pereira et al 2009}. However, the exact mechanism suppressing FGF23 degradation in CKD is unknown and its excretion in the urine and clearance by dialysis is minimal {Isakova et al 2011}. As CKD progresses and less viable nephrons are available, the phosphaturic effect of FGF23 is blunted leading to hyperphosphataemia.

Hyperphosphataemia and high FGF23 are important as these biochemical markers have also been associated with increased mortality {Block et al 2004; Isakova et al 2018}. The association between hyperphosphataemia and increased mortality is likely via increased vascular calcification {Cozzolino et al 2005; Jono et al 2000; Reynolds et al 2004; Scialla et al 2013}. The association between FGF23 and mortality is most likely via left ventricular hypertrophy (LVH) rather than vascular calcification {Faul et al 2011; Sarmento-Dias et al

2016; Scialla et al 2013}. LVH is an important mechanism for congestive heart failure and arrhythmia which can cause sudden death. A cohort of 1525 CKD patients with moderate to severe CKD from the Chronic Renal Insufficiency Cohort (CRIC) study had annual measurement of FGF23 over 5 years {Isakova et al 2018}. A higher baseline or a higher time-varying FGF23 was independently associated with increased risk of mortality.

1.2.3 Vitamin D

Vitamin D measured in clinical practice is 25-hydroxyvitamin D (calcidiol) which is the precursor to active 1,25-dihydroxyvitamin D (calcitriol). Calcitriol can be measured but this is usually done in research setting only. Vitamin D exists in two forms; vitamin D_3 (cholecalciferol) and vitamin D_2 (ergocalciferol) as shown in ***Figure 1.3***. Majority (90%) of vitamin D in human is made in the skin, when exposed to sunlight, in the form of vitamin D_3 {Holick et al 2008}. Only 10% of Vitamin D is sourced from diet; either in the form of vitamin D_3 (e.g. oily fish, egg yolk, cheese and beef liver) or D_2 (e.g. plants and fungi). Calcidiol measured in clinical practice is also called 'total 25-hydroxyvitamin D' as it measures both vitamin D_3 and D_2 that have undergone 25-hydroxylation in the liver. Calcidiol then undergoes 1α-hydroxylation in the proximal tubule epithelial cells in the kidneys to form calcitriol. Calcitriol has direct effects on multiple organs such as the parathyroid glands, the skeleton, the kidneys and the intestine when it binds to its Vitamin D receptors {Bikle 2012}. This is shown in ***Figure 1.4***.

Figure 1.4

Calcitriol effects on multiple organs.

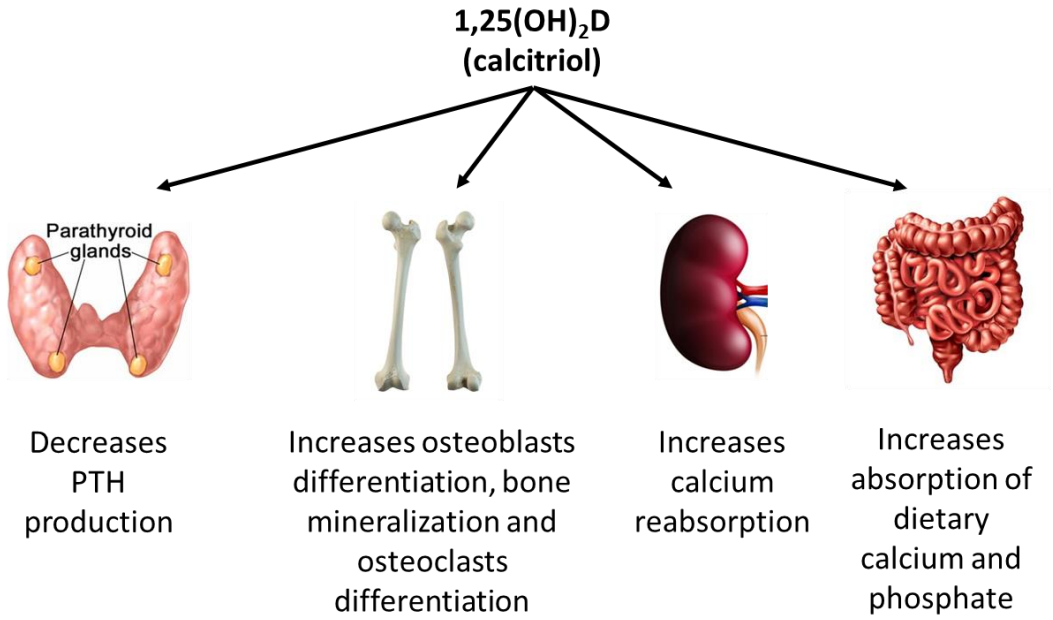

However, measuring calcitriol is challenging as it has a short half-life and low plasma concentration (1,000 times lower than calcidiol concentration). Therefore, calcidiol level remains the only measurement routinely available to assess vitamin D status. This may seem to be a straight forward approach to assess vitamin D status based on the fact that calcidiol is the precursor to calcitriol. Thus, calcidiol level is expected to have a positive relationship with serum calcium and negatively with PTH. However, the association between total calcidiol we measure in clinical practice and calcium and PTH have been inconsistent and this may be explained by the free hormone hypothesis {Bhan et al 2012; Gonzalez et al 2004; Taal et al 2014; Urena-Torres et al 2011}.

Most calcidiol (85 – 90%) in circulation is tightly bound to vitamin D binding protein (VDBP) as it is lipophilic. Some is loosely bound to albumin (10 – 15%) and only < 1% exists in free form. The free hormone hypothesis suggests that the free hormone (albumin-bound and free

hormone) is the biologically active (bioavailable) hormone as it is able to cross plasma membrane due to its small size and lipid permeability {Mendel 1989}. The bioavailable hormone was found to have better correlation with calcium and PTH than total calcidiol {Bhan et al 2012}. Bioavailable hormone can be measured but the methods are technically challenging. It can be calculated using an equation but that would still require measurement of VDBP which is not done in clinical practice {Bikle et al 1986; Powe et al 2011}. Furthermore, the calculated bioavailable calcidiol varied considerably from measured bioavailable calcidiol and only the measured level was shown to be related to PTH {J. B. Schwartz et al 2014}.

However, the discovery of megalin suggests that the free hormone hypothesis may be more important in other 1α-hydroxylation sites but not in the kidneys. In the kidneys, calcidiol/VDBP complex is filtered in the glomerulus and the complex is internalised into the renal proximal tubule by megalin {Nykjaer et al 1999}. Megalin is an endocytic receptor which sits on the luminal surface of tubular epithelial cells. Therefore, 1α-hydroxylation of calcidiol in the kidneys involves total calcidiol and not just the free hormone.

Calcidiol insufficiency and deficiency is common in CKD with the prevalence of up to 90% in dialysis population {Gonzalez et al 2004; Oh et al 2012}. This is often multi-factorial and may include (1) reduced exposure to sunshine due to reduced mobility/increased frailty, (2) dietary restrictions such as low phosphate diet, (3) poor appetite due to uraemia, (4) reduced 25-hydroxylation in the liver due to secondary hyperparathyroidism and (5) reduced VDBP level through heavy proteinuria/nephrotic syndrome or reduced production in malnutrition or inflammation {Doorenbos et al 2012; Laing et al 2002; Michaud et al 2010; Webb et al 1989}.

Calcitriol level is also reduced in CKD and this is partly due to reduced synthesis because of deficiency of its precursor (calcidiol < 10 ng/mL). However, calcitriol level continues to fall with progressive CKD even when calcidiol level is stable and only in the insufficiency range (calcidiol 10 – 30 ng/mL) {O. Gutierrez et al 2005}. This was previously thought to be related to less 1α-hydroxylase activity due to reduced kidney mass in CKD. However, the decline in calcitriol level occurs early in CKD and precedes other CKD complications related to reduce kidney mass such as renal anaemia. Meanwhile, FGF23 rise occurs early in CKD even in those with normal calcidiol level and FGF23 has been shown to be an important predictor of calcitriol level, independent of kidney function {Evenepoel et al 2010; O. Gutierrez et al 2005; Isakova et al 2011; Taal et al 2014}.

There is now an improved understanding on the role that FGF23 plays in vitamin D metabolism (***Figure 1.3***). FGF23 inhibits 1α-hydroxylation in the kidneys and simultaneously increases clearance of calcitriol by increasing 24-hydroxylase activity {Hasegawa et al 2010; Shimada et al 2004}. Some local 1α-hydroxylation occurs in extra-renal sites such as macrophages, colon, prostate and lungs but kidneys are the primary site {Mawer et al 1994; G. G. Schwartz et al 1998; Tangpricha et al 2001}. It should also be noted that 24-hydroxylation removes both calcitriol and calcidiol from circulation.

Calcidiol deficiency is a well-known cause of rickets in children and osteomalacia in adults although this is now rare in the developed world. Calcidiol and calcitriol deficiency in CKD is important as it worsens SHPT. Furthermore, an observational study showed an association between calcidiol and calcitriol deficiency with increased risk of mortality in dialysis population {Wolf et al 2007}. Observational studies support the use of Vitamin D supplementation to control SHPT in CKD but interventional studies have shown variable

outcomes. A meta-analysis by Palmer et al showed that vitamin D compounds do not consistently reduce PTH and beneficial patient-centred outcomes are unproven {Palmer et al 2007}. Furthermore, a recent randomised controlled trial, J-DAVID study, involving 976 haemodialysis patients showed that there is no survival benefit with active vitamin D supplementation but the patients enrolled had iPTH ≤ 180 pg/mL {Shoji et al 2018}. Therefore, uncertainties remain whether vitamin D supplementation is beneficial in CKD with more severe SHPT.

1.2.4 Secondary Hyperparathyroidism

Parathyroid glands have two main receptors which regulate PTH release. Low calcitriol level in CKD is sensed by vitamin D receptor (VDR) on parathyroid glands which stimulates the release of PTH and this is known as secondary hyperparathyroidism (SHPT) {Silver et al 1986}. Hypocalcaemia may also occur in advanced CKD due to low calcitriol level and this is sensed by the calcium sensing receptor (CaSR) on parathyroid gland to stimulate PTH production {Brown 2000}. ***Figure 1.5*** summarises the pathophysiology of SHPT in CKD.

PTH acts directly on bone in response to hypocalcaemia to promote skeletal calcium release via bone resorption. PTH also acts directly on the kidneys by promoting renal tubular re-absorption of calcium and increasing 1α-hydroxylation of calcidiol to make calcitriol. In turn, calcitriol promotes intestinal absorption of calcium. These mechanisms maintain normal calcium level via a negative feedback in healthy individuals. In advanced CKD, normal or mild hypocalcaemia is often observed despite SHPT and this is due to abnormal vitamin D metabolism as previously mentioned.

Figure 1.5

Pathophysiology of secondary hyperparathyroidism in CKD-MBD.

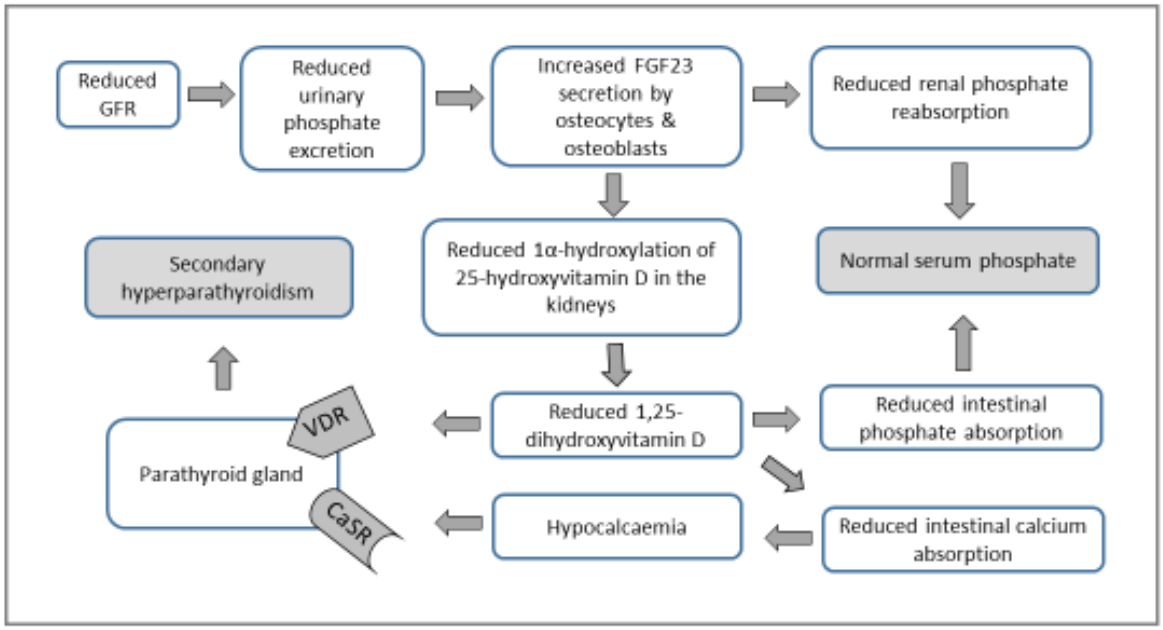

SHPT is a physiological change associated with CKD but uncontrolled SHPT may be harmful. PTH level that is too high or too low is associated with increased mortality in dialysis patients {Floege et al 2011}. The lowest mortality risk is associated with PTH level between 100 – 600 pg/mL (i.e. 2 – 9 times the upper limit of normal for the assay). It is well known that PTH has a direct effect on bone where it stimulates bone turnover. However, CKD patients with SHPT can have low, normal or high bone turnover. Abnormal bone turnover can impact on bone strength and increases the risk of fracture.

SHPT can be detected as early as CKD stage 3 where raised serum PTH is mainly due to increased secretion by parathyroid gland but also partly due to accumulation of PTH fragments. PTH has 84 amino acids sequence with a molecular weight of 9500 Daltons. It has a short half-life of a few minutes once it is released from parathyroid gland into the circulation. It is then metabolised in the liver and kidneys into two main fragments; the N-

terminal and the C-terminal fragments. The N-terminal fragment is fully metabolised in the liver and the C-terminal fragments are usually cleared by the kidneys, thus it accumulates in advanced CKD {Murray et al 2005}.

There are various PTH assays which have been developed over the last few decades with the aim of improving its sensitivity and specificity to detect biologically active PTH molecule (***Figure 1.6***). First generation PTH assays detect either the N-terminal or the C-terminal end of the molecule which also means that the whole molecule and its inactive fragments (mostly the C-terminal fragments) are measured. Second generation assays measure the full length PTH, which is called 'intact PTH' (iPTH). However, the assays detect both 1-84 PTH molecule and the 7-84 PTH fragments {Torres 2006}. This large amino-truncated PTH fragment was initially thought to be biologically inactive but animal studies have shown that 1-84 PTH increases bone resorption when injected into parathyroidectomised rats whilst 7-84 PTH fragments antagonizes the effect of 1-84 PTH in bone {Huan et al 2006; Slatopolsky et al 2000}. This may explain why CKD patients seem to demonstrate skeletal resistance to PTH where bone turnover is suppressed despite SHPT.

Third generation PTH assays, also known as 'whole' PTH assays, measure mainly 1-84 PTH molecules. The assays also detect a post-translational modified form of PTH 1-84 in region 15-20 by phosphorylation of a serine residue known as non-truncated amino-terminal PTH (N-PTH) {Eastell et al 2014}. N-PTH represents up to 15% of PTH detected by the assays in advanced CKD. It is not yet clear whether the whole PTH assays will better predict underlying bone disease in CKD or patient-centred outcomes such as mortality when compared to iPTH assays {Coen, Bonucci, et al 2002; Lehmann et al 2008; Monier-Faugere et al 2001}. Therefore, iPTH assays remain the assays commonly used in clinical practice.

Figure 1.6

Three generations of PTH assays detecting different parts of the PTH molecule {Eastell et al 2014}.

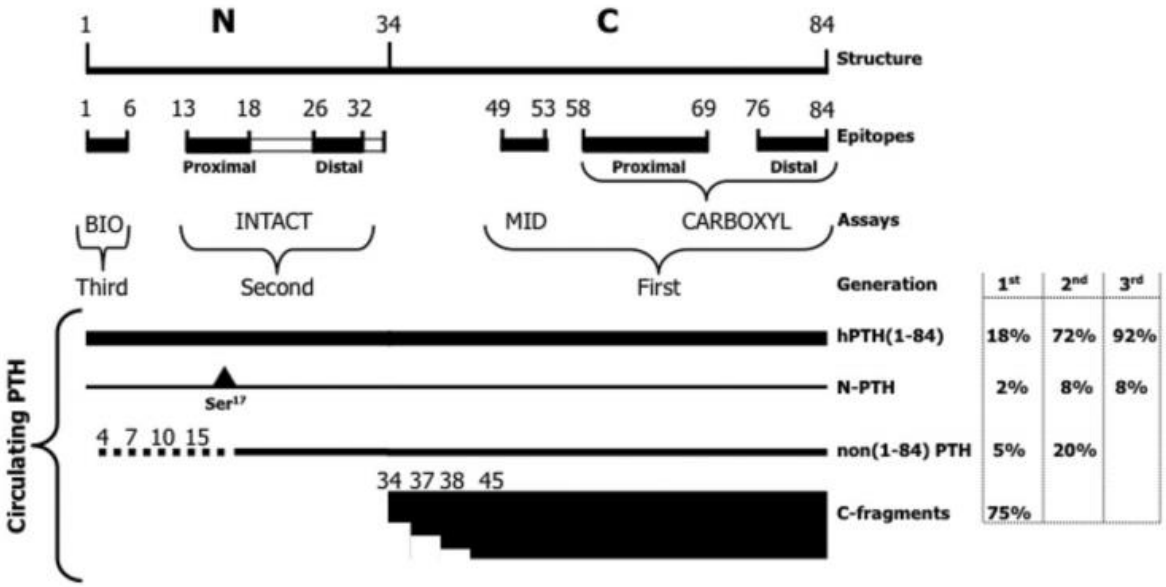

1.2.5 Treatment of Secondary Hyperparathyroidism

Severe SHPT have important consequence because a number of studies in dialysis patients showed that patients with iPTH > 600 pg/mL had the highest risk of mortality {Block et al 2004; Tentori et al 2008}. Very low iPTH is also associated with mortality as shown by U-shaped association between PTH level and mortality in dialysis patients {Floege et al 2011}. PTH and risk of fracture also has a U-shaped association where iPTH level that is too low or too high is associated with increased fracture risk {Fishbane et al 2016; Jadoul et al 2006}. Danese et al assessed USRDS data involving 9007 dialysis patients and found a weak U-shaped association between iPTH and fracture, with the lowest risk found at around iPTH 300 pg/mL {Danese et

al 2006}. Iimori et al examined 485 dialysis patients and found that the risk of fracture is 3.5 times higher with iPTH < 150 pg/mL and 6 times higher with iPTH > 300 pg/mL when compared to those with iPTH level 150 – 300 pg/mL (i.e. 2 – 5 times the upper limit of normal for the assay) {Iimori et al 2012}.

Findings from these observational studies led to KDIGO CKD-MBD guideline recommendation that iPTH level is maintained between 2 to 9 times the upper limit of normal for the assay in dialysis patients {KDIGO 2009}. This equates to around 150 – 600 pg/mL (or 15 – 60 pmol/L). There is no specific recommendation for PTH level in pre-dialysis CKD due to lack of evidence between PTH level and patient-centred outcomes.

Most SHPT treatment focuses on lowering iPTH level although there is no evidence so far that reducing PTH improves mortality or fracture risk in advanced CKD. The Evaluation of Cinacalcet HCl Therapy to Lower Cardiovascular Events (EVOLVE) trial recruited 3883 haemodialysis patients with SHPT (median iPTH 690 pg/mL) who were randomised to receive cinacalcet or placebo. Trial participants received study drug over a two year period and was followed up for up to 5 years. The trial showed that cinacalcet did not reduce the risk of death or the rate of clinical fracture {Chertow et al 2012; S. M. Moe et al 2014}. However, prevention of uncontrolled SHPT may still be important as shown by the observational studies.

Initial treatment for SHPT addresses phosphate intake by restricting dietary phosphate. Dietary restriction is often difficult to sustain or becomes inadequate as CKD progresses. Therefore, phosphate binders are required and these could be calcium-based or non-calcium based binders {KDIGO 2017}. At the same time, calcidiol insufficiency/deficiency requires plain vitamin D supplementation. The use of active vitamin D supplementation such as alfacalcidol or calcitriol is only recommended for dialysis patients who have worsening SHPT

despite sufficient calcidiol levels. This is due to concerns regarding vascular calcification with the use of supplementary active vitamin D.

The next line of treatment aims to lower PTH level in those patients with level above the recommended range who are no longer responding to the treatment outlined above. These patients are likely to have tertiary hyperparathyroidism where a solitary nodule or nodules in parathyroid glands become autonomous. Hypercalcaemia often ensues because the nodules have markedly reduced calcium-sensing receptor (CaSR) and vitamin D receptor (VDR) sensitivities. There are two main approaches to lower PTH level; medical by using calcimimetic or surgical by parathyroidectomy. Calcimimetic increases the sensitivity of CaSR in parathyroid glands to extra cellular calcium concentrations, leading to a reduction in circulating PTH. In the UK, cinacalcet is not part of routine treatment for SHPT largely due to cost. The National Institute of Health and Care Excellence (NICE) guideline recommends its use in patients with uncontrolled SHPT (iPTH > 800 pg/ml) refractory to standard therapy with normal or high adjusted serum calcium or in whom the risk of surgical parathyroidectomy outweighs the benefit {NICE 2007}. In those patients deemed fit for surgical intervention, parathyroidectomy should be considered as there is evidence of potential survival benefit after parathyroidectomy {Iwamoto et al 2012; Sharma et al 2012}. However, one retrospective study involving 235 dialysis patients who underwent parathyroidectomy suggested that patients with persistently very low PTH level (iPTH < 46 pg/mL) post-parathyroidectomy had increased 5-year mortality {Fotheringham et al 2011}.

1.3 Bone in Chronic Kidney Disease

1.3.1 Fracture

CKD patients have increased risk of fracture which is associated with increased morbidity and mortality. A number of studies suggest that even minimal kidney impairment is associated with increased risk of bone loss and fracture {Fried et al 2007; Jamal et al 2010; Kinsella et al 2010}. Indeed, an analysis of the Third NHANES data suggested that the association between prevalent hip fracture and CKD was stronger than many conventional risk factors for fracture such as bone mineral density (BMD), gender, race and age {Nickolas et al 2006}.

The Third NHANES data showed that the prevalence of hip fracture in pre-dialysis CKD is 2-3 times greater than in the general population {Nickolas et al 2006}. Large cohort studies have shown that the incidence of hip fracture in advanced CKD (eGFR 15 - 30 ml/min/1.73m^2) is up to 4 times higher compared to those with eGFR > 60 ml/min/1.73m^2 and this is similar to the incidence in dialysis patients {Dooley et al 2008; Kim et al 2016}. Dialysis patients with fracture also have an associated 2.5 times higher risk of mortality compared to the general population {Alem et al 2000; Coco et al 2000}.

The health care cost of fragility fracture in CKD is substantial. The number of hospital admissions for hip fracture is higher amongst dialysis compared to non-dialysis CKD which is higher those with normal kidney function {Kim et al 2016}. Fracture-related hospitalisation cost in the USA in 2010 was around $660 million for CKD and dialysis patients but this did not include their aftercare which is also substantial as more than 4 in 5 patients were discharged to nursing or intermediary care. A 2010 French National Hospital Database study showed that mean length hospital stay was 5 days longer in dialysis compared to non-dialysis patients and

thus, the cost of hospital stay was higher (Euro 8,500 versus Euro 7,000 respectively) {Maravic et al 2014}. In the UK, the estimated annual cost of all fragility fractures is £2 billion but fracture cost specifically in CKD is unknown {Burge 2001}.

Fractures occur when applied load (force) exceeds bone strength. The risk of fracture is also determined by falls which is increasingly appreciated as an important risk factor in patients with CKD. The risk of serious fall injuries which resulted in fracture, brain injury or joint dislocation increases with worsening CKD {Bowling et al 2016}. The possible mechanisms include frailty and sarcopaenia {Moorthi et al 2017}. The Fracture Triangle summarises the relationship between force, bone strength and falls (***Figure 1.7***).

Figure 1.7

Fracture Triangle and the determinants of bone strength which is affected by CKD.

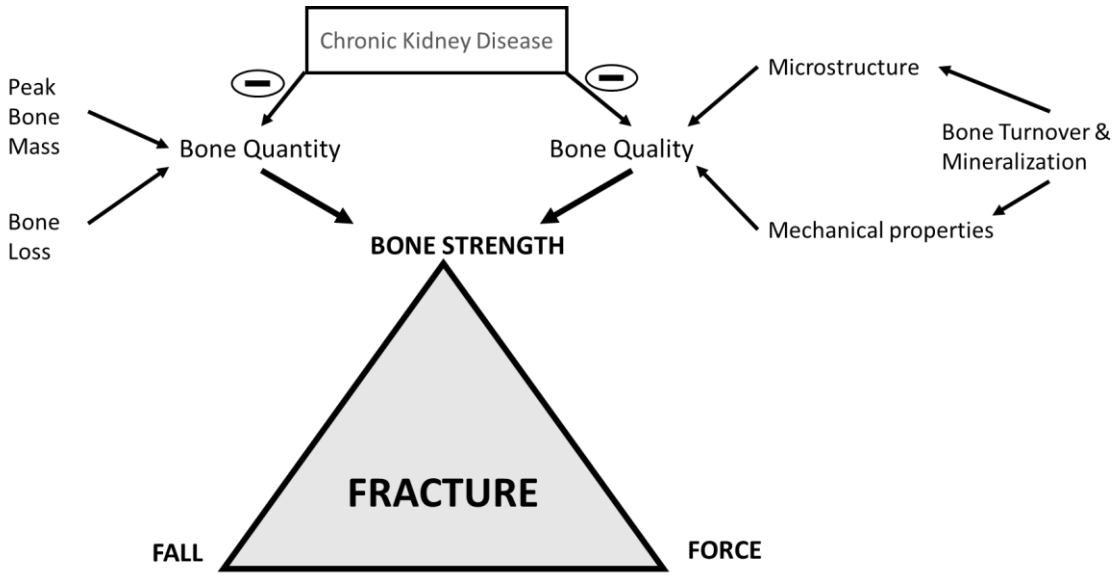

Bone strength is determined by bone quantity and bone quality {NIH 2001}. Bone quantity which can be reflected by BMD or bone volume is determined by peak bone mass in early adulthood and amount of bone loss. Meanwhile, bone quality is reflected by microstructure and mechanical properties which are determined by bone turnover and mineralization. In CKD-MBD, abnormalities of bone quality and quantity are not closely linked which may explain why BMD alone is unable to predict fracture risk in advanced CKD.

1.3.2 Bone Physiology in Health and CKD

Bone undergoes mostly remodelling with minimal bone modelling in adults. Bone remodelling is under the influence of several factors such as PTH, vitamin D, cortisol, thyroid hormone, sex hormones such as oestrogen and testosterone, and growth hormones such as insulin-like growth factor 1 (IGF-1). Bone remodelling in healthy adults occurs at a fairly constant rate with each remodelling cycle of a bone mineral unit taking around 4 months to complete and a whole adult skeleton would be remodelled within 10 years. Remodelling is important for removal of old bone, repair of micro-cracks and adaptation to changes in biomechanical force (e.g. physical activity and weight gain) with new bone which is mechanically stronger. Bone remodelling is also involved in maintaining serum calcium-phosphate balance as skeleton is the biggest calcium and phosphate reservoir.

Bone remodelling starts with activation of bone lining cells and differentiation of osteoclast (OC) precursor which is derived from haematopoietic stem cells {Miller et al 1989}. The maturation and activation of OC precursor are critically dependent on the activity of receptor-activator of NF-κB ligand (RANKL) and macrophage-colony stimulating factor

{Fujikawa et al 2001; Lacey et al 1998}. RANKL is released by osteoblasts (OB) and activates its receptor-activator of NF-κB (RANK), which is expressed on pre-osteoclasts, leading to OC proliferation and activation as shown in ***Figure 1.8***. This process can be attenuated by osteoprotegerin which is an endogenous inhibitor of RANK, also produced by OB {D'Amelio et al 2009}. The mature OC attaches itself to the bone surface by αβ integrin which is mediated by Src kinase to create a seal between itself and the bone surface. This microenvironment enables the collagenolytic enzymes such as cathepsin K and tartrate-resistant acid phosphatase 5b (TRAP5b) to digest bone matrix.

Figure 1.8

Osteoclast activation by RANKL and its inhibition by RANKL decoy receptor osteoprotegerin.

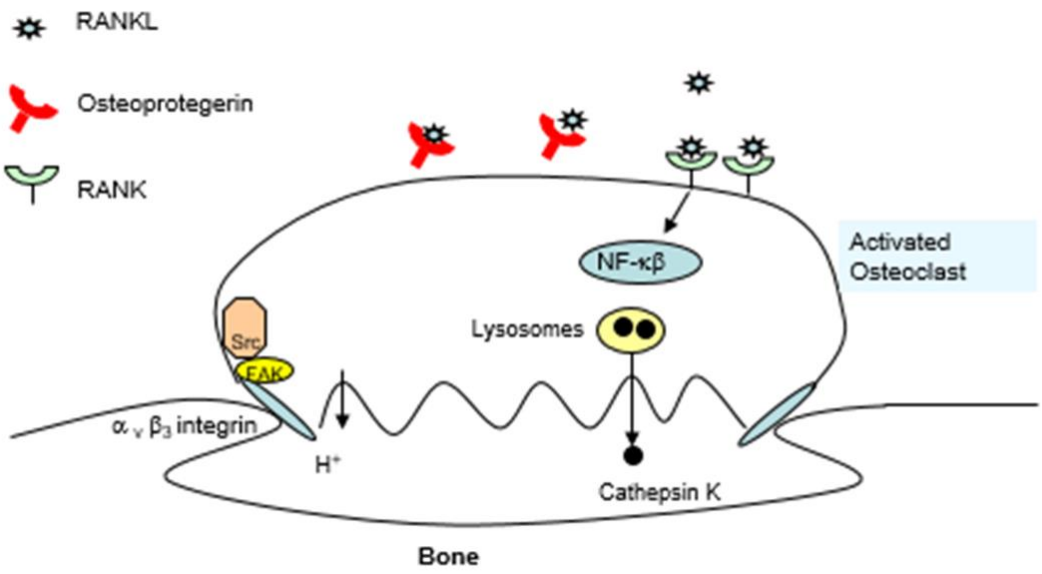

When OC is activated for bone resorption, OB activation follows and this process is tightly coupled in bone remodelling {Nakamura et al 2003}. Coupling has a temporal and spacial relationship which leads to several proposed mechanisms. Bone matrix-derived factors such as IGF-1 and bone morphogenic proteins which are released during matrix degradation has been shown to promote OB activation {G. Chen et al 2012; Crane et al 2014}. Other proposed mechanisms involved cell to cell contact and cytokines released by OC {Ikeda et al 2014}.

OB is derived from mesenchymal stem cells and its differentiation to mature OB is modulated by the Wnt/β-catenin pathyway which is shown in ***Figure 1.9***. This is known as the canonical (classical) pathway where Wnt protein binds to frizzled receptor and its co-receptor LRP5/6 on pre-OB. This leads to translocation of β-catenin into the cell nucleus where it acts on target genes to promote OB differentiation. There are endogenous inhibitors of this process such as sclerostin (produced by osteocytes) and Dickkopf-1 (Dkk-1, produced by OB) which bind to LRP5/6.

OB lays down type I collagen during bone formation and there are molecules released into the circulation during collagen linkage which are N-terminal (PINP) and C-terminal (PICP) peptides. The new unmineralized bone is known as osteoid and undergoes mineralization under the influence of bone alkaline phosphatase (bALP) enzyme and a protein called osteocalcin which are both produced by OB {Price et al 1980; Whyte 1994}. Mineralization with hydroxyapatite crystals is also under the influence of calcium, phosphate, pyrophosphate and vitamin D. Primary mineralization takes 2-3 months and the bone mineral unit remodelling cycle is complete. Secondary mineralization continues beyond this point and may even take years to complete during which there is a slower increase in crystal number and size {Bala et al 2010}.

Figure 1.9

Osteoblast activation by the Wnt/β-catenin pathway.

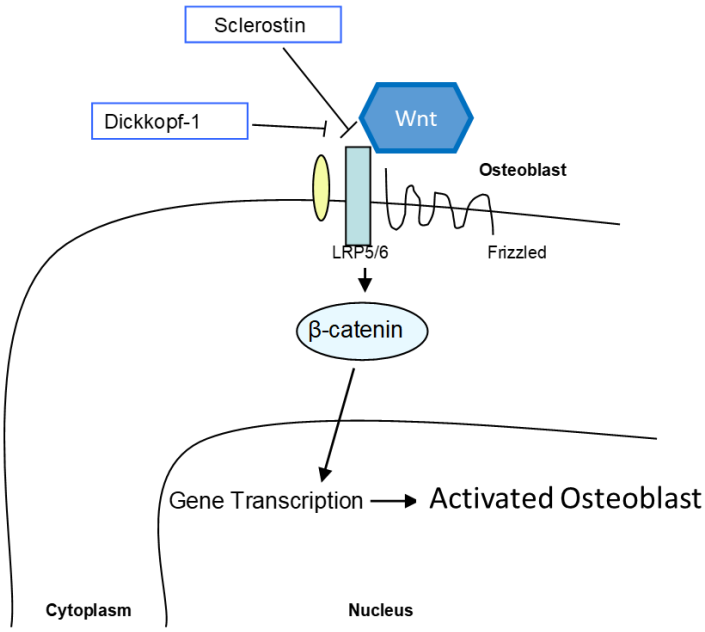

In CKD, bone remodelling and modelling are affected by abnormalities of bone turnover (too high or too low) and mineralization which is known as renal osteodystrophy (ROD). In high bone turnover disease, bone is being replaced at a faster rate before mineralization is complete and often resorption exceeds bone formation which may explain the resulting bone loss. The latter has been demonstrated by a study using mouse model which showed that gene expression of proteins involved in OC differentiation and function such as RANK, RANKL, cathepsin K and TRAP5b rise from early stages of CKD before the onset of SHPT {Sabbagh et al 2012}. In the later stages of CKD, there is also a reduction in gene expression for proteins involved in OB differentiation and bone mineralization such as bALP and osteocalcin. Furthermore, an in vitro study showed that FGF23 together with soluble klotho directly inhibit the Wnt/B-catenin pathway for OB differentiation {Carrillo-Lopez et al 2016}. Thus, bone

formation is relatively suppressed compared to bone resorption even in high bone turnover ROD.

In low bone turnover/adynamic bone disease, bone remodelling is minimal or absent which means that old bones are not replaced, micro-cracks are not repaired and the skeleton is less adapted to changes in mechanical force. Delayed mineralization could also happen when bone turnover is high (mixed bone disease) or low (osteomalacia).

1.3.3 Renal Osteodystrophy and Osteoporosis in CKD

Renal osteodystrophy (ROD) is used exclusively to define bone abnormalities associated with CKD. ROD is a spectrum of bone disease characterised by bone turnover and mineralization abnormalities seen on bone histomorphometry (***Table 1.2***). Osteitis fibrosa is a state of high bone turnover and normal mineralization which is often associated with bone marrow fibrosis. High bone turnover combined with abnormal bone mineralization is known as mixed bone disease. Meanwhile, low bone turnover and abnormal mineralization is known as osteomalacia. Finally, low bone turnover and normal mineralization is known as adynamic bone disease (ABD). Strictly speaking ABD should only be used for bone biopsy which shows absent bone turnover (i.e. no tetracycline label uptake and no OC or OB). However, a spectrum of low to absent bone turnover is often categorised together and labelled as ABD.

An extensive literature review of bone biopsy studies between 1983 and 2006 by KDIGO showed that over 80% of CKD stages 3-5 patients had ROD and the prevalence was up to 98% in dialysis patients {KDIGO 2009}. The predominant type of ROD was high bone turnover disease (50 – 65%) such as osteitis fibrosa and mixed bone disease. Meanwhile, the

prevalence of osteomalacia was only around 10%. The largest bone biopsy series was published by Araujo et al involving 2340 bone biopsies performed between 1985 and 2001 in Brazil which showed that 68% of patients had high bone turnover {Araujo et al 2003}. However, the biopsies were performed in symptomatic dialysis patients for diagnostic purposes which may explain the high proportion of high bone turnover disease.

Table 1.2

Classification of ROD subtypes based on bone turnover and mineralization abnormalities.

ROD subtype	Turnover	Mineralization	Volume
Osteitis fibrosa	High	Normal	May be low, normal or high
Mixed bone disease	High	Abnormal	
Adynamic bone disease (ABD)	Low	Normal	
Osteomalacia	Low	Abnormal	

The natural history of ROD has probably changed from predominantly high bone turnover to predominantly low bone turnover. More recent studies by Malluche et al and Sprague et al involving 630 and 490 dialysis patients respectively demonstrated that up to 60% had low bone turnover or ABD {Malluche et al 2011; Sprague et al 2016}. Furthermore, osteomalacia is becoming less frequent which is consistent with less aluminium toxicity as a result of improved dialysis water treatment, less use of aluminium-based phosphate binders and an increased use of vitamin D to control SHPT {Araujo et al 2003}.

Abnormal bone turnover in CKD may be an important risk factor for fracture as it may affect bone quality and quantity. Material and nano-mechanical abnormalities such as reduced mineral to matrix ratio and lower bone stiffness have been observed in high turnover bone

disease; whereas microstructural abnormalities such as lower trabecular bone volume and reduced trabecular thickness have been observed in low turnover bone disease {Malluche et al 2012}. Piraino et al assessed bone biopsy from 31 dialysis patients and found similar fracture history in those with low and high bone turnover {Piraino et al 1988}. The largest bone biopsy series published by Araujo et al also showed no difference in fracture frequency between low and high bone turnover although it is unclear whether this is based on fracture history or incident fracture {Araujo et al 2003}. Overall, there is no large prospective study assessing the relationship between abnormal bone turnover and fracture incidence.

Patients with low bone volume on bone biopsy are expected to have an increased risk of fracture. However, no bone biopsy study has proven this association because bone biopsy study is difficult to conduct and it would require a large number of participants to assess fracture outcome. Nonetheless, the KDIGO CKD-MBD guideline recommends the inclusion of bone volume assessment and that bone histomorphometry should be reported using the TMV (turnover, mineralization, and volume) classification (***Table 1.2***) {S. Moe et al 2006}.

There is a considerable overlap in the prevalence of osteoporosis and ROD as both may be present in CKD which is common in the elderly. The Third NHANES data showed that 61% of women with osteoporosis had CKD stage 3 and 23% had CKD stage 4 {Klawansky et al 2003}. Osteoporosis is defined by bone mineral density (BMD) T-score < -2.5 as measured on dual energy X-ray absorptiometry (DXA). BMD T-score is the number of standard deviations above or below the average BMD value for healthy young gender-matched adults. The clinical utility of DXA in evaluating those at increased risk of fracture and monitoring response to treatment is well established in the general population {Austin et al 2012; Jacques et al 2012; Kanis et al 2010}. However, the ability of BMD measured by DXA in CKD population to predict fracture

risk is weak as the overall fracture risk in advanced CKD not only relates to low BMD but also due to ROD which affects bone quality {Hsu et al 2002; Jamal et al 2002; Piraino et al 1988}. Accurate diagnosis of osteoporosis and ROD subtypes in CKD is challenging but it is needed to guide treatment decision to reduce fracture risk.

1.3.4 Bone-specific Treatment to Reduce Fracture Risk

Patients with mild to moderate CKD without obvious CKD-MBD biochemical abnormalities (such as SHPT) and low BMD consistent with osteoporosis are less likely to have overt ROD (i.e. their bone turnover and mineralization may be normal). BMD seems to predict fracture in those with eGFR > 30 ml/min/1.73m^2 with absent biochemical abnormalities associated with CKD-MBD {Yenchek et al 2012}. Bone-specific management should be focussed on osteoporosis treatment to reduce fracture risk which includes anti-resorptive (e.g. bisphosphonate or denosumab) or anabolic (e.g. teriparatide) agents.

In contrast, patients with advanced CKD (eGFR < 30 ml/min/1.73m^2) with CKD-MBD biochemical abnormalities and low BMD (osteopaenia or osteoporosis) are more likely to have ROD. Bone-specific management so far has focussed on controlling SHPT and using vitamin D supplementation although there is no evidence from interventional study to show that these approaches reduce fracture risk. Furthermore, patients with advanced CKD and SHPT may have low bone turnover ROD and controlling the SHPT may result in ABD which is also detrimental to bone health.

Overall, accurate diagnosis of ROD subtypes is crucial before considering any bone specific treatment. This is even more important in those who have suffered fragility fracture as it is

well known that a previous fracture is a good predictor of future fractures {Kanis et al 2018}. Previously, bone-specific treatment to reduce fracture risk in advanced CKD have been limited as bisphosphonates are contraindicated in patients with eGFR < 30 ml/min/1.73m^2. This is because bisphosphonates have been associated with worsening kidney function due to acute tubular necrosis and nephrotic range proteinuria due to focal segmental glomerulosclerosis {Toussaint, Elder, et al 2009}. However, denosumab is now available and not contra-indicated in CKD although the risk of hypocalcaemia is high in advanced CKD {Block et al 2012}. Denosumab is an antibody to RANKL and thus, it is an anti-resorptive treatment which suppresses bone turnover. Denosumab should not be given to patients with pre-existing low bone turnover or ABD. On the other hand, teriparatide is a recombinant PTH and thus it is an anabolic agent which stimulates bone turnover. Teriparatide is not contraindicated in advanced CKD but it should not to be given to patients with pre-existing high bone turnover. It is now possible to use these treatment options in advanced CKD but evidence on their fracture risk reduction in this population is limited. Large randomised controlled trials of denosumab and teriparatide have largely excluded advanced CKD patients with SHPT. Additionally, these agents need to be tailored to individual bone turnover status as incorrect diagnosis of ROD subtypes and treatment may cause further damage to bone health. A large interventional trial using these agents tailored to individuals' bone turnover status to assess fracture outcome is unlikely to happen when bone biopsy is still required to diagnose ROD subtypes. Therefore, further research into non-invasive tests to replace bone biopsy is required to address this limiting step in such clinical trial.

1.4 Diagnostic Test for Renal Osteodystrophy

1.4.1 Bone Biopsy

Bone biopsy is the gold standard test to diagnose ROD as there are currently no biomarkers or imaging tools that can accurately predict ROD subtypes. Trans-iliac bone biopsy carries low risk of morbidity and so far there is no known mortality {Hernandez et al 2008}. The KDIGO CKD-MBD guideline recommends performing bone biopsy in various settings such as persistent bone pain, unexplained fractures, unexplained hypercalcaemia, unexplained hypophosphatemia and possible aluminium toxicity {KDIGO 2009}. The guideline also specifies that bone biopsy is required prior to therapy with anti-resorptive agents in patients with CKD-MBD.

Bone biopsy can be assessed quantitatively and reported using histomorphometry standardised nomenclature, symbols and units as published by the American Society of Bone Mineral Research Histomorphometry Nomenclature Committee in 1987 {Parfitt et al 1987}. The published nomenclature included static and dynamic parameters. Dynamic parameters give an indication of bone turnover and mineralization over time (rate) but requires tetracycline bone labelling beforehand. This unified system of terminology allows direct comparison between bone biopsy studies. There are semi-automated histomorphometry software systems available but it is still time and labour-consuming process which requires the expertise of bone technicians. Therefore, most bone biopsies in clinical setting are assessed using qualitative method which is quicker but this method is non-standardised and has a high degree of inter-assessor variability.

Quantitative histomorphometry parameters of bone turnover, mineralization and volume require normal reference ranges to determine normal/abnormal parameters for classification of ROD subtypes. There is no unifying consensus on normal reference ranges worldwide and there is also a debate that normal range may differ between different ethnicities and geography. Furthermore, normal range in healthy adults may differ with each decade of life and gender. The group with extensive publications on bone biopsies of ROD led by Hartmut Malluche published normal reference values in 1982 {Malluche et al 1982}. The study examined bone biopsy parameters from each decade of life (first to eighth) from 84 normal American subjects using quantitative histomorphometry. The bone biopsies were taken from 63 men and 21 women (12 were pre-menopausal). Each decade of life group had between 5 to 19 subjects. However, only static parameters were obtained as the subjects were deceased. Subsequently, the same group published a reference range for dynamic parameters of bone turnover and mineralization in adults {Malluche et al 2011}. Normal bone turnover was defined as bone formation rate/bone surface (BFR/BS) of 1.8 – 3.8 mm^3/cm^2/year (or 18 – 38 $\mu m^3/\mu m^2$/year) and normal mineralization was defined as osteoid thickness (O.Th) ≤ 20 µm and mineralization lag time (MLT) ≤ 50 days. Normal bone volume in the study was defined as bone volume/tissue volume (BV/TV) 16.8 – 22.9%.

Parfitt et al examined bone mineralization in 142 healthy women aged 20 – 74 years who received double tetracycline labelling prior to biopsy {Parfitt et al 1997}. The study included 34 black (19 pre-menopausal, 15 post-menopausal) and 108 white (42 pre-menopausal, 66 post-menopausal) women. The study reported O.Th < 20 µm and MLT < 100 days for this group of healthy women. There are countries such as Brazil and Venezuela which have used their own reference ranges in a multi-centre bone biopsy study {Sprague et al 2016}. There is no UK-specific reference ranges but adopting the reference ranges published by Malluche et

al and Parfitt et al is reasonable given that both countries (the UK and the USA) have predominantly Caucasian population.

There are some limitations inherent to bone biopsy which is mostly performed on unilateral iliac crest. It is easy to access the iliac crest and it is not in close proximity to blood vessels or nerves. However, bone sample from this site may not be representative of the whole skeleton as shown by Hiller et al {Hiller et al 2017}. The group examined bone biopsy samples from the iliac crest, proximal tibia and lumbar spine from 10 cadavers and found that there was no correlation between bone volume/tissue volume (BV/TV) of the three sites. However, earlier studies showed that iliac crest BV/TV had moderate to strong association with lumbar spine BV/TV {Amling et al 1996; Dempster et al 1993; Thomsen et al 2002}. Iliac crest BV/TV was also weakly associated with proximal femur BV/TV {Fazzalari et al 1989}. Overall, iliac crest BV/TV cannot infer the same results for other skeletal sites.

Furthermore, pelvic bone fracture is extremely rare in CKD unlike other fracture sites such as the hip, ankle, wrist and lumbar spine {Wagner et al 2014}. However, bone biopsy of common fracture sites such as the lumbar spine is not possible and have high risk of complications. Taking bone biopsy intra-operatively during fracture fixation such as in hip fracture is not recommended as the bone surrounding the fracture may have also sustained damage.

It is acceptable to obtain bone biopsy sample from either the right or the left iliac crest but we need to be aware of the potential difference between the two sides. Studies by Parisien et al and Chappard et al involving paired iliac crest bone biopsy samples from 30 cadavers showed that there was 11 - 15% intra-individual variability between the two sides {Chappard et al 2008; Parisien et al 1988}.

It is important that interpretation of bone biopsy results takes these limitations into consideration especially when deciding treatment options. All the studies mentioned above only assessed bone volume which is a static measurement. Tetracycline bone labelling was not possible as the studies examined cadavers. No studies have assessed bone turnover or mineralization status at different skeletal sites or in paired samples from both iliac crests using bone biopsy samples.

Although bone biopsy is the gold standard test for ROD, it is rarely performed as it is an invasive and painful procedure. Furthermore, very few centres have the expertise to perform the procedure and carry out quantitative histomorphometry {Evenepoel et al 2017}. ROD also moves from one subtype to another under the influence of worsening CKD, worsening SHPT, PTH resistance in bone, and treatment such as phosphate binder, vitamin D and calcimimetic {Coen et al 1996}. Repeated bone biopsy to monitor these treatment effects on bone is almost impossible. Hence, further research is needed to find non-invasive tools which can predict bone histomorphometry features of ROD.

1.4.2 Overview of Non-invasive Tests

Serum calcium and phosphate are poor predictors for ROD as the levels are maintained in the normal range even in advanced CKD by mechanisms already discussed. PTH is also a poor predictor of ROD although extremely high (greater than 600 pg/mL) or extremely low (less than 100 pg/mL) iPTH level may predict high or low bone turnover respectively in CKD {Garrett et al 2013}. However, the majority of CKD patients have PTH level between these values where bone turnover may still be abnormal. A study by Ferreira et al involving 91 haemodialysis patients found that half of the patients had ABD despite having median iPTH

range of 150-400 pg/mL over a one-year period prior to bone biopsy {Ferreira et al 2008}. Barretto et al studied 101 haemodialysis patients and found that 10 - 15% of patients had low bone turnover despite having iPTH > 300 pg/mL {F. C. Barreto et al 2008}. The positive predictive value (PPV) for iPTH > 300 pg/ml for identifying high bone turnover ROD was only 62% in that study. The PPV may be improved with higher cut off level as shown by Herberth et al involving 141 dialysis patients {Herberth et al 2009}. iPTH ≥ 420 pg/mL was found to have an 84% PPV for identifying high bone turnover. Despite this seemingly favourable PPV for identifying high bone turnover, iPTH is still not robust enough as a diagnostic test. Furthermore, these studies were performed in haemodialysis patients only and may not be applicable to pre-dialysis CKD with SHPT. Meanwhile, iPTH < 150 pg/mL had hugely variable PPV (51 – 97%) for identifying low bone turnover in dialysis patients {F. C. Barreto et al 2008; Carmen Sanchez et al 2000; Urena et al 1996}. Overall, these routinely available biochemical tests are unable to predict bone turnover status accurately but bone turnover markers (BTMs) may have better accuracy as these are markers which are directly released from bone.

Bone imaging may also have a role in predicting ROD subtypes given all the structural changes associated with abnormal bone turnover and mineralization. DXA is a widely available bone imaging technique which measures BMD for the assessment of osteoporosis and fracture risk in the general population. However, its role in predicting ROD subtypes is poor as BMD measured on DXA has been found to be low or normal in all subtypes of ROD {Gerakis et al 2000; Piraino et al 1988}. Bone imaging technique which can measure bone microstructure such as that seen on bone biopsy has been coined as virtual bone biopsy and may have a better accuracy to predict ROD subtypes.

Advances in bone imaging technology and the development of new BTMs present opportunities for less invasive alternatives to bone biopsy but these need further evaluation in CKD. Studies directly comparing these non-invasive tools with bone histomorphometry are rare. Most studies compared novel BTMs with other bone markers or imaging but not directly with bone histomorphometry. Furthermore, most studies examined haemodialysis patients only and excluded peritoneal dialysis and pre-dialysis CKD patients.

1.4.3 Bone Turnover Markers (BTMs)

There are several circulating BTMs which are released directly from bone during bone remodelling and modelling (***Table 1.3***). However, their use in clinical practice is not currently recommended due to limited evidence on their correlation with bone histomorphometry or fracture risk in CKD. Furthermore, some of the bone turnover markers are excreted by the kidneys and thus, may accumulate in advanced CKD. Hence, further research into their diagnostic accuracy in this population is needed.

Bone Resorption Markers

C-terminal and N-terminal telopeptides of type I collagen (CTX and NTX) are released during collagen degradation. Although these are released during degradation of type I collagen from anywhere in the body, the skeleton is by far the biggest site of type I collagen. Thus, measured CTX and NTX reflect bone resorption. These markers accumulate in advanced CKD but a number of studies found that there is a significant negative association between these

markers and BMD in CKD {Hamano et al 2009; Nakashima et al 2005; Okuno et al 2005}. This suggests that high bone turnover ROD is associated with bone loss as reflected by low BMD.

Table 1.3

Bone turnover markers released during bone resorption and bone formation.

Bone Resorption Markers
C-terminal telopeptide of type I collagen (CTX)
N-terminal telopeptide of type I collagen (NTX)
Tartrate-resistant acid phosphatase 5b (TRAP5b)*
Osteoprotegerin§
Bone Formation Markers
Bone alkaline phosphatase (bALP)*
N-terminal procollagen type I peptide (PINP)*
C-terminal procollagen type I peptide (PICP)
Osteocalcin§
Sclerostin

*Symbols: *bone turnover markers which do not accumulate in advanced CKD,§ bone regulatory markers.*

Serum tartrate-resistant acid phosphatase 5b (TRAP5b) could be a better predictor of bone resorption in CKD as it does not accumulate in renal impairment {Yamada et al 2008}. TRAP5b is released by OC during bone matrix degradation and it is also released into the circulation where it is degraded into fragments and then removed by the liver. A study by Lehmann et al using bone biopsy from 96 dialysis patients showed that TRAP5b had moderate predictive value for high bone turnover {Lehmann et al 2008}. However, TRAP5b was unable to predict high bone turnover in pre-dialysis CKD.

Osteoprotegerin (OPG) is an endogenous inhibitor of RANKL and thereby attenuates OC activation and bone resorption {D'Amelio et al 2009}. Although OPG accumulates in CKD and is not removed by haemodialysis, there is evidence from one study in 39 haemodialysis patients showing that it has significant negative correlation with bone turnover on histomorphometry {Coen, Ballanti, et al 2002; Kazama et al 2002}. Assays to measure serum RANKL are available but the stability of this molecule remains inconclusive and reference ranges have not been established {Rogers et al 2005}.

Bone Formation Markers

Bone alkaline phosphatase (bALP) is exclusively produced by bone and is metabolized in the liver. Thus, bALP level is not affected by CKD or dialysis {Sardiwal et al 2012}. BALP shows positive correlation with bone turnover on histomorphometry and when measured simultaneously with PTH, markedly high or low values predict underlying bone turnover {Magnusson et al 2001; Moore et al 2009; Urena et al 1996}. Although bALP is the most reliable BTM studied in advanced CKD so far, its level could fall even though PTH level remains high e.g. with vitamin D supplementation {Palmer et al 2007}. A combination of bALP and markers other than PTH may improve the sensitivity of bALP in predicting bone turnover in patients with SHPT {Takano et al 2011}.

Type I collagen synthesis during bone formation releases N-terminal (PINP) and C-terminal (PICP) peptides into the circulation. ***Figure 1.10*** shows type I procollagen structure and its PINP and PICP domains. Circulating PINP is present in trimeric and monomeric forms; trimeric (intact) PINP does not accumulate in CKD {Ueda et al 2002}. No studies have so far compared these two propeptides of PINP directly with bone histomorphometry but intact PINP has

shown strong correlation with other BTMs {Ueda et al 2002}. A small study found a positive association between PICP and bone turnover on histomorphometry {Eriksen et al 1993}. However, no similar study has been repeated in CKD, probably because PICP is a less stable peptide with a short half-life.

Figure 1.10

Type I procollagen and the domains representing biochemical markers {Marcius M 2006}.

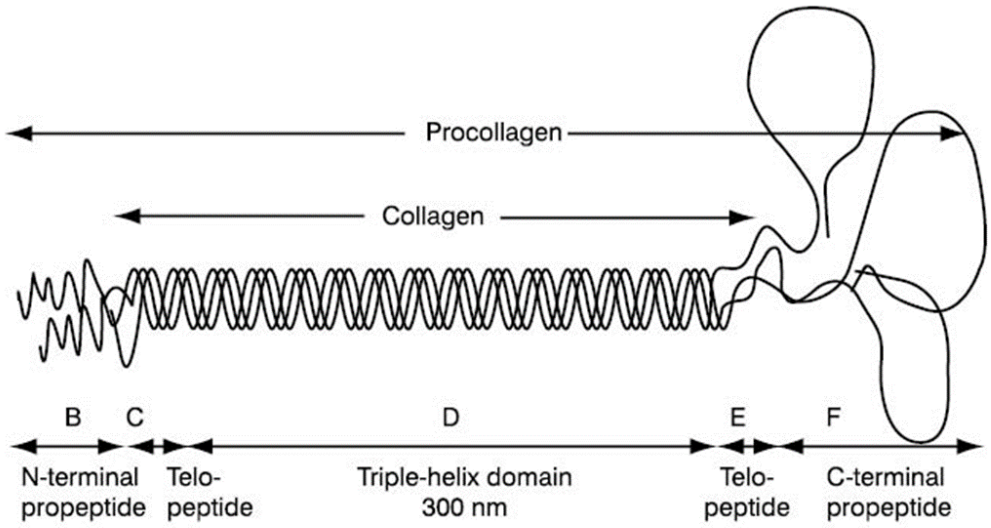

Sclerostin and Dickkopf-1 (Dkk-1) are inhibitors of the Wnt/β-catenin signalling pathway for OB differentiation. A study by Cejka et al which involved 60 dialysis patients found that sclerostin was negatively associated with bone turnover on histomorphometry {Cejka, Herberth, et al 2011}. The same study found that Dkk-1 level was not related to any bone turnover parameters.

Finally, osteocalcin is produced by OB and therefore, a marker of bone formation. However, it also accumulates in advanced CKD {Delmas et al 1983}. Two studies in haemodialysis

patients showed that osteocalcin can predict low bone turnover but bALP which does not accumulate in CKD had better diagnostic accuracy than osteocalcin {Coen et al 1998; Couttenye et al 1996}.

Other Bone-related Markers

High FGF23 has been shown to be associated with poor skeletal mineralisation in conditions such as hereditary or acquired hypophosphatemic rickets and osteomalacia. However, its role to predict abnormal bone mineralization in ROD is unknown. Although FGF23 is produced mainly by osteocytes, some is released by osteoblasts. It is also important to note that FGF23 release is not dependent on bone turnover {Andrukhova et al 2018; Pereira et al 2009; Wesseling-Perry et al 2009}. An animal study showed that FGF23 suppresses alkaline phosphatase in CKD and impairs mineralization {Andrukhova et al 2018}. In contrast, a study involving 32 paediatric and young adults with CKD stages 2-5D showed that bone expression of FGF23 was associated with improved mineralization {Pereira et al 2009}. Therefore, the effect of high circulating FGF23 on the skeleton remains inconclusive.

1.4.4 Bone Imaging

Dual Energy X-ray Absorptiometry (DXA)

ROD is associated with bone microstructural changes. Typically, high bone turnover results in thinner and more porous cortical bone, but it may also result in thickened trabecular bone {Malluche et al 2011; Nickolas et al 2013}. Despite these changes, the change in BMD assessed

by DXA may be very little or absent because DXA is a 2-dimensional imaging technique which cannot discriminate between cortical and trabecular bone. BMD measured on DXA has been found to be low or normal in all subtypes of ROD {Gerakis et al 2000; Piraino et al 1988}. Furthermore, BMD could be overestimated in CKD due to VC. For example, lumbar spine BMD could be overestimated by the presence of abdominal aortic calcification (AAC) which is highly prevalent in advanced CKD {Honkanen et al 2008}. Overall, BMD by DXA is unable to predict ROD subtypes.

The sensitivity and specificity of DXA in predicting ROD on bone histomorphometry may be improved by using specialist software known as trabecular bone score (TBS) which can be derived from DXA lumbar spine scans. This is an index of microarchitecture derived from grey level variations in the DXA image and it correlates with trabecular number and separation {Pothuaud et al 2008}. TBS derived from lumbar spine DXA has never been assessed directly with bone biopsy in CKD and the effect of AAC on TBS is unknown.

Computed Tomography (CT)

Peripheral quantitative computerised tomography (pQCT) is able to discriminate cortical from trabecular bone; and allows accurate calculation of volumetric BMD for each bone compartment. Recently, the development of high-resolution pQCT (HR-pQCT) has enabled an even more powerful analysis of bone microstructure in each bone compartment such as trabecular number and thickness and cortical thickness and porosity. Cross-sectional studies have indicated that HR-pQCT identifies abnormal trabecular microstructure and BMD in CKD and dialysis patients {Bacchetta et al 2010; Cejka, Patsch, et al 2011; Negri et al 2012; Nickolas et al 2010}. Longitudinal and cross-sectional studies using HR-pQCT suggest that there is a

significant reduction in cortical area, density and thickness as well as an increase in cortical porosity in CKD and dialysis patients {Negri et al 2012; Nickolas et al 2013}. These findings are important as suggested by one study involving 74 dialysis patients by Cejka et al {Cejka, Patsch, et al 2011}. The study found that virtually all parameters of bone microstructure were significantly associated with previous fragility fracture whilst there was no significant association between fracture and BMD on DXA. Whilst HR-pQCT may offer a more accurate assessment of bone microstructure in CKD, no studies have assessed direct relationship between imaging abnormalities with underlying bone histomorphometry in ROD.

1.5 Vascular Calcification in CKD

1.5.1 Prevalence and Complications

Vascular calcification (VC) is highly prevalent in CKD with around 50 - 90% of CKD stages 3-5D patients having evidence of VC {KDIGO 2009}. This prevalence is much higher than the general population as demonstrated by Rodrigues-Garcia et al {Rodriguez-Garcia et al 2009}. The study enrolled 193 haemodialysis patients and 624 participants from a random-based general population cohort and showed a significantly higher prevalence of aortic calcification in haemodialysis patients (79% versus 38%).

VC presence in CKD is important as it is associated with increased cardiovascular and all-cause mortality {Z. Chen et al 2016; Lamarche et al 2018; Matsuoka et al 2004; Rodriguez-Garcia et al 2009; Shantouf et al 2010}. Data from United States Renal Data System (USRDS) consistently reported that half of dialysis and kidney transplant patients died from cardiovascular disease {USRDS 2015; USRDS 2018}. The predominant cardiovascular deaths

were due to congestive heart failure and arrhythmia/cardiac arrest rather than deaths due to thromboembolic events.

VC is also associated with fractures which probably compounds increased mortality risk in these patients {Fusaro et al 2013; Rodriguez-Garcia et al 2009}. Rodrigues-Garcia et al found that dialysis patients with VC had 4 - 7 times increased rate of prevalent vertebral fractures compared to those without VC {Rodriguez-Garcia et al 2009}. The study also found that prevalent vertebral fracture was independently associated with mortality after 2 years of follow up, particularly in women with vertebral fracture who had 6 times increased risk of mortality compared to women without vertebral fracture.

1.5.2 Pathogenesis

It is likely that multiple factors result in VC in CKD (***Figure 1.11***). It is thought that the transformation of vascular smooth muscle cells (VSMCs) into osteoblast-like cells allows mineral deposition in the vasculature similar to that in bone formation {Jono et al 2000}. This cellular transformation is partly under the influence of hyperphosphataemia and hypercalcaemia {Reynolds et al 2004}. However, CKD patients could still have severe VC despite persistently normal serum phosphate and calcium levels which suggests that there must be other promoters of VC process. These may include alkaline phosphatase, vitamin D, osteocalcin and bone mineralizing proteins. Inflammation has also been identified as a promoter of VC. VSMCs death may be increased in CKD by factors such as uraemia and calcium-phosphate abnormalities and in turn, this leads to local inflammation that releases cytokines which promotes VC.

There are a number of endogenous VC inhibitors in the circulation which prevents spontaneous calcification of extra-skeletal tissues such as Fetuin A and Matrix Gla protein (MGP) {Ketteler, Wanner, et al 2003}. It is proposed that there is a greater imbalance between VC promoters and these circulating VC inhibitors in CKD. Deficiency of these proteins is common in CKD and has been associated with VC {H. Y. Chen et al 2016; Cranenburg et al 2009; Kanbay et al 2010}.

Vitamin K deficiency is also common in CKD due to low dietary intake and this may play a role in VC {Cranenburg et al 2012}. Vitamin K is a substrate for the Vitamin-K dependent carboxylase enzyme which converts specific glutamic acid residues of a small number of proteins to glutamic carboxyl by the addition of CO_2. Vitamin K2, but not vitamin K1, is responsible for regulating MGP which is a Gla containing protein {Fusaro et al 2011}. In vitamin K2 deficiency, an increase in the level of dephosphorylated-uncarboxylated MGP (dp-uc MGP) which is an inactive VC inhibitor is observed {Cranenburg et al 2012}. Dp-uc MGP has been shown to be associated with VC {Cranenburg et al 2009}. Furthermore, randomised controlled trials in dialysis patients have shown that vitamin K2 therapy leads to a reduction in dp-uc MGP level {Caluwe et al 2014; Westenfeld et al 2012}. Meanwhile, vitamin K antagonist (VKA) such as warfarin is associated with increased VC and high dp-uc MGP level {Fusaro et al 2015; Reynolds et al 2004}. Dp-uc MGP level falls after stopping the VKA {Delanaye et al 2015}.

Figure 1.11

Pathophysiological mechanisms which promote vascular calcification in CKD {Evrard et al 2015}.

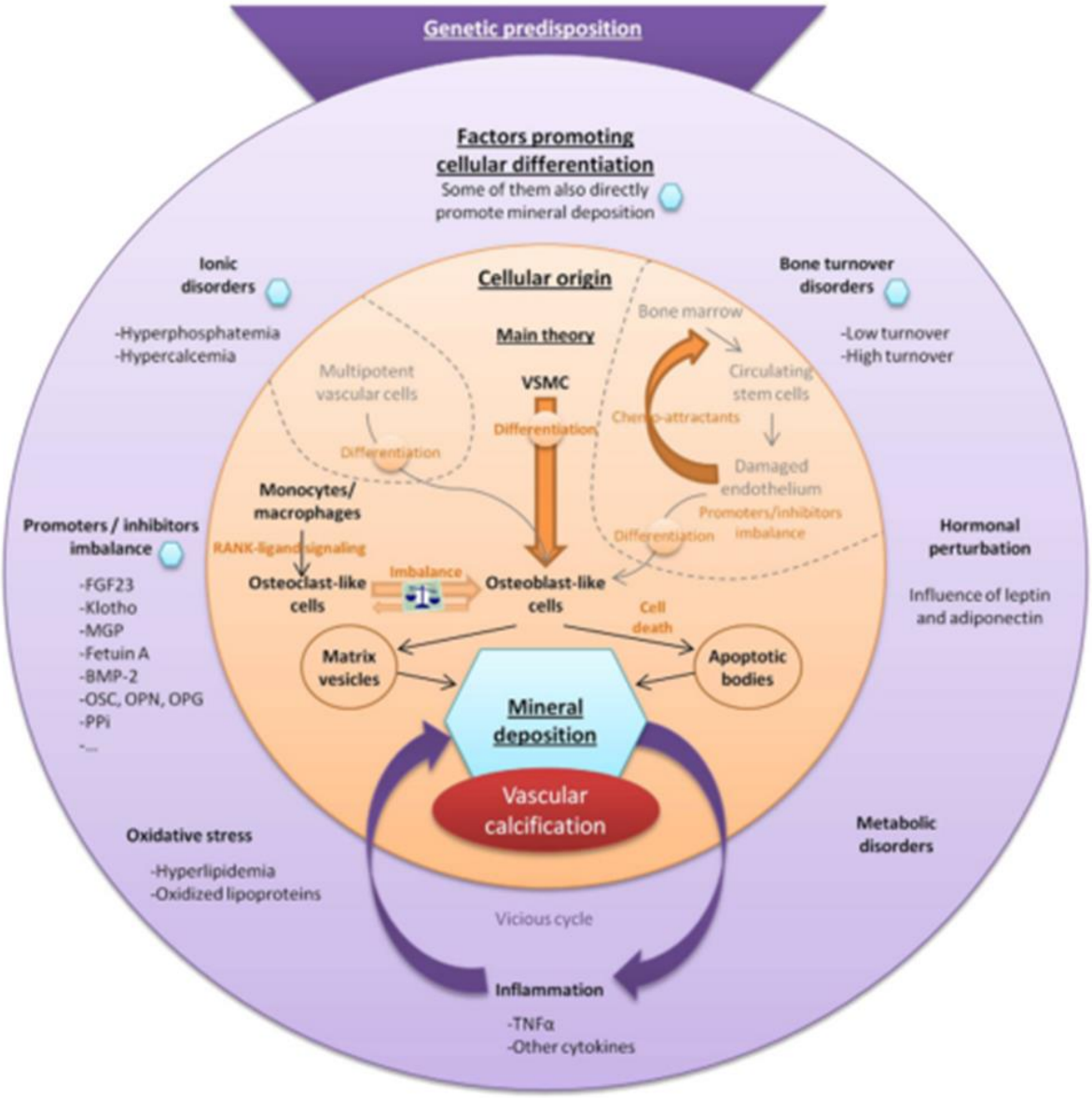

1.5.3 Relationship with Biochemistry and Bone Abnormalities

Hormones which regulate mineral metabolism (i.e. PTH, vitamin D and FGF23) are probably involved in VC process although the relationship is unclear. Furthermore, VC may relate to the treatment used to treat biochemical abnormalities of CKD-MBD. Calcium-based phosphate binders are widely used in managing hyperphosphatemia in advance CKD but there has been serious concerns regarding positive calcium balance and worsening VC {Block et al 2012}. This led to a growing number of studies assessing the impact of calcium-based versus non-calcium based phosphate binders in CKD. A meta-analysis by Jamal et al showed that non-calcium-based binders had a 22% reduction in all-cause mortality in dialysis and pre-dialysis CKD when compared to calcium-based phosphate binders {Jamal et al 2013}. A recent systematic review by Ruospo et al showed that a non-calcium based phosphate binder, i.e. sevelamer, lowers all-cause mortality by 50% in dialysis patients when compared to calcium-based phosphate binders {Ruospo et al 2018}.

There may also be a link between VC and bone abnormalities in CKD. London et al showed that VC is associated with low bone turnover in a study involving 58 dialysis patients {London et al 2004}. VC and bone turnover relationship is further supported by a one-year prospective study in 64 dialysis patients which showed that VC progression may be attenuated if bone turnover change towards normal from a baseline of high or low bone turnover {D. V. Barreto et al 2008}. However, other studies found that VC relates to low bone volume rather than abnormal bone turnover or mineralization {Adragao et al 2009; Barreto et al 2005}. Further studies are needed to confirm the VC and bone relationship as previous studies are limited and mainly involved dialysis patients only.

1.5.4 Treatment

Well established treatment to control SHPT such as phosphate binders and cinacalcet have not been shown to reverse VC although some have shown attenuation of VC progression. Although Ruospo et al systematic review showed a reduction in mortality in dialysis patients using sevelamer compared to those using calcium-based phosphate binders, no effect could be ascertained about the impact of phosphate binders on VC due to limited number of studies reporting on VC outcome {Ruospo et al 2018}.

Cinacalcet is effective in controlling severe SHPT but its benefit on VC is uncertain. ADVANCE Trial which randomised patients into cinacalcet plus low dose vitamin D or vitamin D alone showed that there was no significant difference in coronary artery calcification score between the groups over a one-year period {Raggi et al 2011}. Following that, EVOLVE trial which was a double-blind, placebo-controlled trial randomised 3883 haemodialysis patients with moderate to severe SHPT to cinacalcet or placebo {Wheeler et al 2014}. There was no significant difference in fatal and non-fatal cardiovascular events of any type (atherosclerotic or non-atherosclerotic) between the groups. These findings suggest that VC reversal may not be possible once VC is well established and thus, cardiovascular benefit was not seen. Future studies into treatment of VC may need to focus on early VC prevention in the early stages of CKD and this may also involve simultaneous assessment of ROD. In the first instance, a more sensitive VC imaging test rather than the currently recommended lateral abdominal X-ray is needed as a screening tool for VC in CKD. Ideally, the imaging technique should be able to simultaneously assess VC and bone microstructure but with relatively low dose radiation.

1.6 Summary

CKD-MBD is highly prevalent in CKD and is associated with increased risk of fracture, cardiovascular disease and mortality. CKD-MBD biochemical abnormalities lead to bone abnormalities of ROD but clinical practice so far has focused on correction of SHPT without accurate information on bone turnover and mineralization from bone biopsy. Furthermore, bone-specific treatment to reduce fracture risk could only be initiated after confirmation of ROD subtypes which currently could only be diagnosed on bone biopsy. Routinely available surrogate markers such as PTH, calcium and phosphate, and bone imaging technique such as DXA are unable to predict bone turnover and mineralization abnormalities of ROD. Advances in imaging technology and new bone biomarkers present opportunities for less invasive alternatives to bone biopsy but these need further evaluation in CKD. The use of these tests alone or in combination can only be established by determining their ability to predict bone histomorphometry parameters on bone biopsy.

1.7 Study Aims and Hypothesis

Aim 1:

To evaluate the role of high resolution bone imaging and bone biomarkers as an alternative to bone biopsy to diagnose and classify ROD in advanced CKD.

Objectives:

- To describe bone histomorphometry patterns of advanced CKD
- To describe the bone microstructural changes detected on imaging in advanced CKD
- To describe the level of bone turnover markers (BTMs) in advanced CKD
- To test the diagnostic accuracy of bone imaging and BTMs to identify advanced CKD patients with ROD

Hypothesis 1:

Bone imaging and BTMs are able to diagnose and classify ROD in advanced CKD better than the routinely available iPTH.

Aim 2:

To assess the relationship between vascular calcification (VC) and its biomarkers and bone characteristics in advanced CKD.

Objectives:

- To describe VC severity in advanced CKD
- To describe the relationship between VC and its biomarkers in advanced CKD
- To describe the relationship between VC and bone characteristics detected on imaging and bone biopsy in advanced CKD

Hypothesis 2:

VC is associated with its biomarkers, bone microstructure on imaging and bone biopsy measurements of turnover, mineralization and volume.

Chapter 2. Methodology

2.1 Study Design and Participants

This was a cross-sectional study in patients with CKD stages 4-5D (eGFR < 30ml/min/1.73m^2), aged between 30 and 80 years old who were under the care of nephrologists at the Sheffield Kidney Institute, Sheffield Teaching Hospitals NHS Foundation Trust. CKD patients with earlier stages of CKD are less likely to have ROD and therefore, were excluded from the study. Patients younger than 30 years old were excluded to ensure that only mature adult skeletons were assessed.

The exclusion criteria included patients who had fracture or any orthopaedic surgery in the preceding six months; started or changed the dose of phosphate binders, vitamin D (plain or active metabolites) or calcimimetic within four weeks of study entry; received anti-resorptive agents (such as bisphosphonates or denosumab) or systemic glucocorticoid in the preceding six months; previously received anabolic agent such as teriparatide; and pregnancy or breastfeeding. Additionally, patients with known allergy to tetracycline, demeclocycline or bupivacaine local anaesthetic were excluded because these were required for bone biopsy procedure. Patients on warfarin or ticagrelor were excluded because of potential increased risk of bleeding after bone biopsy. Patients on aspirin, clopidogrel or dipyridamole could be enrolled but the medication was stopped at least 5 days before bone biopsy providing that they did not have coronary angioplasty and stenting in the last 12 months.

We also recruited age and gender-matched control participants with eGFR ≥ 60 ml/min/1.73m². The age match was within +/- 2 years from the age of each CKD patient. The exclusion criteria included fracture or any orthopaedic procedure within 6 months of study entry; known osteoporosis or low impact fracture; have a functioning kidney transplant; started or changed the dose of vitamin D; have received bisphosphonates, denosumab or

systemic glucocorticoid within 6 months of study entry; have previously received teriparatide; and pregnancy or breastfeeding,

We collected medical and demographic data using an approved fracture risk questionnaire (Appendix 1). The study adhered to the *Declaration of Helsinki* and was approved by the South Yorkshire Research Ethics Committee (REC ref: 13/YH/0078). All participants were recruited solely for research and gave written informed consent for the study. CKD patients were re-consented prior to bone biopsy using the Sheffield Teaching Hospitals NHS Foundation Trust approved consent form for medical procedure. Our first participant was recruited in July 2013 and the final participant completed the final study visit in May 2015.

2.2 Bone Biopsy

2.2.1 Bone Biopsy Procedure

Bone biopsy was only performed in CKD patients because the control participants were unlikely to have bone turnover, mineralization or volume abnormalities on bone biopsy. To assess mineralisation and bone turnover, patients received four days of tetracycline (250mg, four times a day) and after a 10-day intermission, a further two days of demeclocycline (300mg, twice a day). Trans-iliac bone biopsy was performed within 2 - 4 days of the last dose of demeclocycline. Each participant was supplied with a schedule clearly indicating the date, type and dose of antibiotic to be taken. The participants marked the doses they had taken on the schedule and this was checked by the operator before the procedure to ensure the doses were taken correctly.

Double tetracycline labelling allowed the identification of two fluorescent labels, circumscribing areas of new bone formed during the labelling intermission, when viewed under fluorescent microscopy. The distance between the two labels determined the mineral apposition rate (MAR). MAR was used to calculate bone formation rate/bone surface (BFR/BS) which was the main assessment of bone turnover status.

Patients on aspirin were advised to stop the aspirin 5 days prior to the procedure. Bone biopsy for haemodialysis patients was performed the day after a dialysis session to reduce the risk of bleeding and haematoma with heparin exposure. Peritoneal dialysis (PD) patients did not have PD fluid dwell when they attended for the procedure. Iliac crest biopsy was obtained with patient lying supine and most biopsies were performed on the right iliac crest as shown in ***Figure 2.1***.

Figure 2.1

Bone biopsy procedure and the Jamshidi bone biopsy trephine and needle used.

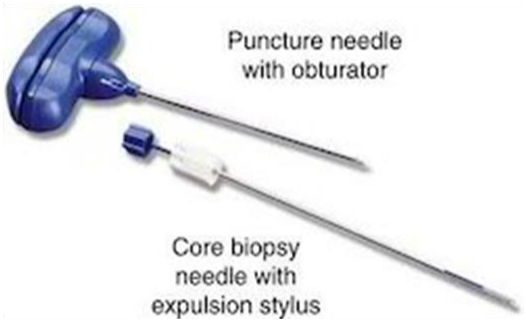

The anterior superior iliac crest was identified and marked. The biopsy entry site was marked 2cm posterior and inferior to the crest. Our modified trans-iliac bone biopsy technique under local anaesthetic (0.5% bupivacaine with adrenaline) used an 8-gauge Jamshidi 4mm trephine and needle. The trephine and needle were inserted together through a small incision in the skin, in an oblique angle pointing towards the opposite shoulder. The needle was removed once it had made firm contact with the bone, leaving the cutting trephine firmly in contact with the periosteum. The trephine was rotated clockwise and counter-clockwise with steady pressure through the full depth of the iliac crest. The sample was extracted from the iliac crest by first rotating the trephine 360° clockwise and then slowly rotating counter-clockwise until the sample was freed. A gauze was immediately applied with firm pressure on the biopsy site. A blue dye was applied gently at the end of the bone sample which was visible at the tip of the trephine to indicate the inner cortical bone. A blunt extractor was then inserted through the top of the trephine to gently push the bone core out. The undecalcified (in its natural state) bone sample was immediately placed in 70% ethanol and shielded from light to preserve fluorescent tetracycline dye within the sample.

2.2.2 Pain Assessment

Pain assessment was performed using the visual analogue scale (VAS). The scale is based on a 100mm horizontal line with a statement at each end for 'no pain' and 'severe pain' (***Figure 2.2***). Patients were asked to score their pain level before the procedure. As soon as procedure was completed, patients were asked to score their pain during the procedure and again 10 minutes later. On Day 2 post-procedure, patients received a phone call from the research nurse to remind them to score their pain level and send back the VAS sheet through the post.

The nurse also checked for any procedure-related complications and advised patients to re-commence aspirin if they were originally on it.

Figure 2.2

Visual Analogue Scale measuring 100mm (not to scale) at four different time points

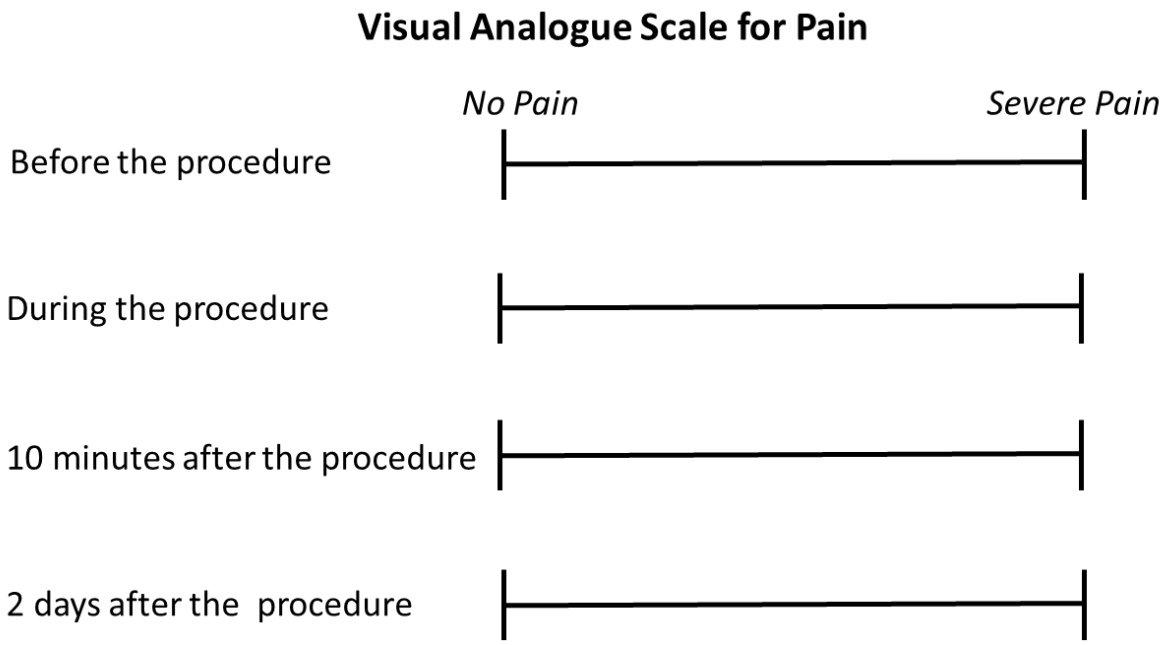

2.2.3 MicroCT

After at least 48 hours immersion in 70% ethanol solution, trabecular bone microarchitecture of the core biopsy sample was assessed using microCT. The core bone sample was removed from the solution and wrapped in cling-film to prevent it from drying out. It was inserted vertically into the scanner in a holder mounted on a brass plinth with the inner cortex, which was marked externally with blue dye, facing the base of the plinth. Using the Skyscan 1172 MicroCT scanner, the entire bone sample was scanned at 4.3 µm resolution with a 360°

rotation. After completion of scanning, the scan images were reconstructed using Skyscan NRecon software and the reconstructed files were analysed using Skyscan CTAn software. A region of interest (ROI) for trabecular bone analysis was created to exclude the cortex and any bone crush artefact around the edges of the biopsy (***Figure 2.3***). The ROI image processing was then performed to assess tissue volume, bone volume, trabecular thickness, trabecular number and trabecular separation.

Figure 2.3

The region of interest selection for bone biopsy microCT trabecular bone analysis.

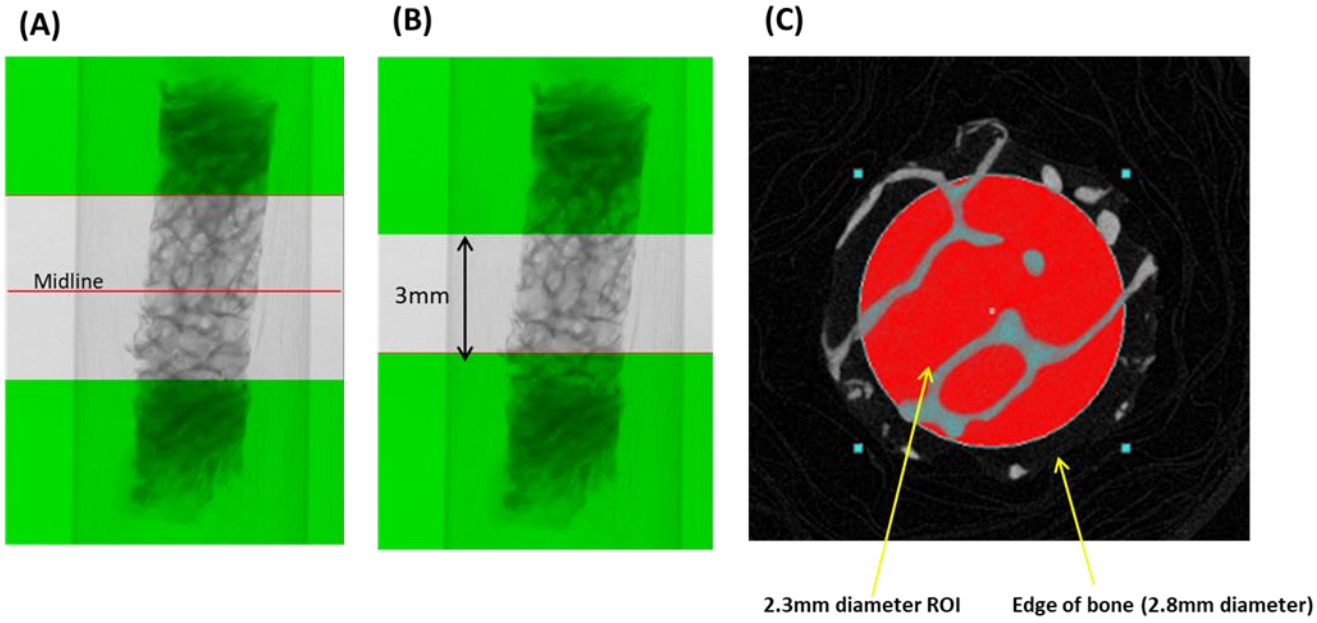

A region of interest (ROI) for microCT analysis was created as follows: (A) The length of the trabecular bone compartment (excluding the cortex) was determined on screen and the midline of the trabecular compartment was calculated; (B) a length of trabecular bone 1.5mm above and 1.5mm below the midline (total length 3mm) was selected for analysis; (C) the ROI for trabecular analysis was drawn using the round ROI tool, and was re-sized to a diameter of 2.3mm to exclude any bone crush artefact around the edges of the biopsy. The ROI was re-drawn if necessary at different levels to check that any edge crush artefact was excluded.

2.2.4 Sample Preparation and Histomorphometry

After microCT, the sample was placed in 80%, 90% and 100% ethanol in turn for at least one week in each solution while remained shielded from light at all time. The sample was then infiltrated and embedded in LR White medium grade resin. The resin block was sectioned at 6 µm thickness using a microtome and for each level sectioned, one sample was prepared for fluorescent microscopy and one sample for light microscopy. Samples were viewed under fluorescent microscopy as shown in ***Figure 2.4*** to identify double tetracycline labelling which appear as two fluorescent labels circumscribing areas of new bone formed. Samples for light microscopy to assess the other histomorphometry quantitative parameters were stained with Masson Goldner trichrome.

The samples were analysed using the Bioquant Osteo histomorphometry system (Bioquant Image Analysis Corporation, Nashville, Tennessee, USA) which uses histomorphometry standardised nomenclature, symbols and units as published by the American Society of Bone Mineral Research (***Table 2.1***) {Parfitt et al 1987}. This unified system of terminology also defines the methodology for each measurement and thus, allows comparison between bone biopsy studies.

Figure 2.4

Bone biopsy histology sections from CKD patients in this study.

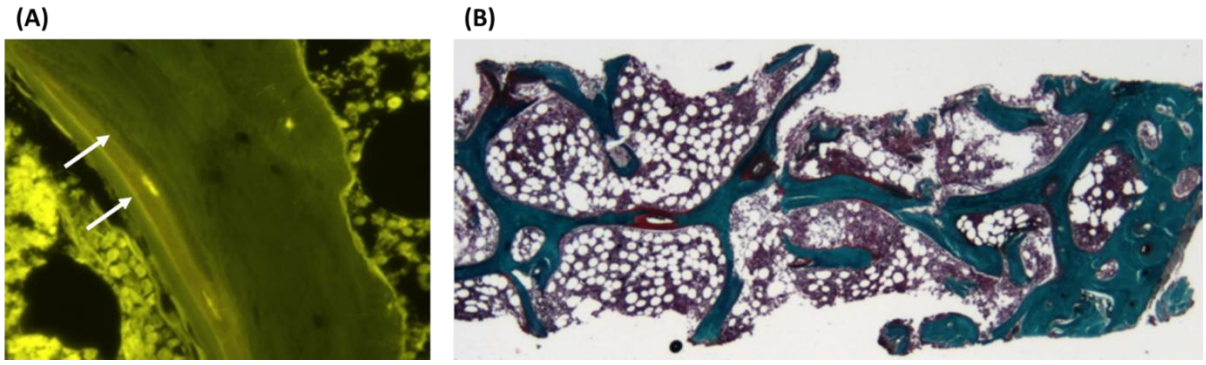

Examples of bone biopsy histology sections: (A) a section viewed under fluorescent microscopy showing double tetracycline labels (white arrows), separated by new bone which was formed during the labelling intermission; (B) a section stained with Masson Goldner trichrome viewed under light microscopy showing thin trabeculae (blue), areas of osteoid (red) and tunnelling resorption in the cortex.

Table 2.1

Dynamic and static nomenclature and units commonly reported on bone histomorphometry. Taken from Recker et al 2012.

Symbols: § the obliquity correction factor (π/4) is applied to convert the thickness expression into 3-dimensional measurement. Abbreviations: iL.Wi, interlabel width; N.iL.Wi, number of interlabel widths measured; dL.Pm, double label perimeter; sL.Pm, single label perimeter; B.Pm, bone perimeter; Ob.Pm, osteoblast perimeter; Oc.Pm, osteoclast perimeter; E.Pm; erosion perimeter; O.Pm, osteoid perimeter; O.Ar, osteoid area; O.Wi, osteoid width; N.O.Wi, number of osteoid widths measured; B.Ar, bone area; Tt.Ar, tissue area measured; BS/TV, bone surface/tissue volume.

Table 2.1

TMV classification	Type	Histomorphometry nomenclature (units)	Definition	Formula
Turnover	Dynamic	BFR/BS (bone formation rate/bone surface, $\mu m^3/\mu m^2$/year)	Rate of bone formation for surface referent	MAR*MS/BS*365
		MAR (mineral apposition rate, µm/day)	The distance between corresponding edges of two consecutive labels over the time between midpoints of labelling period§	(iL.Wi*π)/(d*4)/N.iL.Wi
		MS/BS (mineralizing surface/bone surface, %)	% of bone surface occupied by mineralizing surface	100*(dL.Pm+0.5 sL.Pm)/B.Pm
	Static	Ob.S/BS (osteoblast surface/bone surface, %)	% of bone surface occupied by osteoblasts	100*(Ob.Pm/B.Pm)
		Oc.S/BS (osteoclast surface/bone surface, %)	% of bone surface occupied by osteoclasts	100*(Oc.Pm/B.Pm)
		ES/BS (erosion surface/bone surface, %)	% of bone surface occupied by resorption surface	100*(E.Pm/B.Pm)
Mineralization	Dynamic	MLT (mineralization lag time, days)	Average time lag for osteoid mineralization	(O.Th*OS/BS)/(MAR*MS/BS)
		OMT (osteoid maturation time, days)	Time for mineralization of osteoid forming sites	O.Th/MAR
	Static	O.Th (osteoid thickness, µm)	Average thickness of osteoid seams§	(π*O.Wi)/(4*N.O.Wi)
		OS/BS (osteoid surface/bone surface, %)	% of bone surface occupied by osteoid	100*(O.Pm/B.Pm)
		OV/BV (osteoid volume/bone volume, %)	% of bone tissue occupied by osteoid	100*(O.Ar/B.Ar)
Volume	Static	BV/TV (bone volume/tissue volume, %)	% of marrow space occupied by bone	100*(B.Ar/Tt.Ar)
		Trab Th (trabecular thickness, µm)	Average thickness of trabeculae	(BV/TV)*20/(BS/TV)

The samples in this study fulfilled the histomorphometry minimum acceptable total section area in the standard analysis region of 30 mm^2 {Recker et al 2011}. Quantitative histomorphometry analysis was performed by a single operator to avoid inter-observer variation. Normal bone turnover was defined as bone formation rate/bone surface (BFR/BS) of 18-38 $\mu m^3/\mu m^2$/year {Malluche et al 2011}.

Normal mineralization was defined as osteoid thickness (O.Th) < 20μm and mineralization lag time (MLT) < 100 days {Malluche et al 2011; Parfitt et al 1997}. Other mineralization parameters such as osteoid maturation time (OMT) < 40 days and osteoid volume/bone volume (OV/BV) < 12% were also defined as normal {Lehmann et al 2005; Lima et al 2014}. Normal bone volume was defined as bone volume/tissue volume (BV/TV) 16.8 - 22.9% {Malluche et al 2011}.

2.3 Imaging

2.3.1 Dual-energy X-ray Absorptiometry (DXA)

Principles of DXA

DXA techniques are based on the attenuation of photon energy by bone mineral and soft tissue {NOS 2005; Puumalainen et al 1976}. Photon energy attenuation occurs by photoelectric absorption and Compton scattering as shown in ***Figure 2.5***. In photoelectric absorption, the incident photon energy provides all its energy to an electron and therefore disappears. In Compton scattering, only part of the photon energy is given to an electron and the interaction produces a scattered photon whose direction has changed and whose energy

is reduced. In both situations, photon energy is absorbed by tissue through the electron and it loses kinetic energy in ionising atoms of the tissue.

Figure 2.5

Incident photon energy attenuation by (A) photoelectric absorption and (B) Compton scattering {NOS 2005}.

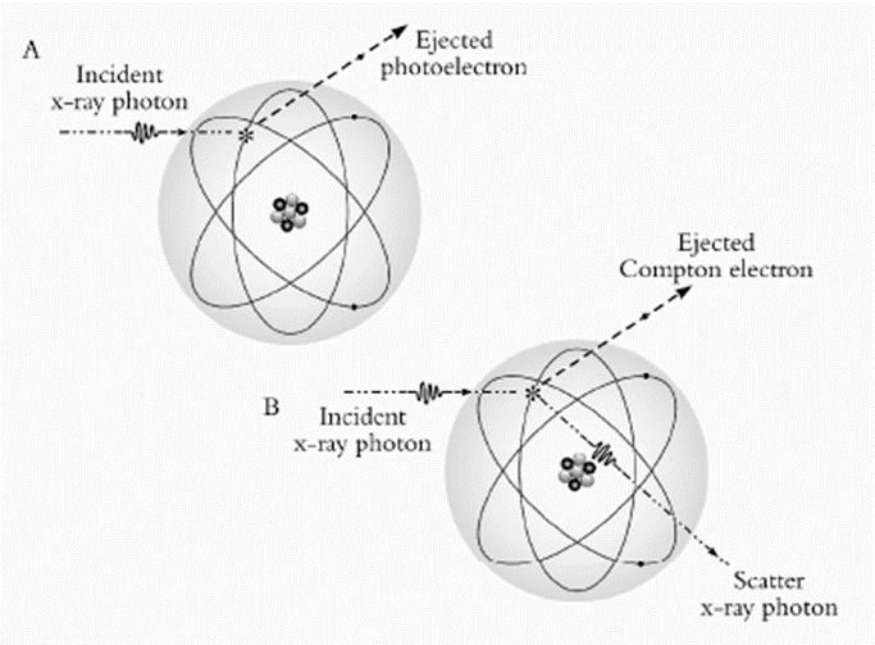

The transmitted intensity of an incident beam depends on the photon energy of the incident beam and the composition, density and thickness of the material it passes through. This is described by an exponential law:

$I_r = I_i \exp(-vx)$

where I_r is the transmitted intensity, I_i is the incident intensity, v is a property of the tissue known as the linear attenuation coefficient and x is the thickness of the tissue. The mass attenuation coefficient of different tissue materials is shown in ***Figure 2.6***.

Figure 2.6

Variation of mass attenuation coefficients with photon energy {Allen 2014}.

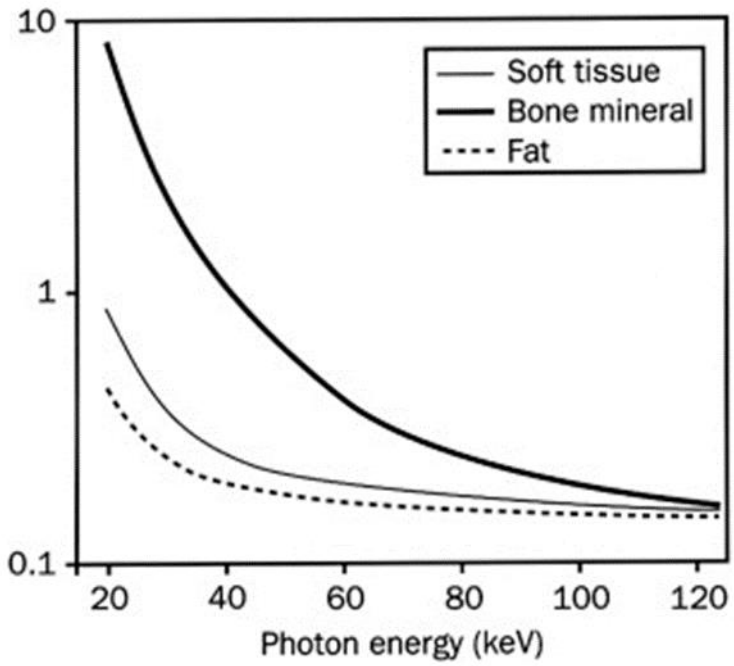

Soft tissue includes muscle, fat, blood and skin which have similar attenuation as they have similar density and mainly composed of carbon, hydrogen and oxygen. Bone mineral have greater attenuation because it has a higher density and includes higher atomic number elements such as calcium and phosphate. Bone mineral (calcium hydroxyapatite) is also distinct from other bone tissue such as collagen and bone marrow.

During DXA scanning, a bone profile is generated in pixel map as the source (which emits X-ray radiation) and detector (which detects X-ray that have not been absorbed) move linearly across the scanned area (***Figure 2.7***). An edge detection algorithm is used to identify the bone edges. The bone density is determined for each pixel of the area being scanned. Areal BMD (g/cm^2) is the mean bone density of these pixels.

Figure 2.7

Bone profile observed as the X-ray moves linearly across the patient, and the corresponding tissue density profiles {Crabtree 2007}.

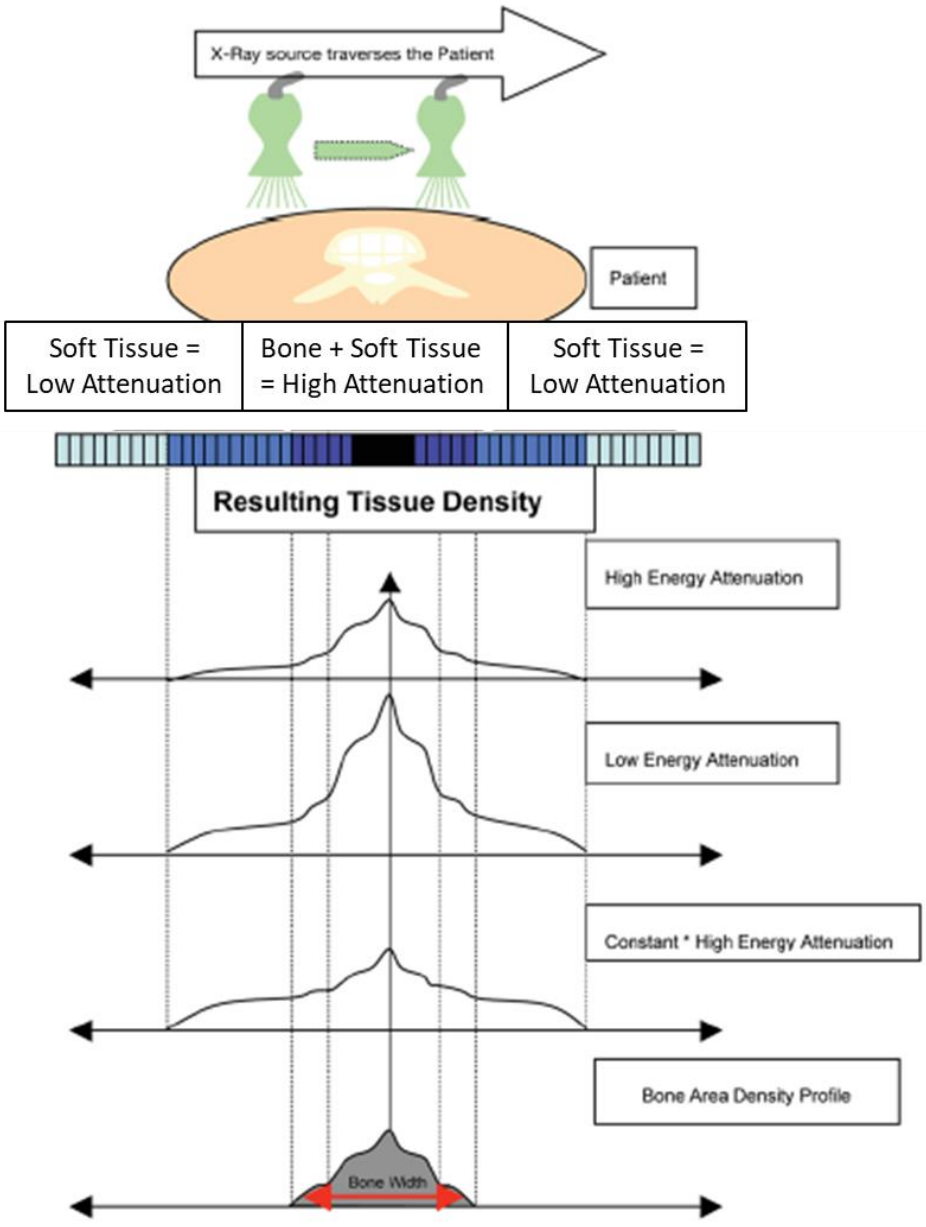

Measurement technique

DXA scan in this study was performed using Hologic Discovery A densitometer (Hologic Inc, Bedford MA, USA) in the array (fan beam) mode. We measured areal BMD for the hip, lumbar spine and forearm which are the usual fracture sites.

Hip

Hip scan was performed on the non-dominant side unless there was a previous fracture or orthopaedic surgery. The patient was laid supine and a positioner was used to hold the hip internally rotated by 25°. The radiation dose was 5µSv.

Figure 2.8

A positioner used during proximal femur DXA scanning

Lumbar Spine

The patient was positioned supine with their legs elevated over a block to reduce lumbar lordosis as shown in ***Figure 2.9***. Their arms were raised above their head to keep clear of the lateral scanning field. The patient's lumbar spine was scanned in the antero-posterior (A-P)

and lateral projections. The lateral projection was used for Vertebral Fracture Assessment and abdominal aortic calcification score. The radiation dose was 2µSv.

Figure 2.9

Positioning of patient for A-P (left image) and lateral (right image) lumbar spine DXA scan.

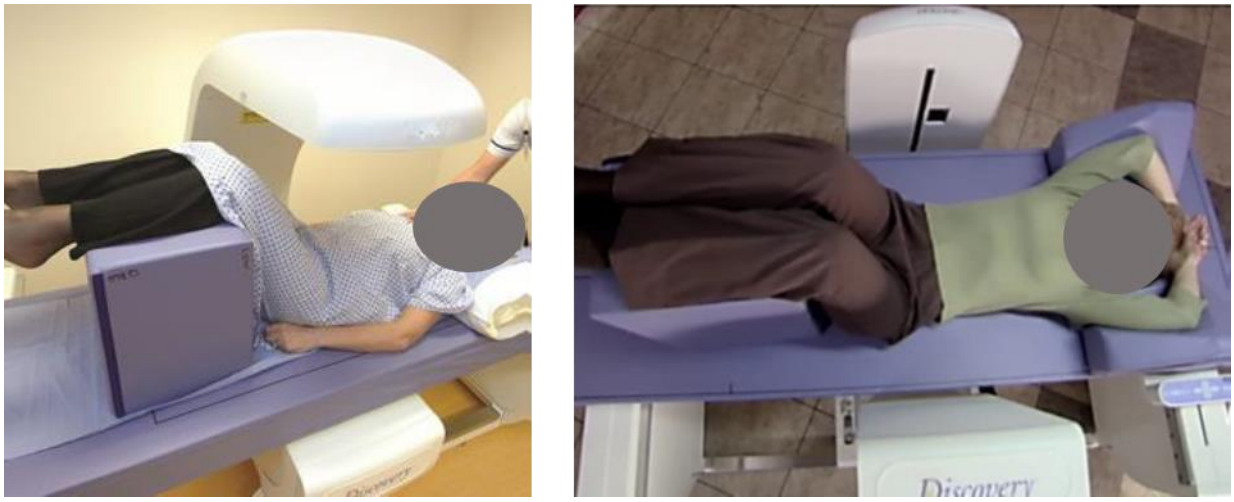

Forearm

Forearm scan was performed on the non-dominant side unless there had been a previous fracture or an arterio-venous (A-V) fistula present in which case the opposite side was scanned. This is because the presence of an A-V fistula has been associated with lower BMD compared to the non-fistula side {Muxi et al 2009}.The patient was seated on the opposite side from the C-arm of the scanner with their side against the table and the arm resting on the table top. An arm support with straps kept the arm in a secure position (***Figure 2.10***). The radiation dose was 2µSv. One CKD patient did not have a forearm scan due to previous bilateral wrist fractures.

Figure 2.10

Forearm positioning during DXA scanning

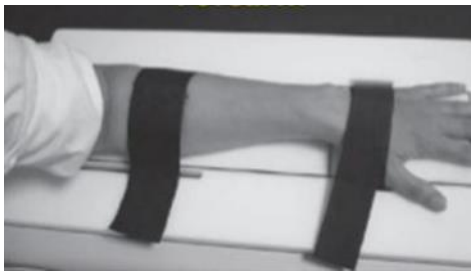

Image Analysis

The hip scan image was checked for proper patient positioning. With internal rotation, the lesser trochanter should be small but visible. The region of interest (ROI) for the hip was a rectangle placed with its superior border 5 lines above the head of the femur, its inferior border 10 lines below the lesser trochanter, its medial border 5 lines from the medial side of the head of the femur and its lateral border 5 lines from the lateral edge of the greater trochanter (***Figure 2.11***). The total hip was indicated by the outer outline of the bone margins. The midline was placed along the central axis of the hip. The neck of femur box was placed close to (but not touching) the greater trochanter. The trochanteric line was placed inferior to the maximum curve of the greater trochanter. The Ward's area was placed automatically by the software.

Figure 2.11

The region of interest on hip DXA image.

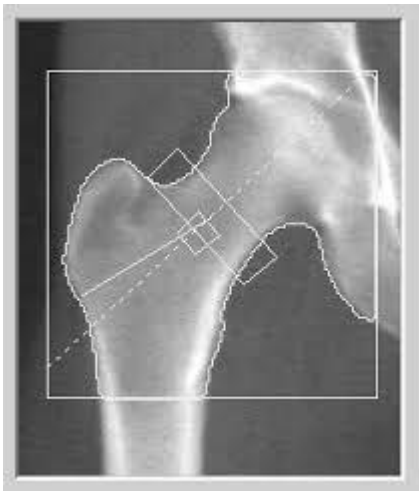

Lumbar spine scans were checked for vertebral fracture and other causes leading to falsely high BMD such as degenerative changes and osteophytes. The ROI for the AP lumbar spine image was placed from the T12/L1 intervertebral space to the L4/L5 intervertebral space (***Figure 2.12***). The vertebral lines were placed in the remaining intervertebral spaces in between. The decision to exclude vertebrae from further analysis was done in accordance to the recommendations by the National Osteoporosis Society 2011. A clearly abnormal vertebrae such as fracture were excluded. A T-score difference of more than 1 standard deviation between adjacent vertebrae was also indicative of BMD result that was likely to be inaccurate. A minimum of two evaluable vertebrae was required for analysis. One CKD patient lumbar spine scan in this study was excluded due to multiple vertebral fractures.

Figure 2.12

Region of interest on lumbar spine DXA image.

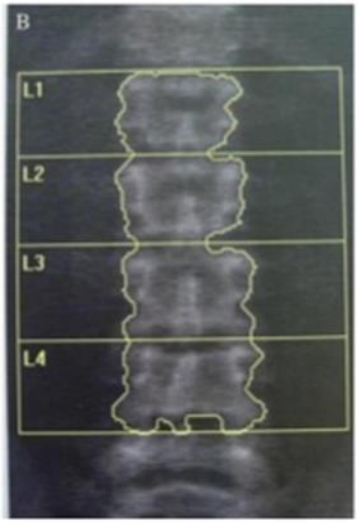

For the forearm ROI, the reference line was placed at the distal tip of the ulna styloid process as shown in ***Figure 2.13***. The forearm ROI was divided into three regions called ultradistal (UD), middistal (MID) and 1/3 radius. The UD ROI did not contain the radial endplate and measured 15 mm in length proximal to the radial endplate. 1/3 radius ROI was 20 mm in length centred at a distance equal to 1/3 of the forearm length measured from the distal tip of the ulna. The MID ROI was between UD and 1/3 radius ROIs.

Figure 2.13

The region of interest on the forearm DXA scan image

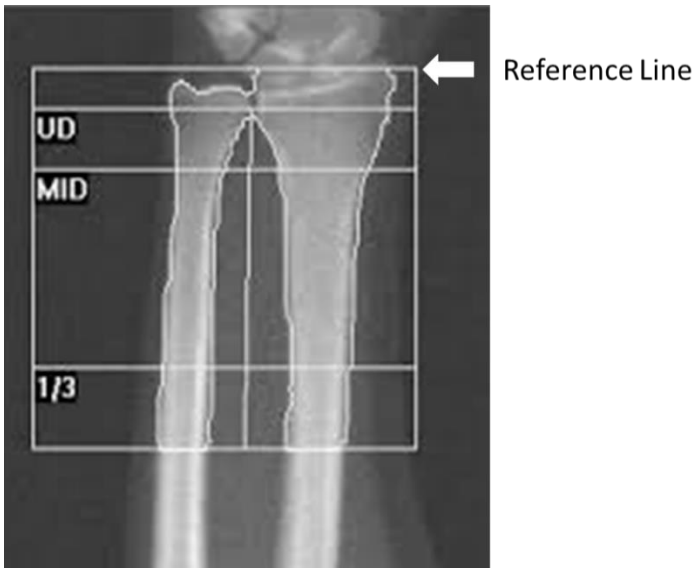

Mean areal BMD (g/cm^2) for lumbar spine (L1-4), total hip and 1/3 radius were calculated using Hologic APEX software (version 3.4.2). BMD T-score is the number of standard deviations (SD) above or below the average BMD value for healthy young gender-matched adults. BMD T-score was calculated by the software using the formula:

BMD T-score = (observed BMD – young normal BMD) / (SD of young normal BMD)

The young normal (peak) BMD reference data for lumbar spine and forearm is gender specific and was provided by the manufacturer. The young normal BMD reference data for the hip was taken from the Third National Health and Nutrition Examination Survey (NHANES III) database for women/men aged 30 years old. This is in accordance with recommendations by the International Committee for Standards in Bone Measurement.

BMD Z-score is the number of standard deviations above or below the average BMD value for age and gender-matched healthy adults. The age and gender-matched BMD reference data for all three sites was provided by the manufacturer. BMD Z-score was calculated by the manufacturer software using the formula:

BMD Z-score = (observed BMD – age and gender-matched BMD) / (SD of age and gender-matched BMD)

Quality Control

A device-specific anthropomorphic spine phantom is scanned daily for quality control (***Figure 2.14***). A weekly scan of European Spine Phantom (Quality Assurance in Radiology and Medicine, Moehrendorf, Germany) is also performed. *In vivo* precision for DXA BMD in our centre is 1.6% for lumbar spine, 1.5% for total hip, 2.9% for femoral neck, 1.7% for 1/3 radius and 1.5% for total radius and ulna.

Figure 2.14

Quality assurance plots for Hologic Discovery A densitometer during the study period (July 2013 – May 2015). Area (**i**), BMC (**ii**), BMD (**iii**).

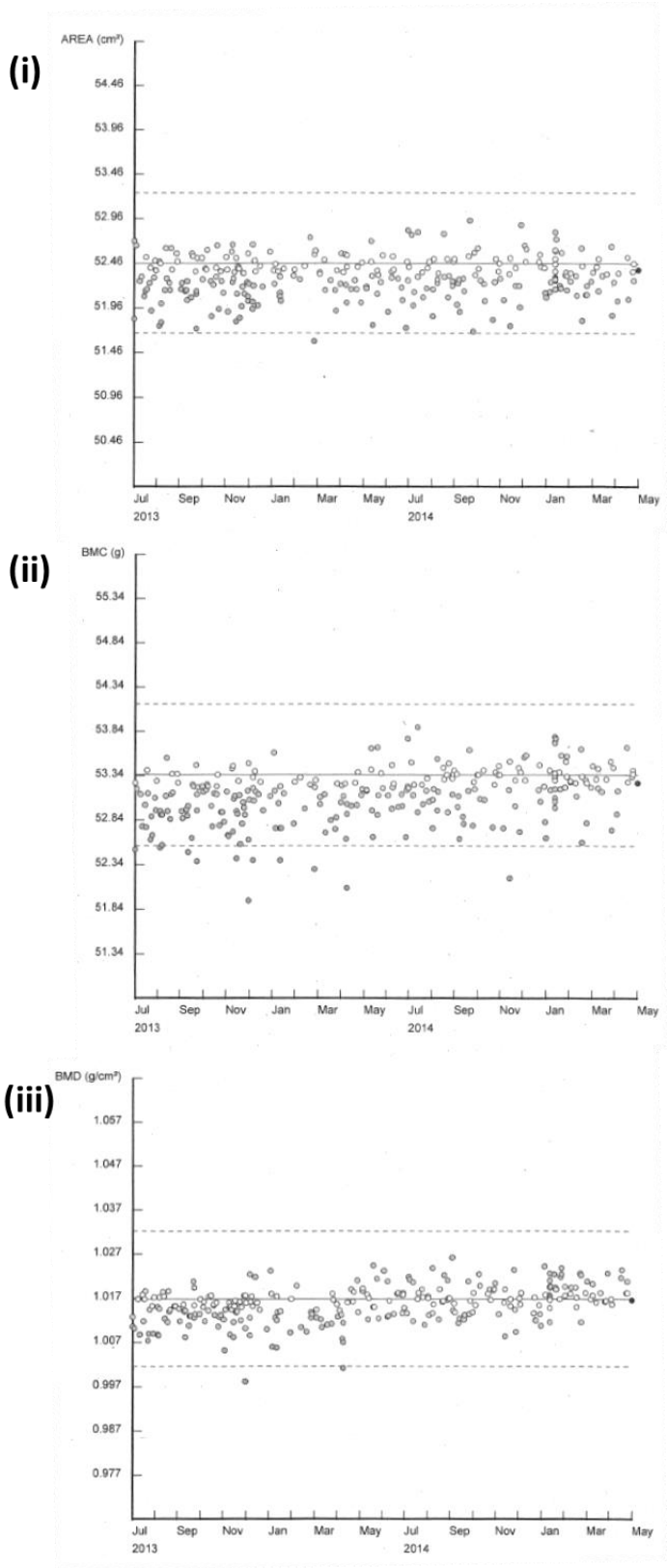

2.3.2 High Resolution Peripheral Quantitative Computed Tomography (HR-pQCT)

Principles of HR-pQCT

Quantitative computed tomography (QCT) uses the same principles as DXA where the attenuation of X-ray beam is used to calculate the density of tissue that it passes through. It uses a standard X-ray computed tomography (CT) scanner with a calibration standard to convert Hounsfield Units of the CT image to bone mineral density. QCT has the advantage of measuring the tissue density of known thickness to give a three-dimensional information and to allow a true measurement of volumetric BMD (mg/cm^3). It also allows the differentiation of cortical from trabecular bone which may be advantageous for assessing bone changes associated with ROD.

High resolution peripheral QCT (HR-pQCT) has a much higher resolution (82 µm) than QCT (1-2 mm) but with a smaller field of view. It is only used at peripheral skeletal sites such as wrist (for distal radius) and ankle (for distal tibia). Scanning takes 3 minutes for each site and the effective radiation dose during each scan is 3 µSV. Spine or hip QCT would involve a higher effective dose of radiation (200 – 400 µSV).

Measurement Technique

The distal radius and tibia were scanned using HR-pQCT (XtremeCT, Scanco Medical AG, Zurich, Switzerland) using a standard protocol. Scans were performed on the non-dominant forearm and lower leg unless there had been a previous fracture or an arterio-venous (A-V) fistula present in which case the opposite side was scanned. The forearm or lower leg was positioned horizontally in the scan gantry, immobilised in a carbon cast.

A scout view scan was initially performed to identify anatomical landmarks and to define a 9.02 mm ROI (***Figure 2.16***). A reference line was manually placed on the notch of the articular surface of the distal radius and on the endplate of the distal tibia. The first image slice was scanned 9.5 mm proximal to the radius reference line and 22.5 mm proximal to the tibia reference line.

HR-pQCT scans were acquired in the high-resolution mode (image matrix = 1,536 x 1,536) using a source potential of 60 kVp, a tube current of 900 mA, and an integration time of 100 ms. Each scan resulted in the acquisition of a total of 110 image slices (stack height = 9.02 mm) at an isotropic resolution of 82 µm. A maximum of one repeat scan at either or both anatomical sites was performed in the event of patient movement.

Figure 2.15

A volunteer undergoing a radius scan on HR-pQCT.

Figure 2.16

A scout view scan for radius (left image) and tibia (right image).

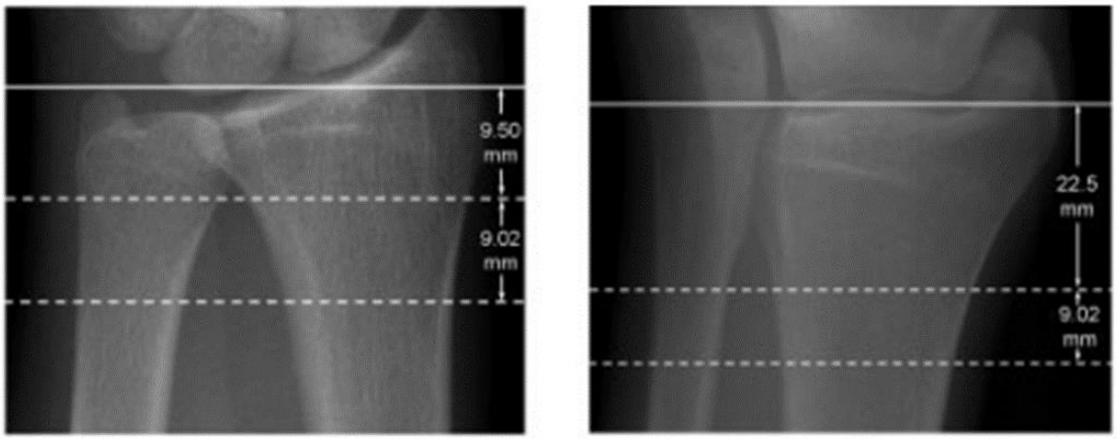

Image Analysis

All images were graded by a single operator. Images were visually graded using a grading scheme described by Engelke et al (***Figure 2.17***); grade 1 (perfect), grade 2 (slight movement), grade 3 (moderate movement) and grade 4 (significant movement) {Engelke et al 2012}. Any images with an unacceptable degree of movement artefact (grade 4) were excluded from further analysis. We excluded images of 9 radii from controls, 11 radii from CKD, one tibia from control and two tibiae from CKD due to movement artefact. One CKD patient did not have radius HR-pQCT performed due to previous bilateral wrist fractures.

HR-pQCT images were analysed using the manufacturer standard software (Scanco Medical AG, version 6.0). The two-dimensional image stack was reconstructed into three-dimensional image which then underwent a validated auto-segmentation method to separate cortical from trabecular bone (***Figure 2.18***).

Figure 2.17

HR-pQCT scan images of the radius and images grading scheme {Paggiosi et al 2014}.

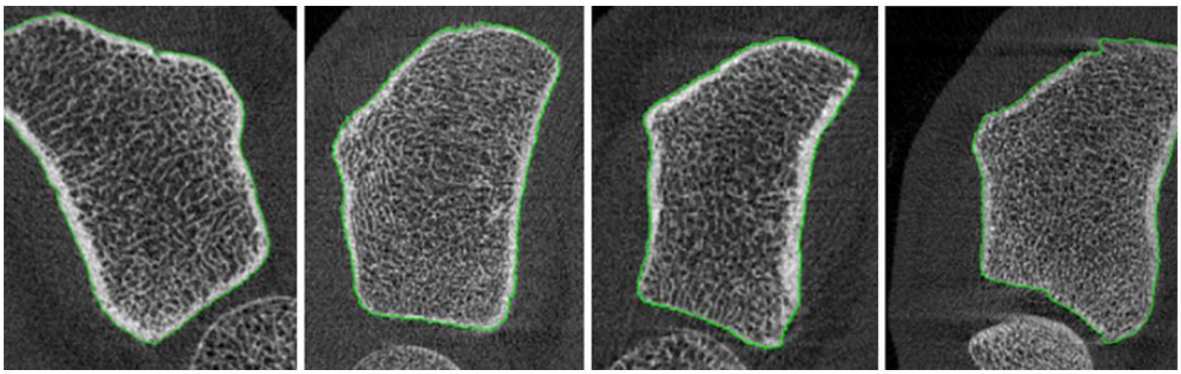

From left to right: GI = perfect, G2 = slight movement, G3 = moderate movement, and G4 = significant movement (unacceptable image quality).

Figure 2.18

Segmentation of cortical bone from trabecular bone of the radius (left) and tibia (right) {Nickolas et al 2010}.

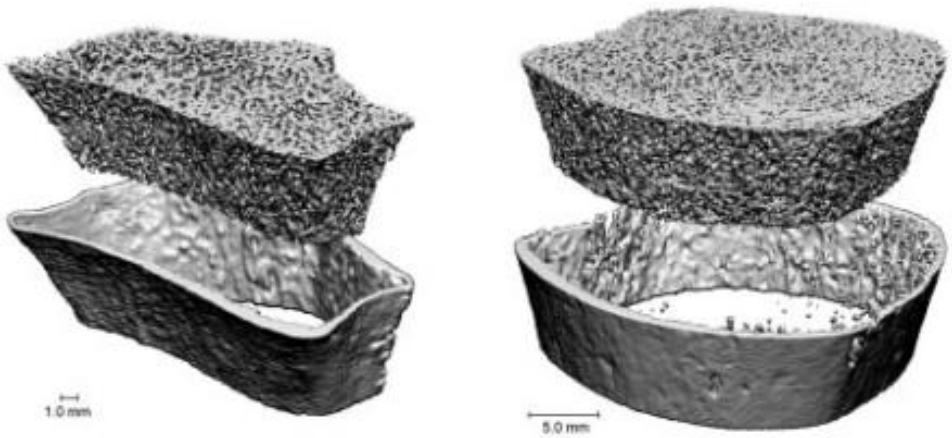

Volumetric bone mineral density (vBMD, mg/cm^3) were calculated as the average of bone densities for the total bone, trabecular bone and cortical bone. Most of trabecular bone microstructural measurements were derived rather than directly measured from the images because HR-pQCT resolution is relatively close to the size of individual trabeculae. The bone volume fraction (BV/TV, %) was determined from trabecular vBMD assuming that the density of fully mineralized bone is 1200mg HA/cm^3. BV/TV was calculated using the formula:

BV/TV (%) = (vBMD/1200) x 100

The average number of trabeculae (Tb.N, 1/mm) was directly measured from the images. Average trabecular thickness and separation were calculated using the formulae:

Trabecular thickness (Tb.Th, mm) = (BV/TV)/Tb.N

Trabecular separation (Tb.Sp, mm) = (1 - BV/TV)/Tb.N

Cortical thickness (Ct.Th, mm) was directly measured from the images following segmentation of cortical bone from trabecular bone. Cortical BV/TV (%) was calculated using the same formula as for trabecular BV/TV. The extended cortical measurement was performed for cortical porosity. The cortical bone image was binarized and cortical porosity was calculated as the percentage of void voxels from the total cortical voxels {Burghardt et al 2010}.

Quality Control

A device-specific phantom was scanned daily for quality control. Our centre *in vivo* precisions of HR-pQCT were reported to be 0.2 - 5.5% for bone density, 1.2 - 7.0% for microstructural

and 3.4 - 20.3% for extended cortical bone measurements at both the radius and tibia {Paggiosi et al 2014}.

Quality assurance was performed by the scanning operator to ensure that the vBMD matches the known vBMD measurements on the phantom (i.e. 0, 100, 200, 400 and 800 mgHA/cm^3) (***Figure 2.19***). The microstructure phantom was also used to ensure the spatial resolution was within the range specified for the phantom.

Figure 2.19

Device-specific HR-pQCT phantoms to test vBMD (left) and spatial resolution (right).

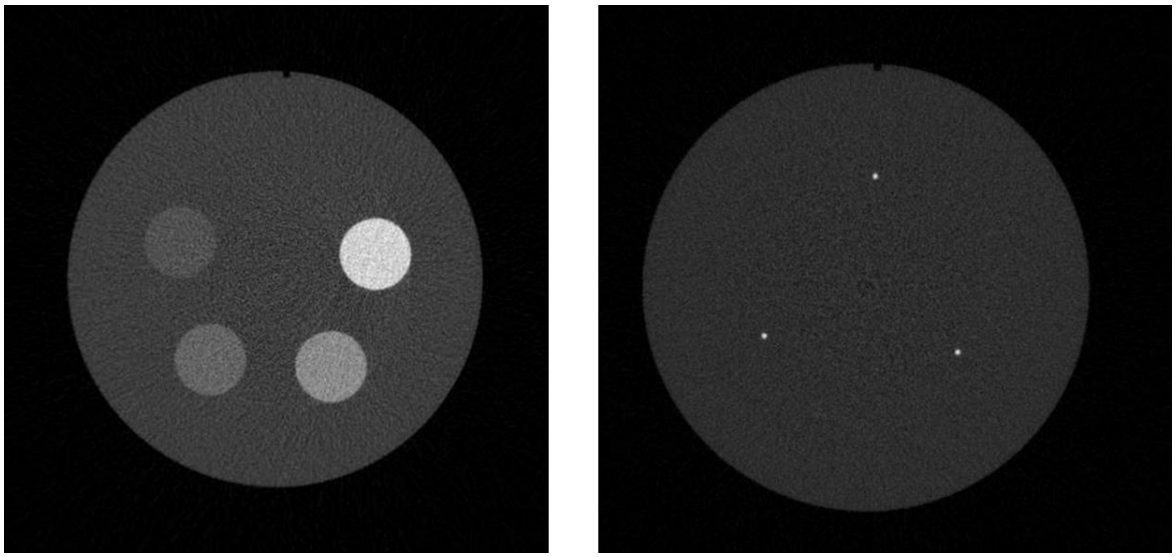

2.3.3 Vascular Calcification Imaging

Abdominal Aortic Calcification (AAC)

AAC was assessed from lateral spine Vertebral Fracture Assessment (VFA) images acquired using DXA. VFA uses single-energy images of the thoraco-lumbar spine in the lateral supine

position. The VFA images were scored by a single experienced operator using an 8-point scale (AAC-8) as shown in **Figure 2.20**. The AAC-8 scale estimates the total length of calcification on the anterior and posterior walls of the abdominal aorta in front of vertebrae L1 to L4 as described by Kaupilla et al {Kauppila et al 1997}. The semi-quantitative scoring system is as follows: 0, no calcification seen; 1, if the total length of calcification is equal to the height of 1 vertebra or less; 2, if the total length of calcification is >1 vertebra but ≤ the height of 2 vertebrae; 3, if the total length of calcification is >2 vertebrae but ≤ the height of 3 vertebrae; and finally 4, if the total length of calcification is >3 vertebrae. Each anterior and posterior walls were scored from 0 to 4, thus the total score ranged from 0 to 8.

There are three different scoring systems described by Kaupilla et al; AAC-24, AAC-8 and AAC-4 scores. There were no significant differences between the scoring systems when they were used to measure AAC severity in 617 men and women at baseline and follow up 25 years later {Kauppila et al 1997}. AAC-8 scoring method on the VFA has high diagnostic accuracy for detecting AAC when compared with the standard lateral abdominal radiograph {Schousboe et al 2007}. A total of 5 VFA images could not be assessed for AAC due to increased body size and the resulting poor VFA images.

Figure 2.20

AAC scoring systems using lateral lumbar X-ray {Kauppila et al 1997}.

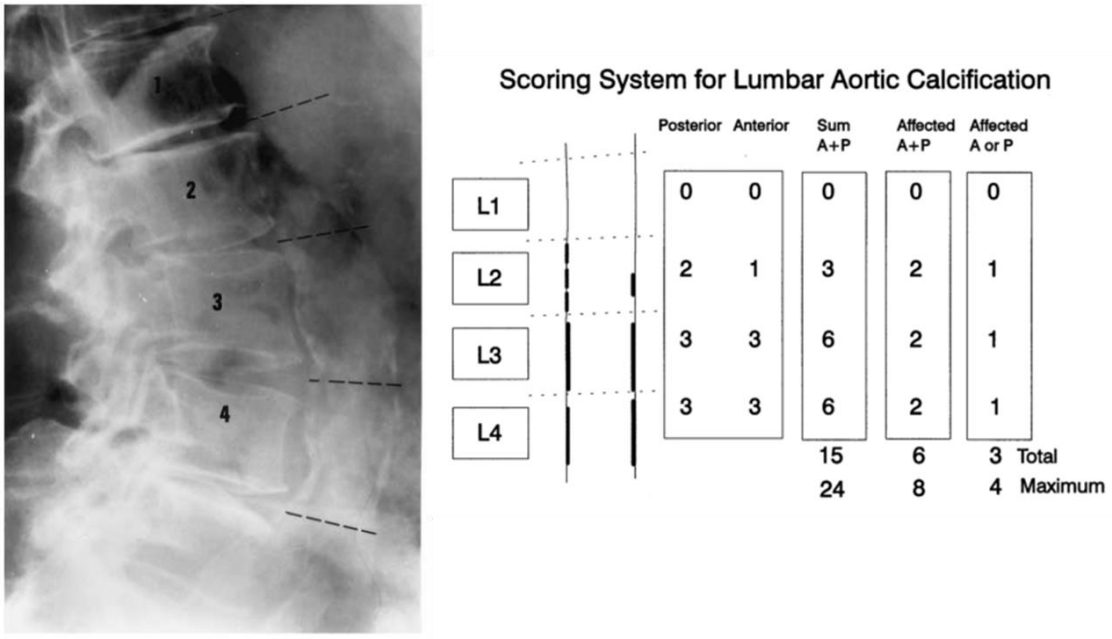

Ankle Arteries Calcification

Ankle vascular calcification (VC) was assessed from HR-pQCT images of distal tibia as shown in ***Figure 2.21***. All images were graded by a single experienced operator, and any images with unacceptable degree of movement artefact (motion grade 4) were excluded from further analysis. A semi-automated software (version 6.5) determined the presence or absence of arterial calcification in the areas corresponding to the anatomical position of anterior tibial artery, posterior tibial artery, interosseous branches or smaller intramuscular or subcutaneous arterioles {Patsch et al 2014}.

Figure 2.21

A cross-sectional axial image from distal tibia HR-pQCT which also shows vascular calcification in the ankle arteries.

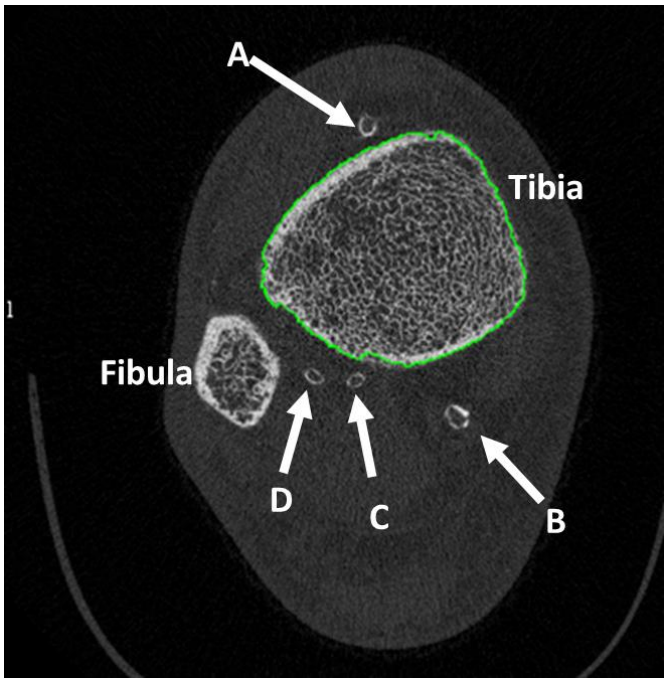

This image shows circular hyperdensity shapes corresponding to anatomical territory of arteries in the ankle. Symbols: A, anterior tibial artery; B, posterior tibial artery; C, perforating branch of peroneal artery; D, peroneal artery.

Arterial calcifications were defined as tubular hyperdensity structure of circular, semi-circular, or crescent-like shape. Bones corresponding to tibia and fibula, cutaneous calcifications (which usually appear as a hyperdense spot rather than tubular shape) and other non-vascular soft tissue calcifications were excluded from the ROI (***Figure 2.22***). Each image slice was then checked by the operator to ensure that the ROI included the calcified arteries only. The operator may still have to do minor manual adjustment of the vascular contour if there was enlargement due to bone movement artefact, or presence of adjacent cutaneous or soft

tissue calcification. The calcification mass for the length of the scan image (9.02 mm) was calculated using the formula:

VC mass (mgHA) = [total volume of vascular calcification (mm^3) x mean calcification density ($mgHA/cm^3$)]/1000

Scans with absent vascular calcification were recorded as zero mgHA. Typical post-scan processing time for ankle VC assessment per participant was 10-20 minutes. A total of three HR-pQCT scans could not be assessed for ankle VC due to movement artefact.

Figure 2.22

Non-vascular, high-density regions that should be excluded from quantitative analysis of vascular calcifications {Patsch et al 2014}.

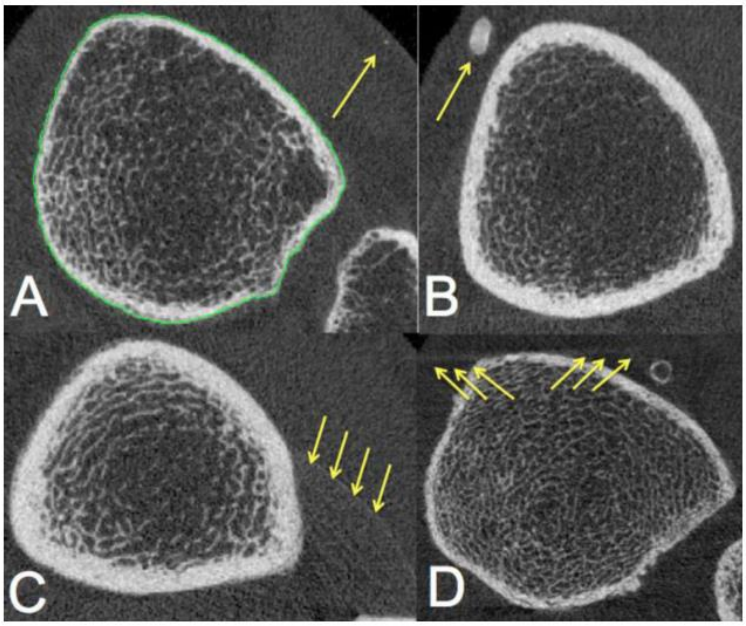

Examples of findings that can mimic arterial calcifications are shown above and highlighted with arrows A) intra-cutaneous spotted calcifications, B) non-vascular, most likely post-traumatic soft tissue calcification, C) focal pixel artefact, D) skeletal motion artefacts.

2.4 Biochemistry

Fasting blood samples were collected once between 7 and 10 am after an overnight fast from 10pm the night before. For haemodialysis patients, fasting blood samples were taken on the day after their routine haemodialysis session. Peritoneal dialysis (PD) is a continuous renal replacement therapy, thus no specific day was required for fasting blood sample collection from PD patients.

Blood samples were collected in SST II tubes (for serum sample) and K3-EDTA tubes (for plasma sample). One SST II sample tube was sent to the biochemistry laboratory at the Northern General Hospital soon after collection for creatinine, calcium, phosphate and total alkaline phosphatase analysis. The rest of the samples were left to clot for 30 minutes and then centrifuged for 10 minutes at 3000 rpm and 4°C temperature. Serum and plasma samples were then divided into 1 ml aliquots and stored at -80^{0}C until the end of the study. Biochemical analyses for bone turnover markers and vascular calcification biomarkers were performed at the Bone Biochemistry Laboratory, Mellanby Centre for Bone Research, the University of Sheffield. The samples were assayed in duplicates when using manual assays.

2.4.1 Principles of Immunoassays

Most biomarker concentrations in this study were measured using immunoassays. Immunoassay has a monoclonal antibody which binds to its antigen at a specific site of the analyte molecule. The antibody has a high affinity for the antigen and thus provides a specific and accurate test. The quantity of the antibody-bound antigen can be measured using labelled antigen or labelled antibody. The label may have an enzyme (e.g. enzyme

immunoassay [EIA] or enzyme-linked immunosorbent assay [ELISA]) or a radioisotope which is known as radioimmunoassay (RIA). Most of the assays are sandwich assays where antigen in the sample is bound to the antibody site and then a labelled antibody is bound to the antigen (***Figure 2.23***). The amount of labelled antibody is then measured which is directly proportional to the concentration of antigen (analyte).

Figure 2.23

Principles of sandwich immunoassay. Taken from http://www.novateinbio.com/3-elisa-kits.

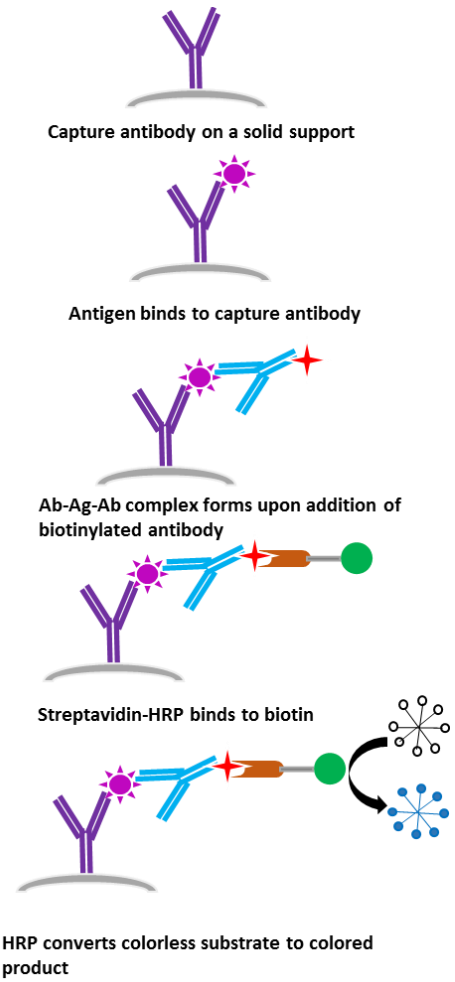

Abbreviations: Ab, antibody; Ag, antigen; HRP, horseradish peroxidase.

Enzyme Immunoassay (EIA) or Enzyme-linked Immunosorbent Assay (ELISA)

ELISA is a widely used EIA and uses the same principal methods as EIA. ELISA method used in this study was a plate-based assay technique using commercially available kits. Some kits had pre-coated plates, otherwise the method began with a careful coating step and incubation with capture antibody which was adsorbed onto a 96-well polystyrene wells. The plate then underwent a series of washes using manufacturer-provided washer solution to remove any excess unbound antibody. Then a substrate (participant sample) was added for further incubation. The capture antibody was specific for the antigen of interest (analyte) and had a high affinity for the antigen. Thus, the antigen was immobilized on the plate surface. The non-bound molecules could then be washed away with a series of washes. Then a detection antibody was added which bound to the target antigen already immobilized on the plate. Finally, a chromogenic substrate which fluoresce when light was shone upon it was added to allow measurement of the amount of antigen present. This was measured using spectrophotometer and is known as absorbance. The concentration of an analyte can be determined by converting its absorbance using a standard curve constructed from antigens of known concentration. An example of a standard curve is shown in ***Figure 2.24***.

Figure 2.24

An example of a standard curve constructed using five standard samples for converting absorbance to analyte concentration. Taken from intact FGF23 ELISA (Immutopics, Quidel, California, USA).

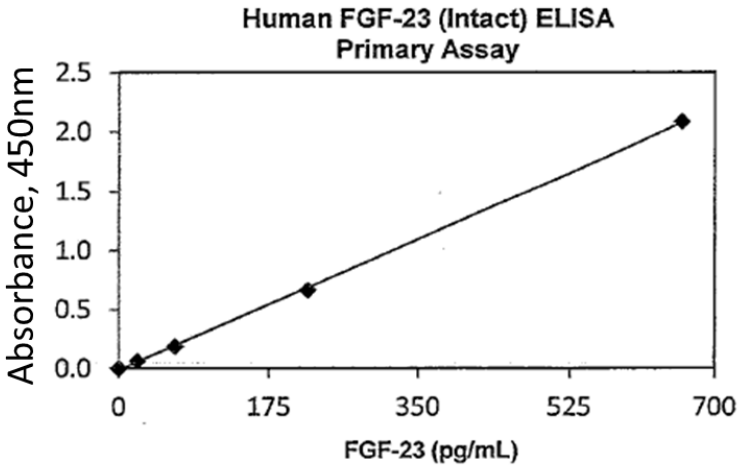

Chemiluminescent Immunoassay (CLIA)

The principles of CLIA is similar to ELISA but the substrate added in the final step is an enzyme which creates a chemical reaction. As the excited state of the chemical reaction returns to resting state, it emits a photon of light instead of developing a particular colour (as described for ELISA). The photon is detected by a specific spectrometry. Luminescence is converted to antigen concentration through a standard curve.

Electrochemiluminescence Immunoassay (ECLIA)

ECLIA has the same principles as CLIA but it does not depend on chemical reaction to emit light. Instead, a voltage is applied to the electrode covering the plate surface to induce

chemiluminescence which can then be measured by a photomultiplier. The analyte concentration can be converted from the luminescence using a standard curve.

2.4.2 Principles of Enzymatic Assay

In enzymatic assay, an enzyme acts by catalysing a specific reaction of the substrate to be assayed. One of the reactants, products or the rate of the reaction can be measured and then converted to the concentration of the substrate.

2.4.3 CKD-MBD Biochemistry

Calcium, Phosphate and Creatinine

Serum calcium, phosphate and creatinine were analysed on Roche Cobas c701/702 autoanalyser (Roche Diagnostics, England, UK) on the same day as blood sample collection. The analysis was performed in the Laboratory Medicine Department at the Northern General Hospital which complies with its internal and external quality control management. The intra-assay and inter-assay coefficient of variations (CVs) for all the biochemistry tested were ≤5%.

Serum calcium was analysed using the NM-BAPTA method. Calcium ions reacted with 5-nitro-5'-methyl-BAPTA (NM-BAPTA) under alkaline conditions to form a complex. This complex reacted in the second step with ethylenediamine tetraacetic acid (EDTA). The change in absorbance was directly proportional to the calcium concentration and was measured photometrically. Serum albumin-adjusted calcium was automatically calculated using serum albumin of 43 g/L as the normal value.

The formula is:

Serum albumin-adjusted calcium (mmol/L) = Serum calcium (mmol/L) + [0.0172 x (43 g/L – serum albumin g/L)]

Serum phosphate was analysed using a method based on the reaction of phosphate ions with ammonium molybdate to form a phosphomolybdate complex. With careful pH control, this complex formed molybdenum blue which can be measured at 600 to 700 nm wavelength using a spectrophotometer.

Calcium x phosphate product was calculated using the formula:

Calcium x phosphate product ($mmol^2/L^2$) = serum albumin-adjusted calcium (mmol/L) x serum phosphate (mmol/L)

Serum creatinine was analysed using the kinetic colorimetric assay which is based on the Jaffé method. In alkaline solution, creatinine formed a yellow-orange complex with picrate. The rate of dye formation was proportional to the creatinine concentration in the specimen.

Estimated glomerular filtration rate (eGFR) was calculated using Modification of Diet in Renal Disease (MDRD) study equation which was used by our biochemistry lab during the study period. The formula from the MDRD study is shown below {Levey et al 1999}. The MDRD equation preceded the CKD-EPI equation.

MDRD eGFR formula ($ml/min/1.73m^2$) = $186 \times [(P_{Cr})/88.4]^{-1.154} \times (age)^{-0.203}$ x (0.742 if female) x (1.210 if African American)

Intact Parathyroid Hormone (iPTH)

Serum iPTH was analysed using the CLIA method on the Immuno Diagnostic Systems (IDS) iSYS autoanalyser (IDS, Boldon, UK). Two polyclonal antibodies against human PTH were utilised. An antibody recognising the C-terminal region (amino acids 39-84) was used as the capture antibody. For detection, an acridinium conjugated antibody recognising the N-terminal region (amino acids 13-34) was used. In addition to full-length PTH (amino acids 1-84), the large PTH fragment (amino acids 7-84) was also detected.

Assay precision evaluated by the manufacturer used 3 serum controls which were assayed using three lots of reagents in duplicate, twice per day for 20 days on three instruments. The manufacturer reported an inter-assay CV of ≤ 8%. In-house quality control (QC) was performed prior to the sample analysis for the study. QC was performed using 3 control samples provided by the manufacturer (serum-like matrix) with known concentrations of iPTH (low, normal, high) and one in-house serum sample. The in-house inter-assay CV was < 7%. The assay range was 5 – 5000 pg/mL.

25-hydroxyvitamin D

Serum total 25-hydroxyvitamin D (25(OH)D) was analysed using the CLIA method on the IDS iSYS autoanalyser. Samples were subjected to a pre-treatment step to denature the vitamin D binding protein (VDBP). The treated samples were then neutralised in assay buffer and a specific anti-25(OH)D antibody labelled with acridinium was added. Following an incubation step, magnetic particles linked to 25(OH)D were added. Following a further incubation step, the magnetic particles were “captured” using a magnet. After a washing step and addition of

trigger reagents, the light emitted by the acridinium label was measured using spectrometer. The luminescence was inversely proportional to the concentration of 25(OH)D in the original sample. Assay precision evaluated by the manufacturer used three serum controls (6.7, 25.8, and 74.4 ng/mL) which were assayed using three lots of reagents in quadruplicate once per day for 20 days on two instruments. The manufacturer reported an inter-assay CV of < 17%. In-house QC was performed prior to the analysis for the study samples using three control samples provided by the manufacturer with varying levels of 25(OH)D and one in-house serum sample. The in-house inter-assay CV was < 7%. The assay range was 5 – 140 ng/mL.

Fibroblast Growth Factor 23 (FGF23)

Plasma intact FGF23 was analysed using Immutopics Human FGF23 (Intact) ELISA manual kit (Quidel, California, US). This sandwich assay uses biotinylated monoclonal antibody for capture and enzyme-conjugated (horseradish peroxidase) antibody for detection. The sample was firstly incubated with biotinylated antibody in a streptavidin-coated microtitre well. After washing to remove unbound antibody, the well was incubated with the enzyme-conjugated antibody. Following another wash, the enzyme antibody bound to the well was incubated with a substrate solution in a timed reaction and then measured using spectrophotometer at 450 nm wavelength. The enzymatic activity of the antibody complex bound to the well was directly proportional to the amount of FGF23 in the sample. The concentration of FGF23 in the sample was determined using a standard curve.

Assay precision evaluated by the manufacturer used two samples of different FGF23 concentrations in 20 duplicates measured by a single assay and duplicates from two samples measured by 20 assays. The manufacturer provided intra-assay CV was < 4% and the inter-

assay CV was ≤ 9%. Samples from this study were measured in duplicates and the intra-assay CV was < 5%. QC was performed using two control samples provided by the manufacturer and one in-house plasma sample. The in-house intra-assay CV was < 5%. The assay lower limit of detection was 1.5 pg/mL. Six CKD samples had levels between the highest standard (30,000 pg/mL) and 500,000 pg/mL. We were unable to re-assay the samples post dilution. Therefore, the samples were recorded as 30,000pg/mL.

2.4.4 Bone Turnover Markers

Alkaline Phosphatase (ALP)

Serum total ALP (tALP) was analysed on Roche Cobas c701/702 analyser (Roche Diagnostics, England) on the same day as blood sample collection using an enzymatic assay. P-nitrophenyl phosphate (colourless) was cleaved by ALP into phosphate and p-nitrophenol. The p-nitrophenol (yellow) released was directly proportional to the catalytic ALP activity. It was determined by measuring the absorbance at 409 nm wavelength. The intra-assay and inter-assay CVs for tALP were ≤ 5%.

Serum bone ALP (bALP) was analysed using the Ostase BAP assay on IDS iSYS autoanalyser. This assay uses the ELISA method. Samples were added to a biotin labelled BAP-specific monoclonal antibody. Following an incubation step, magnetic particles labelled with streptavidin were added. Following a second incubation step, the magnetic particles were captured by a magnet and a wash step performed to remove unbound bALP. Then it was incubated with an enzyme substrate. The amount of substrate turnover (enzyme activity) was determined using spectrophotometer by measuring the absorbance at different time points.

The signal was proportional to the amount of bALP present in the test sample. Assay precision evaluated by the manufacturer used five serum samples which were assayed using three lots of reagents in duplicate twice per day for 20 days on two instruments. The manufacturer reported an inter-assay CV of ≤ 9%. QC was performed using three control samples provided by the manufacturer with varying levels of bALP and one in-house serum sample. The in-house inter-assay CV was < 7%. The assay range was 1 – 75 µg/mL.

N-terminal Procollagen Type I Propeptide (PINP)

We measured serum PINP using two different assays. Total PINP assay measures the trimeric and monomeric forms of PINP, whereas intact PINP assay measures the trimeric form of PINP only.

Total PINP was analysed using the ECLIA method on the Cobas e411 automated analyser (Roche Diagnostics, Germany). The sample was firstly incubated with biotinylated monoclonal PINP-specific antibody. Then microparticles and a monoclonal PINP-specific antibody labelled with a ruthenium were added to form a sandwich complex. The interaction of biotin and streptavidin formed the solid phase which were then captured by electrodes. The mixture was then aspirated into the measuring cell where the streptavidin-labelled microparticles were magnetically captured onto the surface of the electrode. Unbound substances were removed with washer solution. Application of a voltage to the electrode then induced chemiluminescent emission which was measured by a photomultiplier. Substrate concentration was determined via a calibration curve. Assay precision evaluated by the manufacturer used three different pooled human sera and three control samples, 6 times daily for 10 days. The manufacturer reported an inter-assay CV of < 4%. QC was performed

using three control samples provided by the manufacturer and one in-house sample. The in-house inter-assay CV was < 7%. The assay range was 5 - 1200 ng/mL.

Intact PINP was analysed using the CLIA method on the IDS iSYS autoanalyser. Samples were incubated with a biotinylated anti-PINP monoclonal antibody, an acridinium labelled monoclonal antibody, streptavidin labelled magnetic particles and an assay buffer. The magnetic particles were captured using a magnet and a wash step performed. Trigger reagents were added and the resulting light emitted by the acridinium label was directly proportional to the concentration of intact PINP in the original sample. Assay precision evaluated by the manufacturer used three serum controls which were assayed using three lots of reagents in quadruplicate once per day for 20 days on two analysers. The manufacturer reported an inter-assay CV of ≤ 6%. QC was performed using three control samples with varying levels of PINP provided by the manufacturer and one in-house serum sample. The in-house inter-assay CV was < 7%. The assay range was 2 - 230 ng/mL.

Osteocalcin

Serum osteocalcin was analysed using IDS iSYS N-mid Osteocalcin assay which is based the CLIA method. Two highly specific monoclonal antibodies against human osteocalcin were utilised. An antibody recognising the mid-region (amino acids 20-29) was used as the capture antibody and for detection, an acridinium conjugated antibody recognising the N-terminal region (amino acids 10-16) was used. In addition to intact osteocalcin (amino acid 1-49), the N-terminal-Mid fragment (amino acids 1-43) was also detected. Samples were incubated with both labelled antibodies for a period of time. Streptavidin coated magnetic particles were then added and following a further incubation step, the particles were captured using a

magnet. After a washing step and addition of trigger reagents, the light emitted by the acridinium label was measured using a spectrometer. The luminescence was directly proportional to the concentration of osteocalcin in the original sample. Assay precision evaluated by the manufacturer used six serum controls which were assayed using three lots of reagents in duplicate twice per day for 20 days on two instruments. The manufacturer reported an inter-assay CV of < 9.5%. QC was performed using three control samples with varying degree of osteocalcin level provided by the manufacturer and one in-house serum sample. The in-house inter-assay CV was < 7%. The assay range was 2 - 200 ng/mL.

C-terminal Telopeptide of Type I Collagen (CTX)

Serum CTX was analysed using the IDS iSYS autoanalyser CTX-I (CrossLaps) assay which uses the CLIA method. Two highly specific monoclonal antibodies were used. The antibodies were against the amino acid sequence of EKAHD-ß-GGR, where the aspartic acid residue was (D) ß-isomerized. In order to obtain a specific signal in IDS iSYS CTX-I assay, two chains of EKAHD-ß-GGR must be cross-linked. Samples were incubated with both labelled antibodies for a period of time. Streptavidin coated magnetic particles were then added and following a further incubation step, the particles were “captured” using a magnet. After a washing step and addition of trigger reagents, the light emitted by the acridinium label was measured using a spectrometer. The luminescence was directly proportional to the concentration of CTX-I in the original sample. Assay precision evaluated by the manufacturer used five serum controls which were assayed using three lots of reagents in duplicate twice per day for 20 days on three analysers. The manufacturer reported an inter-assay CV of < 9%. QC was performed using three control samples with varying degree of CTX level provided by the manufacturer

and one in-house serum sample. The in-house inter-assay CV was < 7%. The assay range was 0.033 – 6.000 ng/mL.

Tartrate-resistant acid phosphatase 5b (TRAP5b)

Serum TRAP5b was analysed using the IDS iSYS autoanalyser TRAcP 5b (BoneTRAP) assay which uses the ELISA method. Serum sample was added to a biotinylated anti-TRAcP antibody and magnetic particles labelled with Streptavidin and incubated. Following a wash step the magnetic particles, bound to the biotinylated antibody-TRAcP complex, were captured using a magnet. A further wash step was performed to remove any unbound analyte. An enzyme substrate was then added for further incubation. The amount of substrate turnover was determined spectrophotometrically by measuring the absorbance at different time points. The signal was directly proportional to the amount of TRAcP 5b present in the original sample.

Assay precision evaluated by the manufacturer used four serum controls assayed using three lots of reagents in quadruplicate once per day for 20 days on two systems. The manufacturer reported an inter-assay CV of 5 - 14%. QC was performed using three control samples provided by the manufacturer and one in-house serum sample. The in-house inter-assay CV was < 7%. The assay range was 0.9 – 14.0 U/L.

Osteoprotegerin (OPG)

Serum OPG was analysed using a manual ELISA kit by Biomedica (Vienna, Austria). The sample was incubated with analyte-specific biotinylated antibody. The analyte and the labelled derivative competed for the binding site on the biotinylated antibody. Streptavidin conjugate

was added to bind the immunocomplexes. Unbound reagent was washed away using manufacturer provided wash buffer. The substrate was added for further incubation. After a specified time, stop solution was added and the absorbance was read immediately using 450 nm wavelength. A standard curve was constructed from which sample concentration was obtained. Assay precision evaluated by the manufacturer used 4 samples of known concentration measured 8 times on one assay kit and 4 samples which were measured by 3 assay kit lots. The manufacturer reported an inter-assay CV of ≤ 9%. Samples from this study were analysed in duplicates and the intra-assay CV was < 5%. QC was performed using one control sample provided by the manufacturer and one in-house serum sample. The in-house inter-assay CV was < 7%. The assay range was 0 – 22 pmol/L.

2.4.5 Vascular Calcification Markers

Matrix Gla Protein (MGP)

Two species of matrix Gla protein (MGP) were measured using Immuno Diagnostic Systems (IDS) assays; these were total uncarboxylated (t-uc) MGP and dephosphorylated-uncarboxylated (dp-uc) MGP.

Plasma t-uc MGP was analysed using manual ELISA kit from IDS. Antibody specific for ucMGP had been pre-coated onto a microplate. Standards and samples were pipetted into the wells and any ucMGP present was bound by the immobilized antibody. After removing any unbound substances, a biotin-conjugated antibody specific for ucMGP was added to the wells. After washing, avidin conjugated Horseradish Peroxidase (HRP) was added to the wells. Following a wash to remove any unbound avidin-enzyme reagent, a substrate solution was

added to the wells and colour developed in proportion to the amount of ucMGP bound in the initial step. The colour development was stopped and the intensity of the colour was measured. The manufacture reported an inter-assay CV of < 11%. QC was performed using three control samples provided by the manufacturer and one in-house plasma sample. The in-house intra-assay CV was < 5%.

Plasma dp-uc MGP was analysed using the IDS iSYS autoanalyser InaKtif MGP assay which uses the CLIA method. Plasma sample was incubated with magnetic particles coated with murine monoclonal antibodies dpMGP, an acridinium labelled murine monoclonal antibodies ucMGP and an assay buffer. The magnetic particles were captured using a magnet and a wash step performed to remove any unbound analyte. Trigger reagents were added; the resulting light emitted by the acridinium label was directly proportional to the concentration of dp-ucMGP in the original sample.

Assay precision evaluated by the manufacturer used 7 plasma controls/samples assayed in duplicate, twice per day for 20 days on one system. The manufacturer reported an inter-assay CV of ≤ 8.2%. QC was performed using three control samples provided by the manufacturer and one in-house plasma sample. The in-house inter-assay CV was <7%. The assay range was 300 – 12,000 pmol/L.

Fetuin A

Fetuin A was measured using manual ELISA kit by BioVendor (Brno, Czech Republic). The standards, quality controls and samples were incubated in microplate wells pre-coated with polyclonal anti-human fetuin A antibody. After 60 minutes incubation and washing, polyclonal

anti-human fetuin A antibody, conjugated with horseradish peroxidase (HRP) was added to the wells and incubated for 60 minutes with captured fetuin A. Following another washing step, the remaining HRP conjugate was allowed to react with the substrate solution. The reaction was stopped by addition of acidic solution and absorbance of the resulting yellow product was measured. The absorbance was proportional to the concentration of fetuin A. A standard curve was constructed by plotting absorbance values against concentrations of standards. Concentrations of participant samples were determined using this standard curve. Assay precision evaluated by the manufacturer used two samples of known concentration measured 8 times on one assay kit and two samples which were measured by 6 assay kit lots. The manufacturer reported intra-assay CV of < 4% and inter-assay CV of < 6.5%. Samples from this study were measured in duplicates. The in-house intra-assay CV was < 5%. QC was performed using two control samples (low and high concentrations) provided by the manufacturer. The in-house inter-assay CV was < 7%. The assay range was 2 – 100 ng/mL.

2.5 Statistical Analysis

All statistical analyses were performed by computer using IBM SPSS Statistics software (version 22, IBM Corp, New York, USA) and MedCalc Statistical software (version 16.8.4, MedCalc Software, Ostend, Belgium).

2.5.1 Normality Testing

Data were checked for normal or skewed distribution. Data with a normal distribution forms a symmetrical bell-shaped distribution where the peak of the curve lies above the mean and

median, and 95% of the data lies within 1.96 standard deviations above and below the mean. Further assessment for normal distribution was done by checking that the ratio of skewness to its standard error lies within -2 to +2 and that the ratio of kurtosis to its standard error also lies within -2 to +2. Samples of data with normal distribution allow the use of parametric statistical tests. Samples of data with skewed distribution require the use of non-parametric tests. Where this is not possible, the data can be transformed using $\log_{10}$ and the resulting normal distribution data can be tested using parametric tests.

2.5.2 Summary Statistics

We calculated mean and standard deviation for normal distribution data or median and interquartile range for data with skewed distribution.

2.5.3 Testing Group Differences

The comparison of characteristics of CKD and controls was done using one of these statistical tests. Student t-test was used to compare the mean values of two independent sets of data which have normal distribution. Mann-Whitney U test was used to compare the median values of two independent sets of data which have skewed distribution. Chi-squared test was used to compare group difference for categorical data. $p<0.05$ was used to indicate statistical significance.

Where there were more than two groups for comparison e.g. low, normal and high bone turnover groups, we used one-way analysis of variance (ANOVA) to compare variables with normal distribution and *post-hoc* Tukey analysis for pairwise comparison. Kruskall-Wallis test

was used to compare more than two groups with variables which have skewed distribution. *Post-hoc* analysis for pairwise comparison was performed using Mann-Whitney U test.

2.5.4 Testing Relationship between Variables

The direction (positive or negative) and strength of associations between two continuous variables were tested using one of these two statistical tests. Pearson's correlation was used to determine the association between two independent variables with normal distribution. Spearman rank correlation was used to determine the association between two independent variables where at least one set of data had skewed distribution. The correlation coefficient (rho) for both tests can lie between -1 and +1. Negative value indicates inverse association. A rho value of exactly -1 or +1 indicates a perfect linear association whereas a rho value close to zero indicates no association. $p<0.05$ was used to indicate statistical significance.

Multiple correlation was used to determine how well a dependent variable can be predicted using a linear function of a set of other variables. Multiple correlation is based on Pearson's correlation and its correlation coefficient (R^2) can lie between 0 and 1. The higher value indicates better predictability of the dependent variable by the independent variables.

2.5.5 Z-scores

DXA BMD T-score calculation and the reference data used have already been described in this chapter. DXA BMD Z-scores were obtained from the Hologic software which used a larger number of participants to represent the normal population.

However, there is no large reference data for HR-pQCT measurements to enable the calculation of T-scores (the number of standard deviations from the mean of gender-matched young) or Z-scores (the number of standard deviations from the mean of age and gender-matched controls). Z-scores are particularly useful to indicate how different the result is compared to controls with similar age and gender. When we examined the relationship between HR-pQCT measurements and bone turnover (BFR/BS), we wanted to control for the effect of age and gender on bone microarchitecture measured on HR-pQCT. Thus we calculated the HR-pQCT measurement Z-scores. We selected 43 controls in this study who were age- and gender-matched to the 43 CKD patients with bone histomorphometry data. The control group mean and standard deviation were calculated. The Z-scores of HR-pQCT measurements were calculated using the formula:

Z-score = [(CKD patient value) – (control group mean)] / control group standard deviation

2.5.6 Receiver Operating Characteristic (ROC) Analysis

ROC analysis is used to assess the diagnostic accuracy of a test to identify patients with a disease. ROC analysis is based on the dichotomous (yes or no) answer which requires a diagnostic threshold to differentiate those with the disease from those without.

To test the diagnostic accuracy of non-invasive tests (e.g. bone turnover markers or bone imaging) to identify patients with low bone turnover in this study, the CKD patients were firstly grouped into 'Low' and 'Not Low' bone turnover categories based on BFR/BS as shown on histomorphometry. BFR/BS < 18 $\mu m^3/\mu m^2$/year is 'Low' bone turnover and BFR/BS ≥ 18

$\mu m^3/\mu m^2$/year is 'Not Low' bone turnover which included patients with normal and high bone turnover.

Similarly, to test the diagnostic accuracy of non-invasive tests to identify patients with high bone turnover, the CKD patients were grouped into 'High' and 'Not High' bone turnover categories. BFR/BS > 38 $\mu m^3/\mu m^2$/year is 'High' bone turnover and BFR/BS ≤ 38 $\mu m^3/\mu m^2$/year is 'Not High' bone turnover which included patients with normal and low bone turnover. The proportion of patients with low bone turnover (26%) and high bone turnover (40%) in this study were used as the prevalence of the disease.

For a hypothetical perfect diagnostic test, the probability distributions of test results indicating presence or absence of the disease do not overlap and the chosen threshold value is in between the distributions. This is shown in ***Figure 2.25***. In reality, most diagnostic tests probability distribution of those with and without the disease overlap (***Figure 2.26***). It means that any threshold value will lead to misclassification of some patients with the disease as normal, and some normal patients as diseased.

Figure 2.25

The probability distributions of the results of a hypothetical perfect diagnostic test {van Erkel et al 1998}.

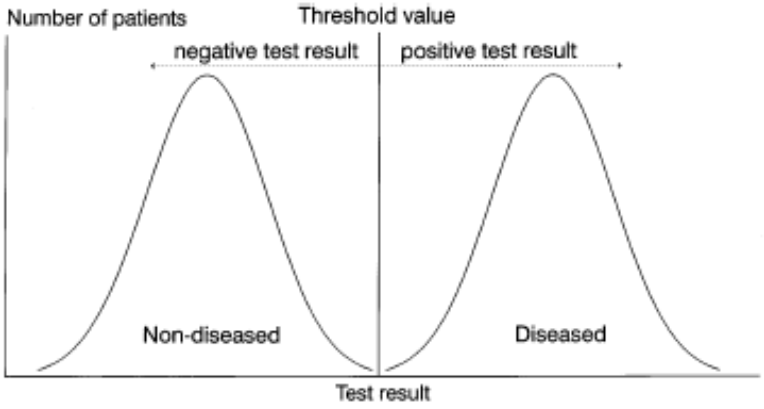

Figure 2.26

Realistic probability distributions of the results of a diagnostic test showing an overlap of those with and without the condition {van Erkel et al 1998}.

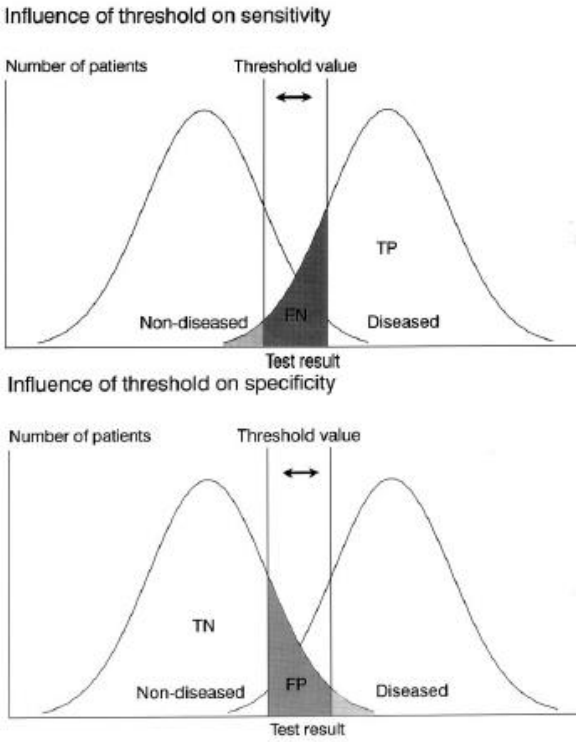

Figure 2.27 summarises the formulae used to calculate sensitivity, specificity, and predictive values of a diagnostic test. A lower threshold value for a diagnostic test decreases the number of false negative results but at the same time, increases the number of false positive results. This approach increases sensitivity but reduces the specificity of the test. Meanwhile, a higher threshold value for the diagnostic test increases the number of false negatives and decreases the number of false positive results. This approach reduces sensitivity but increases specificity of the test. Overall, there is a trade-off between sensitivity and specificity for any given threshold value.

Figure 2.27

Diagnostic test summary statistics and the formulae used.

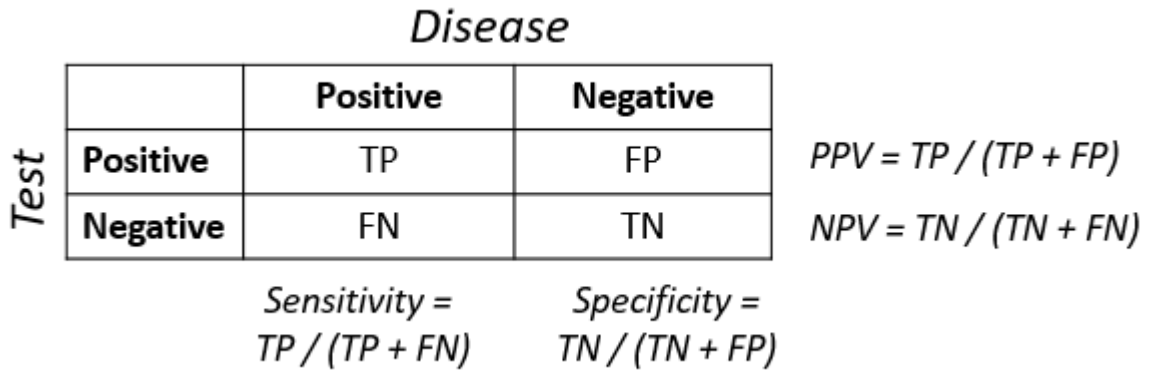

Abbreviations: TP, true positive; FP, false positive; TN, true negative; FP, false positive; PPV, positive predictive value; NPV, negative predictive value.

The ROC curve is a graphical representation of the reciprocal relationship between sensitivity and specificity, calculated for all possible threshold values of the diagnostic test (***Figure 2.28***). The vertical axis shows the sensitivity and the horizontal axis shows 1 – specificity. Each point on the ROC curve represents the combination of sensitivity and specificity at a given threshold value. Youden index is the point on the ROC curve where the optimum sensitivity and specificity of the test lies when sensitivity and specificity are given equal weight. The Youden index is associated with a threshold for the diagnostic test. The positive and negative predictive values can also calculated for this threshold.

Figure 2.28

(a) The ROC curve and (b) graphical presentation of the different threshold values (1 - 5) corresponding with points on the ROC curve {van Erkel et al 1998}.

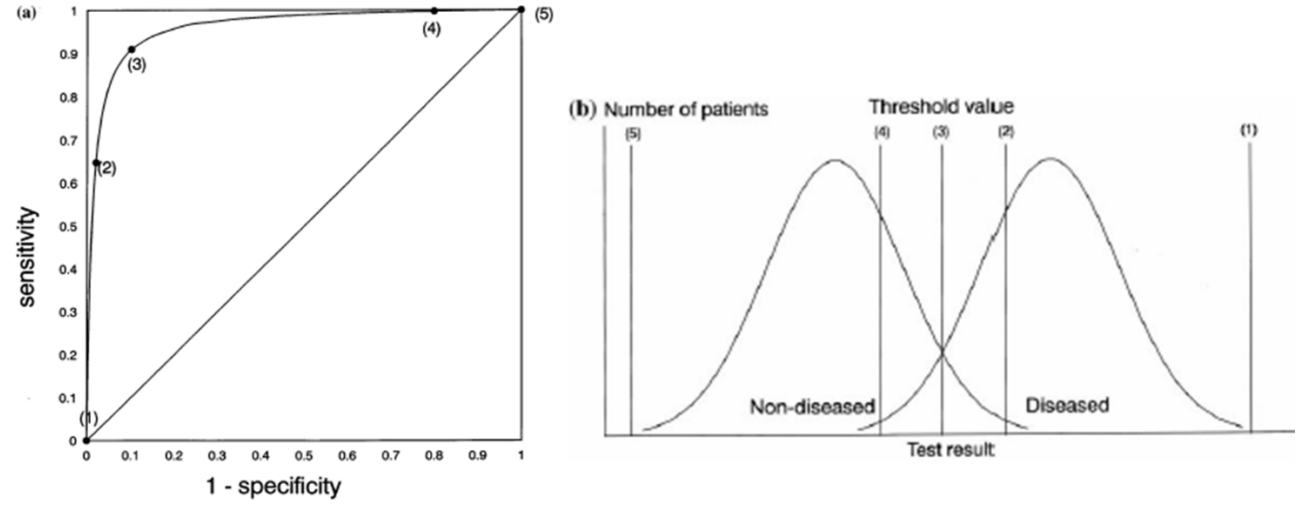

The area under the ROC curve (AUC) reflects the diagnostic accuracy of a test and is used for comparison between diagnostic tests. The diagnostic accuracy classification based on AUC is 0.6-0.7 as poor, 0.7-0.8 as fair, 0.8-0.9 as good and 0.9-1.0 as excellent diagnostic accuracy. Comparison of ROC AUCs is performed using non-parametric Wilcoxon test to determine if one diagnostic test was significantly better than the other. The null hypothesis (i.e. the two diagnostic tests had similar accuracy) was rejected if $p<0.05$. Two diagnostic tests can also be combined to determine if a combination of tests has improved diagnostic accuracy. Combining two tests (variables) is performed using a linear regression analysis to give a new set of variable which can then be tested using ROC analysis.

Although diagnostic accuracy classification based on AUC is widely used, it is important to be aware that AUC may be subjected to measurement errors which would result in a biased estimate. In general, a large measurement error would result in estimated AUC being lower than the true AUC, classifying the diagnostic tool as inaccurate when it is actually useful {Schisterman et al 2001} . There are 4 potential sources of measurement error in a diagnostic study; the participants (e.g. through selection bias or disease verification bias), the situation (e.g. temporal change), the measurer (e.g. inter-observer variability and use of automated versus manual assays) and the laboratory equipment performance (e.g. coefficient of variation and limit of detection). Although measurement errors cannot be totally eliminated, we had taken steps to reduce it in this study.

Chapter 3. Bone Biopsy Patterns in Advanced CKD

3.1 Introduction

Renal osteodystrophy (ROD) is a common complication of chronic kidney disease (CKD) which affects bone quality through changes in bone turnover, mineralization and microarchitecture {Malluche et al 2012}. The changes lead to increased risk of fractures with associated increased mortality in CKD {Block et al 2004; Kim et al 2016; Tentori et al 2014}. Treatment to reduce fracture risk in advanced CKD can only be initiated after accurate diagnosis of ROD {KDIGO 2009}. ROD is a spectrum of bone disease and bone biopsy is the gold standard diagnostic test because it directly assesses the abnormalities in a tissue sample. Quantitative bone histomorphometry using the TMV classification assesses bone turnover (T), mineralization (M) and volume (V) {S. Moe et al 2006}.

Bone biopsy is an invasive procedure which makes collecting large number of samples for research difficult and time consuming. Some studies reported large number of samples (greater than 500) which were collected over a number of years, but often involved multiple centres for sample collection and analysis, and may have been performed for clinical indication which could have introduced bias {Malluche et al 2011; Sprague et al 2016}. Another way of obtaining a large number of bone biopsy sample is to perform bone biopsies during renal transplantation. This approach is also preferred by renal patients as they are already under general anaesthetic. Tetracycline bone labelling is possible prior to living-donor renal transplantation but not for transplantation from deceased donors, who constitute the majority of the cases, due to the unpredictability of deceased donor transplantation. This has led to some studies using static parameters to assess bone turnover status although normal ranges have not been fully defined {Lehmann et al 2005; Viaene et al 2016}. ***Table 2.1*** shows

all dynamic and static parameters commonly reported on histomorphometry using standardised nomenclature and the formulae used to derive those parameters.

The aims of this chapter were to describe the bone histomorphometry features of advanced CKD patients who underwent a bone biopsy and to test if histomorphometry static parameters can replace dynamic parameters in diagnosing ROD.

3.2 Methodology

3.2.1 Bone Biopsy Procedure, MicroCT and Histomorphometry

The bone biopsy technique, bone biopsy-related pain assessment, bone sample preparation, microCT and histomorphometry techniques have been described in the Chapter 2 of this thesis

3.2.2 Statistical Analysis

Data are presented as mean (standard deviation, SD) or median (interquartile range, IQR). Differences between low, normal and high bone turnover groups were tested using one-way ANOVA or Kruskal-Wallis test depending on the distribution of the variables. The associations between bone turnover (BFR/BS) and other continuous variables were tested using Pearson's correlation. $p<0.05$ indicates statistical significance.

Additional statistical method used in this chapter was Kappa (κ) statistic to test that the histomorphometry static measurements were truly independent of the dynamic measurement of bone turnover. It estimates the agreement between dynamic and static

measurements, controlling for random chance {McHugh 2012}. A 95% confidence intervals which crosses zero indicates that there is no agreement between the dynamic and static measurements (i.e. all measurements were independent of each other). Kappa statistics was performed using IBM SPSS Statistics software (version 22, IBM Corp, New York, USA).

We also performed method comparison analysis for trabecular bone volume measurement using histomorphometry and microCT. Bland-Altman plot and Passing & Bablok regression method on MedCalc (version 18.10) were used. The Bland-Altman plot displayed a scatter diagram of the differences plotted against the averages of the two measurements. The plot was used to visualize any relationship between the differences and the magnitude of measurements, to identify any systematic bias and possible outliers.

The Passing-Bablok procedure fits the parameters *a* and *b* of the linear equation $y = a + b\,x$ using non-parametric methods. The coefficient *b* is calculated by taking the shifted median of all slopes of the straight lines between any two points, disregarding lines for which the points are identical or $b = -1$. The median is shifted based on the number of slopes where $b < -1$ to create an unbiased estimator. The intercept *a* is calculated by $a = \text{median}(y_i - b\,x_i)$. Passing and Bablok also defined a method for calculating a 95% confidence interval for both *a* and *b*. The Passing-Bablok procedure is valid only when a linear relationship exist between x and y, which can be assessed by a Cusum test. The results are interpreted as follows; if 0 is in the CI of *a*, and 1 is in the CI of *b*, the two methods are comparable within the investigated concentration range. If 0 is not in the CI of *a*, there is a systematic difference and if 1 is not in the CI of *b* then there is a proportional difference between the two methods.

3.3 Results

3.3.1 Patient Characteristics, Pain Score and Sample Adequacy

Out of 69 CKD patients, 54 patients had bone biopsy performed/attempted but samples were only obtained from 49 patients. 15 patients did not have bone biopsy due to side effects from tetracycline antibiotic (N=5), withdrawal of consent (N=9) and one patient died prior to bone biopsy due to haemorrhagic stroke which was unrelated to the study. Side effects of tetracycline antibiotics included nausea, vomiting, loss of appetite and loose stool which were known side effects. The symptoms resolved within a few days of stopping the antibiotic.

45 out of 54 patients (83%), who had bone biopsy performed/attempted, completed the visual analogue scale (VAS). **Figure 3.1** shows the pain score at different time points. Pain score during the procedure was significantly higher compared to pre-procedure pain score ($p<0.001$) although the level of pain varied greatly within the group (mean [SD] was 43 [27] mm). The pain level improved 10 minutes post-procedure (median (IQR) was 4 [0- 12.5] mm) although not completely back to baseline level ($p=0.001$). Pain level reported 2 days post-procedure was similar to that at 10 minutes post-procedure. Very few patients required simple painkillers such as paracetamol in the 48-hour period post procedure.

Only 43 out of 49 samples obtained were evaluable for histomorphometry. The remaining 6 samples were reviewed by a second assessor (Dr David Hughes, Consultant Clinical Histopathologist, Sheffield Teaching Hospitals NHS Trust) who confirmed that they were unsuitable for histomorphometry as the samples mainly contained soft tissue.

Figure *3.2* summarises the number of patients for each ROD subtype as characterised by bone turnover and mineralization status. Amongst the 43 patients with evaluable bone samples, 28 (65%) were pre-dialysis CKD, mean (SD) age was 59 (12) years, 77% were male, 26% had diabetes, and 26% had previous fragility fracture. All 43 samples evaluable for histomorphometry met the minimum acceptable total section area in the standard analysis region of 30 mm^2. In this study, the median (IQR) for total section area was 36.14 (32.22 – 41.27) mm^2.

Figure 3.1

Pain score using Visual Analogue Scale at different time points (N= 45)

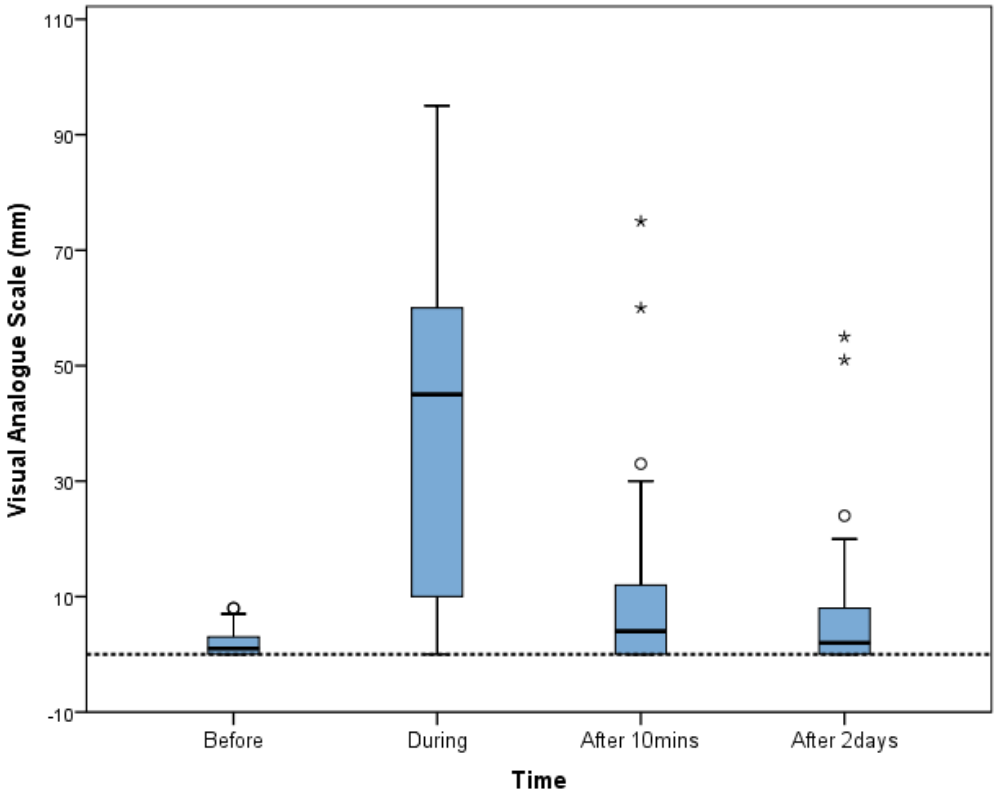

Figure 3.2

ROD subtypes in advanced CKD as classified by bone turnover (T), mineralization (M) and volume (V) status.

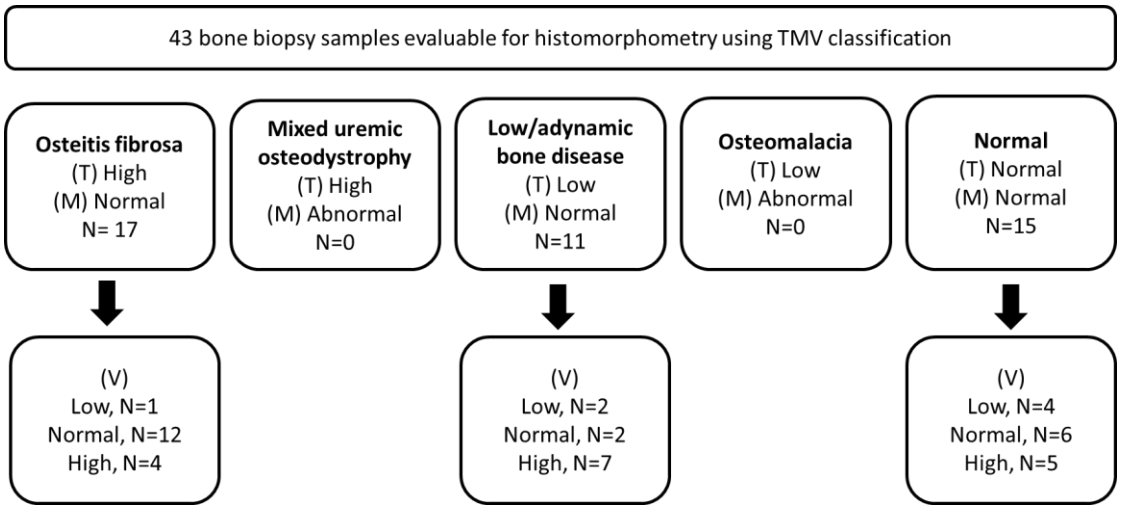

3.3.2 Bone Turnover

We had a wide range of bone turnover in our samples; median (IQR) for BFR/BS was 32.12 (17.76 – 48.25) $\mu m^3/\mu m^2$/year. Patients were divided into low (26%), normal (34%) and high (40%) bone turnover categories based on BFR/BS < 18, between 18 and 38, and > 38 $\mu m^3/\mu m^2$/year respectively. This is shown in **Table 3.1**.

Mineral apposition rate (MAR) and mineralising surface/bone surface (MS/BS) which were used to calculate BFR/BS were also significantly different across the bone turnover categories. Post hoc analysis showed that MAR and MS/BS were significantly different for all pairwise comparisons except for MAR between low and normal bone turnover categories. Static parameters of bone turnover such as osteoclast surface/bone surface (OcS/BS), osteoblast surface/bone surface (ObS/BS) and erosion surface/bone surface (ES/BS) only had weak to

moderate positive correlations with BFR/BS (***Figure 3.3***) and hence, did not show significant differences across the bone turnover categories. OcS/BS and ES/BS which measured osteoclasts and its erosion surfaces showed strong positive correlation (rho= 0.816, p<0.001).

Figure 3.3

Associations between dynamic and static parameters of bone turnover.

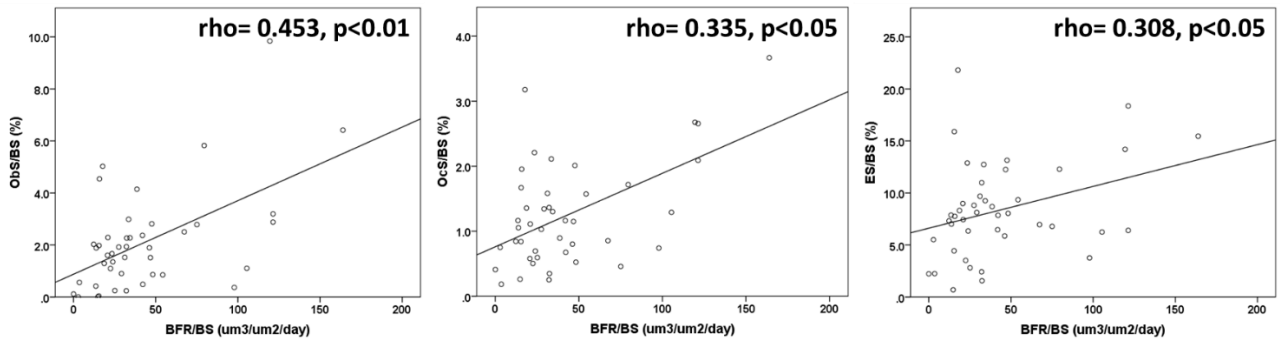

Table 3.1

Dynamic and static parameters on bone histomorphometry in low, normal and high bone turnover groups (N=43)

Parameters	Low (N=11)	Normal (N=15)	High (N=17)	P value
BFR/BS ($\mu m^3/\mu m^2$/year)	13.79 (3.59 – 15.49)	27.51 (22.48 – 32.18)	67.41 (46.46 – 112.45)	**<0.001** [a]
MAR (µm/day)	0.720 (0.396)	1.002 (0.349)	1.302 (0.256)	**<0.001** [b,c]
MS/BS (%)	3.83 (2.53 – 5.41)	7.81 (5.32 – 8.77)	14.56 (9.31 – 20.81)	**<0.001** [a]
ObS/BS (%)	0.56 (0.04 – 2.02)	1.61 (1.10 – 2.27)	2.51 (0.98 – 3.67)	0.07
OcS/BS (%)	0.85 (0.41 – 1.67)	1.11 (0.58 – 1.36)	1.16 (0.77 – 2.05)	0.4
ES/BS (%)	7.53 (6.25)	7.59 (3.60)	9.53 (4.03)	0.4
OS/BS (%)	29.12 (14.08)	38.61 (18.57)	46.82 (22.93)	0.08
OV/BV (%)	2.21 (1.43 – 5.49)	5.46 (2.62 – 7.62)	6.93 (3.08 – 12.59)	**0.01** [b]
MLT (days)	55.6 (21.1 – 192)	41.1 (25.6 – 62.8)	27.4 (15.1 – 36.9)	**<0.01** [b,c]
OMT (days)	6.9 (6.0)	8.0 (3.2)	8.7 (2.8)	0.5
O.Th (µm)	7.29 (1.97)	8.91 (2.36)	10.84 (3.16)	**<0.01** [b]
BV/TV (%)	23.88 (18.12 – 28.61)	20.10 (15.39 – 24.17)	19.42 (18.30 – 24.46)	0.5
Trab Th (µm)	160 (33.2)	143.6 (39.7)	140.9 (20.6)	0.3

Symbols indicating statistically significant post hoc analysis for [a]all pairwise comparisons, [b]pairwise comparison between low and high bone turnover groups, and [c]pairwise comparison between normal and high bone turnover groups.

3.3.3 Bone Mineralization

There was no significant correlation between mineralization lag time (MLT) and osteoid maturation time (OMT) although both are dynamic parameters of mineralization. Osteoid thickness (O.Th) which is a static parameter of mineralization was moderately correlated with OMT (rho = 0.544, $p<0.001$) but it did not correlate with MLT. Osteoid surface/bone surface (OS/BS) and osteoid volume/bone volume (OV/BV) showed strong positive correlation (rho = 0.906, $p<0.001$). However, only OV/BV was correlated with O.Th (rho = 0.62, $p<0.01$).

None of the patients in this study had abnormal mineralization. All patients had O.Th < 20 µm although 7 patients had MLT > 100 days. These 7 patients also had OMT < 40 days and OV/BV < 12% which further support that they have normal mineralization status. In fact, all our patients had normal OMT with mean (SD) of 8.0 (3.9) days.

Static mineralization parameters were then assessed for their association with bone turnover (BFR/BS). O.Th, OV/BV and OS/BS showed positive correlations with BFR/BS (***Figure 3.4***). When patients were divided into low, normal and high bone turnover categories, only O.Th and OV/BV showed significant differences across the bone turnover categories (**Table 3.1**) Post hoc analysis showed that the parameters were significantly different between low and high bone turnover categories.

Figure 3.4

Associations between dynamic parameter of bone turnover and static parameters of mineralization

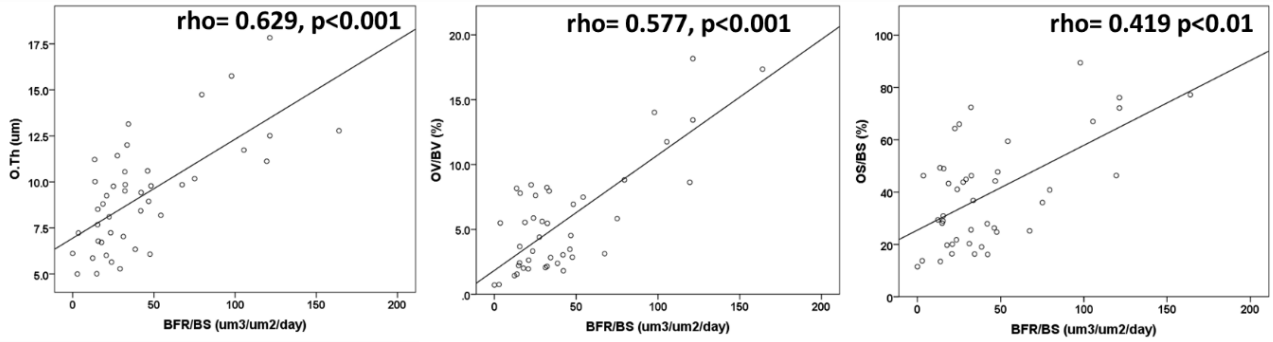

Mineralization dynamic parameters were also assessed for their association with bone turnover. There was a moderate negative association between MLT and BFR/BS (rho = -0.415, p<0.01). MLT was also significantly different across the bone turnover categories (**Table 3.1**). Post hoc analysis showed that MLT was different for 'low versus high' and 'normal versus high' bone turnover categories. The relationship between MLT and BFR/BS is better visualized in ***Figure 3.5*** which shows that prolonged MLT (greater than 100 days) can occur in some patients with normal and low bone turnover but all patients with high bone turnover (BFR/BS > 38 $\mu m^3/\mu m^2$/year) had normal MLT. There was no correlation between OMT and BFR/BS.

Figure 3.5

Distribution of patients based on bone turnover (BFR/BS) and mineralization lag time (MLT).

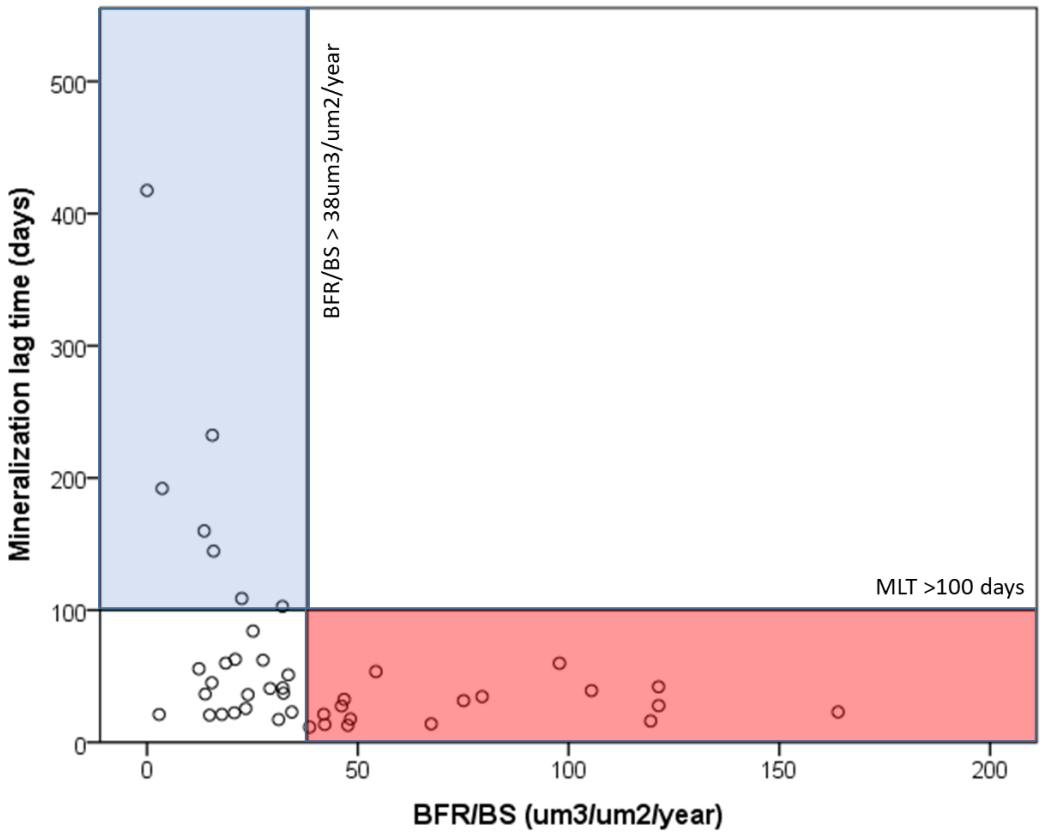

Prolonged MLT was found in 7 patients with normal/low bone turnover (blue shaded area) but all patients with high bone turnover had normal MLT (red shaded area).

3.3.4 Bone Volume

Bone volume/tissue volume (BV/TV) was strongly correlated with trabecular thickness (Tb.Th) (rho = 0.730, p<0.001). BV/TV and Tb.Th did not correlate with age and both parameters had similar distribution in male and female groups, indicating that there was no age and gender effects on these parameters. Only 7 out of 43 patients (16%) had low bone volume as defined by BV/TV < 16.8%. Amongst the 7 patients with low bone volume, 6 were pre-dialysis CKD and

one patient was on peritoneal dialysis, mean (SD) age was 56 (15) years, all were males and two had history of fragility fracture. No correlation was found between BV/TV and BFR/BS.

We also measured trabecular bone volume of the core biopsy sample using microCT and found that BV/TV on microCT and BV/TV on histomorphometry were highly correlated (rho = 0.904, p<0.001). Similarly to BV/TV on histomorphometry, there was no correlation between BV/TV measured by microCT with BFR/BS.

Methods comparison between measuring BV/TV on histomorphometry and microCT is shown in ***Figure 3.6***. Passing-Bablock regression showed that BV/TV on microCT measured lower than BV/TV on histomorphometry [MicroCT BV/TV = -3.13 + 1.10 (Histo BV/TV)] but the two methods were interchangeable (Cusum test of linearity p=0.53 which indicated no deviation from linearity). The Bland-Altman plot showed no bias between the mean differences of the two methods. Passing-Bablock regression analysis of trabecular number showed that there was a proportional difference in trabecular number detected by the two methods (***Figure 3.7***). Meanwhile, there was no difference for trabecular thickness detected by the two methods (***Figure 3.8***).

Figure 3.6

Method comparison for bone volume assessment of bone biopsy using histomorphometry and microCT.

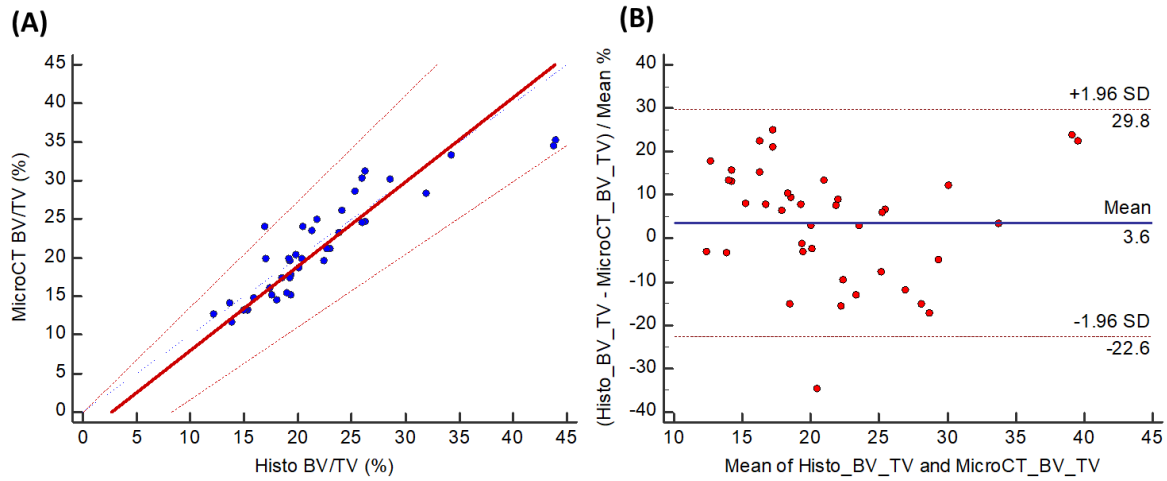

(A) Passing-Bablock regression equation: MicroCT BV/TV = -3.13 + 1.10 (Histo BV/TV)

Intercept (95% CI) = -3.13 (-8.01 to -0.22). Both methods differ by this constant amount.

Slope (95% CI) = 1.10 (0.95 to 1.37). No proportional difference between the two methods.

Cusum test of linearity p = 0.53. No significant deviation from linearity.

(B) Bland-Altman plot: *no bias*

Figure 3.7

Method comparison for trabecular number in bone biopsy using histomorphometry and microCT.

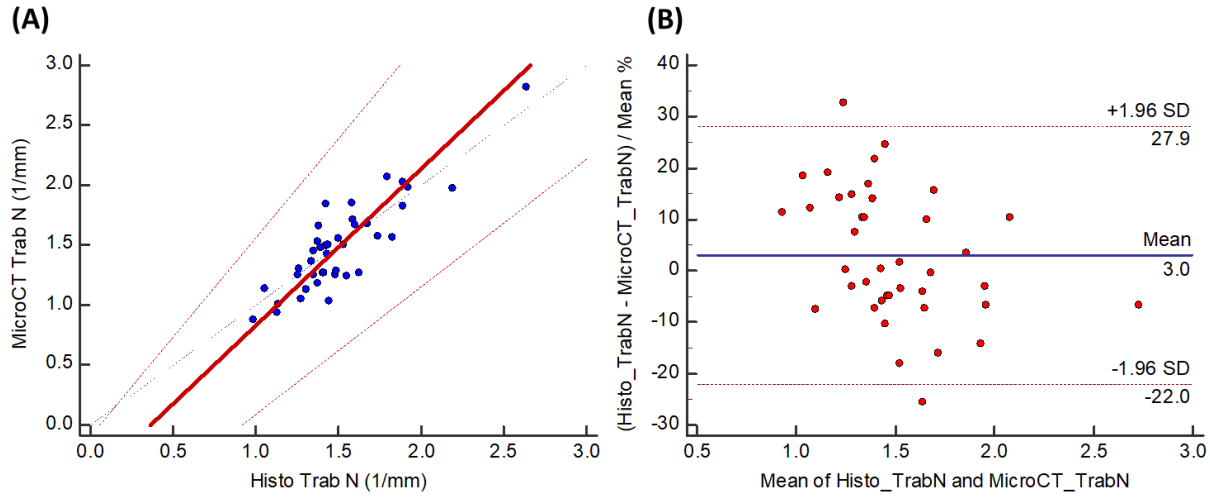

(A) Passing-Bablock regression equation: MicroCT Trab N = -0.49 + 1.31 (Histo Trab N)

Intercept (95% CI) = -0.49 (-0.99 to -0.10). Both methods differ by this constant amount.

Slope (95% CI) = 1.31 (1.07 to 1.66). There is proportional difference between the two methods.

Cusum test of linearity p = 0.53. No significant deviation from linearity.

(B) Bland-Altman plot: *no bias.*

Figure 3.8

Method comparison for trabecular thickness in bone biopsy using histomorphometry and microCT.

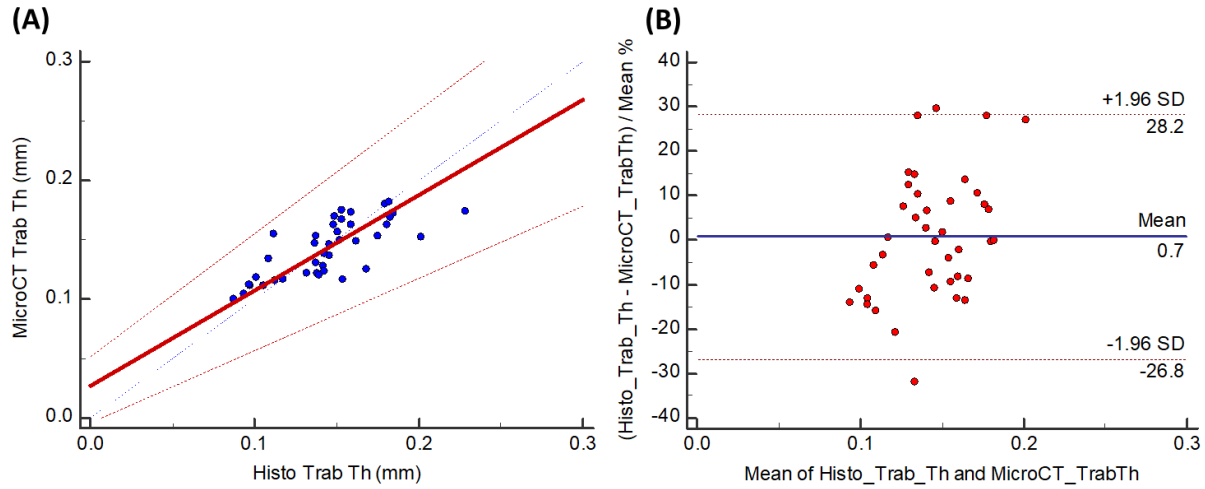

(A) Passing-Bablock regression equation: MicroCT Trab Th = 0.03 + 0.80 (Histo Trab Th)

Intercept (95% CI) = 0.03 (-0.01 to 0.05). Both methods do not differ by this constant amount.

Slope (95% CI) = 0.80 (0.61 to 1.04). No proportional difference between the two methods.

Cusum test of linearity p=0.53. No significant deviation from linearity.

(B) Bland-Altman plot: *no bias.*

3.3.5 Diagnostic Accuracy of Static Parameters to Identify Low and High Bone Turnover

Using static parameters in receiver operating characteristics (ROC) analysis to identify low bone turnover as assessed by BFR/BS, we found that OV/BV had area under the ROC curve (AUC) of 0.764 and O.Th had AUC of 0.770 (***Figure 3.9***). The other static parameters had non-significant AUCs. For identifying high bone turnover, osteoblast surface/bone surface

(ObS/BS) had AUC 0.697, OV/BV had AUC 0.719 and O.Th had AUC 0.744 for predicting high bone turnover (***Figure 3.10***). Diagnostic accuracy summary statistics for identifying low and high bone turnover using these static parameters are shown in ***Table 3.2***.

Figure 3.9

Receiver operating characteristics (ROC) curves for predicting low bone turnover

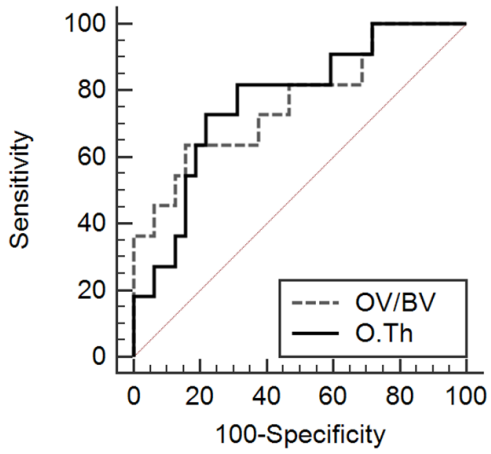

Figure 3.10

Receiver operating characteristics (ROC) curves for predicting high bone turnover

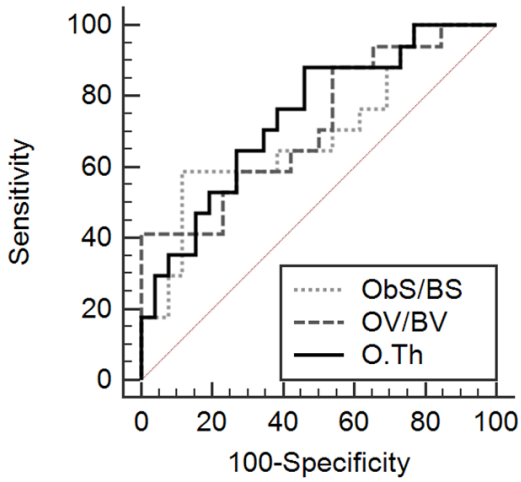

Table 3.2

Receiver operating characteristics (ROC) summary statistics for predicting low and high bone turnover using static parameters.

Static	AUC (95% CI)	Youden	Sensitivity	Specificity	PPV	NPV
For predicting low bone turnover						
OV/BV	0.764 (0.610 – 0.880)	≤ 2.4%	64	84	58	87
O.Th	0.770 (0.616 – 0.884)	≤ 7.7 μm	73	78	53	89
For predicting high bone turnover						
ObS/BS	0.697 (0.538 – 0.827)	> 2.3%	59	89	77	77
OV/BV	0.719 (0.562 – 0.846)	> 8.4%	41	100	100	72
O.Th	0.744 (0.588 – 0.865)	> 8.1 μm	88	54	56	88

OV/BV and O.Th have fairly similar AUCs for differentiating low and high bone turnover (AUCs 0.70 – 0.80). Using Kappa (κ) statistic, we tested whether the static measurements of osteoid were truly independent of the dynamic measurement of bone turnover. The linear weighted κ (95% CI) for agreement between BFR/BS and OV/BV was 0.04 (-0.01 to 0.10). The linear weighted κ (95% CI) for agreement between BFR/BS and O.Th was 0.06 (-0.003 to 0.12). The 95% CI crossed zero, thus there was no agreement between BFR/BS and the two static parameters (i.e. all measurements were independent of each other).

3.4 Discussion

Bone biopsy is the gold standard test to diagnose ROD but it is invasive and painful; thus limiting its use as a diagnostic tool. The traditionally used 7 – 8 mm diameter Bordier trephine needle would require sedation/general anaesthetic and a hospital stay after bone biopsy. However, a modified trans-iliac bone biopsy technique using a smaller 4 mm inner diameter Jamshidi needle has allowed this procedure to be done under local anaesthetic as a day case procedure. This technique is preferred in our centre and in around 40% of bone biopsy centres in Europe {Evenepoel et al 2017}.

Despite using a smaller biopsy needle, there was significant pain experienced by our participants during the procedure. The level of pain varied greatly within the group which may reflect different pain tolerance between individuals. The bone biopsy site, the use of disposable single-use Jamshidi bone biopsy needle, the bone biopsy operator and the technique were the same for all participants. There was some pain/discomfort reported after 2 days, fairly similar to the level reported 10 minutes post procedure. No studies have previously reported the level of pain experienced by participants of trans-iliac bone biopsy. The closest comparison can be made with one study which assessed pain relating to bone marrow biopsy using VAS {Tanasale et al 2013}. Their 202 participants reported pain experienced at 5 minutes post procedure with a median of 19 mm on the VAS. This is around halfway between our results for pain score 'during' and '10-minutes post procedure'. Thus suggesting that pain relating to bone biopsy under local anaesthetic from anterior-inferior or posterior iliac approach are fairly similar. There was no biopsy associated morbidity or mortality in our study. Worldwide morbidity associated with bone biopsy is extremely rare and mortality has never been reported {Hernandez et al 2008; Malluche et al 1994}.

88% of samples obtained in this study were adequate for histomorphometry analysis; falling within the range of previously reported 74 – 99% sample adequacy in other studies {Behets et al 2014; Malluche et al 2011; Viaene et al 2016}. The inadequate samples contained mainly soft tissue and this could have been due to patient or operator-dependent factors. However, the findings of inadequate sample did not cluster in the early stage of this study to suggest operator's experience as a factor.

The dynamic assessment of bone turnover on bone biopsy uses double tetracycline labelling to measure MAR which is required to calculate BFR/BS or activation frequency (Ac.f). We used BFR/BS to assess bone turnover and the proportion of patients with low, normal and high bone turnover in this study was similar to previous studies {Bervoets et al 2003; Couttenye et al 1996}. BFR/BS has been reported with or without Ac.f to determine bone turnover status in other studies {Malluche et al 2011; Malluche et al 2008}. Ac.f was not assessed in our study and thus, we cannot confirm its association with BFR/BS. Ac.f represents the probability that a new bone remodelling cycle will be initiated at any site on the trabecular bone surface. It is calculated by dividing BFR/BS by wall thickness and thus, it is a highly derived parameter which has inherent issues in calculation, assumptions and interpretation {Recker et al 2011}. There is no evidence to suggest that Ac.f measurement is superior to BFR/BS in the assessment of bone turnover. Furthermore, measuring wall thickness requires a dedicated section stained with Toluidine blue at each level sectioned for histomorphometry. This would have increased the risk of not having adequate sample to fulfil the minimum acceptable criteria for tissue area for histomorphometry given that we used a smaller diameter needle. Ac.f is not a routine histomorphometry measurement in clinical setting.

Some studies have used static parameters to assess bone turnover status. Lehmann et al studied 132 patients with CKD stages 3 - 5 who had bone biopsy {Lehmann et al 2005}. Only 95 patients (72%) had tetracycline prior to bone biopsy. Static parameters OcS/BS and ObS/BS were used to classify patients into low, normal and high bone turnover; OcS/BS < 1%, 1 - 2.1% and > 2.1% respectively and ObS/BS < 1%, 1 - 3.2% and > 3.2% respectively. A decade later, Viaene et al published a study of 81 end stage renal disease patients who were having renal transplantation {Viaene et al 2016}. Tetracycline bone labelling was not possible at the time of bone biopsy and static parameter ObS/BS was used to classify patients into low (< 1%), normal (1 - 3.2%) and high (> 3.2%) bone turnover. These thresholds were similar to the Lehman et al study although these were based on their previously unpublished data on a separate cohort of 27 dialysis patients where ObS/BS showed modest correlation with BFR/BS (rho = 0.64).

There is an increasing preference to obtain bone biopsy for research during renal transplantation but this method has its limitations. Firstly, it only includes renal transplant recipients and effectively exclude more frail and elderly patients who are more likely to have worse bone health. Secondly, the accuracy of using purely static parameters to diagnose renal osteodystrophy is unknown. Hence, we assessed the diagnostic accuracy of static parameters for identifying bone turnover status in our samples as assessed by dynamic parameter BFR/BS.

We found that ObS/BS, O.Th and OV/BV can identify patients with high bone turnover with statistically significant AUCs. O.Th and OV/BV also have statistically significant AUCs for identifying low bone turnover. However, all AUCs were below 0.80 which means that these static parameters are not robust enough as diagnostic tests to replace BFR/BS. They cannot

determine bone turnover status accurately and should not be used to guide treatment decisions.

We used BFR/BS as a measure of bone turnover and adopted the previously published normal range {Malluche et al 2011; Sprague et al 2016}. However, normal range of BFR/BS is generally inconsistent and varied across bone biopsy studies due to geographical variance, race and local experience {Parfitt 2003; Sprague et al 2016}. It is almost impossible to establish normal range because it would require bone biopsies from living, healthy people. Furthermore, normal range in healthy adults may differ with each decade of life and gender. The difficulties in establishing normal range inevitably results in the difficulties in establishing abnormalities. We did not explore whether the static parameters in our study had higher accuracy if different ranges and units of BFR/BS were applied.

Malluche et al examined bone biopsy samples from each decade of life (first to eighth) from 84 normal American subjects using quantitative histomorphometry {Malluche et al 1982}. The number of bone biopsy samples obtained for each decade of life ranged from 5 to 19 samples. There was no difference in bone histomorphometry measurements between pre-menopausal women and their age-matched men suggesting that there was no gender difference in bone histomorphometry in the young. Bone density of the samples gradually increased during childhood to early adulthood, peaked in the third decade of life and gradually declined reaching its lowest value in the eighth decade. Only static parameters were obtained in this study as the subjects were deceased. Subsequently, the same author used a reference range for dynamic parameters of bone turnover and mineralization in adults based on further studies of healthy adults {Malluche et al 2011}.

Another study which examined bone biopsies from healthy adults was published by Parfitt et al {Parfitt et al 1997}. The study involved 142 normal women; 61 were pre-menopausal and 81 were post-menopausal women. The participants had bone labelling which allowed the measurements of dynamic and static parameters but the study was focussed on bone mineralization assessment.

Osteomalacia is a subtype of ROD characterized by low bone turnover and abnormal mineralization. However, there is no consensus about the exact definition of abnormal mineralization in CKD patients {Ott 2008}. Generally, 2 criteria must be fulfilled using O.Th for static measurement, and MLT *or* OMT for dynamic measurement of mineralization. O.Th > 12.5 µm indicates early abnormal mineralization whereas O.Th > 20 µm indicates established abnormal mineralization {Lima et al 2014; Malluche et al 2011; Ok et al 2016; Parfitt et al 1997; Parfitt et al 2004}. The clinical implications of this difference is unknown. One study used MLT > 50 days {Malluche et al 2011}, but others used MLT > 100 days or OMT > 40 days to define abnormal mineralization {Lima et al 2014; Ok et al 2016; Parfitt et al 1997}. Given all the different thresholds, we pre-specified that O.Th > 20 µm and MLT > 100 days define abnormal mineralization in this study. Based on these strict criteria, none of our patients had abnormal mineralization. This is not unusual as the prevalence of osteomalacia is low (5 - 10%) {KDIGO 2009}. Other studies have also reported the absence of osteomalacia in their cohort {Coen et al 1998; Moore et al 2009; Yessayan et al 2017}.

Although all our patients had normal mineralization status, 7 patients had prolonged MLT > 100 days but normal OMT. One possible explanation for the difference is that MLT takes into account mineralizing surfaces involved whereas OMT does not. In an example of high bone turnover state, more bone mineral units are active and therefore, more bone surfaces are

involved in the process of resorption, formation and mineralization. Hence, MLT becomes shorter in those with high bone turnover as we observed in our study (***Figure 3.5***). Overall, MLT has the advantage of providing a more comprehensive assessment of mineralization but it is very dependent on bone turnover. Meanwhile, OMT was fairly similar across all bone turnover categories in our study. This begs the question of which dynamic parameter (MLT or OMT) is better suited to assess mineralization. Our study has not managed to answer this question given that all our patients had normal O.Th and OMT.

The classification of ROD subtypes is defined mainly by bone turnover and mineralization status. Bone volume assessment is also recommended as patients with low bone volume are expected to have increased risk of fracture {KDIGO 2009; S. Moe et al 2006}. Bone volume correlates well with BMD at other skeletal sites and studies have found that low BMD at the spine, radius and tibia are associated with fracture in CKD {Nickolas et al 2011; West et al 2015}. Osteoporosis can also occur in patients with advanced CKD, so ROD and osteoporosis can co-exist {Cunningham et al 2004; Klawansky et al 2003}. However, there is no evidence so far that low bone volume on iliac crest bone biopsy is associated with fracture.

There is contradicting evidence on the relationship between bone turnover and bone volume {Malluche et al 2012; Schober et al 1998}. In our study, bone volume on histomorphometry had no relationship with bone turnover. This supports the notion that bone volume is a separate entity to low or high bone turnover ROD {Ott 2008}. Risk factors for osteoporosis such as age, gender and corticosteroid use were addressed in this study. We excluded patients taking oral corticosteroid. We also found that bone volume on histomorphometry was not affected by age or gender, although it is known that bone microarchitecture and BMD of other skeletal sites are affected by these factors {Amin et al 2012}.

Despite the lack of relationship between bone volume on histomorphometry and bone turnover, it does not mean that there is no relationship between bone volume at other skeletal sites and bone turnover. High risk fracture sites in CKD-MBD are the hip, lumbar spine and distal bones (wrist and ankle) whereas iliac bone fracture is extremely rare {Wagner et al 2014}. Furthermore, Hiller et al showed that bone volume from trans-iliac bone biopsy is not comparable to bone volume from proximal tibia and lumbar spine bone biopsies {Hiller et al 2017}. Hence, bone volume assessment on bone biopsy may be useful but it may not be representative of other skeletal sites. This limitation is important when interpreting bone biopsy results and deciding on treatment options.

New developments of microCT have opened up possibilities that bone volume assessment of biopsy samples could be done quicker and without sample preparation that is required for histomorphometry. Another advantage of microCT is its ability to measure bone volume of the whole trabecular bone area in a core biopsy sample whereas histomorphometry bone volume assessment is limited to the number of sections prepared to fulfil the minimum acceptable criteria of tissue area. One limitation of microCT is it only detects calcified bone and not osteoid {Pereira et al 2015}. This limitation is particularly important when assessing advanced CKD patients who may have osteomalacia.

In our study where all patients had normal mineralization status, we have shown that bone volume measured on microCT was highly correlated to that measured on histomorphometry. When we compared the two methods, microCT measured lower bone volume compared to histomorphometry but the two methods were interchangeable. Further analysis revealed that the difference was due to lower trabecular number detected by microCT. Meanwhile, no difference was detected for trabecular thickness. These findings are likely due to the

difference in the image resolution of microCT (4.3 μm) and histomorphometry which uses light microscopy (0.4 to 0.7 μm).

Similarly to our results, a study by Uchiyama et al involving 15 adult patients with various metabolic bone diseases showed that bone volume on microCT and histomorphometry were highly correlated (rho ≥ 0.9) {Uchiyama et al 1997}. However, the two methods showed a lower correlation (rho = 0.7) in bone volume in a study involving 68 paediatric dialysis patients where majority of them had osteomalacia {Pereira et al 2015}. This highlights the limitation of microCT as described above. Another study showed that bone volume assessment by histomorphometry and microCT of biopsies from three different skeletal sites (iliac crest, tibia and lumbar spine) were comparable {Hiller et al 2017}. Overall, microCT may be a useful alternative and complimentary tool to assess bone volume.

There are several strengths in our study. We included CKD stages 4-5 and dialysis patients and thus, our findings are applicable to dialysis and non-dialysis advanced CKD. Bone biopsy was performed purely for research rather than for specific clinical indications. Hence, the patients in this study were representative of our clinical experience where most advanced CKD patients with ROD are asymptomatic. All our patients received tetracycline bone labelling which allowed dynamic assessment of bone turnover and mineralization. Finally, the proportion of our patients with low, normal and high bone turnover was similar to previous studies.

There are also several limitations; this was a single centre observational study with a small number of samples evaluable for histomorphometry. All histomorphometry was performed by a single operator and we did not have a second independent assessor to assess intra-observer variability. We selected 5 random histology sections to re-measure osteoid thickness

and mineralization lag time and the measurements performed by the single operator were similar to the initial measurements (data not shown). The initial classification of ROD in those 5 patients did not change. The operator was blinded to participants' characteristics and histomorphometry analysis was semi-automated, thus histomorphometry assessment in this study was unlikely to be subjected to bias.

We used bone biopsy needles with smaller diameter (4 mm). There has been no direct comparison between small (less than 5 mm) and large (7 – 8 mm) diameter bone biopsy samples for the diagnosis of ROD. Previous experience by histopathologists suggested that bone changes such as high or low bone turnover, or abnormal mineralization is usually not subtle in ROD. Hence, samples fulfilling the minimal acceptable tissue area (30 mm^2) in the standard analysis region for histomorphometry is adequate to make a diagnosis of ROD as recommended by the International Bone and Mineral Society {Recker et al 2011}. It is unusual for histomorphometry operators to section a specimen to exhaustion beyond the required minimal acceptable tissue area. One example which may prompt an operator to do extra sections is when there is total absence of tetracycline label in the standard analysis region when the patients have confirmed that tetracycline had been taken as instructed. However, this extended label search is not recommended as the gain of finding the label is small compared to the extra work required and it does not change the diagnosis of low/absent bone turnover {Foldes et al 1990; Recker et al 2011}. Nonetheless, we must acknowledge the limitations of bone biopsy which are universal to any tissue biopsy procedure. This includes sampling error, single site sampling and limited tissue which mean that the sample may not be representative of the whole skeleton.

We did not measure activation frequency (Ac.f) as discussed above and we did not do aluminium staining on the samples. The likelihood of aluminium toxicity in our patients was low because the use of aluminium-based phosphate binders in our centre was extremely rare and modern dialysis water treatment ensured that aluminium exposure was minimised. Importantly, all our patients had normal mineralization status.

To conclude, there was a wide range of bone turnover in advanced CKD patients who had bone biopsy in this study and the proportions of low, normal and high bone turnover patients were similar to previously published studies. All patients had normal bone mineralization and only 16% had low bone volume. Double tetracycline bone labelling is important for the assessment of bone turnover and mineralization in bone biopsy sample. Static parameters are not robust enough to replace the dynamic parameters to classify patients into ROD subtypes. Correct diagnosis is paramount as it can affect treatment decisions and it allows direct comparison between research studies. Ideally, these findings need to be confirmed in bigger studies using similar patient population but bone biopsy studies have its challenges. This work supports the call for a consensus on normal ranges for static and dynamic parameters of bone turnover and mineralization which are not yet fully defined.

Chapter 4. Bone Microstructure in Advanced CKD

4.1 Introduction

CKD patients have increased risk of fracture which is associated with increased morbidity and mortality. Moderate to severe CKD is associated with a two-fold increase in hip fracture risk as shown by the Third NHANES data involving over 6000 participants {Nickolas et al 2006}. A large observational study, Dialysis Outcomes and Practice Pattern Study (DOPPS), showed that fracture risk is even higher in dialysis patients. DOPPS, which involved nearly 35,000 haemodialysis patients, showed an excess fracture risk of 3-8 fold compared to the general population {Tentori et al 2014}. The incidence of fracture in dialysis population is 150 – 450 fractures per 10,000 patient-years whereas the incidence is 40 – 100 fractures per 10, 000 person-years in the general population {Curtis et al 2016; Tentori et al 2014}. Furthermore, mortality and re-hospitalisation rates are also increased 2-9 times in the first year after a fracture compared to the overall haemodialysis population {Tentori et al 2014}.

This increased risk of fracture in advanced CKD is due to a combination of poor bone quality due to ROD and low BMD. ROD is associated with bone microstructural, material and nanomechanical abnormalities leading to poor bone strength {Malluche et al 2012}. Bone microstructure also worsens with worsening CKD such that dialysis patients have thinner cortical bone compared to pre-dialysis CKD {Carvalho et al 2016}. Even in patients with stable CKD over 2-years (i.e. already on dialysis or with little CKD progression), BMD and bone microstructure worsens with time {Malluche et al 2017; Nickolas et al 2013; West et al 2015}. This indicates that prolonged exposure to CKD-MBD biochemical abnormalities such as SHPT results in bone loss and those patients who subsequently fractured had even greater bone loss.

Although low BMD can be detected by DXA, some of the bone changes associated with ROD such as bone microstructural impairment could only be detected using high resolution bone imaging. A meta-analysis of 13 studies in CKD stages 3-5D showed that BMD was significantly lower in patients with fractures compared to those without fractures, independent of dialysis status {Bucur et al 2015}. Nickolas et al also showed that advanced CKD patients with fracture not only had lower BMD but also worse bone microstructure at the distal radius and tibia as measured by HR-pQCT {Nickolas et al 2010}. However, Cejka et al showed that BMD by DXA was not associated with fracture but bone microarchitecture was, especially of distal tibia {Cejka, Patsch, et al 2011}. This highlights that BMD alone may not identify patients with increased fracture risk. This could be because the magnitude of difference in BMD is not as large as the difference in bone microstructure between patients who had fracture and those without fracture {Nickolas et al 2010}.

Trabecular bone score (TBS) is a grey-level index derived from lumbar spine (LS) DXA images and may give a better estimate of trabecular microstructure in the LS vertebrae {Pothuaud et al 2008}. A study in moderate CKD patients suggests that fracture risk was associated with TBS but not BMD {Naylor et al 2016}. However, it is well known that LS BMD is often over-estimated in advanced CKD who have high prevalence of abdominal aortic calcification (AAC). Whether TBS is equally affected as LS BMD by AAC severity in this population needs further evaluation.

Bone biopsy from iliac bone is the gold standard test to diagnose ROD. Classically, bone turnover and mineralization status on biopsy were used to classify ROD subtypes. In 2009, the KDIGO CKD-MBD guideline recommended that bone volume assessment is included in bone biopsy analyses and this is known as the TMV (turnover, mineralization and volume)

classification {KDIGO 2009}. The recommendation was made because patients with low bone volume on bone biopsy is also thought to have increased risk of fracture. However, bone biopsy is invasive and painful. Bone imaging could be a non-invasive alternative to bone biopsy but the exact relationship between iliac bone microstructure and bone microstructure elsewhere is not entirely certain.

The main aims of this chapter were to assess bone microstructure in advanced CKD and to assess if bone imaging could be a non-invasive alternative to bone volume assessment on biopsy.

4.2 Methodology

4.2.1 Bone Imaging

Recruitment of participants and bone imaging methods using DXA and HR-pQCT have been described in Chapter 2 of this thesis. AAC assessment using lateral LS DXA has also been described to assess its impact on LS BMD and TBS.

TBS values were obtained using LS DXA images using TBS iNsight software (version 3.0.2.0, Medimaps, Pessac, France). TBS is based on the pixel gray-level variations in the DXA image using the same LS BMD region of interest (***Figure 4.1***). A two-dimensional projection image of a porous trabecular structure has a low number of gray-level variations of high amplitude, whereas the projection of a well-structured trabecular bone produces an image with a large number of gray-level variations of small amplitude. TBS was derived from an experimental variogram of those projected images, calculated as the sum of the squared gray-level differences between pixels at a specific distance and angle. TBS was then calculated as the

slope of the log-log transform of the variogram {Pothuaud et al 2008}. TBS was calculated as the mean value of the individual measurement of vertebrae L1 - L4. TBS has a short-term *in vivo* precision of 1.4 - 2.1% {Briot et al 2013; Hans et al 2011}. Participants in this study were divided into three TBS categories; TBS < 1.23 which is associated with high risk, TBS between 1.23 and 1.31 which is associated with moderate risk and TBS > 1.31 which is associated with low risk of major osteoporotic fracture {McCloskey et al 2016}.

Figure 4.1

Examples of gray-level variations detected by TBS software. Taken from https://www.medimapsgroup.com

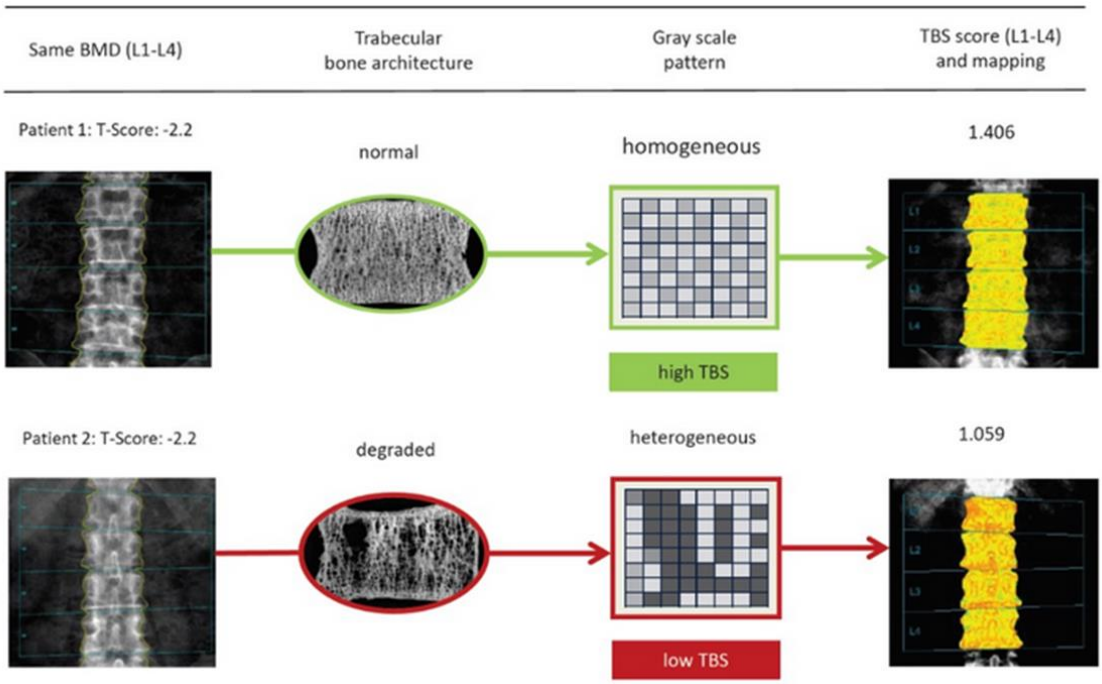

4.2.2 Statistical Analysis

In this chapter, we divided participants into low BMD and normal BMD groups based on areal BMD T-score for TH and 1/3 radius measured by DXA. According to WHO criteria, osteoporosis is defined by BMD T-score < -2.5 and osteopenia is defined by BMD T-score between -1.0 and -2.5. Low BMD group in this study had T-score < -1.0 (i.e. osteopaenia and osteoporosis) and normal BMD group had T-score ≥ -1.0.

Statistical analysis used in this chapter have been described in Chapter 2. Data are presented as mean (standard deviation, SD) or median (interquartile range, IQR). Group differences were tested using Student t test for continuous variables with normal distribution, Mann-Whitney U test for continuous variables with skewed distribution and Chi squared test for categorical variables. We used Pearson's correlation to test the relationship between two continuous variables. ROC analysis was used to test diagnostic accuracy of bone imaging measurements using DXA and HR-pQCT to identify CKD patients with low bone volume on trans-iliac bone biopsy.

4.3 Results

4.3.1 Participants' Demographics

69 advanced CKD stages 4-5D patients and 68 age and gender-matched control participants were recruited into the study. Demographics of each group are shown in ***Table 4.1***. There were 44 pre-dialysis CKD stages 4-5 patients with median (IQR) eGFR of 13 (11 - 16) ml/min/1.73m^2 and 25 dialysis patients (haemodialysis and peritoneal dialysis). Median (IQR) eGFR for controls was 81 (72 to >90) ml/min/1.73m^2.

4.3.2 Bone Microstructure in CKD and Controls

On HR-pQCT, CKD patients had lower total, cortical and trabecular volumetric BMD at the distal radius and distal tibia compared to controls (***Table 4.1***). CKD patients also had thinner trabeculae and lower trabecular bone volume (bone volume/tissue volume [BV/TV]) at both sites. Additionally, CKD patients had thinner cortical bone at the distal tibia.

Mean total hip (TH) BMD T-score by DXA was significantly lower in CKD compared to controls. However, BMD T-score for 1/3 radius and lumbar spine (LS) were similar in CKD and controls. The number of CKD patients and controls with normal BMD (T-score ≥ -1.0) and low BMD (T-score < -1.0) for TH and 1/3 radius are shown in ***Figure 4.2***.

LS BMD by DXA was likely to have been overestimated in CKD as 48% (N=33) had AAC detected. Meanwhile, only 22% (N=15) of controls had AAC detected and they had significantly lower AAC score compared to CKD (1.04 [0.05 - 16.52] in CKD versus 0 [0 - 0.55] mgHA in controls, p<0.001).

Table 4.1

Demographics and imaging parameters in CKD patients and control participants.

Variables	CKD (N=69)	Control (N=68)	p values
Age, years	62 (12)	62 (12)	
Male, N	53	53	
BMI (kg/m^2)	27 (4.1)	28 (4.3)	0.3
Diabetes	28%	0%	**<0.001**
Previous fragility fracture	22%	7%	**<0.05**
HRpQCT distal radius			
Total vBMD (mg/cm^3)	266.2 (75.56)	308.47 (74.2)	**0.003**
Cortical vBMD (mg/cm^3)	782.58 (110.66)	821.04 (88.7)	**0.04**
Trabecular vBMD (mg/cm^3)	156.69 (46.17)	184.6 (41.42)	**0.001**
Cortical thickness (mm)	0.61 (0.27)	0.71 (0.26)	0.06
Cortical porosity (%)	3.0 (2.3 – 4.2)	3.2 (2.0 – 3.8)	0.4
Cortical BV/TV (%)	90.0 (85.4 – 92.1)	90.7 (88.6 – 93.4)	0.1
Trabecular thickness (mm)	0.064 (0.012)	0.073 (0.013)	**<0.001**
Trabecular number (1/mm)	2.01 (0.363)	2.11 (0.296)	0.14
Trabecular separation	0.434 (0.371 – 0.496)	0.4 (0.349 – 0.443)	0.06
Trabecular BV/TV (%)	13.1 (3.8)	15.4 (3.5)	**0.001**
HRpQCT distal tibia			
Total vBMD (mg/cm^3)	276.99 (63.67)	314.97 (61.2)	**0.001**
Cortical vBMD (mg/cm^3)	819.85 (88.67)	858.7 (67.89)	**0.005**
Trabecular vBMD (mg/cm^3)	172.12 (41.06)	189.99 (41.12)	**0.01**
Cortical thickness (mm)	1.05 (0.36)	1.25 (0.35)	**0.001**
Cortical porosity (%)	7.1 (5.7 – 10.4)	6.8 (4.7 – 10.3)	0.2
Cortical BV/TV (%)	86.2 (6.0)	88.1 (4.9)	0.05
Trabecular thickness (mm)	0.075 (0.014)	0.081 (0.013)	**0.01**
Trabecular number (1/mm)	1.92 (0.35)	1.97 (0.4)	0.4
Trabecular separation	0.444 (0.395 – 0.522)	0.425 (0.359 – 0.523)	0.2
Trabecular BV/TV (%)	14.3 (3.4)	15.8 (3.4)	**0.01**
DXA BMD T-score			
Total hip	-0.9 (1.0)	-0.1 (1.1)	**<0.001**
1/3 radius	-1.0 (1.5)	-0.8 (1.5)	0.4
Lumbar spine	-0.4 (1.7)	-0.4 (1.6)	0.98
LS TBS	1.28 (0.14)	1.32 (0.14)	0.1

Figure 4.2

The number of CKD and controls with normal and low BMD measured by DXA.

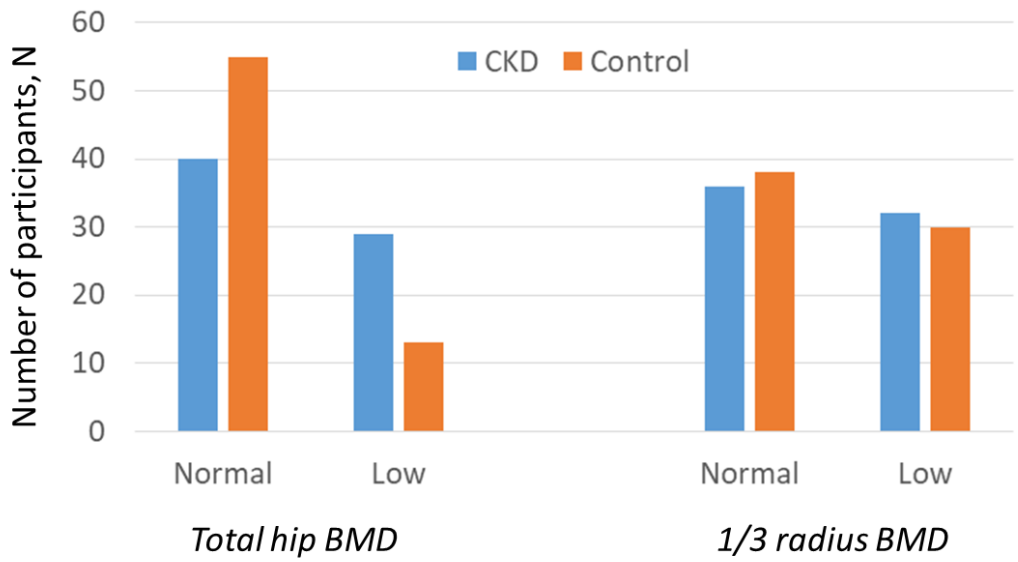

Mean TBS from lumbar spine DXA was also similar in CKD and controls but there were more CKD patients with low TBS (TBS < 1.23) compared to controls (***Figure 4.3***). TBS positively correlated with LS BMD T-score in both groups (Pearson's rho = 0.475, p<0.001 in CKD and rho = 0.451, p<0.001 in controls). We also found that TBS positively correlated with LS BMD T-score in CKD patients with AAC (N= 32, rho = 0.499, p=0.004) and without AAC (N= 32, rho 0.425, p<0.05). Meanwhile in the control group, TBS correlated with LS BMD T-score only in controls without AAC (N=52, rho = 0.51, p<0.001). No associations were found between TBS and AAC in CKD and controls.

TBS in CKD correlated weakly with TH BMD T-score (rho = 0.248, p<0.05) but not with 1/3 radius BMD T-score (rho = 0.220, p=0.07). TBS in the control group positively correlated with BMD T-score at both sites (rho = 0.355, p<0.01 for TH and rho = 0.368, p<0.01 for 1/3 radius).

Figure 4.3

The number of CKD and control participants based on TBS categories.

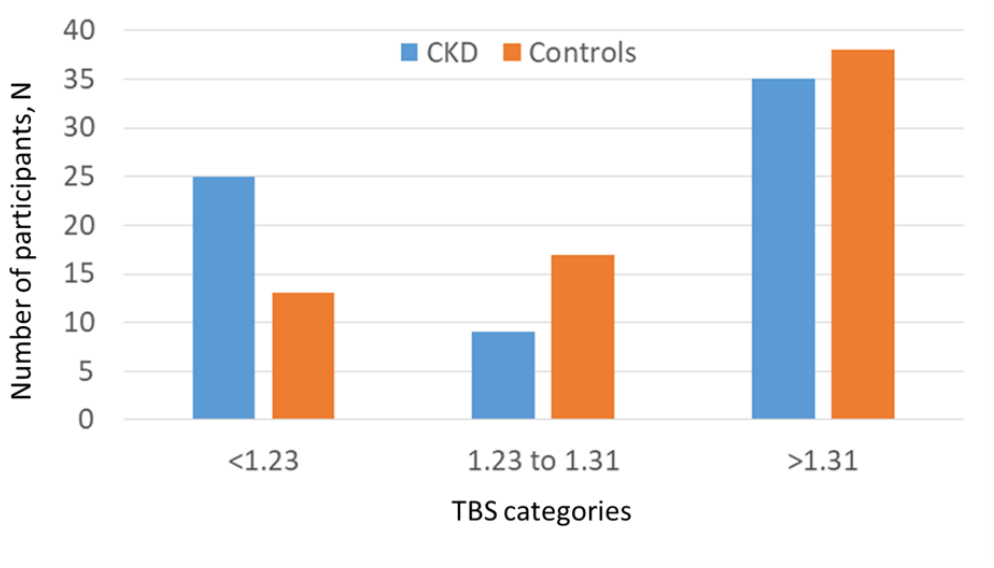

4.3.3 Bone Microstructure in CKD patients with Low BMD on DXA

TH and 1/3 radius BMD T-scores on DXA were positively correlated in CKD (rho = 0.494, p<0.001) (**Figure 4.4**). CKD patients with low TH BMD (T-score < -1.0) had worse trabecular microstructure at distal radius measured by HR-pQCT compared to those with normal TH BMD; there were thinner trabeculae and lower trabecular number (**Table 4.2**). There was no difference in distal radius cortical bone microstructure. CKD with low TH BMD also had worse bone microstructure at the distal tibia affecting both trabecular and cortical bone compartments. There were lower trabecular number and thinner trabeculae as well as thinner and more porous cortical bone.

Table 4.2

Differences in bone microstructure measured by HR-pQCT between CKD patients with normal and low TH BMD on DXA

Variables	Normal TH BMD	Low TH BMD	p values
Number of patients, N	40	29	
HRpQCT distal radius			
Total vBMD (mg/cm^3)	290 (70)	236 (72)	<0.01
Cortical vBMD (mg/cm^3)	800 (96)	760 (125)	NS
Trabecular vBMD (mg/cm^3)	179 (38)	129 (41)	<0.001
Cortical thickness (mm)	0.67 (0.27)	0.55 (0.26)	NS
Cortical porosity (%)	3.0 (2.3 to 4.2)	3.2 (1.9 to 4.3)	NS
Cortical BV/TV (%)	90.8 (85.7 to 92.5)	89.8 (84.8 to 91.1)	NS
Trabecular thickness (mm)	0.069 (0.011)	0.058 (0.011)	0.001
Trabecular number (1/mm)	2.12 (0.25)	1.82 (0.40)	<0.001
Trabecular separation (mm)	0.403 (0.348 to 0.445)	0.496 (0.409 to 0.547)	<0.001
Trabecular BV/TV (%)	14.9 (3.2)	10.7 (3.4)	<0.001
HRpQCT distal tibia			
Total vBMD (mg/cm^3)	306 (53)	239 (57)	<0.001
Cortical vBMD (mg/cm^3)	849 (74)	781 (92)	<0.01
Trabecular vBMD (mg/cm^3)	189 (33)	150 (40)	<0.001
Cortical thickness (mm)	1.20 (0.32)	0.86 (0.31)	<0.001
Cortical porosity (%)	6.4 (5.1 to 8.9)	8.9 (6.3 to 12.2)	<0.05
Cortical BV/TV (%)	88.0 (5.7)	84.2 (6.0)	<0.05
Trabecular thickness (mm)	0.078 (0.012)	0.071 (0.016)	<0.05
Trabecular number (1/mm)	2.03 (0.34)	1.77 (0.32)	<0.01
Trabecular separation (mm)	0.426 (0.355 to 0.500)	0.476 (0.434 to 0.571)	<0.01
Trabecular BV/TV (%)	15.8 (2.8)	12.5 (3.3)	<0.001

Figure 4.4

The relationship between total hip and 1/3 radius BMD T-scores in CKD.

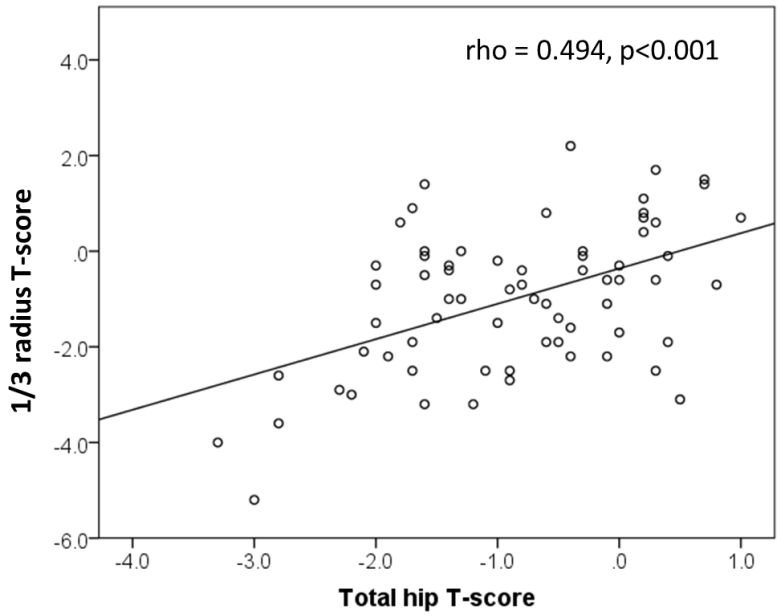

CKD patients with low 1/3 radius BMD (T-score < -1.0) had thinner cortical bone and lower trabecular number at the ultradistal radius when measured by HR-pQCT compared to CKD with normal BMD (***Table 4.3***). There was no difference in cortical porosity or trabecular thickness. CKD patients with low 1/3 radius BMD also had worse bone microstructure in both the trabecular and cortical bone compartments of the distal tibia measured by HR-pQCT. The trabecular number was lower and cortical bone was thinner and more porous. The relationship between LS DXA BMD T-score and bone microstructure at distal radius and tibia in CKD was not analysed because of high percentage of CKD patients with AAC present.

Table 4.3

Differences in BMD and microstructure measured by HR-pQCT between CKD with normal and low 1/3 radius BMD.

Variables	Normal 1/3 radius BMD	Low 1/3 radius BMD	p values
Number of patients, N	36	32	
HRpQCT distal radius			
Total vBMD (mg/cm^3)	290 (76)	242 (68)	<0.05
Cortical vBMD (mg/cm^3)	813 (95)	754 (118)	<0.05
Trabecular vBMD (mg/cm^3)	173 (42)	141 (45)	<0.01
Cortical thickness (mm)	0.69 (0.27)	0.54 (0.25)	<0.05
Cortical porosity (%)	2.9 (1.7 to 4.2)	3.1 (2.6 to 4.3)	NS
Cortical BV/TV (%)	90.0 (86.5 to 92.4)	89.2 (83.6 to 91.1)	NS
Trabecular thickness (mm)	0.066 (0.011)	0.063 (0.013)	NS
Trabecular number (1/mm)	2.18 (0.24)	1.86 (0.39)	<0.001
Trabecular separation (mm)	0.402 (0.348 to 0.495)	0.473 (0.399 to 0.540)	0.001
Trabecular BV/TV (%)	14.4 (3.5)	11.8 (3.8)	<0.01
HRpQCT distal tibia			
Total vBMD (mg/cm^3)	294 (59)	258 (65)	<0.05
Cortical vBMD (mg/cm^3)	859 (70)	779 (88)	<0.001
Trabecular vBMD (mg/cm^3)	176 (38)	167 (45)	NS
Cortical thickness (mm)	1.18 (0.32)	0.93 (0.35)	<0.01
Cortical porosity (%)	6.1 (5.0 to 8.5)	8.9 (6.4 to 11.5)	<0.01
Cortical BV/TV (%)	88.3 (5.2)	84.1 (6.2)	<0.01
Trabecular thickness (mm)	0.073 (0.014)	0.077 (0.014)	NS
Trabecular number (1/mm)	2.02 (0.32)	1.79 (0.37)	<0.01
Trabecular separation (mm)	0.443 (0.377 to 0.499)	0.498 (0.399 to 0.559)	<0.05
Trabecular BV/TV (%)	14.7 (3.1)	13.9 (3.8)	NS

4.3.4 Relationship between Bone Microstructure on Bone Biopsy and Bone Imaging

43 out of 69 CKD patients had trans-iliac bone biopsy evaluable for histomorphometry. Trabecular bone volume/tissue volume (BV/TV) on bone biopsy was similar in males and females and there was no association with age. Bone biopsy BV/TV positively correlated with TH T-score (rho = 0.368, p<0.05) but no correlation was found with 1/3 radius T-score.

CKD patients with low TH BMD measured by DXA had lower trabecular BV/TV on biopsy compared to patients with normal TH BMD (19.3 [16.2 - 22.1] and 23.6 [19.2 - 30.9] % respectively, p<0.01) (***Figure 4.5***). This is due to thinner trabeculae on bone biopsy (0.135 [0.029] mm versus 0.156 [0.031] mm, p<0.05) but trabecular number was similar to those with normal TH BMD. Bone biopsy trabecular BV/TV, trabecular thickness and trabecular number did not correlate with bone microstructure of distal radius and tibia measured by HR-pQCT.

Figure 4.5

Bone volume and trabecular thickness in bone biopsy samples from CKD patients with normal and low total hip BMD measured by DXA.

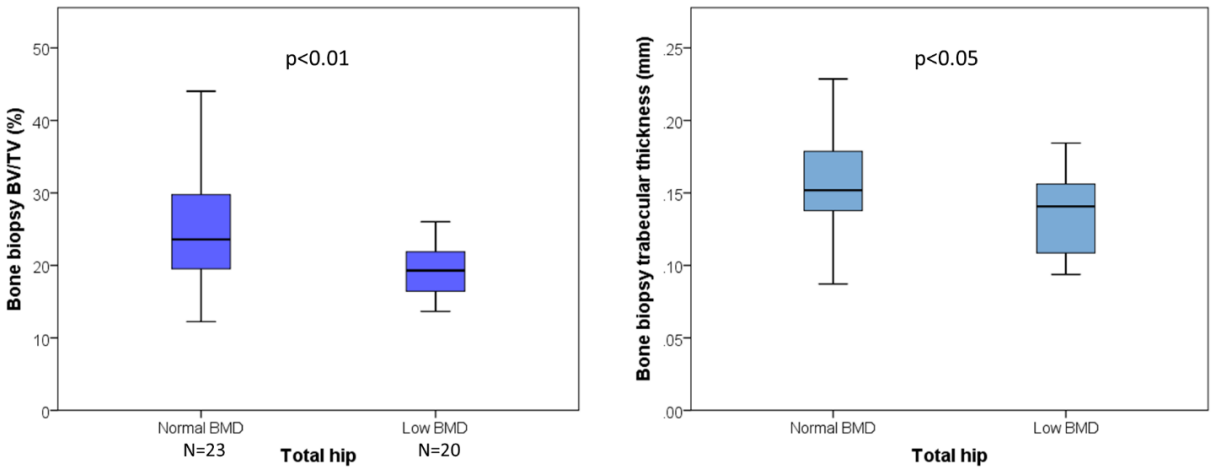

Seven out of 43 patients (16%) had low trabecular BV/TV defined by BV/TV < 16.8% on bone biopsy. ROC analysis showed that TH T-score by DXA had an AUC (95% CI) of 0.692 (0.533 - 0.824) for identifying patients with low BV/TV. The Youden criterion for TH T-score was ≤ -0.4 which had 100% sensitivity, 40% specificity, 24% positive predictive value (PPV) and 100% negative predictive value (NPV) for identifying patients with low BV/TV on biopsy. AUC for 1/3 radius T-score was not significant.

On HR-pQCT, only cortical porosity had significant AUCs for identifying CKD with low BV/TV on bone biopsy; AUC (95% CI) of 0.722 (0.548 - 0.858) for distal radius and 0.690 (0.528 - 0.823) for distal tibia. In comparison of ROC curves analysis, AUCs for TH T-score and cortical porosity by HR-pQCT were similar ($p>0.05$). ROC analysis was also performed using the combined TH T-score and cortical porosity to determine if the AUCs could be improved. This revealed exactly the same AUCs as that of cortical porosity at the distal radius and tibia.

4.4 Discussion

We found that advanced CKD patients have lower BMD and worse bone microstructure when compared to age and gender-matched healthy controls. This is consistent with findings in studies involving pre-dialysis CKD and dialysis patients. Bachetta et al examined 70 patients with CKD stages 2 - 4 using HR-pQCT and compared them with gender and age-matched population-based cohorts who had normal renal function {Bacchetta et al 2010}. The study found that even mild to moderate CKD patients had trabecular and cortical bone impairment such as less trabeculae and thinner cortical bone. These bone microstructure impairment are also found in dialysis patients and are often more severe than those in pre-dialysis CKD {Carvalho et al 2016; Cejka, Patsch, et al 2011; Negri et al 2012}.

Trabecular bone impairment could be due to thinning of trabeculae, loss of trabecular number or both {Khosla et al 2006}. Greater bone resorption than bone formation in bone remodelling underlies these abnormalities. The lower trabecular BMD and bone volume in advanced CKD in this study is due to thinner trabeculae rather than lower trabecular number. This finding was consistent at the distal radius and tibia although PTH effects on bone usually result in both thinner trabeculae and lower trabecular number {Stein et al 2013}. Our study also showed that cortical bone thinning in CKD only occurs at the tibia but not at the radius. This could be due to higher mechanical force going through the tibia compared to the radius, thus the tibial cortical bone is thicker and can be more accurately measured {Frank et al 2012}.

When BMD was measured by DXA in our study, only TH BMD T-score was lower in CKD than control. There was no difference at the other two skeletal sites between CKD and control. Our finding is similar to a study by Negri et al which showed that dialysis patients had significantly lower TH BMD T-score but not for 1/3 radius when compared to age- and gender- matched controls {Negri et al 2012}. However, they found that LS BMD T-score was also lower in dialysis patients. In contrast to our study and Negri et al study, Urena et al showed that dialysis patients had significantly lower BMD at mid radius but not at the femoral neck or LS when compared to age- and gender-matched population {Urena et al 2003}. Therefore, low BMD in advanced CKD is not consistent across all skeletal sites measured by DXA. Similar to our study, the studies by Negri et al and Urena et al recruited patients with a wide range of iPTH and ALP. Thus, it is uncertain if high bone turnover associated with SHPT would be more likely to have lower BMD at certain skeletal sites only.

Similar BMD T-score at 1/3 radius was observed in our CKD and controls despite significant differences in BMD by HR-pQCT at the distal radius. This contrasting finding is likely due to

the different bone types at these two different locations within the radius. The 1/3 radius measured by DXA mainly consists of cortical bone (greater than 90%) whereas ultradistal radius measured by HR-pQCT has less cortical bone (around 75%) {Wahner et al 1985}. We have demonstrated on HR-pQCT of distal radius that trabecular bone was significantly impaired in CKD whereas cortical bone measurements were similar in both groups, consistent with similar BMD at 1/3 radius measured by DXA. Similar BMD at LS in CKD and controls in this study was probably due to the overestimation of BMD in CKD who have AAC. DXA is a 2-dimensional imaging which cannot differentiate increased density detected from bone or other extra-skeletal calcification such as vascular calcification. It is well known that AAC predisposes to artefactual overestimate of LS BMD {Drinka et al 1992}.

Spine TBS may give a better estimate of trabecular microstructure in the LS vertebrae than BMD as shown in a study by Krueger et al involving 429 non-CKD women {Krueger et al 2014}. The study showed that TBS and LS BMD were weakly correlated but TBS of 1.30 identified 70% of women with fracture who did not have osteoporosis when assessed by BMD. The Canadian Multicentre Osteoporosis Study (CaMOS) also showed that TBS is associated with higher fracture risk in those with moderate CKD, independent of BMD {Naylor et al 2016}. A meta-analysis by McCloskey et al which utilized data from nearly 18,000 participants showed that TBS < 1.23 was associated with highest risk of major osteoporotic fracture {McCloskey et al 2016}. The studies did not involve advanced CKD but some had studied the effect of age on bone. Therefore, some participants may have had mild to moderate CKD. In our study, more CKD patients had TBS < 1.23 compared to controls despite similar mean TBS in the two groups. Meanwhile, other studies have reported lower TBS in dialysis patients compared to healthy controls {Yavropoulou et al 2017; Yoon et al 2018}.

TBS was positively associated with LS BMD in this study but no relationship was found between TBS and AAC score. Meanwhile, a study by Aleksova et al involving 146 patients with CKD stages 5-5D showed that TBS was positively associated with LS BMD and inversely associated with AAC score {Aleksova, Kurniawan, & Elder 2018; Aleksova, Kurniawan, Vucak-Dzumhur, et al 2018}. Further study is needed to confirm the exact relationship between TBS and LS bone microstructure in advanced CKD population who have high prevalence and more severe AAC.

DXA BMD T-score (rather than absolute BMD value) is reported widely in clinical practice to determine if an individual has normal or low BMD. T-score is the number of standard deviation that individual's BMD is above or below the mean of 30-year old men/women. According to WHO criteria, osteoporosis is defined by BMD T-score < -2.5 and osteopenia is defined by BMD T-score between -1.0 and -2.5. Rather than reporting on associations between BMD T-score and bone microstructure as previously reported by other studies, we explored the difference in bone microstructure in CKD with normal (T-score ≥ -1.0) and low BMD (T-score < -1.0). We found that CKD patients with low BMD at the hip or 1/3 radius also had worse bone microstructure at the radius and tibia. Cortical bone tended to be thinner and more porous, and trabecular bone tended to be thinner and there were less trabeculae. Thus far, our results suggest that there were significant bone microstructure abnormalities in patients who have low BMD by DXA.

Bone volume assessment is recommended by the KDIGO CKD-MBD guideline in addition to bone turnover and mineralization assessment of bone biopsy to diagnose ROD. Meanwhile, the usual fracture sites for CKD are the hip, vertebrae, wrist and ankle but pelvic bone fracture (i.e. bone biopsy site) is extremely rare. Thus, clinical relevance of bone volume assessment

on biopsy is questionable. However, we have shown that there is a positive relationship between iliac bone biopsy trabecular bone volume and TH BMD T-score. Further analysis showed that patients with low TH BMD T-score had low iliac bone volume due to thinner trabeculae and not because of lower trabecular number. In contrast, a study by Adragao et al involving 38 haemodialysis patients showed that femoral neck BMD by DXA was not associated with trabecular bone volume of iliac bone biopsy {Adragao et al 2010}. This difference may be because Adragao et al measured femoral neck BMD and our study measured TH BMD. TH BMD measurement is known to have lower precision error and smaller BMD change with hip rotation compared to femoral neck BMD {Rosenthall 2004}. A study by Cohen et al in non-CKD patients showed that TH BMD and iliac bone volume had similar association as shown in our study {Cohen et al 2010}.

Despite the relationship between trabecular bone volume on bone biopsy and TH BMD T-score, we found that there was no relationship between bone volume on biopsy and BMD or bone microstructure of the peripheral bones (distal radius and tibia). A study by Cohen et al examined 54 non-CKD adults and showed that trabecular bone volume on bone biopsy was only modestly associated with trabecular bone microstructure of distal radius on HR-pQCT (rho = 0.3) {Cohen et al 2010}. Marques et al examined 31 CKD patients who were mostly on dialysis and have SHPT, and also found only modest associations between trabecular bone structure on biopsy and trabecular microstructure of distal radius by HR-pQCT {Marques et al 2017}. Our results indicate that bone microstructure on bone biopsy and HR-pQCT of peripheral bones correlate poorly which may be due to the different functions of these bones. The tibia, and to a lesser extent the radius, are load-bearing bones whereas the iliac crest is non-weight bearing.

The proportion of our CKD patients with low bone volume on bone biopsy is the same as in the study by Adragao et al which indicated that CKD patients in our study was representative of advanced CKD population {Adragao et al 2010}. Our CKD participants were enrolled purely for research and not for any medical indications such as bone pain or unexplained fracture. We also used the same cut off value of BV/TV < 16.8% as Adragao et al to diagnose low trabecular bone volume on biopsy. This cut off value was taken from historical histomorphometric results of 84 normal individuals published by Malluche et al {Malluche et al 1982}. We found that TH BMD T-score could identify patients with low bone volume on bone biopsy but the AUC was < 0.80 which meant that TH BMD T-score is not robust enough as a clinical diagnostic test. A study by Blomquist et al involving 46 dialysis patients reported that TH BMD had AUC of 0.75 to identify patients with low bone volume on bone biopsy {Blomquist et al 2015}. It should be noted that 80% of patients in that study were assessed as having low bone volume on bone biopsy and it was based on qualitative assessment rather than quantitative histomorphometry.

Cortical porosity measurement using HR-pQCT could also identify patients with low bone volume on biopsy in our study. Again, the AUCs were < 0.80 and thus, not robust enough as an alternative to bone biopsy. The diagnostic accuracies of TH BMD by DXA and cortical porosity measurements by HR-pQCT were similar and combining the two imaging techniques did not improve their diagnostic accuracy. This is important because it shows that HR-pQCT did not perform better than DXA in identifying advanced CKD with low bone volume on biopsy. Overall, both imaging techniques are still not robust enough to replace trans-iliac bone biopsy but this may be due to the fact that we were scanning bone sites (peripheral skeleton) which were away from the biopsy site (axial skeleton). Furthermore, Hiller et al also

showed in a small study of 12 cadavers that there was significant intra-individual heterogeneity of bone microstructure from one bone site to another {Hiller et al 2017}.

This study has several limitations. We had small sample size for CKD patients with bone biopsy data but nonetheless, we have shown that the proportion of patients with low bone volume was similar to other study. We did not perform quantitative computed tomography (QCT) of LS vertebrae to determine its BMD separate from AAC. Lateral LS DXA was performed but we did not measure LS BMD using these lateral view images. Although this has been done in previous studies to separate LS BMD from AAC, anterior-posterior view of LS images is the gold standard for measuring BMD by DXA and lateral view can under-estimate BMD {Toussaint et al 2010}. We analysed the results of our pre-dialysis and dialysis patients together although dialysis patients may have worse bone microstructure {Carvalho et al 2016}. Furthermore, our dialysis patients included haemodialysis (HD) and peritoneal dialysis (PD) patients; and HD patients may have worse bone microarchitecture than PD patients {Pelletier et al 2012}. However, analysing the subgroups would have resulted in small numbers and thus, our findings need to be interpreted in the context of CKD stages 4-5D.

This study also has several strengths; we were able to show the difference between bone microstructure in advanced CKD and their age and gender-matched healthy controls. We simultaneously performed bone imaging using DXA and HR-pQCT and thus were able to show the relationship between the different bones in CKD. Finally, we performed bone biopsy, which is an invasive procedure, in asymptomatic patients who were representative of most advanced CKD patients in clinical practice.

Conclusion, TH BMD T-score by DXA is associated with bone microstructural impairment in advanced CKD. CKD patients with low TH BMD have lower BMD and worse bone

microstructure in the peripheral skeleton and lower bone volume on trans-iliac bone biopsy. Bone imaging is currently not robust enough to be an alternative to bone volume assessment on bone biopsy despite the improvement in imaging techniques.

Chapter 5. Diagnostic Accuracy of Bone Turnover Markers and Bone Imaging to diagnose Renal Osteodystrophy

This work has been peer reviewed and published as "Diagnostic Accuracy of Biomarkers and Imaging for Bone Turnover in Renal Osteodystrophy". Syazrah Salam, Orla Gallagher, Fatma Gossiel, Margaret Paggiosi, Arif Khwaja, Richard Eastell. J Am Soc Nephrol. 2018 May;29(5):1557-1565. doi: 10.1681/ASN.2017050584.

5.1 Introduction

ROD is characterized by abnormal bone turnover, mineralization and volume which can only be assessed on bone histomorphometry (gold standard test) {KDIGO 2009}. However, bone biopsy is invasive and rarely performed due to patients' reluctance or limited expertise in the procedure and bone histomorphometry. Hence, current clinical practice still relies on iPTH although it has been shown to have low sensitivity and specificity to assess bone turnover {F. C. Barreto et al 2008; Herberth et al 2009; Sprague et al 2016}. The poor diagnostic accuracy of iPTH limits its use to guide therapies that target BMD or bone turnover.

Very high levels of both bALP and iPTH are strongly predictive of high bone turnover in CKD {Bervoets et al 2003; Coen et al 1998; Couttenye et al 1996; Fletcher et al 1997; Lehmann et al 2008; Sprague et al 2016; Urena et al 1996}. However, bALP has better predictive ability than iPTH for low bone turnover {Bervoets et al 2003; Couttenye et al 1996; Sprague et al 2016; Urena et al 1996}. There are other bone turnover biomarkers which are directly released during the process of bone resorption (e.g. collagen type 1 cross-linked C-telopeptide [CTX] and tartrate-resistant acid phosphatase 5b [TRAP5b]) and bone formation (e.g. procollagen type I N-terminal propeptide [PINP]), thus are potentially more accurate in assessing bone turnover in CKD.

The changes in BMD and microarchitecture associated with high or low bone turnover cannot be adequately assessed by DXA which is a 2-dimensional imaging technique {Nickolas et al 2013}. However, HR-pQCT can detect microstructural changes in both the cortical and trabecular bone compartments. Previous studies using HR-pQCT showed that CKD patients had thinner cortical bone and lower trabecular bone volume compared to healthy controls {Bacchetta et al 2010; Cejka, Patsch, et al 2011; Negri et al 2012}.

The emergence of bone biomarkers and HR-pQCT offer the possibility of replacing bone biopsy, but their diagnostic accuracy for predicting bone turnover in advanced CKD is unknown. We aimed to simultaneously test if biomarkers and HR-pQCT can identify advanced CKD patients with low and high bone turnover as shown on histomorphometry. We also tested whether these non-invasive tests have better diagnostic accuracy than iPTH.

5.2 Methodology

5.2.1 Study Design and Population

This was a cross-sectional study in CKD stages 4 - 5 (including dialysis) patients, aged 30-80 years old. The exclusion criteria included fracture/orthopaedic surgery in the preceding six months; started/changed the dose of phosphate binders, vitamin D or calcimimetics within four weeks of study entry; and received anti-resorptive, anabolic agent or systemic glucocorticoid in the preceding six months. All patients attending our Nephrology centre who fulfilled the inclusion and exclusion criteria were invited to take part in the study. We also recruited age- and gender-matched controls with estimated glomerular filtration rate (eGFR) ≥60 ml/min/1.73m^2. The exclusion criteria were similar to CKD group and we also excluded participants with known osteoporosis. The study adhered to the *Declaration of Helsinki* and was approved by the South Yorkshire Research Ethics Committee. All participants gave written informed consent. All samples and imaging studies were obtained purely for research and are summarised below. The full methodology is described in Chapter 2 of this thesis.

5.2.2 Bone Biomarkers

Fasting morning blood samples were taken, stored at -80^{0}C and analysed at the end of the study. For haemodialysis patients, blood samples were taken on the day after their haemodialysis session. We measured serum iPTH, bALP, intact PINP, CTX, TRAP5b and 25-hydroxyvitamin D using the IDS-iSYS auto-analyser (Immunodiagnostic Systems, United Kingdom). Total PINP was measured using the Cobas e411 automated immunoassay (Roche Diagnostics, Germany). We measured fasting serum calcium, phosphate, total alkaline phosphatase (tALP) and creatinine on Roche Cobas c701/702 analyser (Roche Diagnostics, England) on the same day as sample collection. eGFR was calculated using the Modification of Diet in Renal Disease (MDRD) equation.

5.2.3 Bone Imaging

HR-pQCT of the distal radius and tibia were performed using XtremeCT (Scanco Medical AG, Switzerland) using a standard protocol. The images were analysed with standard software (Scanco Medical AG, version 6.0) for volumetric BMD (mg/cm^3) and microarchitectural parameters. The extended cortical measurement was also performed.

DXA of the lumbar spine (L1 - 4), hip and forearm were performed using Hologic Discovery A densitometer (Hologic Inc, USA). Mean areal BMD (g/cm^2) was calculated using Hologic APEX software (version 3.4.2).

5.2.4 Bone Biopsy and Histomorphometry

Trans-iliac bone biopsy was only performed in CKD patients using tetracycline bone labelling. A trans-iliac bone biopsy was performed under local anaesthetic using an 8-gauge Jamshidi 4mm trephine and needle. The samples were analysed using the Bioquant Osteo histomorphometry system (Bioquant Image Analysis Corporation) which uses standardised nomenclature {Parfitt et al 1987}. The samples fulfilled the histomorphometry minimum acceptable total section area in the standard analysis region of $30mm^2$ {Recker et al 2011}. All histomorphometry analysis was performed by a single operator and normal bone turnover was defined as BFR/BS of 18-38 um^3/um^2/year {Malluche et al 2011}.

5.2.5 Statistical Analysis

To examine the relationship between HR-pQCT measurements and BFR/BS, we used HR-pQCT Z-scores to control for the effect of age and gender on bone microarchitecture. We selected 43 controls who were age- and gender-matched to the 43 CKD patients with bone histomorphometry and the control mean and standard deviation were calculated. The Z-scores were obtained by subtracting the control group mean from HR-pQCT raw values in CKD patients, which was then divided by the control group standard deviation. DXA BMD Z-scores were obtained from the Hologic software which uses a larger number of participants to represent the normal population.

For receiver operating characteristic (ROC) analysis to assess the diagnostic accuracy of BTMs and imaging, CKD patients were grouped into Low/Not Low and High/Not High bone turnover categories based on bone turnover on histomorphometry (BFR/BS). The proportion of low

bone turnover (26%) and high bone turnover (40%) in this study were used as the prevalence of the disease. We classified area under the ROC curve (AUC) of 0.6-0.7 as poor, 0.7-0.8 as fair, 0.8-0.9 as good and 0.9-1.0 as excellent diagnostic accuracy. Combining variables for ROC analysis were performed using regression analysis. Diagnostic accuracy summary statistics included sensitivity and specificity. We also included the Youden criteria which is the cut off level that optimizes the diagnostic tool differentiating ability when equal weight is given to sensitivity and specificity. The associated positive (PPV) and negative predictive values (NPV) for the Youden criteria were also specified.

5.3 Results

5.3.1 Participants and the Bone Turnover on Histomorphometry

The demographics of 69 advanced CKD stages 4 - 5 (including dialysis) patients and 68 age- and gender-matched control participants are shown in ***Table 5.1***. There were 44 pre-dialysis CKD patients with median (IQR) eGFR of 13 (11 - 16) ml/min/1.73m^2 and 25 dialysis patients (haemodialysis and PD). Median (IQR) eGFR for controls was 81 (72 to >90) ml/min/1.73m^2.

49 bone biopsies were performed but only 43 samples were adequate for histomorphometry analysis. Amongst these 43 patients, 28 (65%) were pre-dialysis CKD, mean (SD) age was 59 (12) years, 77% were male, 26% had diabetes, and 26% had previous fragility fracture. Their current medications are shown in ***Table 5.2*** but none were taking calcimimetics. Based on BFR/BS on histomorphometry, 26% of patients had low, 34% had normal and 40% had high bone turnover.

Table 5.1

Demographics, biomarkers and imaging parameters in CKD and controls.

Variables	CKD (N=69)	Control (N=68)	p values
Age, years	62 (12)	62 (12)	
Male, N	53	53	
BMI (kg/m^2)	27 (4.1)	28 (4.3)	0.3
Diabetes	28%	0%	**<0.001**
Previous fragility fracture	22%	7%	**<0.05**
Biomarkers			
iPTH (pg/mL)	188 (121 – 280)	32 (27 – 45)	**<0.001**
Intact PINP (ng/mL)	67.5 (42.8 – 107.7)	38.5 (31.8 – 55.3)	**<0.001**
Total PINP (ng/mL)	125 (72.8 – 237.2)	41.4 (33.7 – 56.7)	**<0.001**
bALP (µg/L)	22.3 (16.6 – 33.3)	17 (12.9 – 20.2)	**<0.001**
tALP (IU/L)	88 (73 – 126)	65.5 (55.3 – 78)	**<0.001**
CTX (ng/mL)	1.49 (0.76 – 2.39)	0.27 (0.19 – 0.5)	**<0.001**
TRAP5b (U/L)	4.9 (3.2 – 6.9)	3.8 (3.3 – 4.5)	**0.001**
Adjusted calcium (mmol/L)	2.28 (0.15)	2.28 (0.07)	0.9
Phosphate (mmol/L)	1.53 (0.3)	1.06 (0.15)	**<0.001**
25-hydroxyvitamin D (ng/mL)	22.9 (9.4)	23.9 (7.0)	0.5
HRpQCT distal radius			
Total vBMD (mg/cm^3)	266.2 (75.56)	308.47 (74.2)	**0.003**
Cortical vBMD (mg/cm^3)	782.58 (110.66)	821.04 (88.7)	**0.04**
Trabecular vBMD (mg/cm^3)	156.69 (46.17)	184.6 (41.42)	**0.001**
Cortical thickness (mm)	0.61 (0.27)	0.71 (0.26)	0.06
Cortical porosity (%)	3.0 (2.3 – 4.2)	3.2 (2.0 – 3.8)	0.4
Cortical BV/TV (%)	90.0 (85.4 – 92.1)	90.7 (88.6 – 93.4)	0.1
Trabecular thickness (mm)	0.064 (0.012)	0.073 (0.013)	**<0.001**
Trabecular number (1/mm)	2.01 (0.363)	2.11 (0.296)	0.14
Trabecular separation (mm)	0.434 (0.371 – 0.496)	0.4 (0.349 – 0.443)	0.06
Trabecular BV/TV (%)	13.1 (3.8)	15.4 (3.5)	**0.001**
HRpQCT distal tibia			
Total vBMD (mg/cm^3)	276.99 (63.67)	314.97 (61.2)	**0.001**
Cortical vBMD (mg/cm^3)	819.85 (88.67)	858.7 (67.89)	**0.005**
Trabecular vBMD (mg/cm^3)	172.12 (41.06)	189.99 (41.12)	**0.01**
Cortical thickness (mm)	1.05 (0.36)	1.25 (0.35)	**0.001**
Cortical porosity (%)	7.1 (5.7 – 10.4)	6.8 (4.7 – 10.3)	0.2
Cortical BV/TV (%)	86.2 (6.0)	88.1 (4.9)	0.05
Trabecular thickness (mm)	0.075 (0.014)	0.081 (0.013)	**0.01**
Trabecular number (1/mm)	1.92 (0.35)	1.97 (0.4)	0.4
Trabecular separation (mm)	0.444 (0.395 – 0.522)	0.425 (0.359 – 0.523)	0.2
Trabecular BV/TV (%)	14.3 (3.4)	15.8 (3.4)	**0.01**
DXA BMD Z-score			
Forearm	-0.4 (1.5)	0.2 (1.4)	**0.02**
Total hip	-0.2 (1.0)	0.6 (1.1)	**<0.001**
Lumbar spine	0.4 (1.7)	0.5 (1.6)	0.7

Table 5.2

Biomarkers and imaging parameters for low, normal and high bone turnover categories in CKD (N = 43).

Variables	Low (N=11)	Normal (N=15)	High (N=17)	p value
BFR/BS ($um^3/um^2/day$)	13.8 (3.6 – 15.5)	27.5 (22.5 – 32.2)	67.4 (46.5 – 112.5)	**<0.001**
Medications				
Vitamin D	45%	13%	47%	
Calcium-based phosphate binder	9%	20%	41%	
Non-Calcium based phosphate binder	0%	7%	6%	
Biomarkers				
iPTH (pg/mL)	172 (119 – 292)	172 (86 – 194)	347 (161 – 381)	**<0.05**
Intact PINP (ng/mL)	44.1 (29.2 -68.4)	81.1 (54.3 – 92.4)	107.9 (63.5 – 182)	**<0.005**
Total PINP (ng/mL)	76.3 (51.7 – 159.3)	127.3 (68.4 – 221.7)	214 (110.6 – 403)	**<0.05**
bALP (µg/L)	17.7 (5.6)	25.9 (8.7)	34.4 (13.3)	**<0.005**
tALP (IU/L)	82 (53 – 86)	94 (82 – 127)	115 (82 – 156)	**<0.05**
CTX (ng/mL)	1.01 (0.68)	1.46 (0.67)	2.65 (1.68)	**<0.005**
TRAP5b (U/L)	3.2 (2.9 – 4.3)	5.2 (3.2 – 7.4)	5.8 (4.8 – 8.5)	**<0.05**
Adjusted calcium (mmol/L)	2.27 (2.22 – 2.33)	2.32 (2.26 – 2.35)	2.24 (2.14 – 2.40)	0.6
Phosphate (mmol/L)	1.48 (1.30 – 1.77)	1.61 (1.43 – 1.83)	1.30 (1.25 – 1.55)	0.1
25-hydroxyvitamin D (ng/mL)	23 (9.9)	23.7 (8.2)	22.6 (10.3)	0.95
HR-pQCT radius Z-score				
Total vBMD	-0.11 (0.63)	-1.06 (0.66)	-0.97 (1.08)	**<0.05**
Cortical vBMD	0.49 (-0.47 to 0.9)	-0.63 (-1.4 to -0.14)	-0.84 (-1.67 to 0.15)	0.09
Trabecular vBMD	-0.31 (0.83)	-1.03 (0.57)	-1.11 (1.31)	0.16
Cortical thickness	0.07 (0.8)	-0.76 (0.82)	-0.64 (0.98)	0.1
Cortical porosity	-0.51 (-0.95 to -0.02)	-0.12 (-0.94 to 1.58)	0.10 (-0.47 to 0.90)	0.15
Cortical BV/TV	0.72 (-0.08 to 0.97)	-0.2 (-1.48 to 0.27)	-0.23 (-1.46 to 0.27)	**<0.05**
Trabecular thickness	-0.43 (-0.82 to -0.18)	-1.14 (-1.57 to -0.79)	-1.21 (-1.77 to 0.11)	0.07
Trabecular number	-0.03 (1.01)	-0.11 (0.84)	-0.66 (1.58)	0.39
Trabecular separation	-0.13 (-0.5 to 0.71)	0.30 (-0.39 to 0.55)	0.59 (-0.50 to 1.18)	0.5
Trabecular BV/TV	-0.30 (0.82)	-1.01 (0.57)	-1.09 (1.31)	0.17

HR-pQCT tibia Z-score				
Total vBMD	-0.34 (0.91)	-1.05 (0.90)	-0.92 (1.13)	0.21
Cortical vBMD	0.26 (-0.93 to 0.44)	-0.60 (-2.0 to 0.31)	-0.21 (-2.0 to 0.13)	0.13
Trabecular vBMD	-0.48 (0.92)	-0.63 (0.88)	-0.70 (1.11)	0.86
Cortical thickness	-0.18 (0.92)	-1.1 (0.86)	-0.86 (1.16)	0.1
Cortical porosity	-0.31 (0.52)	0.43 (1.26)	0.31 (1.17)	0.23
Cortical BV/TV	0.36 (-0.15 to 0.73)	-0.43 (-1.82 to 0.70)	0.14 (-2.12 to 0.37)	0.17
Trabecular thickness	-0.70 (-0.87 to 0.23)	-0.93 (-1.62 to 0.21)	-0.78 (-1.66 to 0.14)	0.44
Trabecular number	-0.31 (1.23)	-0.03 (0.76)	-0.07 (0.92)	0.74
Trabecular separation	0.56 (-0.75 to 0.84)	-0.09 (-0.30 to 0.55)	-0.04 (-0.44 to 0.52)	0.66
Trabecular BV/TV	-0.46 (0.91)	-0.60 (0.88)	-0.67 (1.10)	0.86
DXA BMD Z-score				
Forearm	-0.24 (0.88)	-0.31 (0.99)	-0.94 (1.33)	0.18
Total hip	-0.07 (0.76)	-0.35 (0.96)	-0.38 (1.05)	0.68
Lumbar spine	-0.10 (-0.5 to 0.6)	0.2 (-0.8 to 1.0)	0 (-0.8 to 1.3)	0.86

5.3.2 Biomarkers and Imaging in CKD and Controls

CKD patients had significantly higher biomarker levels compared to controls (***Table 5.1***). On HR-pQCT, CKD patients had lower volumetric BMD, and lower trabecular thickness and trabecular bone volume at the distal radius and distal tibia compared to controls. Additionally, CKD patients had thinner cortical bone at the tibia. **Figure 5.1** shows examples of 3-dimensional reconstruction of HR-pQCT images at both sites in this study.

Areal BMD Z-score by DXA at the forearm and total hip were also lower in CKD compared to controls (***Table 5.1***). 59% of the CKD group had osteopaenia (T score -1.0 to -2.5), and 25% had osteoporosis (T score < -2.5) as assessed by BMD at the three sites. In the control group, 51% had osteopaenia, and 12% had osteoporosis.

Figure 5.1

Examples of HR-pQCT 3-dimensional images of distal radius and distal tibia from a control participant and a CKD patient in this study. This CKD patient demonstrated trabecular bone impairment whereas the control participant had normal bone microarchitecture.

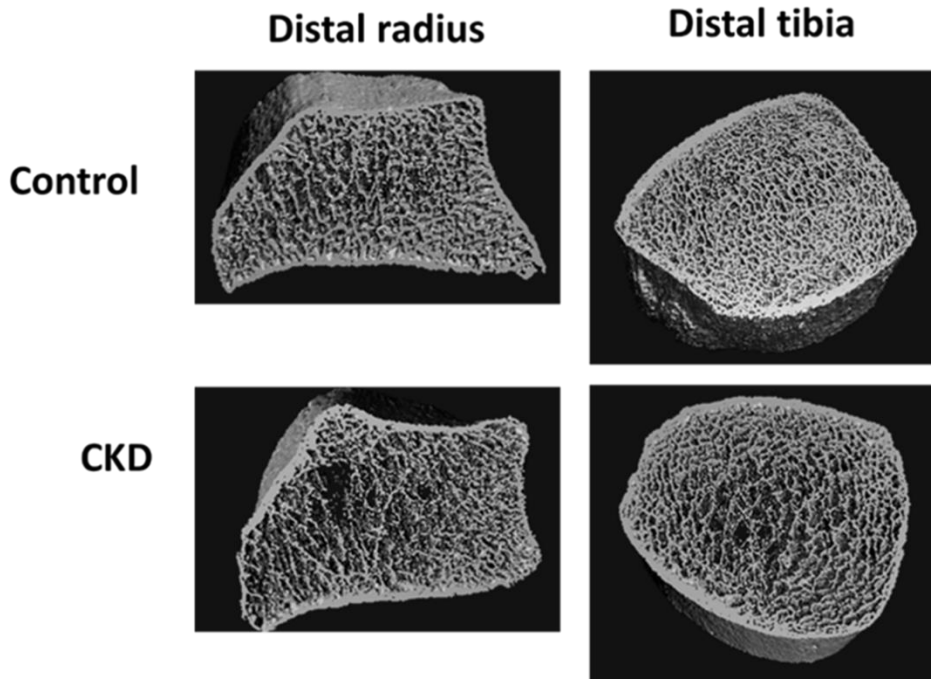

5.3.3 Relationship between Bone Turnover on Histomorphometry and Biomarkers and Imaging in CKD

In 43 CKD patients with bone histomorphometry data, all biomarkers were significantly correlated with each other (***Table 5.3***). iPTH was positively associated with BFR/BS (rho = 0.42, $p<0.01$) but the other biomarkers showed higher correlations with bone turnover (***Figure 5.2***). There were significant differences for all the biomarkers between low, normal and high bone turnover categories (***Table 5.2***).

Table 5.3

Correlations between all bone turnover markers in 43 advanced CKD patients with bone histomorphometry data.

	Intact PINP	Total PINP	bALP	tALP	CTX	TRAP5b
iPTH	0.619	0.523	0.621	0.508	0.567	0.504
Intact PINP		0.813	0.866	0.762	0.732	0.741
Total PINP			0.749	0.698	0.591	0.575
bALP				0.869	0.710	0.672
tALP					0.542	0.548
CTX						0.709

All Spearman's rho correlations are significant at ≤0.001 (2-tailed).

Figure 5.2

All biomarkers showed positive correlations with bone turnover on histomorphometry.

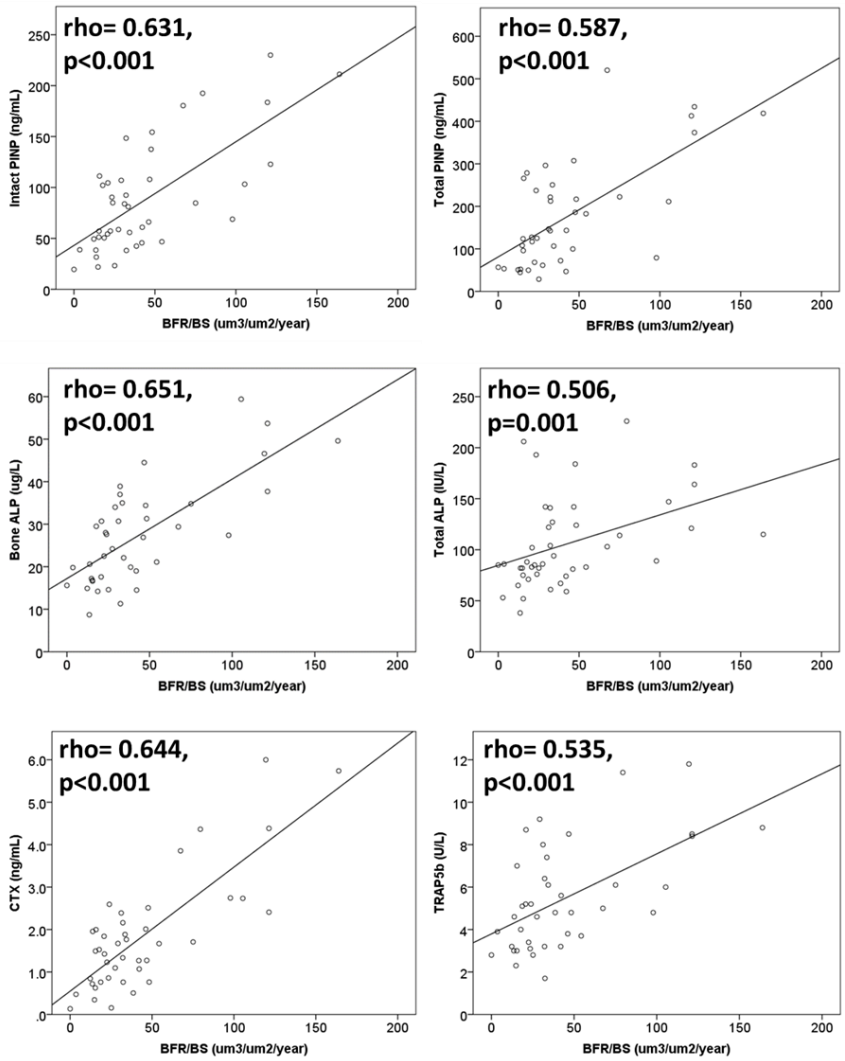

Bone turnover on histomorphometry was negatively associated with radius Z-scores for BMD and microarchitecture (***Figure 5.3***) but no significant associations were found with tibia HR-pQCT Z-scores. Differences were only significant for radius HR-pQCT total BMD and cortical bone volume ($p<0.05$) between the three bone turnover categories (***Table 5.2***). On DXA, only the forearm BMD Z-score was significantly associated with bone turnover (rho = -0.307, $p<0.05$). No significant differences were found for DXA BMD Z-scores between the bone turnover categories.

Figure 5.3

Distal radius HR-pQCT parameters showed negative correlations with bone turnover on histomorphometry (N = 43).

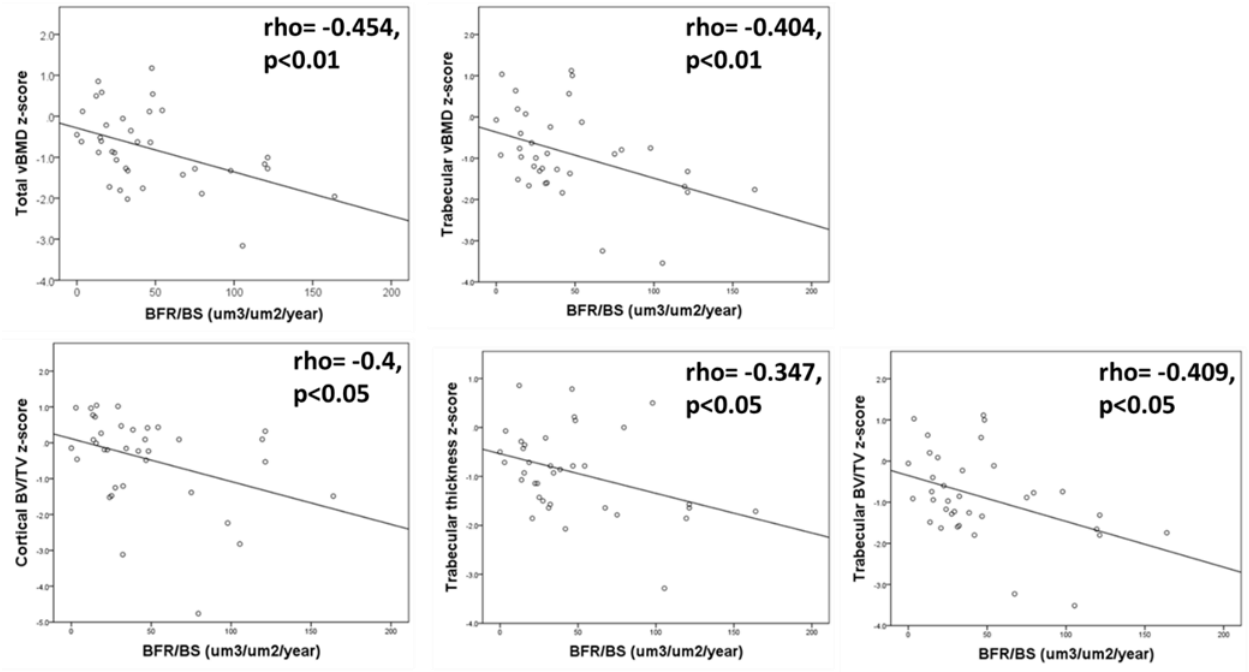

5.3.4 Diagnostic Accuracy of Biomarkers and Imaging for Low Bone Turnover

In ROC analysis for discriminating Low from Not Low bone turnover, AUC for bALP was 0.824, intact PINP was 0.794 and TRAP5b were 0.799 (***Table 5.4***). These AUCs were significantly better ($p<0.05$) than AUC for iPTH which was 0.563 (***Figure 5.4***). Combining biomarkers did not improve the AUC.

Radius HR-pQCT Z-scores for total BMD and cortical bone volume had AUC of 0.811 and 0.802 respectively for discriminating low bone turnover (***Figure 5.4***). However, these AUCs were not significantly better than iPTH AUC. Tibia HR-pQCT Z-scores only had AUCs ≤0.70. All three sites DXA BMD Z-scores also had non-significant AUCs (***Table 5.5***). Combining bALP and radius total BMD Z-score did not improve the AUC (***Table 5.4***).

Table 5.4

Diagnostic accuracy of biomarkers and radius HR-pQCT for identifying patients with low bone turnover.

Variables	AUC (95% CI)	Criterion	Sensitivity (%)	Specificity (%)	PPV (%)	NPV (%)
Biomarkers						
iPTH	0.563 (0.401 to 0.715)	≤183 pg/mL	70	53	32	85
Intact PINP	0.794 (0.641 to 0.903)	≤57 ng/mL	80	75	50	92
Total PINP	0.719 (0.557 to 0.848)	≤124 ng/mL	80	68	44	91
bALP	0.824 (0.671 to 0.926)	≤21 µg/L	89	77	53	96
tALP	0.753 (0.598 to 0.871)	≤88 IU/L	91	63	46	95
CTX	0.766 (0.610 to 0.882)	≤0.84 ng/mL	60	84	55	87
TRAP5b	0.799 (0.643 to 0.909)	≤4.6 U/L	89	71	47	96
Radius HR-pQCT Z-score						
Total vBMD	0.811 (0.646 – 0.922)	>-1.0	100	59	45	100
Cortical BV/TV	0.802 (0.636 – 0.916)	> -0.2	89	63	44	94
Combined variables						
bALP & radius total vBMD Z-score	0.797 (0.621 – 0.916)	Not available	100	58	39	100

Figure 5.4

Biomarkers and distal radius HR-pQCT parameters can discriminate CKD patients with low bone turnover. Receiver operating characteristic curves show that the biomarkers bALP, intact PINP and TRAP5b (panel A) performed significantly better than iPTH in discriminating patients with low bone turnover. Distal radius HR-pQCT parameters (panel B) were not significantly better than iPTH despite area under the curves being >0.80.

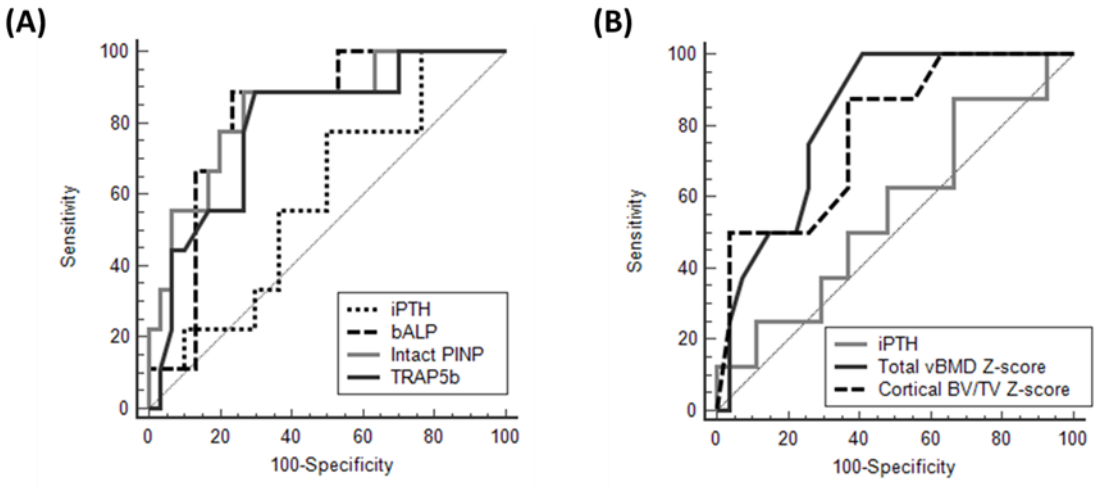

Table 5.5

Diagnostic accuracy of DXA areal BMD Z-scores for identifying advanced CKD patients with low and high bone turnover (N=43).

Areal BMD Z-score	AUC (95% CI)
Low bone turnover	
Forearm	0.645 (0.483 – 0.786)
Total hip	0.598 (0.438 – 0.744)
Lumbar spine	0.554 (0.395 – 0.705)
High bone turnover	
Forearm	0.685 (0.523 – 0.819)
Total hip	0.580 (0.420 – 0.729)
Lumbar spine	0.533 (0.375 – 0.686)

5.3.5 Diagnostic Accuracy of Biomarkers and Imaging for High Bone Turnover

In ROC analysis for discriminating High from Not High bone turnover, iPTH had an AUC of 0.76 which was similar to AUCs for the other biomarkers (***Table 5.6***). Combining biomarkers did not improve the AUC. All bone imaging parameters also had non-significant AUCs (***Table 5.5*** and ***Table 5.7***).

Table 5.6

Diagnostic accuracy of biomarkers for identifying patients with high bone turnover.

Biomarkers	AUC (95% CI)	Criterion	Sensitivity (%)	Specificity (%)	PPV (%)	NPV (%)
iPTH	0.760 (0.603 to 0.878)	>327 pg/mL	53	96	90	75
Intact PINP	0.765 (0.609 to 0.882)	>107 ng/mL	53	92	82	74
Total PINP	0.725 (0.563 to 0.853)	>142ng/mL	75	68	60	81
bALP	0.750 (0.588 to 0.873)	>31 µg/L	56	83	69	74
tALP	0.670 (0.510 to 0.805)	>102 IU/L	65	73	61	76
CTX	0.762 (0.606 to 0.880)	>2.39 ng/mL	53	96	90	75
TRAP5b	0.710 (0.545 to 0.842)	>4.6 U/L	81	58	57	82

Table 5.7

Diagnostic accuracy of HR-pQCT Z-scores for identifying advanced CKD patients with high bone turnover (N = 43).

HR-pQCT Z-scores	Distal radius AUC (95% CI)	Distal tibia AUC (95% CI)
Total vBMD	0.627 (0.450 – 0.782)	0.553 (0.392 – 0.706)
Cortical vBMD	0.569 (0.394 – 0.732)	0.579 (0.417 – 0.729)
Trabecular vBMD	0.625 (0.448 – 0.780)	0.541 (0.381 – 0.696)
Cortical thickness	0.552 (0.377 – 0.717)	0.525 (0.365 – 0.681)
Cortical porosity	0.627 (0.450 – 0.782)	0.548 (0.387 – 0.702)
Cortical BV/TV	0.628 (0.451 – 0.783)	0.576 (0.414 – 0.727)
Trabecular thickness	0.583 (0.407 – 0.744)	0.575 (0.413 – 0.726)
Trabecular number	0.603 (0.427 – 0.762)	0.541 (0.381 – 0.696)
Trabecular separation	0.614 (0.438 – 0.771)	0.533 (0.373 – 0.688)
Trabecular BV/TV	0.628 (0.451 – 0.783)	0.542 (0.382 – 0.697)

5.4 Discussion

This is the first study to simultaneously compare biomarkers and HR-pQCT to bone histomorphometry to determine their diagnostic accuracy in discriminating bone turnover status in advanced CKD patients. BALP and radius HR-pQCT can discriminate low bone turnover, with their AUCs being >0.80. We also found that iPTH, all the biomarkers and bone imaging had similarly suboptimal diagnostic accuracy for discriminating high bone turnover.

BALP, intact PINP and TRAP5b can discriminate patients with low bone turnover better than iPTH, most likely because they do not accumulate in advanced CKD {Koivula et al 2010; Yamada et al 2008}. Secondary hyperparathyroidism is a common complication in advanced CKD and has a major role in CKD mineral bone disorder (CKD-MBD) {KDIGO 2009}. iPTH is a poor diagnostic test to discriminate low bone turnover in advanced CKD patients, partly due to the assay used. A second generation iPTH assay measures the whole (1-84) PTH molecule and the (7-84) PTH fragment. The fragment accumulates in CKD and has an antagonistic effect on bone turnover {Slatopolsky et al 2000}. Despite those limitations, iPTH can still discriminate high bone turnover with similar accuracy as other biomarkers used in this study. iPTH has 90% positive predictive value (PPV) for high bone turnover which is consistent with previous studies {Fletcher et al 1997; Lehmann et al 2008; Urena et al 1996}. The optimal cut off value for discriminating high bone turnover in this study is five times the upper limit of normal, whereas KDIGO CKD-MBD guideline recommends that iPTH level is maintained 2 - 9 times the upper limit of normal in dialysis patients {KDIGO 2009}. The number of dialysis patients in our study was too small for further analysis to make a comparison.

In this study, bALP had AUC > 0.80 and has better diagnostic accuracy for low bone turnover than iPTH which are consistent with previous studies {Bervoets et al 2003; Coen et al 1998;

Couttenye et al 1996; Urena et al 1996}. BALP and other biomarkers in this study had consistently low PPV but high NPV for the optimal threshold (criterion) for low bone turnover. We also found that bALP only had 69% PPV for discriminating high bone turnover whereas previous studies found > 90% PPV {Fletcher et al 1997; Lehmann et al 2008; Urena et al 1996}.

Sprague et al. recently published diagnostic accuracy of biomarkers in predicting bone turnover in 492 dialysis patients from four countries {Sprague et al 2016}. They showed that iPTH had similar diagnostic accuracy to bALP and PINP in predicting high bone turnover. They found that bALP and iPTH had the highest diagnostic accuracy for low bone turnover but we found that iPTH to be a poor diagnostic test for low bone turnover. They also found that combining iPTH and bALP improved the discrimination of both low and high bone turnover but this was not the case in our study. There are differences between the study and ours; firstly, we included pre-dialysis and dialysis patients which may account for the different proportion of patients with low bone turnover. Although our sample size was smaller, the proportion of patients with low bone turnover was similar to other studies {Bervoets et al 2003; Couttenye et al 1996}. In contrast, Sprague et al. reported that around 60% of patients had low bone turnover but most of their biopsies were performed for clinical indication whereas ours were collected purely for research. Our histomorphometry analysis was performed by a single operator to avoid inter-observer variability whereas Sprague et al. had bone histomorphometry analysed in several centres with different ranges of bone turnover defined as normal. The assays used for iPTH and bALP were also different from ours and Sprague et al used total PINP whereas we evaluated total and intact PINP separately.

PINP is cleaved off from type I collagen during bone formation process. Total PINP assay measures the trimeric propeptide and its monomeric fragments, whilst the intact PINP assay

only measures the trimeric propeptide {Koivula et al 2010}. The trimeric propeptide is cleared from circulation by liver endothelial cells {Melkko et al 1994}, whereas the monomeric fragments are cleared by the kidneys, hence the fragments accumulate in advanced CKD {Koivula et al 2010}. We have shown that in advanced CKD, (1) only intact PINP can discriminate low bone turnover better than iPTH and (2) both have suboptimal diagnostic accuracy for high bone turnover. Although total PINP is often used in the field of osteoporosis, we do not recommend its use to assess bone turnover in advanced CKD.

Biomarker profile in dialysis patients may differ from that in non-dialysis CKD even with similar bone turnover status because biomarkers, such as CTX, may be dialysed {Alvarez et al 2004}. Hence, our haemodialysis patients had blood sample taken the day after a dialysis session but we did not assess residual renal function. These issues may have introduced bias in our study. However, the number of pre-dialysis patients was small with <10 patients each in the low and high bone turnover categories which made further analysis in this subgroup questionable.

CKD patients in our study had lower BMD on HR-pQCT compared to controls which was mostly due to trabecular bone impairment. Additionally, CKD patients also had thinner cortical bone at the tibia. Previous studies also found that CKD had lower BMD on HR-pQCT compared to controls due to both trabecular and cortical bone impairment {Bacchetta et al 2010; Cejka, Patsch, et al 2011; Negri et al 2012}. However, we did not match our control participants' BMD to CKD patients and we excluded participants with known osteoporosis which may have introduced bias.

We found that radius BMD and microarchitecture were negatively associated with bone turnover in advanced CKD. Negri et al. showed similar trend on HR-pQCT in female dialysis patients but they used biomarkers as measures of bone turnover rather than bone

histomorphometry {Negri et al 2012}. We also found that normal and high bone turnover CKD patients had significantly lower radius BMD compared to those with low bone turnover, mostly due to lower cortical bone volume. Gerakis et al. described similar finding using DXA in haemodialysis patients who had a bone biopsy {Gerakis et al 2000}. We did not find any difference in DXA BMD between bone turnover categories. Importantly, DXA was unable to discriminate bone turnover status in advanced CKD.

Distal radius HR-pQCT can discriminate low bone turnover from non-low bone turnover patients in this study. However, it is important to recognise that the effects of bone turnover on microarchitecture are dynamic whereas HR-pQCT is a static test. Thus the cross-sectional use of HR-pQCT is perhaps more appropriate in assessing bone volume (static measurement) rather than bone turnover (dynamic measurement) {Marques et al 2017}. Nevertheless, the use of bone imaging could be complementary to biomarkers in discriminating bone turnover status and deciding treatment decisions, for example, in osteoporotic CKD.

We included pre-dialysis and dialysis CKD patients and we assessed bone turnover using the gold standard bone biopsy but there were several limitations to our study. This was a single centre observational study with a small number of participants. However, the proportion of patients with low/high bone turnover was similar to previous studies, and we had a broad range of bone turnover which is important in assessing diagnostic test accuracy. We were unable to assess pre-dialysis and dialysis patients separately. Hence, our results must be interpreted in the context of CKD stages 4-5 and dialysis.

We have interpreted AUC > 0.80 as having good diagnostic accuracy but we need to be mindful that AUC values are approximate. As with any discriminative or predictive tool, AUC

is also subjected to inaccuracy. The interpretation also needs to take into account the importance of missing or misclassifying the diagnosis of ROD using these non-invasive tests.

In conclusion, bALP, intact PINP, TRAP5b and radius HR-pQCT were able to discriminate low bone turnover in advanced CKD patients. Despite poor diagnostic accuracy for low bone turnover, iPTH can discriminate high bone turnover with similar accuracy to other biomarkers in this study. In clinical practice, iPTH and bALP remain the diagnostic tests of choice to discriminate high and low bone turnover. However, we believe that all four biomarkers and radius HR-pQCT can potentially be used for patient selection in clinical trials in advanced CKD as we continue to search for bone-specific treatment to reduce fracture risk in this population.

Chapter 6. Vascular Calcification Relationship with Biomarkers and Bone in CKD

6.1 Introduction

Vascular calcification (VC) is part of CKD-MBD, which is an important complication of CKD {KDIGO 2009}. VC is highly prevalent in CKD and its severity increases with worsening CKD {J. Chen et al 2017; M. Sigrist et al 2006}. Around 50 - 90% of CKD stages 3-5D had evidence of VC and it is associated with increased cardiovascular and all-cause mortality {Z. Chen et al 2016; Lamarche et al 2018; Matsuoka et al 2004; Rodriguez-Garcia et al 2009; Shantouf et al 2010}. Data from United States Renal Data System (USRDS) consistently reported that half of dialysis and kidney transplant patients died from cardiovascular disease {USRDS 2015; USRDS 2018}. VC is also associated with fractures which probably compounds increased mortality risk in these patients {H. Y. Chen et al 2016; Fusaro et al 2013; Rodriguez-Garcia et al 2009}.

VC is not exclusive to CKD patients as post mortem study of the general population showed that the majority of atherosclerotic plaques in the intimal arterial layer had calcification. However, calcification in the media layer of arteries, or arteriosclerosis, is the predominant pattern of calcification in CKD {Gross et al 2007; Schwarz et al 2000}. The systemic nature of media calcification is highlighted by its presence not only in coronary arteries, but also in the large aorta and other peripheral arteries in advanced CKD {Gross et al 2007; S. M. Moe et al 2002; Qureshi et al 2015; N. Wang et al 2008}. Media calcification leads to vessel stiffness which in turn causes end organ damage such as left ventricular hypertrophy, cardiac dysfunction and failure {Toussaint, Lau, et al 2009}. Annual data from USRDS shows that cardiovascular deaths are mainly due to non-thromboembolic events {USRDS 2015}.

VC in CKD is a complex process which involves interactions between calcium and phosphate, vascular calcification promoters and inhibitors, bone abnormalities of ROD, local and systemic inflammation, oxidative stress and various uremic toxins. It is likely that all these

factors work synergistically to initiate and then allow the progression of VC in CKD. There is uncertainty if some factors play a bigger role than others. A review by Evrard et al summarises the complex pathophysiological mechanisms (***Figure 1.11***) which promotes VSMCs transformation into osteoblast-like cells and hydroxyapatite crystal growth in VC {Evrard et al 2015}. There is growing knowledge on circulating inhibitors of VC such as matrix Gla protein (MGP) and fetuin A. MGP inhibits calcium crystal growth and prevents osteoblastic differentiation of VSMCs {Roy et al 2002}. Fetuin A prevents spontaneous precipitation of calcium-phosphate product in the vasculature and other extra-skeletal tissue {Schafer et al 2003}. A number of studies in dialysis patients have consistently shown that low serum fetuin A is associated with VC {H. Y. Chen et al 2016; Kanbay et al 2010; Stenvinkel et al 2005; A. Y. Wang et al 2005}.

There are also circulating markers which are released from bone, such as osteocalcin and osteoprotegerin (OPG), which may have effects on VSMCs. Osteocalcin may be a VC promoter as high osteocalcin level stimulates VSMCs differentiation and mineralization in experimental model {Idelevich et al 2011}. OPG inhibits osteoclast differentiation and maturation in bone but circulating OPG may be a VC inhibitor. Experimental studies have shown that OPG reduces osteoblastic transformation of VSMCs and blocks alkaline phosphatase (ALP) activity to prevent bone matrix formation and mineralization in the vasculature {Orita et al 2007; Zhou et al 2013}. The evidence for these biomarkers relationship with VC is still limited but VC is thought to be the result of an imbalance between these circulating promoters and inhibitors.

KDIGO CKD-MBD guideline suggests that a lateral abdominal X-ray can be used to detect the presence of VC as a reasonable alternative to computed tomography (CT) based imaging {KDIGO 2017}. Although CT is more sensitive, lateral abdominal X-ray has much lower

radiation dose (0.3 mSv) than CT (2 - 10 mSv). Lateral lumbar spine images using DXA can also be used to assess abdominal aortic calcification (AAC) and has low radiation dose (0.05 mSv) {Schousboe et al 2006}. Meanwhile, HR-pQCT of distal radius and tibia has steadily been used in more research into the effects of CKD on bone microarchitecture over the last decade. It has high resolution and low radiation dose (0.003 mSV) and peripheral arteries calcification is often seen as incidental findings on the scan images. Patsch et al developed a quantitative method to measure peripheral arteries calcification on HR-pQCT images {Patsch et al 2014}. The technique using HR-pQCT images of the ankle (distal tibia) was validated against coronary artery calcification quantified by multi-detector CT in 46 haemodialysis patients. There was a significant positive correlations between the two methods (rho = 0.6).

However, it is unclear if HR-pQCT would identify more advanced CKD patients with VC compared to DXA detection of AAC. The relationship between ankle VC and VC biomarkers and bone structure is also unknown. Therefore, the aims of our study were:

1. To compare the presence and severity of vascular calcification in abdominal aorta using DXA and peripheral (ankle) arteries using HR-pQCT in CKD and controls
2. To assess the relationship between ankle VC and its biomarkers in CKD
3. To assess the relationship between ankle VC and bone structure (on imaging and bone biopsy) in CKD.

6.2 Methodology

6.2.1 Vascular Calcification and Bone Imaging

Participants' demographics, bone imaging techniques using DXA and HR-pQCT, and bone biopsy technique have been described in Chapter 2 of this thesis. VC was assessed for the abdominal aorta and ankle arteries. AAC images were obtained from lateral lumbar spine DXA and ankle VC images were obtained from distal tibia HR-pQCT. The scoring method and VC mass quantification have been described in Chapter 2.

6.2.2 Vascular Calcification Biomarkers

The full assay methodologies have been described in Chapter 2 of this thesis. We measured osteocalcin using the automated Immuno Diagnostic Systems (IDS) iSYS N-mid osteocalcin assay. Fetuin A was measured using ELISA by Biovendor. Both species of MGP were measures using IDS assays; these were total uncarboxylated (t-uc) MGP and dephosphorylated-uncarboxylated (dp-uc) MGP. Osteoprotegerin (OPG) was measured using ELISA by Biomedica and intact FGF23 was measured using ELISA by Immutopics. We also measured serum adjusted calcium, phosphate, iPTH and tALP, bALP and 25-hydroxyvitamin D using methods that have been fully described in Chapter 2.

6.2.3 Statistical Analysis

Full statistical analysis has been described in Chapter 2 of this thesis. Data are presented as mean (standard deviation, SD) or median (interquartile range, IQR). Group differences

between CKD and controls were tested using Students t test or Mann-Whitney U test depending on the distribution of the variables, or Chi squared test for categorical variables. Ankle VC and AAC have skewed distribution, therefore its relationship with biomarkers and imaging measurements were tested using Spearman's correlation for univariate analysis. For multivariate analysis, variables with skewed distribution were firstly $\log_{10}$ transformed before multiple correlation test was performed. ROC analysis was performed to determine the diagnostic accuracy of VC biomarkers in identifying CKD patients with ankle VC. $p<0.05$ indicated statistical significance.

6.3 Results

6.3.1 Vascular Calcification in CKD and Controls

We recruited 69 CKD stages 4-5D and 68 age- and gender-matched control participants who had eGFR > 60ml/min/1.73m^2. Higher proportion of CKD patients had AAC and ankle VC than healthy controls (***Table 6.1***). More CKD patients had ankle VC (75%) than AAC (48%) detected but the difference was not statistically significant ($p = 0.25$). The number of CKD patients with vascular calcification detected at both or one of the two sites is shown in ***Figure 6.1***. CKD patients also had significantly higher ankle VC mass and AAC score compared to controls. Ankle VC mass and AAC score were weakly correlated in both groups but only reached statistical significance in CKD (rho = 0.28, $p<0.05$ in CKD and rho = 0.24, $p=0.05$ in controls). The relationship in CKD group is shown in ***Figure 6.2***.

Table 6.1

Vascular calcification characteristics in CKD and controls.

Vascular calcification	CKD (N=69)	Controls (N=68)	p value
Imaging			
AAC detected, N (%)	33 (48%)	15 (22%)	**0.001**
AAC score	1 (0 – 3)	0 (0 – 0)	**<0.001**
Ankle VC detected, N (%)	52 (75%)	21 (31%)	**<0.001**
Ankle VC, mgHA	1.043 (0.05 – 16.52)	0 (0 - 0.55)	**<0.001**
Biochemistry			
Adjusted calcium, mmol/L	2.28 (0.15)	2.28 (0.07)	0.9
Phosphate, mmol/L	1.53 (0.3)	1.06 (0.15)	**<0.001**
Ca x PO4, $mmol^2/L^2$	3.33 (2.97 – 3.91)	2.39 (2.17 – 2.64)	**<0.001**
25-hydrovitamin D, ng/ml	22.9 (9.4)	23.9 (7.0)	0.5
iPTH, pg/ml	188 (121 – 280)	32 (27 – 45)	**<0.001**
Intact FGF23, pg/ml	484 (258 – 2437)	59 (47 – 72)	**<0.001**
tALP, IU/L	88 (73 – 126)	66 (55 – 78)	**<0.001**
bALP, µg/L	22 (17 – 33)	17 (13 – 20)	**<0.001**
Osteocalcin, ng/ml	105 (59)	16 (5)	**<0.001**
OPG, pmol/L	8.16 (5.60 – 11.17)	4.06 (3.23 – 5.03)	**<0.001**
t-uc MGP, nmol/L	2064 (1257 – 2903)	4919 (3194 – 6773)	**<0.001**
dp-uc MGP, pmol/L	1479 (1055 – 2148)	443 (346 – 557)	**<0.001**
Fetuin A, µg/ml	239 (39)	266 (49)	**0.001**

Figure 6.1

The number of CKD patients with detectable vascular calcification in the ankle arteries (ankle VC) and abdominal aorta (AAC).

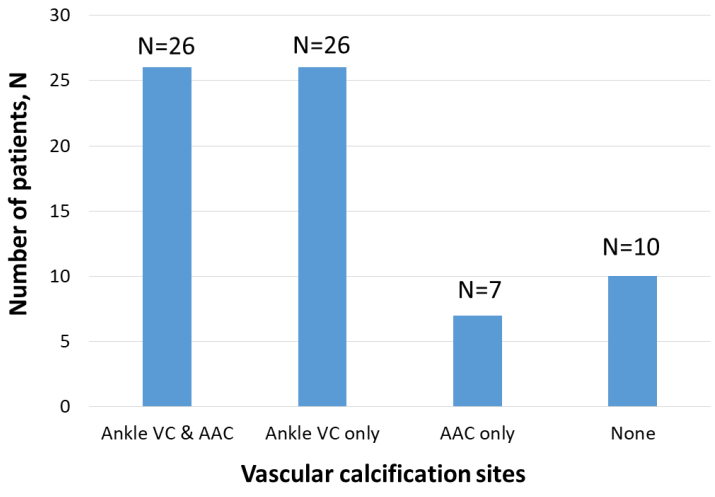

Figure 6.2

Relationship between AAC score and ankle VC in CKD patients.

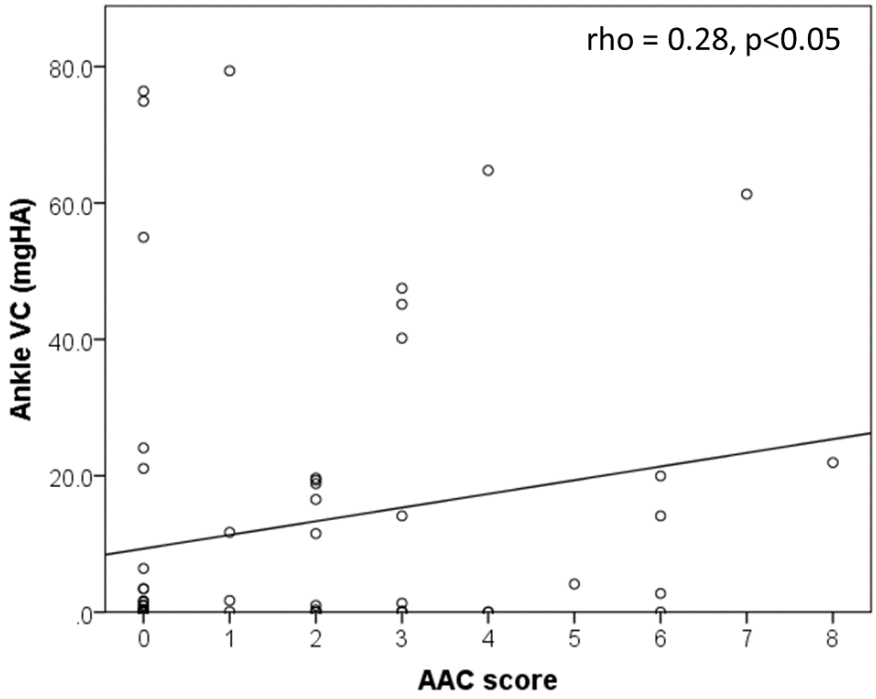

Ankle VC and AAC were positively correlated with age in CKD (rho = 0.41, p=0.001 and rho = 0.35, p<0.01 respectively). In the control group, only ankle VC correlated with age (rho= 0.29, p<0.05). 28% of advanced CKD patients had diabetes mellitus (type 1 and type 2) whereas none in the control group had diabetes. CKD patients with diabetes had significantly higher ankle VC compared to non-diabetic CKD (median [IQR] of 24.07 [3.42 – 61.30] vs 0.23 [0- 3.78] mgHA, p<0.001) (***Figure 6.3***). There was no difference between AAC score in CKD patients with and without diabetes.

Figure 6.3

Ankle VC mass in advanced CKD patients with and without diabetes.

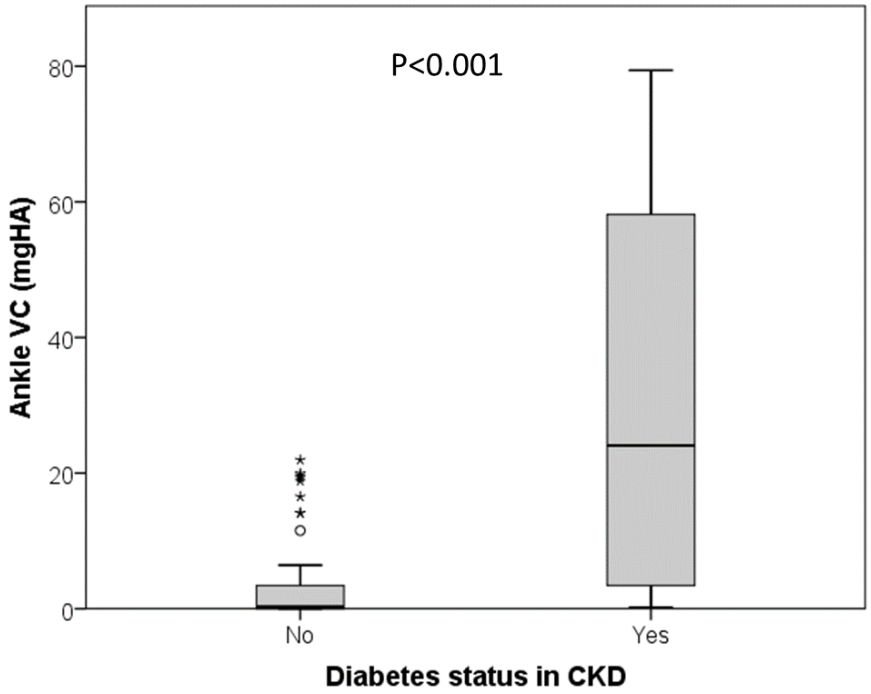

6.3.2 Vascular Calcification Biomarkers

We found that CKD had significantly higher levels of serum phosphate, calcium x phosphate (CaxPO4) product, iPTH and intact FGF23 than the controls (***Table 6.1***). Serum adjusted calcium and 25-hydroxyvitamin D levels were similar in both groups. The vascular calcification markers tALP, bALP, osteocalcin, OPG and dp-uc MGP were also significantly higher in CKD than controls. Meanwhile, other markers such as fetuin A and t-uc MGP were significantly lower in CKD than controls.

The relationship between vascular calcification and its biomarkers was only analysed for ankle VC given that a higher proportion of CKD had ankle VC rather than AAC. Ankle VC positively correlated with serum phosphate, CaxPO4 product, iPTH, intact FGF23, tALP, bALP,

osteocalcin, OPG and dp-uc MGP (***Table 6.2***). There was also a trend towards negative correlation with fetuin A (rho -0.229, p=0.07).

Table 6.2

Relationships between vascular calcification and its biomarkers in CKD.

Biomarkers	**Ankle VC** (N=67)	**p values**
Adjusted calcium	0.032	0.8
Phosphate	**0.286**	**<0.05**
Ca x PO4	**0.308**	**0.01**
25-hydroxyvitamin D	-0.083	0.5
iPTH	**0.381**	**<0.01**
Intact FGF23	**0.397**	**0.001**
tALP	**0.411**	**<0.001**
bALP	**0.286**	**<0.05**
Osteocalcin	**0.317**	**<0.05**
OPG	**0.395**	**0.001**
t-uc MGP	0.03	0.8
dp-uc MGP	**0.308**	**<0.05**
Fetuin A	-0.229	0.07

ROC analysis for identifying CKD patients with ankle VC showed that a number of markers had AUC ranging between 0.66 and 0.73 (***Table 6.3***). These markers are phosphate, CaxPO4 product, iPTH, intact FGF23, tALP, osteocalcin, OPG and dp-uc MGP. In ROC AUC comparison analysis, none of these markers had significantly higher AUC than the other. Furthermore, combinations of biomarkers did not improve the AUC.

Table 6.3

Diagnostic accuracy of biomarkers for identifying patients with ankle VC.

Biomarkers	AUC (95% CI)	Criterion	Sensitivity (%)	Specificity (%)	PPV (%)	NPV (%)
Phosphate	0.692 (0.568 -0.799)	>1.44 mmol/L	65	73	90	38
Ca x PO4	0.710 (0.587 – 0.815)	>3.31 $mmol^2/L^2$	62	80	91	38
iPTH	0.725 (0.602 – 0.828)	>194 pg/mL	59	100	100	42
Intact FGF23	0.722 (0.598 – 0.825)	>408 pg/mL	67	80	92	41
tALP	0.662 (0.536 – 0.773)	>124 IU/L	35	100	100	31
Osteocalcin	0.676 (0.547 – 0.789)	>104 ng/mL	50	93	96	37
OPG	0.715 (0.586 – 0.822)	>6.54 pmol/L	77	67	88	48
dp-uc MGP	0.690 (0.560 – 0.802)	>1497 pmol/L	60	93	97	41

6.3.3 Vascular Calcification and Bone Microstructure

Ankle VC in CKD had statistically significant correlations with distal tibia cortical bone microstructure measured by HR-pQCT (**Table 6.4**). Ankle VC was associated with lower cortical bone BMD and bone volume, and thinner and more porous cortical bone. No association was found with trabecular bone of distal tibia.

Ankle VC only weakly correlated with distal radius cortical BV/TV measured by HR-pQCT (rho = -0.27, $p<0.05$). There were only trends towards lower BMD, thinner and more porous cortical bone of distal radius on HR-pQCT. Ankle VC in CKD did not correlate with DXA BMD T-score for total hip. There was a trend towards negative correlation with 1/3 distal radius BMD T-score (rho = -0.22, $p = 0.07$).

Table 6.4

Relationships between ankle VC and bone characteristics on imaging in CKD.

Imaging sites	**Ankle VC** (N=67)	
DXA BMD T-score	**Rho**	**p values**
Total hip	-0.17	0.2
1/3 distal radius	-0.22	0.07
HR-pQCT radius		
Total vBMD	-0.24	0.08
Cortical vBMD	-0.23	0.09
Trabecular vBMD	-0.12	0.4
Cortical thickness	-0.24	0.08
Cortical porosity	0.23	0.09
Cortical BV/TV	-0.27	**<0.05**
Trabecular thickness	-0.12	0.4
Trabecular number	-0.10	0.5
Trabecular separation	0.12	0.4
Trabecular BV/TV	-0.12	0.4
HR-pQCT tibia		
Total vBMD	-0.23	0.07
Cortical vBMD	-0.44	**<0.001**
Trabecular vBMD	0.05	0.7
Cortical thickness	-0.35	**<0.01**
Cortical porosity	0.40	**0.001**
Cortical BV/TV	-0.50	**<0.001**
Trabecular thickness	0.03	0.8
Trabecular number	0.02	0.9
Trabecular separation	-0.06	0.6
Trabecular BV/TV	0.05	0.7

6.3.4 Vascular Calcification and Bone Biopsy

43 out of 69 CKD participants had evaluable bone biopsy samples for histomorphometry. There was no correlation between ankle VC and bone turnover (BFR/BS). All patients with bone biopsy data in this study had normal mineralization status based on O.Th < 20 µm and MLT < 100 days. Ankle VC did not correlate with these mineralization parameters. Bone volume/tissue volume (BV/TV) on histomorphometry was also not correlated with ankle VC. All the correlations remained non-significant when patients without ankle VC were excluded. Overall, ankle VC did not correlate with bone turnover, mineralization or volume on bone histomorphometry in this study.

6.3.5 Independent Factors for Vascular Calcification

Univariate analyses identified a number of factors which significantly correlated with ankle VC in CKD. In multivariate analysis using all these significant variables and eGFR, the adjusted R^2 was 0.617 which meant that 61.7% of ankle VC variability was explained by the combination of all the variables listed in ***Table 6.5***. However, none of the variables reached statistical significance to be an independent factor for ankle VC.

Table 6.5

Multivariate analysis of the factors associated with ankle VC in CKD. The model R^2 = 0.617.

Variables	Standardised coefficients, β	p values
Demographics		
Age	0.431	0.80
eGFR	0.171	0.49
Diabetes	0.386	0.07
Biomarkers		
Phosphate	0.846	0.07
Log CaxPO4	-0.371	0.41
Log iPTH	-0.171	0.56
Log intact FGF23	0.377	0.09
Log tALP	-0.178	0.72
Log bALP	0.563	0.31
Osteocalcin	-0.045	0.89
OPG	-0.077	0.74
Log dp-uc MGP	-0.042	0.86
HR-pQCT tibia		
Cortical vBMD	0.723	0.30
Cortical thickness	-0.050	0.89
Log cortical porosity	0.000	1.0
Cortical BV/TV	-0.581	0.26

6.4 Discussion

Advanced CKD patients stages 4 - 5D had more VC than their age and gender-matched healthy controls in this study which is consistent with previously published studies {Krasniak et al 2007; Rodriguez-Garcia et al 2009}. A study by Rodrigues-Garcia et al involving 193 dialysis patients showed that the prevalence of aortic calcification was 79% compared to 38% in the general population {Rodriguez-Garcia et al 2009}. These proportions are similar to the ankle VC detected in the CKD and control groups in our study. However, ankle VC mass in the CKD group of our study was lower (median of 1.04 mgHA) than ankle VC mass reported by Patsch et al (median of 6.65 mgHA) {Patsch et al 2014}. This was expected because they studied dialysis patients only and we included pre-dialysis and dialysis patients in our study.

Age is a known strong risk factor for VC and previous studies in dialysis patients showed increasing severity of vascular calcification with age, often regardless of other factors such as dialysis vintage, dyslipidaemia, PTH level and hypertension {Adragao et al 2009; Fabbian et al 2005; Krasniak et al 2007; S. M. Moe et al 2003; Nitta et al 2018}. However, young or paediatric patients with advanced CKD also has VC {Kanbay et al 2010; Shroff et al 2008}, suggesting that other factors also play active roles in VC. Diabetes mellitus is another strong risk factor as shown by previous studies in dialysis and non-dialysis CKD {Garcia-Canton et al 2011; Gorriz et al 2015; Malluche et al 2015; Patsch et al 2014}. Diabetes is associated with 2 - 5 times increased likelihood of having more severe VC. In our study, we found that age was associated with ankle VC and AAC in CKD. However, CKD patients with diabetes had more severe ankle VC whereas there was no difference in AAC score between CKD with and without diabetes. This suggested that ankle VC was an active process rather than just passive changes associated with ageing. The relationships between ankle VC and the risk factors assessed in

CKD in our study is summarised in ***Figure 6.4***. Although collectively these factors explain 62% of the variability in ankle VC mass, none of the factors was identified as an independent factor for ankle VC which confirms that ankle VC in advanced CKD is multi-factorial.

Figure 6.4

Summary of the relationships between ankle VC and its biomarkers and bone in CKD.

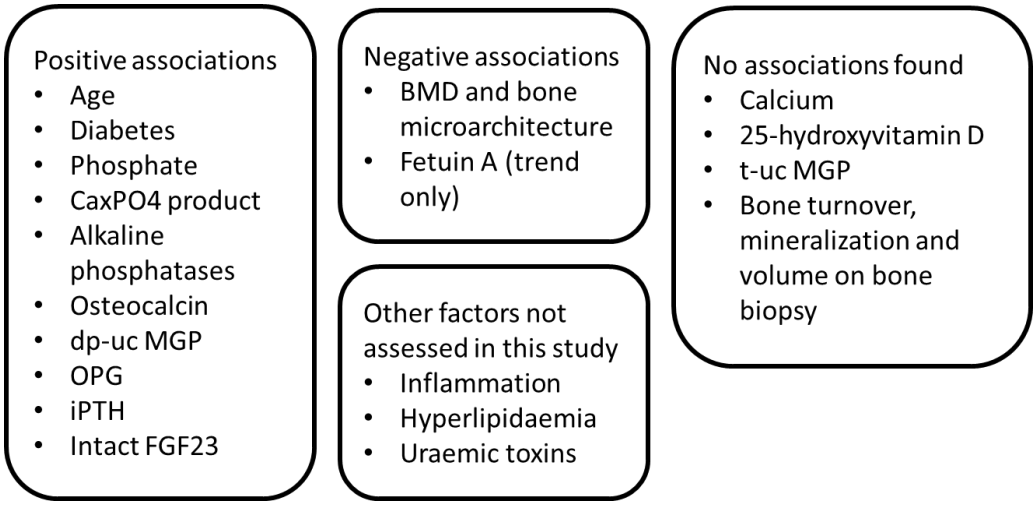

There are biochemical abnormalities of CKD-MBD which are promoters of vascular calcification, namely calcium, phosphate, iPTH and alkaline phosphatases. A study by Block et al using a database with over 40,000 haemodialysis patients showed that abnormalities of these CKD-MBD biochemistry were associated with increased mortality {Block et al 2004}. Hypercalcaemia and hyperphosphataemia are known to be positively associated with VC {London et al 2008; Raggi et al 2002} . The Chronic Renal Insufficiency Cohort (CRIC) study was a large study involving 1500 patients with mild-moderate CKD which showed that serum phosphate was associated with the prevalence and severity of coronary arteries calcification

{Scialla et al 2013}. In our study, serum phosphate in CKD was higher than healthy controls and it was positively associated with ankle VC. Raised serum phosphate encourages vascular smooth muscles cells (VSMCs) to differentiate into osteogenic phenotype, leading to mineral deposition {Giachelli 2003; Jono et al 2000}.

CKD patients in our study had similar serum calcium as healthy controls and it was not associated with ankle VC. However, CaxPO4 product was positively associated with ankle VC. An ex vivo study by Shroff et al assessing human blood vessels from pre-dialysis and dialysis patients showed that only the combination of high calcium and high phosphate medium (and therefore, high CaxPO4 product) increased VC significantly in these patients {Shroff et al 2010}. This suggested that CaxPO4 product play a role in VC in advanced CKD. However, there are also a number of studies that found no relationship between VC and CaxPO4 product. A study by Sigrist et al also showed that calcium, phosphate and CaxPO4 product were not associated with VC progression in CKD stages 4-5D {M. K. Sigrist et al 2007}. Furthermore, a study by Fabian et al showed that CaxPO4 product was similar in dialysis patients with and without AAC {Fabbian et al 2005}. VC and CaxPO4 product relationship was also assessed in an interventional trial called Treat to Goal Study which assessed VC progression in 200 dialysis patients who were randomised to calcium-based phosphate binder and sevelamer (non-calcium based binder) {Chertow et al 2002}. Calcium-based binder group had higher serum calcium level and higher VC progression despite similar serum phosphate and CaxPO4 product levels in both groups. These contrasting findings have only emphasised that calcium, phosphate and CaxPO4 product should still be simultaneously assessed in relation to VC.

CKD patients in our study had similar 25-hydroxyvitamin D level as healthy controls and it was not associated with ankle VC. VC association with 25-hydroxyvitamin D have been mixed;

some studies showed no associations {Kanbay et al 2010; Ulutas et al 2018}, but most showed inverse association between VC and 25-hydroxyvitamin D level {Fusaro et al 2013; Garcia-Canton et al 2011; Krasniak et al 2007; S. Y. Lee et al 2012; Matias et al 2009; F. Wang et al 2015}.

High tALP and bALP are known to promote VSMCs transformation into osteoblast-like cells in experimental model {N. X. Chen et al 2002}. In our study, CKD patients had significantly higher tALP and bALP than healthy controls although it is known that alkaline phosphatases levels are not affected by reduced renal clearance {Magnusson et al 2001}. We found that both markers were positively associated with ankle VC. Previous studies showed that the association between alkaline phosphatases and VC have been mixed. Morena et al reported that tALP was positively associated with moderate to severe VC in pre-dialysis CKD although the association was not found with bALP {Morena et al 2015}. Ishimura et al did not assess tALP but found that bALP was positively associated with VC in dialysis patients {Ishimura et al 2014}. Sigrist et al also found that tALP was associated with VC progression over 24-months in dialysis and pre-dialysis CKD {M. K. Sigrist et al 2007}. Despite these supportive findings on the relationship of alkaline phosphatases and VC, several studies did not find any relationship between these markers and VC on imaging {D. V. Barreto et al 2008; Jean et al 2009; Ozkok et al 2012}. Furthermore, a study by Qureshi et al also did not show tALP and bALP association with biopsy proven VC of the inferior epigastric artery {Qureshi et al 2015}.

SHPT and extremely high FGF23 level are the main hormone abnormalities in CKD-MBD. PTH and FGF23 levels rise in response to reduced renal function, reduced renal phosphate excretion, and abnormal vitamin D metabolism. Thus, phosphate, PTH and FGF23 are also surrogate markers of reduced renal function and it is difficult to infer causal relationship

between these markers and VC. In our study, both iPTH and intact FGF23 were positively associated with ankle VC. A recent experimental study showed that high PTH medium promotes osteoblastic transformation of endothelial cells {Cheng et al 2018}. Furthermore, PTH effect on VC may also be indirect via increased bone turnover with secondary hyperparathyroidism which releases phosphate from bone and promotes VC. Malluche et al showed that the presence and progression of VC was associated with iPTH > 540 pg/mL in a study of 213 dialysis patients {Malluche et al 2015}. Although bone biopsy was not performed, this level of iPTH is almost certainly associated with high bone turnover. However, VC has also been associated with low bone turnover or adynamic bone disease. In a study of 58 dialysis patients, London et al showed that severe VC was associated with low PTH and low bone turnover confirmed on histomorphometry {London et al 2004}. Another study by Tomiyama et al also showed similar association in pre-dialysis CKD {Tomiyama et al 2010}. It is likely that reduced phosphate uptake by bone in low bone turnover ROD leads to hyperphosphatemia which promotes VC. Despite the positive association between VC and iPTH in our study, we did not find any relationship between VC and bone turnover on histomorphometry.

We found that intact FGF23 was positively associated with ankle VC in our study. It is likely that this relationship was indirect through serum phosphate. FGF23 is produced by osteocytes in the bone and its main action is via its high affinity to bind with its co-receptor, klotho, in the kidneys to promote phosphaturia {Saito et al 2003}. Klotho is not found in VSMCs and two *in vitro* studies also showed that it was phosphate, and not FGF23, which induced VC {Jimbo et al 2014; Scialla et al 2013; van Venrooij et al 2014}.

In addition to the VC promoters discussed so far, there is growing knowledge on circulating inhibitors of VC (e.g. MGP and fetuin A) but the evidence is still limited. MGP is a VC inhibitor

which is produced by VSMCs and endothelial cells {Luo et al 1997; Schlieper et al 2010}. MGP inhibits calcium crystal growth locally and prevents osteoblastic differentiation of VSMCs {Roy et al 2002}. MGP is dependent on vitamin K for its activation and undergoes two post-translational modifications: glutamate carboxylation and serine phosphorylation {Schurgers et al 2007}. The active forms of this inhibitor is the carboxylated and/or phosphorylated MGP. We measured two different species of MGP in this study; total uncarboxylated (t-uc) MGP and dephosphorylated-uncarboxylated (dp-uc) MGP. The t-uc MGP detected is mainly in the phosphorylated form which is an active VC inhibitor. We found that CKD patients had lower level of t-uc MGP compared to healthy controls but it was not associated with ankle VC mass in CKD. A study by Cranenburg et al also showed that t-uc MGP level was lower in dialysis patients compared to healthy controls {Cranenburg et al 2009}. Unlike our findings, they found that t-uc MGP was inversely associated with VC in dialysis patients.

The other MGP species measured in our study was the dp-uc MGP which is the inactive VC inhibitor. We found that its level was significantly higher in CKD compared to healthy controls and it was positively associated with ankle VC. This is consistent with findings by Schurgers et al where dp-uc MGP was significantly associated with aortic calcification in 107 patients with CKD stages 2 - 5D {Schurgers et al 2010}. The evidence is very limited to suggest if dp-uc MGP may be a better marker for VC compared to t-uc MGP in both pre-dialysis and dialysis patients.

Fetuin A, also known as alpha- 2 Heremans Schmid glycoprotein, is a potent systemic VC inhibitor which is produced by the liver. Circulating fetuin A prevents spontaneous precipitation of calcium-phosphate product in the vasculature and in other extra-skeletal tissues {Schafer et al 2003}. It inhibits VC via several mechanisms: (1) Fetuin A is incorporated intracellularly in VSMC to inhibit calcification, (2) prevents VSMC apoptosis and (3)

encourages the uptake of apoptotic VSMC by adjacent viable VSMC and thus, reduces local inflammation which is another factor promoting VC {Reynolds et al 2005; Schlieper et al 2010}. A number of studies predominantly in dialysis patients consistently showed that low serum fetuin A was associated with VC {H. Y. Chen et al 2016; Kanbay et al 2010; Stenvinkel et al 2005; A. Y. Wang et al 2005}. We only found a trend towards lower fetuin A with increasing ankle VC mass in our study. This may have been due to small number of patients and we included pre-dialysis and dialysis patients. It is well known that dialysis patients tend to have more severe VC than pre-dialysis CKD {M. Sigrist et al 2006}. Another possible explanation may be due to the relationship between fetuin A and inflammation which was not assessed in our study. Fetuin A and C-reactive protein (CRP) are predominantly made in the liver and they have an inverse relationship {Ketteler, Bongartz, et al 2003; Lebreton et al 1979; Stenvinkel et al 2005; A. Y. Wang et al 2005}. Inflammation is a known promoter of VC and CRP has been positively associated with VC in a number of studies involving dialysis patients {Ishimura et al 2004; Krasniak et al 2007; Stompor et al 2003}. When assessed simultaneously, it was CRP but not fetuin A which was independently associated with VC in dialysis patients {Jung et al 2006; Schlieper et al 2009}.

There are also circulating markers released from bone which may have effects on VSMCs (e.g. osteocalcin and OPG). Osteocalcin is produced primarily by osteoblasts and thus, is also a marker of bone formation. It is a vitamin K-dependent protein which has a high affinity for hydroxyapatite and has been found in calcified atherosclerotic plaque and calcified aortic valve {Hauschka et al 1989; Levy et al 1983}. The exact role of osteocalcin in VC is not fully understood but it is thought to be a VC promoter as high osteocalcin level stimulates VSMCs differentiation and mineralization in experimental model {Idelevich et al 2011}. We found that osteocalcin level was significantly higher in advanced CKD than in controls. The marked

increase is due to a combination of high bone turnover disease in some of our CKD patients and accumulation of osteocalcin with reduced renal clearance {Yamada et al 2008}. Although some osteocalcin is removed during dialysis, the level rebounds within several hours {Carlson et al 2017}. We found that osteocalcin was positively associated with ankle VC, thus supporting the evidence that osteocalcin is a VC promoter. However, findings from other studies have been different to ours despite only involving dialysis patients who were expected to have higher osteocalcin level than pre-dialysis CKD. Three studies found no relationship and one study found an inverse association between osteocalcin and VC {Avila et al 2017; Fusaro et al 2017; Ishimura et al 2014; Ramirez-Sandoval et al 2016}.

Another bone marker which may have effects on VC in CKD is OPG. It is produced mainly by osteoblasts and can be detected in the circulation, but it can also be produced locally by VSMCs {Bucay et al 1998}. OPG is a decoy receptor for RANKL and prevents osteoclast differentiation in bone {Lacey et al 1998}. Via the same mechanism, it is also thought to block the remodelling process in VC {Bucay et al 1998}. Furthermore, OPG can also reduce osteoblastic transformation of VSMCs and block ALP activity to prevent bone matrix formation and mineralization in the vasculature as shown in experimental studies {Orita et al 2007; Zhou et al 2013}. Consistent with the mechanisms described, an animal study showed that OPG was inversely associated with VC {Bennett et al 2006}. However, human studies have shown the opposite, even in those without CKD {Schoppet et al 2003}. Our study and others showed that OPG was positively associated with VC in pre-dialysis and dialysis patients {Avila et al 2017; S. M. Lee et al 2017; Morena et al 2015; Nascimento et al 2014; Nitta et al 2003; Ozkok et al 2012; Pateinakis et al 2013; Ramirez-Sandoval et al 2016}. Although OPG is excreted by the kidneys and is not removed by dialysis, studies in dialysis patients showed that those with VC had significantly higher OPG level than those without VC {D. V. Barreto et

al 2008; Jean et al 2009; Kazama et al 2002; Morena et al 2015}. There are two possible explanations for these conflicting observations. OPG secreted by VSMCs may be a local VC inhibitor but higher circulating OPG level may not have the same protective effect {Morena et al 2012}. OPG production by VSMCs could also be a compensatory mechanism to inflammation from pre-existing VC, thus higher level is observed with increasing VC severity {Deuell et al 2012}.

Assessment of ankle VC using HR-pQCT is only available in a few research centre and is currently not available in clinical practice. In this study, we have identified a number of markers which were associated with ankle VC in CKD. Furthermore, we found that biomarkers such as phosphate, CaxPO4 product, iPTH, intact FGF23, tALP, osteocalcin, OPG and dp-uc MGP can identify CKD patients with ankle VC. However, these biomarkers are not robust enough as diagnostic tests because their AUCs were <0.80. Therefore, imaging of VC is still the only way of assessing the presence of VC.

The bone-vascular abnormalities are an important sequelae of CKD-MBD. In a study involving 193 dialysis patients, Rodriguez-Garcia et al showed that patients with VC had 6 times higher risk of vertebral fractures than those without {Rodriguez-Garcia et al 2009}. Female patients with vertebral fractures in the study also had 5 times increased risk of mortality. More recently, Chen et al reported a study involving 685 dialysis patients and found that patients with VC had double the risk of fractures compared to those without VC {H. Y. Chen et al 2016}. This may be partly explained by the association between lower BMD and VC in these patients {Adragao et al 2008; Z. Chen et al 2016; Malluche et al 2015}. A longitudinal study also showed that VC progression was associated with bone loss in CKD {Watanabe et al 2012}. Simultaneous assessment of bone and VC at the distal tibia using HR-pQCT in our study

revealed that lower cortical BMD and worse cortical bone microarchitecture at the tibia were associated with ankle VC. Meanwhile, ankle VC had no relationship with total hip BMD or distal radius BMD and microstructure. Our findings are similar to a study by Cejka et al which assessed coronary artery calcification (CAC) and bone characteristics using DXA and HR-pQCT in 66 dialysis patients {Cejka et al 2014}. The study found that high CAC was associated with lower BMD and lower trabecular bone volume at the distal tibia. No association was found between CAC and DXA BMD. Our study and Cejka et al study confirmed that VC was associated with lower BMD and microarchitecture of distal tibia only but not with the sites typically assessed using DXA.

Studies assessing the direct relationship between VC and bone turnover, mineralization and microstructure using bone biopsy is very limited. Two studies in dialysis patients found that low bone volume on iliac bone biopsy, but not bone turnover, was associated with increased VC {Adragao et al 2009; Barreto et al 2005}. However, we did not find any relationship between VC and bone turnover, mineralization or volume on bone biopsy in our study. This could be due to small number of patients with bone biopsy data and the inclusion of pre-dialysis and dialysis CKD. Dialysis patients tend to have worse VC and worse bone characteristics than pre-dialysis CKD.

There are several strengths in this study. We used two different imaging techniques (DXA and HR-pQCT) which allowed simultaneous assessment of VC and bone. Assessment of ankle VC using HR-pQCT is relatively new but it has been validated against the more sensitive VC imaging using computed tomography of coronary arteries in CKD {Patsch et al 2014}. There is also growing evidence on the importance of bone microstructure assessment in CKD-MBD which can be done using HR-pQCT. We also assessed the relationship between VC and bone

in CKD using bone biopsy to determine the direct association between VC and bone turnover, mineralization and volume. Finally, we simultaneously assessed VC, its biomarkers and bone characteristics in CKD and healthy controls.

There are also several limitations to our study. We did not assess coronary artery calcification using computed tomography in this study but VC is a systemic process. Inflammation is a known promoter of VC but we did not assess this in our study. We also did not assess other factors such as hyperlipidaemia or hypercholectrolemia but evidence showed that VC in advanced CKD is independent of these traditional VC risk factors {Fabbian et al 2005; Krasniak et al 2007}. We also had a small number of patients with bone biopsy data but bone biopsy was not performed with the primary aim to assess its relationship with VC in this study.

To conclude, ankle VC assessed by HR-pQCT is an alternative method to detect VC in advanced CKD. Ankle VC in CKD was associated with age, diabetes, mineral abnormalities, VC promoters, low BMD and worse bone microarchitecture. Currently, no interventions involving the correction of biochemical abnormalities in CKD-MBD could reverse VC once it is established although there is some evidence of VC attenuation. Given the high risk of cardiovascular disease and fracture in advanced CKD, future research on the bone-vascular effects of bone-specific therapy in advanced CKD is needed. HR-pQCT will allow simultaneous assessment of bone microarchitecture and VC in these patients.

Chapter 7. Conclusions and Future Research

Fracture risk is increased in patients with advanced CKD due to bone turnover and mineralization abnormalities known as renal osteodystrophy (ROD). It is common in this patient population and results in bone microstructural and mechanical changes which are associated with increased bone fragility. Bone-specific treatment to reduce fracture risk have been used in patients with osteoporosis with clear benefit on fracture risk reduction. Some of these treatment (e.g. denosumab and teriparatide) are not contraindicated in advanced CKD but a bone biopsy (gold standard test) is required to diagnose their bone turnover before commencing treatment. This would allow the treatment to be tailored to individuals bone turnover status. For example, denosumab is an antiresorptive agent and therefore, should only be given to patients with normal or high bone turnover. Meanwhile, teriparatide is an anabolic agent which should be avoided in patients with high bone turnover disease. However, bone biopsy is rarely performed because it is invasive and painful. Repeated bone biopsy to assess treatment effect is also impossible. Therefore, there is a real need to explore if new non-invasive techniques of assessing bone turnover and microstructure could replace the role of bone biopsy to diagnose and classify ROD.

We have answered this question by simultaneously testing the diagnostic accuracy of novel bone turnover markers (BTMs) and high resolution bone imaging to predict ROD subtypes. We found that BTMs such as bALP, intact PINP and TRAP5b, and bone imaging of distal radius using HR-pQCT were able to discriminate low bone turnover in advanced CKD patients. These non-invasive tests are robust as diagnostic tools and have the potential to be translated into clinical practice.

Vascular calcification (VC) is also common in advanced CKD. Although ROD and VC are both part of CKD-MBD, their direct relationship is uncertain due to limited number of studies

especially those involving bone biopsy. We assessed this relationship in advanced CKD patients by using a new quantitative method of measuring VC in the ankle arteries and directly assessing its severity with bone biopsy and bone microstructure using HR-pQCT. We found that ankle VC was associated with worse bone microstructure of cortical bone at the distal tibia. We also found that ankle VC was associated with CKD-MBD serum biochemistry such as phosphate, iPTH and intact FGF23; mineralization markers such as ALP and osteocalcin; and inactive vascular calcification inhibitor such as dp-uc MGP.

The major strength of this study is bone biopsy which is the gold standard test to diagnose ROD. Furthermore, our bone biopsy histomorphometry included both dynamic and static measurements to assess bone turnover, mineralization and volume as recommended by KDIGO CKD-MBD guideline. Participant recruitment into a bone biopsy study is challenging but we managed to recruit all participants purely for research and not for clinical indications. Therefore, our participants were representative of advanced CKD population with CKD-MBD who are mostly asymptomatic. Furthermore, we used HR-pQCT scan to assess bone microstructure in the peripheral bones which are also known fracture sites in CKD. Our simultaneous assessment of VC and bone microstructure by HR-pQCT is new but important in advanced CKD in whom VC and ROD are common. HR-pQCT is only available in a small number of centres worldwide which are focussed on bone research.

There are several limitations to this study. This was a single centre observational study with a small number of participants. For the primary aim of assessing diagnostic accuracy of non-invasive tests to predict ROD subtypes on bone biopsy, we managed to recruit a representative sample of advanced CKD patients with ROD. The proportion of patients with low, normal and high bone turnover was similar to previously published studies, and we had

a broad range of bone turnover which is important in assessing diagnostic test accuracy. However, we were unable to assess pre-dialysis CKD and dialysis patients separately, or haemodialysis and peritoneal dialysis separately because of small sample size. Small sample size in bone biopsy study is not exclusive to our study. This has been acknowledged by the CKD-MBD Working Group under the European Renal Association and European Dialysis and Transplant Association (ERA-EDTA). We have established collaboration with other European centres to collect all bone biopsy data from CKD into a registry known as the European ROD (EUROD) Initiatives under the umbrella of ERA-EDTA.

Our bone histomorphometry analysis was only performed for trabecular bone. Some bone samples were missing the inner cortex when the biopsy sample was extracted from the patients. All samples had the outer cortex but the risk of crush artefact on the outer cortex is higher. Cortical bone analysis such as bone thickness and volume may be useful in CKD because cortical bone microstructure is affected in CKD. However, information on bone turnover and mineralization which are required for ROD classification should be obtained from trabecular bone as it is the more metabolically active bone compartment. Histomorphometry limited to trabecular bone is also the standard analysis in clinical setting.

We found that distal radius HR-pQCT can discriminate low bone turnover from non-low bone turnover patients in this study. However, we recognise that the effects of bone turnover on microstructure are dynamic and may take a long time (potentially up to a couple of years) to show the associated changes. Meanwhile, any imaging technique is a static test. Thus, the cross-sectional use of HR-pQCT is perhaps more appropriate in assessing bone volume (static measurement) rather than bone turnover (dynamic measurement). This could be confirmed with a longitudinal study assessing bone turnover on bone biopsy and bone microstructure

using HR-pQCT. However, a study using repeated bone biopsy is challenging for the reasons already mentioned.

The future direction of my research may involve the use of the non-invasive diagnostic tools identified in this study to assess the treatment effect of bone specific therapy in advanced CKD. Bisphosphonates used to be the only treatment to reduce fracture risk but it is contraindicated in advanced CKD. New treatment, namely denosumab and teriparatide, have been developed over the last decade and are not contraindicated in advanced CKD. However, these treatment has different effect on bone turnover (anti-resorptive versus anabolic) and therefore must be tailored appropriately to patients bone turnover status. Incorrect treatment, for example further suppression of low bone turnover by denosumab in patients with pre-existing low bone turnover/ABD may be detrimental to bone health. This tailored approach and its benefit to bone and fracture risk need further research. This could be done in a randomised clinical trial in which bone turnover markers we have identified could predict participants' baseline bone turnover status. Assessing fracture outcome in this clinical trial would require a large number of participants and costly. However, the use of BTMs and HR-pQCT as surrogate markers could improve our understanding of the mechanism and structural changes by which these new treatment may reduce fracture risk in advanced CKD. Furthermore, denosumab often requires supplementary calcium and vitamin D to prevent severe hypocalcaemia in advanced CKD and there is a concern that these may also worsen VC. HR-pQCT would allow simultaneous assessment of bone and VC in this type of clinical trial.

The use of BTMs to identify ROD may also be used in future research to further understand a particular type of ROD. Historically, the predominant ROD is high bone turnover disease but

this may have changed now to predominantly low bone turnover/ABD as demonstrated by two large bone biopsy series published in the last decade. Whilst PTH is known to be the main drive for high bone turnover disease, the exact mechanisms leading to ABD is not fully understood. The reason why advanced CKD patients with similar degree of SHPT may have different ROD subtypes is unknown. Our study has shown that CKD patients with low bone turnover disease have better bone microstructure compared to those with high bone turnover disease. However, bone quality, which is one the main determinants of bone strength, in ABD is unknown. BTMs and HR-pQCT can be used towards further research to answer these questions.

References

Adragao, T., Branco, P., Birne, R., Curto, J. D., de Almeida, E., Prata, M. M., et al. (2008). Bone mineral density, vascular calcifications, and arterial stiffness in peritoneal dialysis patients. *Perit Dial Int, 28*(6), 668-672.

Adragao, T., Herberth, J., Monier-Faugere, M. C., Branscum, A. J., Ferreira, A., Frazao, J. M., et al. (2009). Low bone volume--a risk factor for coronary calcifications in hemodialysis patients. *Clin J Am Soc Nephrol, 4*(2), 450-455. doi:10.2215/CJN.01870408

Adragao, T., Herberth, J., Monier-Faugere, M. C., Branscum, A. J., Ferreira, A., Frazao, J. M., et al. (2010). Femoral bone mineral density reflects histologically determined cortical bone volume in hemodialysis patients. *Osteoporos Int, 21*(4), 619-625. doi:10.1007/s00198-009-0988-9

Aleksova, J., Kurniawan, S., & Elder, G. J. (2018). The trabecular bone score is associated with bone mineral density, markers of bone turnover and prevalent fracture in patients with end stage kidney disease. *Osteoporos Int, 29*(6), 1447-1455. doi:10.1007/s00198-018-4468-y

Aleksova, J., Kurniawan, S., Vucak-Dzumhur, M., Kerr, P., Ebeling, P. R., Milat, F., et al. (2018). Aortic vascular calcification is inversely associated with the trabecular bone score in patients receiving dialysis. *Bone, 113*, 118-123. doi:10.1016/j.bone.2018.05.014

Alem, A. M., Sherrard, D. J., Gillen, D. L., Weiss, N. S., Beresford, S. A., Heckbert, S. R., et al. (2000). Increased risk of hip fracture among patients with end-stage renal disease. *Kidney Int, 58*(1), 396-399. doi:kid178 [pii] 10.1046/j.1523-1755.2000.00178.x

Allen, M. K., K. (2014). Skeletal Imaging. In A. M. Burr D (Ed.), *Basic and Applied Bone Biology* (pp. 93 -113): Academic Press.

Alvarez, L., Torregrosa, J. V., Peris, P., Monegal, A., Bedini, J. L., Martinez De Osaba, M. J., et al. (2004). Effect of hemodialysis and renal failure on serum biochemical markers of bone turnover. *J Bone Miner Metab, 22*(3), 254-259. doi:10.1007/s00774-003-0476-9

Amin, S., & Khosla, S. (2012). Sex- and age-related differences in bone microarchitecture in men relative to women assessed by high-resolution peripheral quantitative computed tomography. *J Osteoporos, 2012*, 129760. doi:10.1155/2012/129760

Amling, M., Herden, S., Posl, M., Hahn, M., Ritzel, H., & Delling, G. (1996). Heterogeneity of the skeleton: comparison of the trabecular microarchitecture of the spine, the iliac crest, the femur, and the calcaneus. *J Bone Miner Res, 11*(1), 36-45. doi:10.1002/jbmr.5650110107

Andrukhova, O., Schuler, C., Bergow, C., Petric, A., & Erben, R. G. (2018). Augmented Fibroblast Growth Factor-23 Secretion in Bone Locally Contributes to Impaired Bone Mineralization in Chronic Kidney Disease in Mice. *Front Endocrinol (Lausanne), 9*, 311. doi:10.3389/fendo.2018.00311

Antoniucci, D. M., Yamashita, T., & Portale, A. A. (2006). Dietary phosphorus regulates serum fibroblast growth factor-23 concentrations in healthy men. *J Clin Endocrinol Metab, 91*(8), 3144-3149. doi:10.1210/jc.2006-0021

Araujo, S. M., Ambrosoni, P., Lobao, R. R., Caorsi, H., Moyses, R. M., Barreto, F. C., et al. (2003). The renal osteodystrophy pattern in Brazil and Uruguay: an overview. *Kidney Int Suppl*(85), S54-56. doi:10.1046/j.1523-1755.63.s85.13.x

Austin, M., Yang, Y. C., Vittinghoff, E., Adami, S., Boonen, S., Bauer, D. C., et al. (2012). Relationship between bone mineral density changes with denosumab treatment and risk reduction for vertebral and nonvertebral fractures. *J Bone Miner Res, 27*(3), 687-693. doi:10.1002/jbmr.1472

Avila, M., Mora, C., Prado, M. D. C., Zavala, M., Paniagua, R., & Mexican Collaborative, G. (2017). Osteoprotegerin Is the Strongest Predictor for Progression of Arterial Calcification in Peritoneal Dialysis Patients. *Am J Nephrol, 46*(1), 39-46. doi:10.1159/000477380

Bacchetta, J., Boutroy, S., Vilayphiou, N., Juillard, L., Guebre-Egziabher, F., Rognant, N., et al. (2010). Early impairment of trabecular microarchitecture assessed with HR-pQCT in patients with stage II-IV chronic kidney disease. *J Bone Miner Res, 25*(4), 849-857. doi:10.1359/jbmr.090831

Bala, Y., Farlay, D., Delmas, P. D., Meunier, P. J., & Boivin, G. (2010). Time sequence of secondary mineralization and microhardness in cortical and cancellous bone from ewes. *Bone, 46*(4), 1204-1212. doi:10.1016/j.bone.2009.11.032

Barreto, D. V., Barreto, F. C., Carvalho, A. B., Cuppari, L., Cendoroglo, M., Draibe, S. A., et al. (2005). Coronary calcification in hemodialysis patients: the contribution of traditional and uremia-related risk factors. *Kidney Int, 67*(4), 1576-1582. doi:10.1111/j.1523-1755.2005.00239.x

Barreto, D. V., Barreto Fde, C., Carvalho, A. B., Cuppari, L., Draibe, S. A., Dalboni, M. A., et al. (2008). Association of changes in bone remodeling and coronary calcification in hemodialysis patients: a prospective study. *Am J Kidney Dis, 52*(6), 1139-1150. doi:10.1053/j.ajkd.2008.06.024

Barreto, F. C., Barreto, D. V., Moyses, R. M., Neves, K. R., Canziani, M. E., Draibe, S. A., et al. (2008). K/DOQI-recommended intact PTH levels do not prevent low-turnover bone disease in hemodialysis patients. *Kidney Int, 73*(6), 771-777. doi:5002769 [pii] 10.1038/sj.ki.5002769

Behets, G. J., Spasovski, G., Sterling, L. R., Goodman, W. G., Spiegel, D. M., De Broe, M. E., et al. (2014). Bone histomorphometry before and after long-term treatment with cinacalcet in dialysis patients with secondary hyperparathyroidism. *Kidney Int*. doi:10.1038/ki.2014.349

Bennett, B. J., Scatena, M., Kirk, E. A., Rattazzi, M., Varon, R. M., Averill, M., et al. (2006). Osteoprotegerin inactivation accelerates advanced atherosclerotic lesion progression and calcification in older ApoE-/- mice. *Arterioscler Thromb Vasc Biol, 26*(9), 2117-2124. doi:10.1161/01.ATV.0000236428.91125.e6

Bervoets, A. R., Spasovski, G. B., Behets, G. J., Dams, G., Polenakovic, M. H., Zafirovska, K., et al. (2003). Useful biochemical markers for diagnosing renal osteodystrophy in predialysis end-stage renal failure patients. *Am J Kidney Dis, 41*(5), 997-1007.

Bhan, I., Powe, C. E., Berg, A. H., Ankers, E., Wenger, J. B., Karumanchi, S. A., et al. (2012). Bioavailable vitamin D is more tightly linked to mineral metabolism than total vitamin D in incident hemodialysis patients. *Kidney Int, 82*(1), 84-89. doi:10.1038/ki.2012.19

Bhattacharyya, N., Wiench, M., Dumitrescu, C., Connolly, B. M., Bugge, T. H., Patel, H. V., et al. (2012). Mechanism of FGF23 processing in fibrous dysplasia. *J Bone Miner Res, 27*(5), 1132-1141. doi:10.1002/jbmr.1546

Bikle, D. D. (2012). Vitamin D and bone. *Curr Osteoporos Rep, 10*(2), 151-159. doi:10.1007/s11914-012-0098-z

Bikle, D. D., Gee, E., Halloran, B., Kowalski, M. A., Ryzen, E., & Haddad, J. G. (1986). Assessment of the free fraction of 25-hydroxyvitamin D in serum and its regulation by albumin and the vitamin D-binding protein. *J Clin Endocrinol Metab, 63*(4), 954-959. doi:10.1210/jcem-63-4-954

Block, G. A., Bone, H. G., Fang, L., Lee, E., & Padhi, D. (2012). A single-dose study of denosumab in patients with various degrees of renal impairment. *J Bone Miner Res, 27*(7), 1471-1479. doi:10.1002/jbmr.1613

Block, G. A., Klassen, P. S., Lazarus, J. M., Ofsthun, N., Lowrie, E. G., & Chertow, G. M. (2004). Mineral metabolism, mortality, and morbidity in maintenance hemodialysis. *J Am Soc Nephrol, 15*(8), 2208-2218. doi:10.1097/01.ASN.0000133041.27682.A2

Blomquist, G. A., Davenport, D. L., Mawad, H. W., Monier-Faugere, M. C., & Malluche, H. H. (2015). Diagnosis of low bone mass in CKD-5D patients. *Clin Nephrol*. doi:10.5414/CN108708

Bowling, C. B., Bromfield, S. G., Colantonio, L. D., Gutierrez, O. M., Shimbo, D., Reynolds, K., et al. (2016). Association of Reduced eGFR and Albuminuria with Serious Fall Injuries among Older Adults. *Clin J Am Soc Nephrol, 11*(7), 1236-1243. doi:10.2215/CJN.11111015

Briot, K., Paternotte, S., Kolta, S., Eastell, R., Reid, D. M., Felsenberg, D., et al. (2013). Added value of trabecular bone score to bone mineral density for prediction of osteoporotic fractures in postmenopausal women: the OPUS study. *Bone, 57*(1), 232-236. doi:10.1016/j.bone.2013.07.040

Brown, E. M. (2000). Calcium receptor and regulation of parathyroid hormone secretion. *Rev Endocr Metab Disord, 1*(4), 307-315.

Bucay, N., Sarosi, I., Dunstan, C. R., Morony, S., Tarpley, J., Capparelli, C., et al. (1998). osteoprotegerin-deficient mice develop early onset osteoporosis and arterial calcification. *Genes Dev, 12*(9), 1260-1268.

Bucur, R. C., Panjwani, D. D., Turner, L., Rader, T., West, S. L., & Jamal, S. A. (2015). Low bone mineral density and fractures in stages 3-5 CKD: an updated systematic review and meta-analysis. *Osteoporos Int, 26*(2), 449-458. doi:10.1007/s00198-014-2813-3

Burge, R., Worley, D., Johansen, A. and Bose, U. . (2001). The cost of osteoporotic fractures in the United Kingdom. *Value in Health, 4*, 66–67.

Burghardt, A. J., Buie, H. R., Laib, A., Majumdar, S., & Boyd, S. K. (2010). Reproducibility of direct quantitative measures of cortical bone microarchitecture of the distal radius and tibia by HR-pQCT. *Bone, 47*(3), 519-528. doi:10.1016/j.bone.2010.05.034

Caluwe, R., Vandecasteele, S., Van Vlem, B., Vermeer, C., & De Vriese, A. S. (2014). Vitamin K2 supplementation in haemodialysis patients: a randomized dose-finding study. *Nephrol Dial Transplant, 29*(7), 1385-1390. doi:10.1093/ndt/gft464

Carlson, N., Mortensen, O. H., Axelsen, M., Pedersen, R. S., & Heaf, J. G. (2017). Clearance of Sclerostin, Osteocalcin, Fibroblast Growth Factor 23, and Osteoprotegerin by Dialysis. *Blood Purif, 44*(2), 122-128. doi:10.1159/000465513

Carmen Sanchez, M., Auxiliadora Bajo, M., Selgas, R., Mate, A., Millan, I., Eugenia Martinez, M., et al. (2000). Parathormone secretion in peritoneal dialysis patients with adynamic bone disease. *Am J Kidney Dis, 36*(5), 953-961.

Carrillo-Lopez, N., Panizo, S., Alonso-Montes, C., Roman-Garcia, P., Rodriguez, I., Martinez-Salgado, C., et al. (2016). Direct inhibition of osteoblastic Wnt pathway by fibroblast growth factor 23 contributes to bone loss in chronic kidney disease. *Kidney Int, 90*(1), 77-89. doi:10.1016/j.kint.2016.01.024

Carvalho, C., Magalhaes, J., Neto, R., Pereira, L., Branco, P., Adragao, T., et al. (2016). Cortical bone analysis in a predialysis population: a comparison with a dialysis population. *J Bone Miner Metab*. doi:10.1007/s00774-016-0781-8

Cejka, D., Herberth, J., Branscum, A. J., Fardo, D. W., Monier-Faugere, M. C., Diarra, D., et al. (2011). Sclerostin and Dickkopf-1 in renal osteodystrophy. *Clin J Am Soc Nephrol, 6*(4), 877-882. doi:10.2215/CJN.06550810

Cejka, D., Patsch, J. M., Weber, M., Diarra, D., Riegersperger, M., Kikic, Z., et al. (2011). Bone microarchitecture in hemodialysis patients assessed by HR-pQCT. *Clin J Am Soc Nephrol, 6*(9), 2264-2271. doi:10.2215/CJN.09711010

Cejka, D., Weber, M., Diarra, D., Reiter, T., Kainberger, F., & Haas, M. (2014). Inverse association between bone microarchitecture assessed by HR-pQCT and coronary artery calcification in patients with end-stage renal disease. *Bone, 64*, 33-38. doi:10.1016/j.bone.2014.03.048

Chappard, C., Marchadier, A., & Benhamou, C. L. (2008). Side-to-side and within-side variability of 3D bone microarchitecture by conventional micro-computed tomography of paired iliac crest biopsies. *Bone, 43*(1), 203-208. doi:10.1016/j.bone.2008.02.019

Chen, G., Deng, C., & Li, Y. P. (2012). TGF-beta and BMP signaling in osteoblast differentiation and bone formation. *Int J Biol Sci, 8*(2), 272-288. doi:10.7150/ijbs.2929

Chen, H. Y., Chiu, Y. L., Hsu, S. P., Pai, M. F., Yang, J. Y., & Peng, Y. S. (2016). Relationship between Fetuin A, Vascular Calcification and Fracture Risk in Dialysis Patients. *PLoS One, 11*(7), e0158789. doi:10.1371/journal.pone.0158789

Chen, J., Budoff, M. J., Reilly, M. P., Yang, W., Rosas, S. E., Rahman, M., et al. (2017). Coronary Artery Calcification and Risk of Cardiovascular Disease and Death Among Patients With Chronic Kidney Disease. *JAMA Cardiol, 2*(6), 635-643. doi:10.1001/jamacardio.2017.0363

Chen, N. X., O'Neill, K. D., Duan, D., & Moe, S. M. (2002). Phosphorus and uremic serum up-regulate osteopontin expression in vascular smooth muscle cells. *Kidney Int, 62*(5), 1724-1731. doi:10.1046/j.1523-1755.2002.00625.x

Chen, Z., Qureshi, A. R., Ripsweden, J., Wennberg, L., Heimburger, O., Lindholm, B., et al. (2016). Vertebral bone density associates with coronary artery calcification and is an independent predictor of poor outcome in end-stage renal disease patients. *Bone, 92*, 50-57. doi:10.1016/j.bone.2016.08.007

Cheng, Z. Y., Ye, T., Ling, Q. Y., Wu, T., Wu, G. Y., & Zong, G. J. (2018). Parathyroid hormone promotes osteoblastic differentiation of endothelial cells via the extracellular signal-regulated protein kinase 1/2 and nuclear factor-kappaB signaling pathways. *Exp Ther Med, 15*(2), 1754-1760. doi:10.3892/etm.2017.5545

Chertow, G. M., Block, G. A., Correa-Rotter, R., Drueke, T. B., Floege, J., Goodman, W. G., et al. (2012). Effect of cinacalcet on cardiovascular disease in patients undergoing dialysis. *N Engl J Med, 367*(26), 2482-2494. doi:10.1056/NEJMoa1205624

Chertow, G. M., Burke, S. K., Raggi, P., & Treat to Goal Working, G. (2002). Sevelamer attenuates the progression of coronary and aortic calcification in hemodialysis patients. *Kidney Int, 62*(1), 245-252. doi:10.1046/j.1523-1755.2002.00434.x

Coco, M., & Rush, H. (2000). Increased incidence of hip fractures in dialysis patients with low serum parathyroid hormone. *Am J Kidney Dis, 36*(6), 1115-1121. doi:10.1053/ajkd.2000.19812

Coen, G., Ballanti, P., Balducci, A., Calabria, S., Fischer, M. S., Jankovic, L., et al. (2002). Serum osteoprotegerin and renal osteodystrophy. *Nephrol Dial Transplant, 17*(2), 233-238.

Coen, G., Ballanti, P., Bonucci, E., Calabria, S., Centorrino, M., Fassino, V., et al. (1998). Bone markers in the diagnosis of low turnover osteodystrophy in haemodialysis patients. *Nephrol Dial Transplant, 13*(9), 2294-2302.

Coen, G., Bonucci, E., Ballanti, P., Balducci, A., Calabria, S., Nicolai, G. A., et al. (2002). PTH 1-84 and PTH "7-84" in the noninvasive diagnosis of renal bone disease. *Am J Kidney Dis, 40*(2), 348-354. doi:10.1053/ajkd.2002.34519

Coen, G., Mazzaferro, S., Ballanti, P., Sardella, D., Chicca, S., Manni, M., et al. (1996). Renal bone disease in 76 patients with varying degrees of predialysis chronic renal failure: a cross-sectional study. *Nephrol Dial Transplant, 11*(5), 813-819.

Cohen, A., Dempster, D. W., Muller, R., Guo, X. E., Nickolas, T. L., Liu, X. S., et al. (2010). Assessment of trabecular and cortical architecture and mechanical competence of bone by high-resolution peripheral computed tomography: comparison with transiliac bone biopsy. *Osteoporos Int, 21*(2), 263-273. doi:10.1007/s00198-009-0945-7

Coresh, J., Astor, B. C., Greene, T., Eknoyan, G., & Levey, A. S. (2003). Prevalence of chronic kidney disease and decreased kidney function in the adult US population: Third National Health and Nutrition Examination Survey. *Am J Kidney Dis, 41*(1), 1-12. doi:10.1053/ajkd.2003.50007

Coresh, J., Selvin, E., Stevens, L. A., Manzi, J., Kusek, J. W., Eggers, P., et al. (2007). Prevalence of chronic kidney disease in the United States. *JAMA, 298*(17), 2038-2047. doi:10.1001/jama.298.17.2038

Couttenye, M. M., D'Haese, P. C., Van Hoof, V. O., Lemoniatou, E., Goodman, W., Verpooten, G. A., et al. (1996). Low serum levels of alkaline phosphatase of bone origin: a good marker of adynamic bone disease in haemodialysis patients. *Nephrol Dial Transplant, 11*(6), 1065-1072.

Cozzolino, M., Brancaccio, D., Gallieni, M., & Slatopolsky, E. (2005). Pathogenesis of vascular calcification in chronic kidney disease. *Kidney Int, 68*(2), 429-436. doi:10.1111/j.1523-1755.2005.00421.x

Crabtree, N. L., M.; Zemel, B. (2007). Dual-Energy X-Ray Absorptiometry. In A. Sawyer (Ed.), *Bone Densitometry in Growing Patients* (pp. 41 - 57): Humana Press.

Crane, J. L., & Cao, X. (2014). Function of matrix IGF-1 in coupling bone resorption and formation. *J Mol Med (Berl), 92*(2), 107-115. doi:10.1007/s00109-013-1084-3

Cranenburg, E. C., Brandenburg, V. M., Vermeer, C., Stenger, M., Muhlenbruch, G., Mahnken, A. H., et al. (2009). Uncarboxylated matrix Gla protein (ucMGP) is

associated with coronary artery calcification in haemodialysis patients. *Thromb Haemost, 101*(2), 359-366.

Cranenburg, E. C., Schurgers, L. J., Uiterwijk, H. H., Beulens, J. W., Dalmeijer, G. W., Westerhuis, R., et al. (2012). Vitamin K intake and status are low in hemodialysis patients. *Kidney Int, 82*(5), 605-610. doi:10.1038/ki.2012.191

Craver, L., Marco, M. P., Martinez, I., Rue, M., Borras, M., Martin, M. L., et al. (2007). Mineral metabolism parameters throughout chronic kidney disease stages 1-5--achievement of K/DOQI target ranges. *Nephrol Dial Transplant, 22*(4), 1171-1176. doi:10.1093/ndt/gfl718

Cunningham, J., Sprague, S. M., Cannata-Andia, J., Coco, M., Cohen-Solal, M., Fitzpatrick, L., et al. (2004). Osteoporosis in chronic kidney disease. *Am J Kidney Dis, 43*(3), 566-571.

Curtis, E. M., van der Velde, R., Moon, R. J., van den Bergh, J. P., Geusens, P., de Vries, F., et al. (2016). Epidemiology of fractures in the United Kingdom 1988-2012: Variation with age, sex, geography, ethnicity and socioeconomic status. *Bone, 87*, 19-26. doi:10.1016/j.bone.2016.03.006

D'Amelio, P., Isaia, G., & Isaia, G. C. (2009). The osteoprotegerin/RANK/RANKL system: a bone key to vascular disease. *J Endocrinol Invest, 32*(4 Suppl), 6-9.

Danese, M. D., Kim, J., Doan, Q. V., Dylan, M., Griffiths, R., & Chertow, G. M. (2006). PTH and the risks for hip, vertebral, and pelvic fractures among patients on dialysis. *Am J Kidney Dis, 47*(1), 149-156. doi:S0272-6386(05)01495-2 [pii] 10.1053/j.ajkd.2005.09.024

Delanaye, P., Dubois, B. E., Lukas, P., Peters, P., Krzesinski, J. M., Pottel, H., et al. (2015). Impact of stopping vitamin K antagonist therapy on concentrations of dephospho-uncarboxylated Matrix Gla protein. *Clin Chem Lab Med, 53*(8), e191-193. doi:10.1515/cclm-2015-0073

Delmas, P. D., Wilson, D. M., Mann, K. G., & Riggs, B. L. (1983). Effect of renal function on plasma levels of bone Gla-protein. *J Clin Endocrinol Metab, 57*(5), 1028-1030. doi:10.1210/jcem-57-5-1028

Dempster, D. W., Ferguson-Pell, M. W., Mellish, R. W., Cochran, G. V., Xie, F., Fey, C., et al. (1993). Relationships between bone structure in the iliac crest and bone structure and strength in the lumbar spine. *Osteoporos Int, 3*(2), 90-96. doi:10.1007/bf01623379

Deuell, K. A., Callegari, A., Giachelli, C. M., Rosenfeld, M. E., & Scatena, M. (2012). RANKL enhances macrophage paracrine pro-calcific activity in high phosphate-treated smooth muscle cells: dependence on IL-6 and TNF-alpha. *J Vasc Res, 49*(6), 510-521. doi:10.1159/000341216

Dooley, A. C., Weiss, N. S., & Kestenbaum, B. (2008). Increased risk of hip fracture among men with CKD. *Am J Kidney Dis, 51*(1), 38-44. doi:10.1053/j.ajkd.2007.08.019

Doorenbos, C. R., de Cuba, M. M., Vogt, L., Kema, I. P., van den Born, J., Gans, R. O., et al. (2012). Antiproteinuric treatment reduces urinary loss of vitamin D-binding protein but does not affect vitamin D status in patients with chronic kidney disease. *J Steroid Biochem Mol Biol, 128*(1-2), 56-61. doi:10.1016/j.jsbmb.2011.09.002

Drinka, P. J., DeSmet, A. A., Bauwens, S. F., & Rogot, A. (1992). The effect of overlying calcification on lumbar bone densitometry. *Calcif Tissue Int, 50*(6), 507-510.

Eastell, R., Brandi, M. L., Costa, A. G., D'Amour, P., Shoback, D. M., & Thakker, R. V. (2014). Diagnosis of asymptomatic primary hyperparathyroidism: proceedings of the Fourth

International Workshop. *J Clin Endocrinol Metab, 99*(10), 3570-3579. doi:10.1210/jc.2014-1414

Engelke, K., Stampa, B., Timm, W., Dardzinski, B., de Papp, A. E., Genant, H. K., et al. (2012). Short-term in vivo precision of BMD and parameters of trabecular architecture at the distal forearm and tibia. *Osteoporos Int, 23*(8), 2151-2158. doi:10.1007/s00198-011-1829-1

Eriksen, E. F., Charles, P., Melsen, F., Mosekilde, L., Risteli, L., & Risteli, J. (1993). Serum markers of type I collagen formation and degradation in metabolic bone disease: correlation with bone histomorphometry. *J Bone Miner Res, 8*(2), 127-132. doi:10.1002/jbmr.5650080202

Evenepoel, P., D'Haese, P., Bacchetta, J., Cannata-Andia, J., Ferreira, A., Haarhaus, M., et al. (2017). Bone biopsy practice patterns across Europe: the European renal osteodystrophy initiative-a position paper. *Nephrol Dial Transplant*. doi:10.1093/ndt/gfw468

Evenepoel, P., Meijers, B., Viaene, L., Bammens, B., Claes, K., Kuypers, D., et al. (2010). Fibroblast growth factor-23 in early chronic kidney disease: additional support in favor of a phosphate-centric paradigm for the pathogenesis of secondary hyperparathyroidism. *Clin J Am Soc Nephrol, 5*(7), 1268-1276. doi:10.2215/CJN.08241109

Evrard, S., Delanaye, P., Kamel, S., Cristol, J. P., Cavalier, E., & calcifications, S. S. j. w. g. o. v. (2015). Vascular calcification: from pathophysiology to biomarkers. *Clin Chim Acta, 438*, 401-414. doi:10.1016/j.cca.2014.08.034

Fabbian, F., Catalano, C., Orlandi, V., Conte, M. M., Lupo, A., & Catizone, L. (2005). Evaluation of aortic arch calcification in hemodialysis patients. *J Nephrol, 18*(3), 289-293.

Faul, C., Amaral, A. P., Oskouei, B., Hu, M. C., Sloan, A., Isakova, T., et al. (2011). FGF23 induces left ventricular hypertrophy. *J Clin Invest, 121*(11), 4393-4408. doi:10.1172/JCI46122

Fazzalari, N. L., Moore, R. J., Manthey, B. A., & Vernon-Roberts, B. (1989). Comparative study of iliac crest and proximal femur histomorphometry in normal patients. *J Clin Pathol, 42*(7), 745-748. doi:10.1136/jcp.42.7.745

Ferreira, A., Frazao, J. M., Monier-Faugere, M. C., Gil, C., Galvao, J., Oliveira, C., et al. (2008). Effects of sevelamer hydrochloride and calcium carbonate on renal osteodystrophy in hemodialysis patients. *J Am Soc Nephrol, 19*(2), 405-412. doi:10.1681/ASN.2006101089

Fishbane, S., Hazzan, A. D., Jhaveri, K. D., Ma, L., & Lacson, E., Jr. (2016). Bone Parameters and Risk of Hip and Femur Fractures in Patients on Hemodialysis. *Clin J Am Soc Nephrol*. doi:10.2215/CJN.09280915

Fletcher, S., Jones, R. G., Rayner, H. C., Harnden, P., Hordon, L. D., Aaron, J. E., et al. (1997). Assessment of renal osteodystrophy in dialysis patients: use of bone alkaline phosphatase, bone mineral density and parathyroid ultrasound in comparison with bone histology. *Nephron, 75*(4), 412-419.

Floege, J., Kim, J., Ireland, E., Chazot, C., Drueke, T., de Francisco, A., et al. (2011). Serum iPTH, calcium and phosphate, and the risk of mortality in a European haemodialysis population. *Nephrol Dial Transplant, 26*(6), 1948-1955. doi:10.1093/ndt/gfq219

Foldes, J., Shih, M. S., & Parfitt, A. M. (1990). Frequency distributions of tetracycline-based measurements: implications for the interpretation of bone formation indices in the

absence of double-labeled surfaces. *J Bone Miner Res, 5*(10), 1063-1067. doi:10.1002/jbmr.5650051010

Fotheringham, J., Balasubramanian, S. P., Harrison, B., & Wilkie, M. (2011). Post-parathyroidectomy parathyroid hormone levels: the impact on patient survival - a single-centre study in a stage 5 chronic kidney disease population. *Nephron Clin Pract, 119*(2), c113-120. doi:10.1159/000326683

Frank, A. W., Labas, M. C., Johnston, J. D., & Kontulainen, S. A. (2012). Site-specific variance in radius and tibia bone strength as determined by muscle size and body mass. *Physiother Can, 64*(3), 292-301. doi:10.3138/ptc.2010-40BH

Fried, L. F., Biggs, M. L., Shlipak, M. G., Seliger, S., Kestenbaum, B., Stehman-Breen, C., et al. (2007). Association of kidney function with incident hip fracture in older adults. *J Am Soc Nephrol, 18*(1), 282-286. doi:ASN.2006050546 [pii] 10.1681/ASN.2006050546

Fujikawa, Y., Sabokbar, A., Neale, S. D., Itonaga, I., Torisu, T., & Athanasou, N. A. (2001). The effect of macrophage-colony stimulating factor and other humoral factors (interleukin-1, -3, -6, and -11, tumor necrosis factor-alpha, and granulocyte macrophage-colony stimulating factor) on human osteoclast formation from circulating cells. *Bone, 28*(3), 261-267.

Fusaro, M., Crepaldi, G., Maggi, S., Galli, F., D'Angelo, A., Calo, L., et al. (2011). Vitamin K, bone fractures, and vascular calcifications in chronic kidney disease: an important but poorly studied relationship. *J Endocrinol Invest, 34*(4), 317-323. doi:10.3275/7353 10.1007/BF03347093

Fusaro, M., Gallieni, M., Aghi, A., Iervasi, G., Rizzo, M. A., Stucchi, A., et al. (2017). Cigarette smoking is associated with decreased Bone Gla-protein (BGP) levels in hemodialysis patients. *Curr Vasc Pharmacol*. doi:10.2174/1570161115666170919182421

Fusaro, M., Tripepi, G., Noale, M., Plebani, M., Zaninotto, M., Piccoli, A., et al. (2015). Prevalence of vertebral fractures, vascular calcifications, and mortality in warfarin treated hemodialysis patients. *Curr Vasc Pharmacol, 13*(2), 248-258.

Fusaro, M., Tripepi, G., Noale, M., Vajente, N., Plebani, M., Zaninotto, M., et al. (2013). High prevalence of vertebral fractures assessed by quantitative morphometry in hemodialysis patients, strongly associated with vascular calcifications. *Calcif Tissue Int, 93*(1), 39-47. doi:10.1007/s00223-013-9722-x

Garcia-Canton, C., Bosch, E., Ramirez, A., Gonzalez, Y., Auyanet, I., Guerra, R., et al. (2011). Vascular calcification and 25-hydroxyvitamin D levels in non-dialysis patients with chronic kidney disease stages 4 and 5. *Nephrol Dial Transplant, 26*(7), 2250-2256. doi:10.1093/ndt/gfq650

Garrett, G., Sardiwal, S., Lamb, E. J., & Goldsmith, D. J. (2013). PTH--a particularly tricky hormone: why measure it at all in kidney patients? *Clin J Am Soc Nephrol, 8*(2), 299-312. doi:10.2215/CJN.09580911

Gerakis, A., Hadjidakis, D., Kokkinakis, E., Apostolou, T., Raptis, S., & Billis, A. (2000). Correlation of bone mineral density with the histological findings of renal osteodystrophy in patients on hemodialysis. *J Nephrol, 13*(6), 437-443.

Giachelli, C. M. (2003). Vascular calcification: in vitro evidence for the role of inorganic phosphate. *J Am Soc Nephrol, 14*(9 Suppl 4), S300-304.

Gonzalez, E. A., Sachdeva, A., Oliver, D. A., & Martin, K. J. (2004). Vitamin D insufficiency and deficiency in chronic kidney disease. A single center observational study. *Am J Nephrol, 24*(5), 503-510. doi:10.1159/000081023

Gorriz, J. L., Molina, P., Cerveron, M. J., Vila, R., Bover, J., Nieto, J., et al. (2015). Vascular Calcification in Patients with Nondialysis CKD over 3 Years. *Clin J Am Soc Nephrol*. doi:10.2215/CJN.07450714

Gross, M. L., Meyer, H. P., Ziebart, H., Rieger, P., Wenzel, U., Amann, K., et al. (2007). Calcification of coronary intima and media: immunohistochemistry, backscatter imaging, and x-ray analysis in renal and nonrenal patients. *Clin J Am Soc Nephrol, 2*(1), 121-134. doi:10.2215/CJN.01760506

Gutierrez, O., Isakova, T., Rhee, E., Shah, A., Holmes, J., Collerone, G., et al. (2005). Fibroblast growth factor-23 mitigates hyperphosphatemia but accentuates calcitriol deficiency in chronic kidney disease. *J Am Soc Nephrol, 16*(7), 2205-2215. doi:10.1681/ASN.2005010052

Gutierrez, O. M., Mannstadt, M., Isakova, T., Rauh-Hain, J. A., Tamez, H., Shah, A., et al. (2008). Fibroblast growth factor 23 and mortality among patients undergoing hemodialysis. *N Engl J Med, 359*(6), 584-592. doi:10.1056/NEJMoa0706130

Hamano, T., Tomida, K., Mikami, S., Matsui, I., Fujii, N., Imai, E., et al. (2009). Usefulness of bone resorption markers in hemodialysis patients. *Bone, 45 Suppl 1*, S19-25. doi:10.1016/j.bone.2009.03.663

Hans, D., Goertzen, A. L., Krieg, M. A., & Leslie, W. D. (2011). Bone microarchitecture assessed by TBS predicts osteoporotic fractures independent of bone density: the Manitoba study. *J Bone Miner Res, 26*(11), 2762-2769. doi:10.1002/jbmr.499

Hasegawa, H., Nagano, N., Urakawa, I., Yamazaki, Y., Iijima, K., Fujita, T., et al. (2010). Direct evidence for a causative role of FGF23 in the abnormal renal phosphate handling and vitamin D metabolism in rats with early-stage chronic kidney disease. *Kidney Int, 78*(10), 975-980. doi:10.1038/ki.2010.313

Hauschka, P. V., Lian, J. B., Cole, D. E., & Gundberg, C. M. (1989). Osteocalcin and matrix Gla protein: vitamin K-dependent proteins in bone. *Physiol Rev, 69*(3), 990-1047. doi:10.1152/physrev.1989.69.3.990

Herberth, J., Monier-Faugere, M. C., Mawad, H. W., Branscum, A. J., Herberth, Z., Wang, G., et al. (2009). The five most commonly used intact parathyroid hormone assays are useful for screening but not for diagnosing bone turnover abnormalities in CKD-5 patients. *Clin Nephrol, 72*(1), 5-14.

Hernandez, J. D., Wesseling, K., Pereira, R., Gales, B., Harrison, R., & Salusky, I. B. (2008). Technical approach to iliac crest biopsy. *Clin J Am Soc Nephrol, 3 Suppl 3*, S164-169. doi:10.2215/CJN.00460107

Hiller, R. G., Patecki, M., Neunaber, C., Reifenrath, J., Kielstein, J. T., & Kielstein, H. (2017). A comparative study of bone biopsies from the iliac crest, the tibial bone, and the lumbar spine. *BMC Nephrol, 18*(1), 134. doi:10.1186/s12882-017-0550-5

Holick, M. F., & Chen, T. C. (2008). Vitamin D deficiency: a worldwide problem with health consequences. *Am J Clin Nutr, 87*(4), 1080S-1086S. doi:10.1093/ajcn/87.4.1080S

Honkanen, E., Kauppila, L., Wikstrom, B., Rensma, P. L., Krzesinski, J. M., Aasarod, K., et al. (2008). Abdominal aortic calcification in dialysis patients: results of the CORD study. *Nephrol Dial Transplant, 23*(12), 4009-4015. doi:10.1093/ndt/gfn403

Hsu, C. Y., Cummings, S. R., McCulloch, C. E., & Chertow, G. M. (2002). Bone mineral density is not diminished by mild to moderate chronic renal insufficiency. *Kidney Int, 61*(5), 1814-1820. doi:kid306 [pii] 10.1046/j.1523-1755.2002.00306.x

Huan, J., Olgaard, K., Nielsen, L. B., & Lewin, E. (2006). Parathyroid hormone 7-84 induces hypocalcemia and inhibits the parathyroid hormone 1-84 secretory response to

hypocalcemia in rats with intact parathyroid glands. *J Am Soc Nephrol, 17*(7), 1923-1930. doi:10.1681/ASN.2005101136

Idelevich, A., Rais, Y., & Monsonego-Ornan, E. (2011). Bone Gla protein increases HIF-1alpha-dependent glucose metabolism and induces cartilage and vascular calcification. *Arterioscler Thromb Vasc Biol, 31*(9), e55-71. doi:10.1161/ATVBAHA.111.230904

Iimori, S., Mori, Y., Akita, W., Kuyama, T., Takada, S., Asai, T., et al. (2012). Diagnostic usefulness of bone mineral density and biochemical markers of bone turnover in predicting fracture in CKD stage 5D patients--a single-center cohort study. *Nephrol Dial Transplant, 27*(1), 345-351. doi:10.1093/ndt/gfr317

Ikeda, K., & Takeshita, S. (2014). Factors and mechanisms involved in the coupling from bone resorption to formation: how osteoclasts talk to osteoblasts. *J Bone Metab, 21*(3), 163-167. doi:10.11005/jbm.2014.21.3.163

Isakova, T., Cai, X., Lee, J., Xie, D., Wang, X., Mehta, R., et al. (2018). Longitudinal FGF23 Trajectories and Mortality in Patients with CKD. *J Am Soc Nephrol, 29*(2), 579-590. doi:10.1681/ASN.2017070772

Isakova, T., Wahl, P., Vargas, G. S., Gutierrez, O. M., Scialla, J., Xie, H., et al. (2011). Fibroblast growth factor 23 is elevated before parathyroid hormone and phosphate in chronic kidney disease. *Kidney Int, 79*(12), 1370-1378. doi:10.1038/ki.2011.47

Ishimura, E., Okuno, S., Kitatani, K., Maekawa, K., Izumotani, T., Yamakawa, T., et al. (2004). C-reactive protein is a significant predictor of vascular calcification of both aorta and hand arteries. *Semin Nephrol, 24*(5), 408-412.

Ishimura, E., Okuno, S., Okazaki, H., Norimine, K., Yamakawa, K., Yamakawa, T., et al. (2014). Significant association between bone-specific alkaline phosphatase and vascular calcification of the hand arteries in male hemodialysis patients. *Kidney Blood Press Res, 39*(4), 299-307. doi:10.1159/000355807

Iwamoto, N., Sato, N., Nishida, M., Hashimoto, T., Kobayashi, H., Yamasaki, S., et al. (2012). Total parathyroidectomy improves survival of hemodialysis patients with secondary hyperparathyroidism. *J Nephrol, 25*(5), 755-763. doi:10.5301/jn.5000056

Jacques, R. M., Boonen, S., Cosman, F., Reid, I. R., Bauer, D. C., Black, D. M., et al. (2012). Relationship of changes in total hip bone mineral density to vertebral and nonvertebral fracture risk in women with postmenopausal osteoporosis treated with once-yearly zoledronic acid 5 mg: the HORIZON-Pivotal Fracture Trial (PFT). *J Bone Miner Res, 27*(8), 1627-1634. doi:10.1002/jbmr.1644

Jadoul, M., Albert, J. M., Akiba, T., Akizawa, T., Arab, L., Bragg-Gresham, J. L., et al. (2006). Incidence and risk factors for hip or other bone fractures among hemodialysis patients in the Dialysis Outcomes and Practice Patterns Study. *Kidney Int, 70*(7), 1358-1366. doi:5001754 [pii] 10.1038/sj.ki.5001754

Jamal, S. A., Chase, C., Goh, Y. I., Richardson, R., & Hawker, G. A. (2002). Bone density and heel ultrasound testing do not identify patients with dialysis-dependent renal failure who have had fractures. *Am J Kidney Dis, 39*(4), 843-849. doi:10.1053/ajkd.2002.32006

Jamal, S. A., Swan, V. J., Brown, J. P., Hanley, D. A., Prior, J. C., Papaioannou, A., et al. (2010). Kidney function and rate of bone loss at the hip and spine: the Canadian Multicentre Osteoporosis Study. *Am J Kidney Dis, 55*(2), 291-299. doi:10.1053/j.ajkd.2009.10.049

Jamal, S. A., Vandermeer, B., Raggi, P., Mendelssohn, D. C., Chatterley, T., Dorgan, M., et al. (2013). Effect of calcium-based versus non-calcium-based phosphate binders on

mortality in patients with chronic kidney disease: an updated systematic review and meta-analysis. *Lancet, 382*(9900), 1268-1277. doi:10.1016/S0140-6736(13)60897-1

Jean, G., Bresson, E., Terrat, J. C., Vanel, T., Hurot, J. M., Lorriaux, C., et al. (2009). Peripheral vascular calcification in long-haemodialysis patients: associated factors and survival consequences. *Nephrol Dial Transplant, 24*(3), 948-955. doi:10.1093/ndt/gfn571

Jimbo, R., Kawakami-Mori, F., Mu, S., Hirohama, D., Majtan, B., Shimizu, Y., et al. (2014). Fibroblast growth factor 23 accelerates phosphate-induced vascular calcification in the absence of Klotho deficiency. *Kidney Int, 85*(5), 1103-1111. doi:10.1038/ki.2013.332

Jono, S., McKee, M. D., Murry, C. E., Shioi, A., Nishizawa, Y., Mori, K., et al. (2000). Phosphate regulation of vascular smooth muscle cell calcification. *Circ Res, 87*(7), E10-17.

Jung, H. H., Kim, S. W., & Han, H. (2006). Inflammation, mineral metabolism and progressive coronary artery calcification in patients on haemodialysis. *Nephrol Dial Transplant, 21*(7), 1915-1920. doi:10.1093/ndt/gfl118

Kanbay, M., Nicoleta, M., Selcoki, Y., Ikizek, M., Aydin, M., Eryonucu, B., et al. (2010). Fibroblast growth factor 23 and fetuin A are independent predictors for the coronary artery disease extent in mild chronic kidney disease. *Clin J Am Soc Nephrol, 5*(10), 1780-1786. doi:10.2215/CJN.02560310

Kanis, J. A., Johansson, H., Oden, A., Harvey, N. C., Gudnason, V., Sanders, K. M., et al. (2018). Characteristics of recurrent fractures. *Osteoporos Int, 29*(8), 1747-1757. doi:10.1007/s00198-018-4502-0

Kanis, J. A., McCloskey, E. V., Johansson, H., Oden, A., Strom, O., & Borgstrom, F. (2010). Development and use of FRAX in osteoporosis. *Osteoporos Int, 21 Suppl 2*, S407-413. doi:10.1007/s00198-010-1253-y

Kauppila, L. I., Polak, J. F., Cupples, L. A., Hannan, M. T., Kiel, D. P., & Wilson, P. W. (1997). New indices to classify location, severity and progression of calcific lesions in the abdominal aorta: a 25-year follow-up study. *Atherosclerosis, 132*(2), 245-250.

Kazama, J. J., Shigematsu, T., Yano, K., Tsuda, E., Miura, M., Iwasaki, Y., et al. (2002). Increased circulating levels of osteoclastogenesis inhibitory factor (osteoprotegerin) in patients with chronic renal failure. *Am J Kidney Dis, 39*(3), 525-532. doi:10.1053/ajkd.2002.31402

KDIGO. (2009). KDIGO clinical practice guideline for the diagnosis, evaluation, prevention, and treatment of Chronic Kidney Disease-Mineral and Bone Disorder (CKD-MBD). *Kidney Int Suppl*(113), S1-130. doi:10.1038/ki.2009.188

KDIGO. (2017). KDIGO 2017 Clinical Practice Guideline Update for the Diagnosis, Evaluation, Prevention and Treatment of Chronic Kidney Disease-Mineral and Bone Disorder (CKD-MBD). *Kidney Int Suppl*(7), 1-59.

Ketteler, M., Bongartz, P., Westenfeld, R., Wildberger, J. E., Mahnken, A. H., Bohm, R., et al. (2003). Association of low fetuin-A (AHSG) concentrations in serum with cardiovascular mortality in patients on dialysis: a cross-sectional study. *Lancet, 361*(9360), 827-833. doi:10.1016/S0140-6736(03)12710-9

Ketteler, M., Wanner, C., Metzger, T., Bongartz, P., Westenfeld, R., Gladziwa, U., et al. (2003). Deficiencies of calcium-regulatory proteins in dialysis patients: a novel concept of cardiovascular calcification in uremia. *Kidney Int Suppl*(84), S84-87.

Khosla, S., Riggs, B. L., Atkinson, E. J., Oberg, A. L., McDaniel, L. J., Holets, M., et al. (2006). Effects of sex and age on bone microstructure at the ultradistal radius: a population-

based noninvasive in vivo assessment. *J Bone Miner Res, 21*(1), 124-131. doi:10.1359/JBMR.050916

Kidney Disease: Improving Global Outcomes. (2013). KDIGO 2012 Clinical Practice Guideline for the Evaluation and Management of Chronic Kidney Disease. *Kidney International, 3*(1), 1-150.

Kim, S. M., Long, J., Montez-Rath, M., Leonard, M., & Chertow, G. M. (2016). Hip Fracture in Patients With Non-Dialysis-Requiring Chronic Kidney Disease. *J Bone Miner Res, 31*(10), 1803-1809. doi:10.1002/jbmr.2862

Kinsella, S., Chavrimootoo, S., Molloy, M. G., & Eustace, J. A. (2010). Moderate chronic kidney disease in women is associated with fracture occurrence independently of osteoporosis. *Nephron Clin Pract, 116*(3), c256-262. doi:10.1159/000317207

Klawansky, S., Komaroff, E., Cavanaugh, P. F., Jr., Mitchell, D. Y., Gordon, M. J., Connelly, J. E., et al. (2003). Relationship between age, renal function and bone mineral density in the US population. *Osteoporos Int, 14*(7), 570-576. doi:10.1007/s00198-003-1435-y

Koivula, M. K., Ruotsalainen, V., Bjorkman, M., Nurmenniemi, S., Ikaheimo, R., Savolainen, K., et al. (2010). Difference between total and intact assays for N-terminal propeptide of type I procollagen reflects degradation of pN-collagen rather than denaturation of intact propeptide. *Ann Clin Biochem, 47*(Pt 1), 67-71. doi:10.1258/acb.2009.009110

Krasniak, A., Drozdz, M., Pasowicz, M., Chmiel, G., Michalek, M., Szumilak, D., et al. (2007). Factors involved in vascular calcification and atherosclerosis in maintenance haemodialysis patients. *Nephrol Dial Transplant, 22*(2), 515-521. doi:10.1093/ndt/gfl564

Krueger, D., Fidler, E., Libber, J., Aubry-Rozier, B., Hans, D., & Binkley, N. (2014). Spine trabecular bone score subsequent to bone mineral density improves fracture discrimination in women. *J Clin Densitom, 17*(1), 60-65. doi:10.1016/j.jocd.2013.05.001

Lacey, D. L., Timms, E., Tan, H. L., Kelley, M. J., Dunstan, C. R., Burgess, T., et al. (1998). Osteoprotegerin ligand is a cytokine that regulates osteoclast differentiation and activation. *Cell, 93*(2), 165-176.

Laing, C. J., & Fraser, D. R. (2002). Changes with malnutrition in the concentration of plasma vitamin D binding protein in growing rats. *Br J Nutr, 88*(2), 133-139. doi:10.1079/BJNBJN2002611

Lamarche, M. C., Hopman, W. M., Garland, J. S., White, C. A., & Holden, R. M. (2018). Relationship of coronary artery calcification with renal function decline and mortality in predialysis chronic kidney disease patients. *Nephrol Dial Transplant*. doi:10.1093/ndt/gfy183

Lebreton, J. P., Joisel, F., Raoult, J. P., Lannuzel, B., Rogez, J. P., & Humbert, G. (1979). Serum concentration of human alpha 2 HS glycoprotein during the inflammatory process: evidence that alpha 2 HS glycoprotein is a negative acute-phase reactant. *J Clin Invest, 64*(4), 1118-1129. doi:10.1172/JCI109551

Lee, S. M., Lee, H. W., Son, Y. K., Kim, S. E., & An, W. S. (2017). Abdominal aortic calcification score among several vascular calcification scores of plain radiograph is the most reliable predictor of severe coronary artery calcification in dialysis patients. *Ren Fail, 39*(1), 729-735. doi:10.1080/0886022X.2017.1398666

Lee, S. Y., Kim, H. Y., Gu, S. W., Kim, H. J., & Yang, D. H. (2012). 25-hydroxyvitamin D levels and vascular calcification in predialysis and dialysis patients with chronic kidney disease. *Kidney Blood Press Res, 35*(5), 349-354. doi:10.1159/000335952

Lehmann, G., Ott, U., Kaemmerer, D., Schuetze, J., & Wolf, G. (2008). Bone histomorphometry and biochemical markers of bone turnover in patients with chronic kidney disease Stages 3 - 5. *Clin Nephrol, 70*(4), 296-305.

Lehmann, G., Stein, G., Huller, M., Schemer, R., Ramakrishnan, K., & Goodman, W. G. (2005). Specific measurement of PTH (1-84) in various forms of renal osteodystrophy (ROD) as assessed by bone histomorphometry. *Kidney Int, 68*(3), 1206-1214. doi:10.1111/j.1523-1755.2005.00513.x

Levey, A. S., Bosch, J. P., Lewis, J. B., Greene, T., Rogers, N., & Roth, D. (1999). A more accurate method to estimate glomerular filtration rate from serum creatinine: a new prediction equation. Modification of Diet in Renal Disease Study Group. *Ann Intern Med, 130*(6), 461-470.

Levey, A. S., Stevens, L. A., Schmid, C. H., Zhang, Y. L., Castro, A. F., 3rd, Feldman, H. I., et al. (2009). A new equation to estimate glomerular filtration rate. *Ann Intern Med, 150*(9), 604-612.

Levy, R. J., Gundberg, C., & Scheinman, R. (1983). The identification of the vitamin K-dependent bone protein osteocalcin as one of the gamma-carboxyglutamic acid containing proteins present in calcified atherosclerotic plaque and mineralized heart valves. *Atherosclerosis, 46*(1), 49-56.

Li, B., Cairns, J. A., Fotheringham, J., Tomson, C. R., Forsythe, J. L., Watson, C., et al. (2015). Understanding cost of care for patients on renal replacement therapy: looking beyond fixed tariffs. *Nephrol Dial Transplant, 30*(10), 1726-1734. doi:10.1093/ndt/gfv224

Lima, F., El-Husseini, A., Monier-Faugere, M. C., David, V., Mawad, H., Quarles, D., et al. (2014). FGF-23 serum levels and bone histomorphometric results in adult patients with chronic kidney disease on dialysis. *Clin Nephrol*. doi:10.5414/CN108407

London, G. M., Marchais, S. J., Guerin, A. P., Boutouyrie, P., Metivier, F., & de Vernejoul, M. C. (2008). Association of bone activity, calcium load, aortic stiffness, and calcifications in ESRD. *J Am Soc Nephrol, 19*(9), 1827-1835. doi:10.1681/ASN.2007050622

London, G. M., Marty, C., Marchais, S. J., Guerin, A. P., Metivier, F., & de Vernejoul, M. C. (2004). Arterial calcifications and bone histomorphometry in end-stage renal disease. *J Am Soc Nephrol, 15*(7), 1943-1951.

Luo, G., Ducy, P., McKee, M. D., Pinero, G. J., Loyer, E., Behringer, R. R., et al. (1997). Spontaneous calcification of arteries and cartilage in mice lacking matrix GLA protein. *Nature, 386*(6620), 78-81. doi:10.1038/386078a0

MacNeill, S. J., & Ford, D. (2017). UK Renal Registry 19th Annual Report: Chapter 2 UK Renal Replacement Therapy Prevalence in 2015: National and Centre-specific Analyses. *Nephron, 137 Suppl 1*, 45-72. doi:10.1159/000481364

Magnusson, P., Sharp, C. A., Magnusson, M., Risteli, J., Davie, M. W., & Larsson, L. (2001). Effect of chronic renal failure on bone turnover and bone alkaline phosphatase isoforms. *Kidney Int, 60*(1), 257-265. doi:10.1046/j.1523-1755.2001.00794.x

Malluche, H. H., Blomquist, G., Monier-Faugere, M. C., Cantor, T. L., & Davenport, D. L. (2015). High Parathyroid Hormone Level and Osteoporosis Predict Progression of

Coronary Artery Calcification in Patients on Dialysis. *J Am Soc Nephrol, 26*(10), 2534-2544. doi:10.1681/ASN.2014070686

Malluche, H. H., Mawad, H. W., & Monier-Faugere, M. C. (2011). Renal osteodystrophy in the first decade of the new millennium: analysis of 630 bone biopsies in black and white patients. *J Bone Miner Res, 26*(6), 1368-1376. doi:10.1002/jbmr.309

Malluche, H. H., Meyer, W., Sherman, D., & Massry, S. G. (1982). Quantitative bone histology in 84 normal American subjects. Micromorphometric analysis and evaluation of variance in iliac bone. *Calcif Tissue Int, 34*(5), 449-455.

Malluche, H. H., & Monier-Faugere, M. C. (1994). The role of bone biopsy in the management of patients with renal osteodystrophy. *J Am Soc Nephrol, 4*(9), 1631-1642.

Malluche, H. H., Monier-Faugere, M. C., Blomquist, G., & Davenport, D. L. (2017). Two-year cortical and trabecular bone loss in CKD-5D: biochemical and clinical predictors. *Osteoporos Int*. doi:10.1007/s00198-017-4228-4

Malluche, H. H., Monier-Faugere, M. C., Wang, G., Fraza, O. J., Charytan, C., Coburn, J. W., et al. (2008). An assessment of cinacalcet HCl effects on bone histology in dialysis patients with secondary hyperparathyroidism. *Clin Nephrol, 69*(4), 269-278.

Malluche, H. H., Porter, D. S., Monier-Faugere, M. C., Mawad, H., & Pienkowski, D. (2012). Differences in bone quality in low- and high-turnover renal osteodystrophy. *J Am Soc Nephrol, 23*(3), 525-532. doi:10.1681/ASN.2010121253

Maravic, M., Ostertag, A., Torres, P. U., & Cohen-Solal, M. (2014). Incidence and risk factors for hip fractures in dialysis patients. *Osteoporos Int, 25*(1), 159-165. doi:10.1007/s00198-013-2435-1

Marcius M , V. N., Getaldić-Švarc B. (2006). Analytical evaluation of P1NP assay, a biochemical marker of bone turnover. *Biochemia Medica, 16*(2), 178 - 190.

Marques, I. D., Araujo, M. J., Graciolli, F. G., Reis, L. M., Pereira, R. M., Custodio, M. R., et al. (2017). Biopsy vs. peripheral computed tomography to assess bone disease in CKD patients on dialysis: differences and similarities. *Osteoporos Int*. doi:10.1007/s00198-017-3956-9

Matias, P. J., Ferreira, C., Jorge, C., Borges, M., Aires, I., Amaral, T., et al. (2009). 25-Hydroxyvitamin D3, arterial calcifications and cardiovascular risk markers in haemodialysis patients. *Nephrol Dial Transplant, 24*(2), 611-618. doi:10.1093/ndt/gfn502

Matsuoka, M., Iseki, K., Tamashiro, M., Fujimoto, N., Higa, N., Touma, T., et al. (2004). Impact of high coronary artery calcification score (CACS) on survival in patients on chronic hemodialysis. *Clin Exp Nephrol, 8*(1), 54-58. doi:10.1007/s10157-003-0260-0

Mawer, E. B., Hayes, M. E., Heys, S. E., Davies, M., White, A., Stewart, M. F., et al. (1994). Constitutive synthesis of 1,25-dihydroxyvitamin D3 by a human small cell lung cancer cell line. *J Clin Endocrinol Metab, 79*(2), 554-560. doi:10.1210/jcem.79.2.8045976

McCloskey, E. V., Oden, A., Harvey, N. C., Leslie, W. D., Hans, D., Johansson, H., et al. (2016). A Meta-Analysis of Trabecular Bone Score in Fracture Risk Prediction and Its Relationship to FRAX. *J Bone Miner Res, 31*(5), 940-948. doi:10.1002/jbmr.2734

McHugh, M. L. (2012). Interrater reliability: the kappa statistic. *Biochem Med (Zagreb), 22*(3), 276-282.

Melkko, J., Hellevik, T., Risteli, L., Risteli, J., & Smedsrod, B. (1994). Clearance of NH2-terminal propeptides of types I and III procollagen is a physiological function of the scavenger receptor in liver endothelial cells. *J Exp Med, 179*(2), 405-412.

Mendel, C. M. (1989). The free hormone hypothesis: a physiologically based mathematical model. *Endocr Rev, 10*(3), 232-274. doi:10.1210/edrv-10-3-232

Methven, S., Steenkamp, R., & Fraser, S. (2017). UK Renal Registry 19th Annual Report: Chapter 5 Survival and Causes of Death in UK Adult Patients on Renal Replacement Therapy in 2015: National and Centre-specific Analyses. *Nephron, 137 Suppl 1*, 117-150. doi:10.1159/000481367

Michaud, J., Naud, J., Ouimet, D., Demers, C., Petit, J. L., Leblond, F. A., et al. (2010). Reduced hepatic synthesis of calcidiol in uremia. *J Am Soc Nephrol, 21*(9), 1488-1497. doi:10.1681/ASN.2009080815

Miller, S. C., de Saint-Georges, L., Bowman, B. M., & Jee, W. S. (1989). Bone lining cells: structure and function. *Scanning Microsc, 3*(3), 953-960; discussion 960-951.

Moe, S., Drueke, T., Cunningham, J., Goodman, W., Martin, K., Olgaard, K., et al. (2006). Definition, evaluation, and classification of renal osteodystrophy: a position statement from Kidney Disease: Improving Global Outcomes (KDIGO). *Kidney Int, 69*(11), 1945-1953. doi:10.1038/sj.ki.5000414

Moe, S. M., Abdalla, S., Chertow, G. M., Parfrey, P. S., Block, G. A., Correa-Rotter, R., et al. (2014). Effects of Cinacalcet on Fracture Events in Patients Receiving Hemodialysis: The EVOLVE Trial. *J Am Soc Nephrol*. doi:10.1681/ASN.2014040414

Moe, S. M., O'Neill, K. D., Duan, D., Ahmed, S., Chen, N. X., Leapman, S. B., et al. (2002). Medial artery calcification in ESRD patients is associated with deposition of bone matrix proteins. *Kidney Int, 61*(2), 638-647. doi:10.1046/j.1523-1755.2002.00170.x

Moe, S. M., O'Neill, K. D., Fineberg, N., Persohn, S., Ahmed, S., Garrett, P., et al. (2003). Assessment of vascular calcification in ESRD patients using spiral CT. *Nephrol Dial Transplant, 18*(6), 1152-1158.

Monier-Faugere, M. C., Geng, Z., Mawad, H., Friedler, R. M., Gao, P., Cantor, T. L., et al. (2001). Improved assessment of bone turnover by the PTH-(1-84)/large C-PTH fragments ratio in ESRD patients. *Kidney Int, 60*(4), 1460-1468. doi:10.1046/j.1523-1755.2001.00949.x

Moore, C., Yee, J., Malluche, H., Rao, D. S., Monier-Faugere, M. C., Adams, E., et al. (2009). Relationship between bone histology and markers of bone and mineral metabolism in African-American hemodialysis patients. *Clin J Am Soc Nephrol, 4*(9), 1484-1493. doi:10.2215/CJN.01770408

Moorthi, R. N., & Avin, K. G. (2017). Clinical relevance of sarcopenia in chronic kidney disease. *Curr Opin Nephrol Hypertens, 26*(3), 219-228. doi:10.1097/MNH.0000000000000318

Morena, M., Jaussent, I., Dupuy, A. M., Bargnoux, A. S., Kuster, N., Chenine, L., et al. (2015). Osteoprotegerin and sclerostin in chronic kidney disease prior to dialysis: potential partners in vascular calcifications. *Nephrol Dial Transplant, 30*(8), 1345-1356. doi:10.1093/ndt/gfv081

Morena, M., Jaussent, I., Halkovich, A., Dupuy, A. M., Bargnoux, A. S., Chenine, L., et al. (2012). Bone biomarkers help grading severity of coronary calcifications in non dialysis chronic kidney disease patients. *PLoS One, 7*(5), e36175. doi:10.1371/journal.pone.0036175

Murray, T. M., Rao, L. G., Divieti, P., & Bringhurst, F. R. (2005). Parathyroid hormone secretion and action: evidence for discrete receptors for the carboxyl-terminal region and related biological actions of carboxyl- terminal ligands. *Endocr Rev, 26*(1), 78-113. doi:10.1210/er.2003-0024

Muxi, A., Torregrosa, J. V., Fuster, D., Peris, P., Vidal-Sicart, S., Sola, O., et al. (2009). Arteriovenous fistula affects bone mineral density measurements in end-stage renal failure patients. *Clin J Am Soc Nephrol, 4*(9), 1494-1499. doi:10.2215/CJN.01470209

Nakamura, M., Udagawa, N., Matsuura, S., Mogi, M., Nakamura, H., Horiuchi, H., et al. (2003). Osteoprotegerin regulates bone formation through a coupling mechanism with bone resorption. *Endocrinology, 144*(12), 5441-5449. doi:10.1210/en.2003-0717

Nakashima, A., Yorioka, N., Mizutani, T., Yamagata, Z., Ueno, T., & Takasugi, N. (2005). Serum cross-linked N-terminal telopeptide of type I collagen for evaluation of renal osteodystrophy in hemodialysis patients. *Nephron Clin Pract, 99*(3), c78-85. doi:10.1159/000083418

Nascimento, M. M., Hayashi, S. Y., Riella, M. C., & Lindholm, B. (2014). Elevated levels of plasma osteoprotegerin are associated with all-cause mortality risk and atherosclerosis in patients with stages 3 to 5 chronic kidney disease. *Braz J Med Biol Res, 0*, 0.

Naylor, K. L., Prior, J., Garg, A. X., Berger, C., Langsetmo, L., Adachi, J. D., et al. (2016). Trabecular Bone Score and Incident Fragility Fracture Risk in Adults with Reduced Kidney Function. *Clin J Am Soc Nephrol, 11*(11), 2032-2040. doi:10.2215/CJN.00720116

Negri, A. L., Del Valle, E. E., Zanchetta, M. B., Nobaru, M., Silveira, F., Puddu, M., et al. (2012). Evaluation of bone microarchitecture by high-resolution peripheral quantitative computed tomography (HR-pQCT) in hemodialysis patients. *Osteoporos Int, 23*(10), 2543-2550. doi:10.1007/s00198-011-1890-9

Neovius, M., Jacobson, S. H., Eriksson, J. K., Elinder, C. G., & Hylander, B. (2014). Mortality in chronic kidney disease and renal replacement therapy: a population-based cohort study. *BMJ Open, 4*(2), e004251. doi:10.1136/bmjopen-2013-004251

NICE. (2007). Cinacalcet for the treatment of secondary hyperparathyroidism in patients with end-stage renal disease on maintenance dialysis therapy.

NICE. (2014). *Chronic kidney disease in adults: assessment and management.* Retrieved from https://www.nice.org.uk/guidance/cg182.

Nickolas, T. L., Cremers, S., Zhang, A., Thomas, V., Stein, E., Cohen, A., et al. (2011). Discriminants of prevalent fractures in chronic kidney disease. *J Am Soc Nephrol, 22*(8), 1560-1572. doi:10.1681/ASN.2010121275

Nickolas, T. L., McMahon, D. J., & Shane, E. (2006). Relationship between moderate to severe kidney disease and hip fracture in the United States. *J Am Soc Nephrol, 17*(11), 3223-3232. doi:ASN.2005111194 [pii] 10.1681/ASN.2005111194

Nickolas, T. L., Stein, E., Cohen, A., Thomas, V., Staron, R. B., McMahon, D. J., et al. (2010). Bone mass and microarchitecture in CKD patients with fracture. *J Am Soc Nephrol, 21*(8), 1371-1380. doi:10.1681/ASN.2009121208

Nickolas, T. L., Stein, E. M., Dworakowski, E., Nishiyama, K. K., Komandah-Kosseh, M., Zhang, C. A., et al. (2013). Rapid cortical bone loss in patients with chronic kidney disease. *J Bone Miner Res, 28*(8), 1811-1820. doi:10.1002/jbmr.1916

NIH. (2001). Osteoporosis prevention, diagnosis, and therapy. NIH Consensus Development Panel on Osteoporosis Prevention, Diagnosis & Therapy,. *JAMA, 285*(6), 785-795.

Nitta, K., Akiba, T., Uchida, K., Kawashima, A., Yumura, W., Kabaya, T., et al. (2003). The progression of vascular calcification and serum osteoprotegerin levels in patients on long-term hemodialysis. *Am J Kidney Dis, 42*(2), 303-309.

Nitta, K., Hanafusa, N., Okazaki, M., Komatsu, M., Kawaguchi, H., & Tsuchiya, K. (2018). Association Between Risk Factors Including Bone-Derived Biomarkers and Aortic Arch Calcification in Maintenance Hemodialysis Patients. *Kidney Blood Press Res, 43*(5), 1554-1562. doi:10.1159/000494441

NOS. (2005). *National Osteoporosis Society document on Physical principles and measurement accuracy of bone densitometry*. Retrieved from https://nos.org.uk/media/1725/02_physical_principles.pdf.

Nykjaer, A., Dragun, D., Walther, D., Vorum, H., Jacobsen, C., Herz, J., et al. (1999). An endocytic pathway essential for renal uptake and activation of the steroid 25-(OH) vitamin D3. *Cell, 96*(4), 507-515.

Oh, Y. J., Kim, M., Lee, H., Lee, J. P., Kim, H., Kim, S., et al. (2012). A threshold value of estimated glomerular filtration rate that predicts changes in serum 25-hydroxyvitamin D levels: 4th Korean National Health and Nutritional Examination Survey 2008. *Nephrol Dial Transplant, 27*(6), 2396-2403. doi:10.1093/ndt/gfr763

Ok, E., Asci, G., Bayraktaroglu, S., Toz, H., Ozkahya, M., Yilmaz, M., et al. (2016). Reduction of Dialysate Calcium Level Reduces Progression of Coronary Artery Calcification and Improves Low Bone Turnover in Patients on Hemodialysis. *J Am Soc Nephrol, 27*(8), 2475-2486. doi:10.1681/ASN.2015030268

Okuno, S., Inaba, M., Kitatani, K., Ishimura, E., Yamakawa, T., & Nishizawa, Y. (2005). Serum levels of C-terminal telopeptide of type I collagen: a useful new marker of cortical bone loss in hemodialysis patients. *Osteoporos Int, 16*(5), 501-509. doi:10.1007/s00198-004-1712-4

Orita, Y., Yamamoto, H., Kohno, N., Sugihara, M., Honda, H., Kawamata, S., et al. (2007). Role of osteoprotegerin in arterial calcification: development of new animal model. *Arterioscler Thromb Vasc Biol, 27*(9), 2058-2064. doi:10.1161/ATVBAHA.107.147868

Ott, S. M. (2008). Histomorphometric measurements of bone turnover, mineralization, and volume. *Clin J Am Soc Nephrol, 3 Suppl 3*, S151-156. doi:10.2215/CJN.04301206

Ozkok, A., Caliskan, Y., Sakaci, T., Erten, G., Karahan, G., Ozel, A., et al. (2012). Osteoprotegerin/RANKL axis and progression of coronary artery calcification in hemodialysis patients. *Clin J Am Soc Nephrol, 7*(6), 965-973. doi:10.2215/CJN.11191111

Paggiosi, M. A., Eastell, R., & Walsh, J. S. (2014). Precision of high-resolution peripheral quantitative computed tomography measurement variables: influence of gender, examination site, and age. *Calcif Tissue Int, 94*(2), 191-201. doi:10.1007/s00223-013-9798-3

Palmer, S. C., McGregor, D. O., Macaskill, P., Craig, J. C., Elder, G. J., & Strippoli, G. F. (2007). Meta-analysis: vitamin D compounds in chronic kidney disease. *Ann Intern Med, 147*(12), 840-853.

Parfitt, A. M. (2003). Renal bone disease: a new conceptual framework for the interpretation of bone histomorphometry. *Curr Opin Nephrol Hypertens, 12*(4), 387-403. doi:10.1097/01.mnh.0000079687.89474.dc

Parfitt, A. M., Drezner, M. K., Glorieux, F. H., Kanis, J. A., Malluche, H., Meunier, P. J., et al. (1987). Bone histomorphometry: standardization of nomenclature, symbols, and

units. Report of the ASBMR Histomorphometry Nomenclature Committee. *J Bone Miner Res, 2*(6), 595-610. doi:10.1002/jbmr.5650020617

Parfitt, A. M., Han, Z. H., Palnitkar, S., Rao, D. S., Shih, M. S., & Nelson, D. (1997). Effects of ethnicity and age or menopause on osteoblast function, bone mineralization, and osteoid accumulation in iliac bone. *J Bone Miner Res, 12*(11), 1864-1873. doi:10.1359/jbmr.1997.12.11.1864

Parfitt, A. M., Qiu, S., & Rao, D. S. (2004). The mineralization index--a new approach to the histomorphometric appraisal of osteomalacia. *Bone, 35*(1), 320-325. doi:10.1016/j.bone.2004.02.016

Parisien, M. V., McMahon, D., Pushparaj, N., & Dempster, D. W. (1988). Trabecular architecture in iliac crest bone biopsies: infra-individual variability in structural parameters and changes with age. *Bone, 9*(5), 289-295. doi:10.1016/8756-3282(88)90012-9

Pateinakis, P., Papagianni, A., Douma, S., Efstratiadis, G., & Memmos, D. (2013). Associations of fetuin-A and osteoprotegerin with arterial stiffness and early atherosclerosis in chronic hemodialysis patients. *BMC Nephrol, 14*, 122. doi:10.1186/1471-2369-14-122

Patsch, J. M., Zulliger, M. A., Vilayphou, N., Samelson, E. J., Cejka, D., Diarra, D., et al. (2014). Quantification of lower leg arterial calcifications by high-resolution peripheral quantitative computed tomography. *Bone, 58*, 42-47. doi:10.1016/j.bone.2013.08.006

Pelletier, S., Vilayphiou, N., Boutroy, S., Bacchetta, J., Sornay-Rendu, E., Szulc, P., et al. (2012). Bone microarchitecture is more severely affected in patients on hemodialysis than in those receiving peritoneal dialysis. *Kidney Int, 82*(5), 581-588. doi:10.1038/ki.2012.166

Pereira, R. C., Bischoff, D. S., Yamaguchi, D., Salusky, I. B., & Wesseling-Perry, K. (2015). Micro-CT in the Assessment of Pediatric Renal Osteodystrophy by Bone Histomorphometry. *Clin J Am Soc Nephrol*. doi:10.2215/CJN.04810515

Pereira, R. C., Juppner, H., Azucena-Serrano, C. E., Yadin, O., Salusky, I. B., & Wesseling-Perry, K. (2009). Patterns of FGF-23, DMP1, and MEPE expression in patients with chronic kidney disease. *Bone, 45*(6), 1161-1168. doi:10.1016/j.bone.2009.08.008

PHE. (2014). *Chronic Kidney Disease Prevalence Model*.

Piraino, B., Chen, T., Cooperstein, L., Segre, G., & Puschett, J. (1988). Fractures and vertebral bone mineral density in patients with renal osteodystrophy. *Clin Nephrol, 30*(2), 57-62.

Pothuaud, L., Carceller, P., & Hans, D. (2008). Correlations between grey-level variations in 2D projection images (TBS) and 3D microarchitecture: applications in the study of human trabecular bone microarchitecture. *Bone, 42*(4), 775-787. doi:S8756-3282(07)00866-6 [pii]10.1016/j.bone.2007.11.018

Powe, C. E., Ricciardi, C., Berg, A. H., Erdenesanaa, D., Collerone, G., Ankers, E., et al. (2011). Vitamin D-binding protein modifies the vitamin D-bone mineral density relationship. *J Bone Miner Res, 26*(7), 1609-1616. doi:10.1002/jbmr.387

Price, P. A., & Nishimoto, S. K. (1980). Radioimmunoassay for the vitamin K-dependent protein of bone and its discovery in plasma. *Proc Natl Acad Sci U S A, 77*(4), 2234-2238.

Puumalainen, P., Uimarihuhta, A., & Olkkonen, H. (1976). A new photon scattering method for bone mineral density measurements. *Radiology, 120*(3), 723-724. doi:10.1148/120.3.723

Qureshi, A. R., Olauson, H., Witasp, A., Haarhaus, M., Brandenburg, V., Wernerson, A., et al. (2015). Increased circulating sclerostin levels in end-stage renal disease predict biopsy-verified vascular medial calcification and coronary artery calcification. *Kidney Int, 88*(6), 1356-1364. doi:10.1038/ki.2015.194

Raggi, P., Boulay, A., Chasan-Taber, S., Amin, N., Dillon, M., Burke, S. K., et al. (2002). Cardiac calcification in adult hemodialysis patients. A link between end-stage renal disease and cardiovascular disease? *J Am Coll Cardiol, 39*(4), 695-701.

Raggi, P., Chertow, G. M., Torres, P. U., Csiky, B., Naso, A., Nossuli, K., et al. (2011). The ADVANCE study: a randomized study to evaluate the effects of cinacalcet plus low-dose vitamin D on vascular calcification in patients on hemodialysis. *Nephrol Dial Transplant, 26*(4), 1327-1339. doi:10.1093/ndt/gfq725

Ramirez-Sandoval, J. C., Casanova, I., Villar, A., Gomez, F. E., Cruz, C., & Correa-Rotter, R. (2016). Biomarkers Associated with Vascular Calcification in Peritoneal Dialysis. *Perit Dial Int, 36*(3), 262-268. doi:10.3747/pdi.2014.00250

Recker, R. R., Kimmel, D. B., Dempster, D., Weinstein, R. S., Wronski, T. J., & Burr, D. B. (2011). Issues in modern bone histomorphometry. *Bone, 49*(5), 955-964. doi:10.1016/j.bone.2011.07.017

Reynolds, J. L., Joannides, A. J., Skepper, J. N., McNair, R., Schurgers, L. J., Proudfoot, D., et al. (2004). Human vascular smooth muscle cells undergo vesicle-mediated calcification in response to changes in extracellular calcium and phosphate concentrations: a potential mechanism for accelerated vascular calcification in ESRD. *J Am Soc Nephrol, 15*(11), 2857-2867. doi:10.1097/01.ASN.0000141960.01035.28

Reynolds, J. L., Skepper, J. N., McNair, R., Kasama, T., Gupta, K., Weissberg, P. L., et al. (2005). Multifunctional roles for serum protein fetuin-a in inhibition of human vascular smooth muscle cell calcification. *J Am Soc Nephrol, 16*(10), 2920-2930. doi:10.1681/ASN.2004100895

Rodriguez-Garcia, M., Gomez-Alonso, C., Naves-Diaz, M., Diaz-Lopez, J. B., Diaz-Corte, C., Cannata-Andia, J. B., et al. (2009). Vascular calcifications, vertebral fractures and mortality in haemodialysis patients. *Nephrol Dial Transplant, 24*(1), 239-246. doi:10.1093/ndt/gfn466

Rogers, A., & Eastell, R. (2005). Circulating osteoprotegerin and receptor activator for nuclear factor kappaB ligand: clinical utility in metabolic bone disease assessment. *J Clin Endocrinol Metab, 90*(11), 6323-6331. doi:10.1210/jc.2005-0794

Rosenthall, L. (2004). Range of change of measured BMD in the femoral neck and total hip with rotation in women. *J Bone Miner Metab, 22*(5), 496-499. doi:10.1007/s00774-004-0513-3

Roy, M. E., & Nishimoto, S. K. (2002). Matrix Gla protein binding to hydroxyapatite is dependent on the ionic environment: calcium enhances binding affinity but phosphate and magnesium decrease affinity. *Bone, 31*(2), 296-302.

Ruospo, M., Palmer, S. C., Natale, P., Craig, J. C., Vecchio, M., Elder, G. J., et al. (2018). Phosphate binders for preventing and treating chronic kidney disease-mineral and bone disorder (CKD-MBD). *Cochrane Database Syst Rev, 8*, CD006023. doi:10.1002/14651858.CD006023.pub3

Sabbagh, Y., Graciolli, F. G., O'Brien, S., Tang, W., dos Reis, L. M., Ryan, S., et al. (2012). Repression of osteocyte Wnt/beta-catenin signaling is an early event in the progression of renal osteodystrophy. *J Bone Miner Res, 27*(8), 1757-1772. doi:10.1002/jbmr.1630

Saito, H., Kusano, K., Kinosaki, M., Ito, H., Hirata, M., Segawa, H., et al. (2003). Human fibroblast growth factor-23 mutants suppress Na+-dependent phosphate co-transport activity and 1alpha,25-dihydroxyvitamin D3 production. *J Biol Chem, 278*(4), 2206-2211. doi:10.1074/jbc.M207872200

Sardiwal, S., Gardham, C., Coleman, A. E., Stevens, P. E., Delaney, M. P., & Lamb, E. J. (2012). Bone-specific alkaline phosphatase concentrations are less variable than those of parathyroid hormone in stable hemodialysis patients. *Kidney Int, 82*(1), 100-105. doi:10.1038/ki.2012.77

Sarmento-Dias, M., Santos-Araujo, C., Poinhos, R., Oliveira, B., Silva, I. S., Silva, L. S., et al. (2016). Fibroblast growth factor 23 is associated with left ventricular hypertrophy, not with uremic vasculopathy in peritoneal dialysis patients. *Clin Nephrol, 85*(3), 135-141. doi:10.5414/CN108716

Schafer, C., Heiss, A., Schwarz, A., Westenfeld, R., Ketteler, M., Floege, J., et al. (2003). The serum protein alpha 2-Heremans-Schmid glycoprotein/fetuin-A is a systemically acting inhibitor of ectopic calcification. *J Clin Invest, 112*(3), 357-366. doi:10.1172/JCI17202

Schisterman, E. F., Faraggi, D., Reiser, B., & Trevisan, M. (2001). Statistical inference for the area under the receiver operating characteristic curve in the presence of random measurement error. *Am J Epidemiol, 154*(2), 174-179. doi:10.1093/aje/154.2.174

Schlieper, G., Aretz, A., Verberckmoes, S. C., Kruger, T., Behets, G. J., Ghadimi, R., et al. (2010). Ultrastructural analysis of vascular calcifications in uremia. *J Am Soc Nephrol, 21*(4), 689-696. doi:10.1681/ASN.2009080829

Schlieper, G., Brandenburg, V., Djuric, Z., Damjanovic, T., Markovic, N., Schurgers, L., et al. (2009). Risk factors for cardiovascular calcifications in non-diabetic Caucasian haemodialysis patients. *Kidney Blood Press Res, 32*(3), 161-168. doi:10.1159/000221064

Schober, H. C., Han, Z. H., Foldes, A. J., Shih, M. S., Rao, D. S., Balena, R., et al. (1998). Mineralized bone loss at different sites in dialysis patients: implications for prevention. *J Am Soc Nephrol, 9*(7), 1225-1233.

Schoppet, M., Sattler, A. M., Schaefer, J. R., Herzum, M., Maisch, B., & Hofbauer, L. C. (2003). Increased osteoprotegerin serum levels in men with coronary artery disease. *J Clin Endocrinol Metab, 88*(3), 1024-1028. doi:10.1210/jc.2002-020775

Schousboe, J. T., Wilson, K. E., & Hangartner, T. N. (2007). Detection of aortic calcification during vertebral fracture assessment (VFA) compared to digital radiography. *PLoS One, 2*(8), e715. doi:10.1371/journal.pone.0000715

Schousboe, J. T., Wilson, K. E., & Kiel, D. P. (2006). Detection of abdominal aortic calcification with lateral spine imaging using DXA. *J Clin Densitom, 9*(3), 302-308. doi:10.1016/j.jocd.2006.05.007

Schurgers, L. J., Barreto, D. V., Barreto, F. C., Liabeuf, S., Renard, C., Magdeleyns, E. J., et al. (2010). The circulating inactive form of matrix gla protein is a surrogate marker for vascular calcification in chronic kidney disease: a preliminary report. *Clin J Am Soc Nephrol, 5*(4), 568-575. doi:10.2215/CJN.07081009

Schurgers, L. J., Spronk, H. M., Skepper, J. N., Hackeng, T. M., Shanahan, C. M., Vermeer, C., et al. (2007). Post-translational modifications regulate matrix Gla protein function: importance for inhibition of vascular smooth muscle cell calcification. *J Thromb Haemost, 5*(12), 2503-2511. doi:10.1111/j.1538-7836.2007.02758.x

Schwartz, G. G., Whitlatch, L. W., Chen, T. C., Lokeshwar, B. L., & Holick, M. F. (1998). Human prostate cells synthesize 1,25-dihydroxyvitamin D3 from 25-hydroxyvitamin D3. *Cancer Epidemiol Biomarkers Prev, 7*(5), 391-395.

Schwartz, J. B., Lai, J., Lizaola, B., Kane, L., Markova, S., Weyland, P., et al. (2014). A comparison of measured and calculated free 25(OH) vitamin D levels in clinical populations. *J Clin Endocrinol Metab, 99*(5), 1631-1637. doi:10.1210/jc.2013-3874

Schwarz, U., Buzello, M., Ritz, E., Stein, G., Raabe, G., Wiest, G., et al. (2000). Morphology of coronary atherosclerotic lesions in patients with end-stage renal failure. *Nephrol Dial Transplant, 15*(2), 218-223.

Scialla, J. J., Lau, W. L., Reilly, M. P., Isakova, T., Yang, H. Y., Crouthamel, M. H., et al. (2013). Fibroblast growth factor 23 is not associated with and does not induce arterial calcification. *Kidney Int, 83*(6), 1159-1168. doi:10.1038/ki.2013.3

Shantouf, R. S., Budoff, M. J., Ahmadi, N., Ghaffari, A., Flores, F., Gopal, A., et al. (2010). Total and individual coronary artery calcium scores as independent predictors of mortality in hemodialysis patients. *Am J Nephrol, 31*(5), 419-425. doi:10.1159/000294405

Sharma, J., Raggi, P., Kutner, N., Bailey, J., Zhang, R., Huang, Y., et al. (2012). Improved long-term survival of dialysis patients after near-total parathyroidectomy. *J Am Coll Surg, 214*(4), 400-407; discussion 407-408. doi:10.1016/j.jamcollsurg.2011.12.046

Shimada, T., Hasegawa, H., Yamazaki, Y., Muto, T., Hino, R., Takeuchi, Y., et al. (2004). FGF-23 is a potent regulator of vitamin D metabolism and phosphate homeostasis. *J Bone Miner Res, 19*(3), 429-435. doi:10.1359/JBMR.0301264

Shimada, T., Urakawa, I., Isakova, T., Yamazaki, Y., Epstein, M., Wesseling-Perry, K., et al. (2010). Circulating fibroblast growth factor 23 in patients with end-stage renal disease treated by peritoneal dialysis is intact and biologically active. *J Clin Endocrinol Metab, 95*(2), 578-585. doi:10.1210/jc.2009-1603

Shoji, T., Inaba, M., Fukagawa, M., Ando, R., Emoto, M., Fujii, H., et al. (2018). Effect of Oral Alfacalcidol on Clinical Outcomes in Patients Without Secondary Hyperparathyroidism Receiving Maintenance Hemodialysis: The J-DAVID Randomized Clinical Trial. *JAMA, 320*(22), 2325-2334. doi:10.1001/jama.2018.17749

Shroff, R. C., McNair, R., Figg, N., Skepper, J. N., Schurgers, L., Gupta, A., et al. (2008). Dialysis accelerates medial vascular calcification in part by triggering smooth muscle cell apoptosis. *Circulation, 118*(17), 1748-1757. doi:10.1161/CIRCULATIONAHA.108.783738

Shroff, R. C., McNair, R., Skepper, J. N., Figg, N., Schurgers, L. J., Deanfield, J., et al. (2010). Chronic mineral dysregulation promotes vascular smooth muscle cell adaptation and extracellular matrix calcification. *J Am Soc Nephrol, 21*(1), 103-112. doi:10.1681/ASN.2009060640

Sigrist, M., Bungay, P., Taal, M. W., & McIntyre, C. W. (2006). Vascular calcification and cardiovascular function in chronic kidney disease. *Nephrol Dial Transplant, 21*(3), 707-714. doi:10.1093/ndt/gfi236

Sigrist, M. K., Taal, M. W., Bungay, P., & McIntyre, C. W. (2007). Progressive vascular calcification over 2 years is associated with arterial stiffening and increased mortality

in patients with stages 4 and 5 chronic kidney disease. *Clin J Am Soc Nephrol, 2*(6), 1241-1248. doi:10.2215/CJN.02190507

Silver, J., Naveh-Many, T., Mayer, H., Schmelzer, H. J., & Popovtzer, M. M. (1986). Regulation by vitamin D metabolites of parathyroid hormone gene transcription in vivo in the rat. *J Clin Invest, 78*(5), 1296-1301. doi:10.1172/JCI112714

Slatopolsky, E., Finch, J., Clay, P., Martin, D., Sicard, G., Singer, G., et al. (2000). A novel mechanism for skeletal resistance in uremia. *Kidney Int, 58*(2), 753-761. doi:10.1046/j.1523-1755.2000.00222.x

Sprague, S. M., Bellorin-Font, E., Jorgetti, V., Carvalho, A. B., Malluche, H. H., Ferreira, A., et al. (2016). Diagnostic Accuracy of Bone Turnover Markers and Bone Histology in Patients With CKD Treated by Dialysis. *Am J Kidney Dis, 67*(4), 559-566. doi:10.1053/j.ajkd.2015.06.023

Stein, E. M., Silva, B. C., Boutroy, S., Zhou, B., Wang, J., Udesky, J., et al. (2013). Primary hyperparathyroidism is associated with abnormal cortical and trabecular microstructure and reduced bone stiffness in postmenopausal women. *J Bone Miner Res, 28*(5), 1029-1040. doi:10.1002/jbmr.1841

Stenvinkel, P., Wang, K., Qureshi, A. R., Axelsson, J., Pecoits-Filho, R., Gao, P., et al. (2005). Low fetuin-A levels are associated with cardiovascular death: Impact of variations in the gene encoding fetuin. *Kidney Int, 67*(6), 2383-2392. doi:10.1111/j.1523-1755.2005.00345.x

Stompor, T., Pasowicz, M., Sullowicz, W., Dembinska-Kiec, A., Janda, K., Wojcik, K., et al. (2003). An association between coronary artery calcification score, lipid profile, and selected markers of chronic inflammation in ESRD patients treated with peritoneal dialysis. *Am J Kidney Dis, 41*(1), 203-211. doi:10.1053/ajkd.2003.50005

Taal, M. W., Thurston, V., McIntyre, N. J., Fluck, R. J., & McIntyre, C. W. (2014). The impact of vitamin D status on the relative increase in fibroblast growth factor 23 and parathyroid hormone in chronic kidney disease. *Kidney Int, 86*(2), 407-413. doi:10.1038/ki.2013.537

Takano, M., Okano, K., Tsuruta, Y., Yamashita, T., Echida, Y., Miwa, N., et al. (2011). Correlation of new bone metabolic markers with conventional biomarkers in hemodialysis patients. *Clin Invest Med, 34*(5), E267.

Tanasale, B., Kits, J., Kluin, P. M., Trip, A., & Kluin-Nelemans, H. C. (2013). Pain and anxiety during bone marrow biopsy. *Pain Manag Nurs, 14*(4), 310-317. doi:10.1016/j.pmn.2011.06.007

Tangpricha, V., Flanagan, J. N., Whitlatch, L. W., Tseng, C. C., Chen, T. C., Holt, P. R., et al. (2001). 25-hydroxyvitamin D-1alpha-hydroxylase in normal and malignant colon tissue. *Lancet, 357*(9269), 1673-1674. doi:10.1016/S0140-6736(00)04831-5

Tentori, F., Blayney, M. J., Albert, J. M., Gillespie, B. W., Kerr, P. G., Bommer, J., et al. (2008). Mortality risk for dialysis patients with different levels of serum calcium, phosphorus, and PTH: the Dialysis Outcomes and Practice Patterns Study (DOPPS). *Am J Kidney Dis, 52*(3), 519-530. doi:10.1053/j.ajkd.2008.03.020

Tentori, F., McCullough, K., Kilpatrick, R. D., Bradbury, B. D., Robinson, B. M., Kerr, P. G., et al. (2014). High rates of death and hospitalization follow bone fracture among hemodialysis patients. *Kidney Int, 85*(1), 166-173. doi:10.1038/ki.2013.279

Thomsen, J. S., Ebbesen, E. N., & Mosekilde, L. (2002). Static histomorphometry of human iliac crest and vertebral trabecular bone: a comparative study. *Bone, 30*(1), 267-274. doi:10.1016/s8756-3282(01)00666-4

Tomiyama, C., Carvalho, A. B., Higa, A., Jorgetti, V., Draibe, S. A., & Canziani, M. E. (2010). Coronary calcification is associated with lower bone formation rate in CKD patients not yet in dialysis treatment. *J Bone Miner Res, 25*(3), 499-504. doi:10.1359/jbmr.090735

Tonelli, M., Wiebe, N., Culleton, B., House, A., Rabbat, C., Fok, M., et al. (2006). Chronic kidney disease and mortality risk: a systematic review. *J Am Soc Nephrol, 17*(7), 2034-2047. doi:10.1681/ASN.2005101085

Torres, P. U. (2006). The need for reliable serum parathyroid hormone measurements. *Kidney Int, 70*(2), 240-243. doi:10.1038/sj.ki.5001658

Toussaint, N. D., Elder, G. J., & Kerr, P. G. (2009). Bisphosphonates in chronic kidney disease; balancing potential benefits and adverse effects on bone and soft tissue. *Clin J Am Soc Nephrol, 4*(1), 221-233. doi:CJN.02550508 [pii]10.2215/CJN.02550508

Toussaint, N. D., Lau, K. K., Strauss, B. J., Polkinghorne, K. R., & Kerr, P. G. (2009). Relationship between vascular calcification, arterial stiffness and bone mineral density in a cross-sectional study of prevalent Australian haemodialysis patients. *Nephrology (Carlton), 14*(1), 105-112. doi:10.1111/j.1440-1797.2008.01056.x

Toussaint, N. D., Lau, K. K., Strauss, B. J., Polkinghorne, K. R., & Kerr, P. G. (2010). Using vertebral bone densitometry to determine aortic calcification in patients with chronic kidney disease. *Nephrology (Carlton), 15*(5), 575-583. doi:10.1111/j.1440-1797.2010.01288.x

Uchiyama, T., Tanizawa, T., Muramatsu, H., Endo, N., Takahashi, H. E., & Hara, T. (1997). A morphometric comparison of trabecular structure of human ilium between microcomputed tomography and conventional histomorphometry. *Calcif Tissue Int, 61*(6), 493-498.

Ueda, M., Inaba, M., Okuno, S., Nagasue, K., Kitatani, K., Ishimura, E., et al. (2002). Clinical usefulness of the serum N-terminal propeptide of type I collagen as a marker of bone formation in hemodialysis patients. *Am J Kidney Dis, 40*(4), 802-809. doi:10.1053/ajkd.2002.35692

Ulutas, O., Taskapan, M. C., Dogan, A., Baysal, T., & Taskapan, H. (2018). Vascular calcification is not related to serum fetuin-A and osteopontin levels in hemodialysis patients. *Int Urol Nephrol, 50*(1), 137-142. doi:10.1007/s11255-017-1740-6

Urena-Torres, P., Metzger, M., Haymann, J. P., Karras, A., Boffa, J. J., Flamant, M., et al. (2011). Association of kidney function, vitamin D deficiency, and circulating markers of mineral and bone disorders in CKD. *Am J Kidney Dis, 58*(4), 544-553. doi:10.1053/j.ajkd.2011.04.029

Urena, P., Bernard-Poenaru, O., Ostertag, A., Baudoin, C., Cohen-Solal, M., Cantor, T., et al. (2003). Bone mineral density, biochemical markers and skeletal fractures in haemodialysis patients. *Nephrol Dial Transplant, 18*(11), 2325-2331.

Urena, P., Hruby, M., Ferreira, A., Ang, K. S., & de Vernejoul, M. C. (1996). Plasma total versus bone alkaline phosphatase as markers of bone turnover in hemodialysis patients. *J Am Soc Nephrol, 7*(3), 506-512.

USRDS. (2015). USRDS annual data report: Epidemiology of Kidney Disease in the United States*., 2*.

USRDS. (2018). *Annual report for End-Stage Renal Disease in the United States.* Retrieved from https://www.usrds.org/2018/view/Default.aspx.

van Erkel, A. R., & Pattynama, P. M. (1998). Receiver operating characteristic (ROC) analysis: basic principles and applications in radiology. *Eur J Radiol, 27*(2), 88-94.

van Venrooij, N. A., Pereira, R. C., Tintut, Y., Fishbein, M. C., Tumber, N., Demer, L. L., et al. (2014). FGF23 protein expression in coronary arteries is associated with impaired kidney function. *Nephrol Dial Transplant, 29*(8), 1525-1532. doi:10.1093/ndt/gft523

Viaene, L., Behets, G. J., Heye, S., Claes, K., Monbaliu, D., Pirenne, J., et al. (2016). Inflammation and the bone-vascular axis in end-stage renal disease. *Osteoporos Int, 27*(2), 489-497. doi:10.1007/s00198-015-3233-8

Wagner, J., Jhaveri, K. D., Rosen, L., Sunday, S., Mathew, A. T., & Fishbane, S. (2014). Increased bone fractures among elderly United States hemodialysis patients. *Nephrol Dial Transplant, 29*(1), 146-151. doi:10.1093/ndt/gft352

Wahner, H. W., Eastell, R., & Riggs, B. L. (1985). Bone mineral density of the radius: where do we stand? *J Nucl Med, 26*(11), 1339-1341.

Wang, A. Y., Woo, J., Lam, C. W., Wang, M., Chan, I. H., Gao, P., et al. (2005). Associations of serum fetuin-A with malnutrition, inflammation, atherosclerosis and valvular calcification syndrome and outcome in peritoneal dialysis patients. *Nephrol Dial Transplant, 20*(8), 1676-1685. doi:10.1093/ndt/gfh891

Wang, F., Wu, S., Ruan, Y., & Wang, L. (2015). Correlation of serum 25-hydroxyvitamin D level with vascular calcification in hemodialysis patients. *Int J Clin Exp Med, 8*(9), 15745-15751.

Wang, N., Yang, J., Yu, X., Hu, J., Xing, C., Ju, X., et al. (2008). Radial artery calcification in end-stage renal disease patients is associated with deposition of osteopontin and diminished expression of alpha-smooth muscle actin. *Nephrology (Carlton), 13*(5), 367-375. doi:10.1111/j.1440-1797.2008.00941.x

Watanabe, R., Lemos, M. M., Carvalho, A. B., Rochitte, C. E., Santos, R. D., Draibe, S. A., et al. (2012). The association between coronary artery calcification progression and loss of bone density in non-dialyzed CKD patients. *Clin Nephrol, 78*(6), 425-431. doi:10.5414/CN107515

Webb, A. R., DeCosta, B. R., & Holick, M. F. (1989). Sunlight regulates the cutaneous production of vitamin D3 by causing its photodegradation. *J Clin Endocrinol Metab, 68*(5), 882-887. doi:10.1210/jcem-68-5-882

Wesseling-Perry, K., Pereira, R. C., Wang, H., Elashoff, R. M., Sahney, S., Gales, B., et al. (2009). Relationship between plasma fibroblast growth factor-23 concentration and bone mineralization in children with renal failure on peritoneal dialysis. *J Clin Endocrinol Metab, 94*(2), 511-517. doi:10.1210/jc.2008-0326

West, S. L., Lok, C. E., Langsetmo, L., Cheung, A. M., Szabo, E., Pearce, D., et al. (2015). Bone mineral density predicts fractures in chronic kidney disease. *J Bone Miner Res, 30*(5), 913-919. doi:10.1002/jbmr.2406

Westenfeld, R., Krueger, T., Schlieper, G., Cranenburg, E. C., Magdeleyns, E. J., Heidenreich, S., et al. (2012). Effect of vitamin K2 supplementation on functional vitamin K deficiency in hemodialysis patients: a randomized trial. *Am J Kidney Dis, 59*(2), 186-195. doi:10.1053/j.ajkd.2011.10.041

Wheeler, D. C., London, G. M., Parfrey, P. S., Block, G. A., Correa-Rotter, R., Dehmel, B., et al. (2014). Effects of Cinacalcet on Atherosclerotic and Nonatherosclerotic Cardiovascular Events in Patients Receiving Hemodialysis: The EValuation Of Cinacalcet HCl Therapy to Lower CardioVascular Events (EVOLVE) Trial. *J Am Heart Assoc, 3*(6). doi:10.1161/JAHA.114.001363

Whyte, M. P. (1994). Hypophosphatasia and the role of alkaline phosphatase in skeletal mineralization. *Endocr Rev, 15*(4), 439-461. doi:10.1210/edrv-15-4-439

Wolf, M. (2010). Forging forward with 10 burning questions on FGF23 in kidney disease. *J Am Soc Nephrol, 21*(9), 1427-1435. doi:10.1681/ASN.2009121293

Wolf, M., Shah, A., Gutierrez, O., Ankers, E., Monroy, M., Tamez, H., et al. (2007). Vitamin D levels and early mortality among incident hemodialysis patients. *Kidney Int, 72*(8), 1004-1013. doi:10.1038/sj.ki.5002451

Yamada, S., Inaba, M., Kurajoh, M., Shidara, K., Imanishi, Y., Ishimura, E., et al. (2008). Utility of serum tartrate-resistant acid phosphatase (TRACP5b) as a bone resorption marker in patients with chronic kidney disease: independence from renal dysfunction. *Clin Endocrinol (Oxf), 69*(2), 189-196. doi:10.1111/j.1365-2265.2008.03187.x

Yavropoulou, M. P., Vaios, V., Pikilidou, M., Chryssogonidis, I., Sachinidou, M., Tournis, S., et al. (2017). Bone Quality Assessment as Measured by Trabecular Bone Score in Patients With End-Stage Renal Disease on Dialysis. *J Clin Densitom, 20*(4), 490-497. doi:10.1016/j.jocd.2016.11.002

Yenchek, R. H., Ix, J. H., Shlipak, M. G., Bauer, D. C., Rianon, N. J., Kritchevsky, S. B., et al. (2012). Bone mineral density and fracture risk in older individuals with CKD. *Clin J Am Soc Nephrol, 7*(7), 1130-1136. doi:10.2215/CJN.12871211

Yessayan, L., Moore, C., Lu, M., & Yee, J. (2017). Bone-specific alkaline phosphatase and bone turnover in African American hemodialysis patients. *Hemodial Int, 21*(1), 90-96. doi:10.1111/hdi.12454

Yoon, H. E., Kim, Y., Shin, S. J., Hong, Y. S., & Kang, K. Y. (2018). Factors associated with low trabecular bone scores in patients with end-stage kidney disease. *J Bone Miner Metab*. doi:10.1007/s00774-018-0938-8

Zhou, S., Fang, X., Xin, H., Li, W., Qiu, H., & Guan, S. (2013). Osteoprotegerin inhibits calcification of vascular smooth muscle cell via down regulation of the Notch1-RBP-Jkappa/Msx2 signaling pathway. *PLoS One, 8*(7), e68987. doi:10.1371/journal.pone.0068987

Appendix 1. Lifestyle Questionnaire

Renal Bone Study

Protocol reference: STH17141

Lifestyle Questionnaire

Please fill in this form as best you can. It will take approximately 20 minutes. If you need any help filling in this form please ask when you attend for your appointment.

About You

First Name: ..... Middle Initial..... Surname.....

Address: .....

.....

Telephone number: .....(home)

.....(work/mobile)

Gender: male / female

Occupation (current or before retirement): .....

Date of Birth: ..... / ..... / ..... Age:.....

GP name: .....

GP address: .....

.....

.....

About your lifestyle

How much milk do you use each day (e.g. in drinks, on cereal)?

Less than ½ pint ☐ ½ to 1 pint ☐ More than 1 pint ☐

How often do you eat cheese and/or yoghurt?

Never ☐ Less than once a week ☐ Once/twice a week ☐ Most days ☐

Do you take any of these supplements?

Cod Liver Oil ☐ Glucosamine ☐ Chondroitin ☐ Multivitamins ☐

Calcium ☐ Vitamin D ☐ Other (please state).....

On average, how often do you spend at least half an hour out of doors?

Never ☐ Less than once a week ☐ Once/twice a week ☐ Most days ☐

Do you take regular exercise, including activity at work?

YES ☐ NO ☐

If YES: What type of exercise (e.g. walking, gardening).....

How long do you exercise for each day _ _ hours _ _ minutes

On how many days of the week do you exercise? _ days

Do you drink alcohol?

YES ☐ NO ☐

If YES: How many days a week do you drink alcohol? _ days

On average, how many units of alcohol do you have each week? _ _ units

(1 unit = a single measure of whisky, 1/3 of a pint of beer or ½ a standard glass of red wine)

Do you smoke?

YES ☐ NOT NOW, but in the past ☐ NEVER ☐

If YES: How long have you smoked for? _ _ years _ _ months

If NOT NOW: How old were you when you stopped? _ _ years

About your health

Do you have any other health problems diagnosed by your GP or at hospital?

YES ☐ NO ☐

If YES, please describe.....

.....

.....

.....

Have you ever had any operations?

YES ☐ NO ☐

If YES, please describe (with dates if possible).....

.....

.....

.....

Are you currently taking any medication?

YES ☐ NO ☐

If YES, please list all tablets, medicines, creams, inhalers and injections that you are taking, with doses if possible. Please include prescribed treatment and treatment you buy yourself.

Medication	Dose

Have you ever taken steroid tablets (e.g. prednisolone)

YES ☐ NOT NOW, but in the past ☐ NO ☐

If YES: Approximately when did you start taking them? _ _ years _ _ months ago

What dose are you taking?……

What is the highest dose that you have taken?……

If NOT NOW: Approximately when did you stop? _ _ years _ _ months ago

Are you allergic to anything?

YES ☐ NO ☐

If YES: What you are allergic to?……

Have you taken treatment to make your bones stronger?

(e.g. Alendronate, Alendronic acid (Fosamax), Etidronate (Didronel PMO), Ibandronate (Bonviva), Risedronate (Actonel), Raloxifene (Evista), Strontium ranelate (Protelos), Teriparatide (Forsteo), Zoledronate (Aclasta))

YES ☐ NOT NOW, but in the past ☐ NO ☐

If YES: Which one(s) ……

When did you start taking them? _ _ years _ _ months ago

If NOT NOW: When did you stop taking them? _ _ years _ _ months ago

Fractures

Have you ever broken or fractured any bones?

YES ☐ NO ☐

If YES, please fill in the table below:

Which bone?	Age broken or fractured	How did it happen?	How was it treated?

Have you had any falls in the last 6 months?

YES ☐ NO ☐

If YES: How many?…….

Did you fall because you felt dizzy or had a blackout? (please give details).....

……

…….

Have you ever had severe back pain lasting more than a few days?

YES ☐ NO ☐

If YES: When and how do you think it started? .....

.....

Have you had any back or spine x-rays taken in the last 12 months?

YES ☐ NO ☐

If YES: At which hospital? …….

Family history

Do any of your close relatives have osteoporosis (thin bones)?

YES ☐ NO ☐

If YES: What is their relationship to you? .....

Have any of your close relatives broken a hip?

YES ☐ NO ☐

If YES: What is their relationship to you? .....

How old were they when they broke their hip? _ _ years

Reproductive Health (females only)

How old were you when your periods started? _ _ years

Are you still having regular periods (8 or more each year)?

YES ☐ NO ☐

If NO: How old were you when you had your last period? _ _ years

Did your periods ever stop for more than 3 months? (except during pregnancy and at the menopause) YES ☐ NO ☐

If YES: Please say when and why .....

.....

Have you ever used any of the following forms of contraception?

Combined oral contraceptive pill YES now ☐ NOT NOW, but in the past ☐ NEVER ☐

If NOT NOW: How long did you have them for? _ _ years _ _ months

When did you stop taking them? _ _ years _ _ months

Contraceptive injections YES now ☐ NOT NOW, but in the past ☐ NEVER ☐

If NOT NOW: How long did you have them for? _ _ years _ _ months

When did you stop taking them? _ _ years _ _ months

How many pregnancies beyond 20 weeks have you had? _ _

Have you ever breast fed?

YES ☐ NO ☐

If YES: How many children have you breast fed? _ _

Approximately how long did you breast feed each child for? _ _ months

When did you last stop breast feeding? _ _ years _ _ months ago

Do you experience menopausal symptoms now?

YES ☐ NO ☐

Have you ever taken Hormone Replacement Therapy (HRT)?

YES now ☐ NOT NOW, but in the past ☐ NO ☐

If YES now or NOT NOW: How old were you when you started taking it? _ _ years

How old were you when you stopped taking it? _ _ years

Have you had a hysterectomy?

YES ☐ NO ☐

If YES: How old were you? _ _ years

Had your periods stopped before you had the hysterectomy? YES ☐ NO ☐

Did you experience menopausal symptoms after the hysterectomy? (e.g. flushing, night sweats) YES ☐ NO ☐

If YES, when: Straight away ☐ Months later ☐ Years later ☐

Have you had either of your ovaries removed?

YES ☐ NO ☐

If YES: How old were you? _ _ years

How many ovaries were removed? One ☐ Two ☐

Thank you for completing this questionnaire.